University of Bath

UNIVERSITY OF BATH

PHD

Application of biophysics and bioengineering to the assessment of skin barrier function

Yang, Quan

Award date:
2011

Awarding institution:
University of Bath

[Link to publication](#)

APPLICATION OF BIOPHYSICS AND BIOENGINEERING TO THE ASSESSMENT OF SKIN BARRIER FUNCTION

QUAN YANG

A thesis submitted for the degree of Doctor of Philosophy

University of Bath
Department of Pharmacy and Pharmacology
September 2011

COPYRIGHT

Table of contents

Acknowledgments

My three years in Bath have been very enjoyable, and it is a pleasure to thank the many people who have helped and supported me.

First and foremost, I would like to thank my supervisor Prof. Richard Guy for giving me the opportunity to work in his research group in Bath; for sharing his insights and rounded vision of skin research with me during many stimulating discussions and for his guidance, encouragement and constant support throughout my doctoral studies.

I gratefully acknowledge Prof. Adrian Davis and Dr. Michael Rowan for accepting to evaluate this work.

I would also like to thank Dr. Michael Rowan for his important scientific comments on the development of analytical methods and Dr. Begona Delgaso-Charro for her support and comments throughout my study.

 I wish to thank all my dear friends and colleagues, past and present, from the pharmaceutic group in Bath for their moral and technical support. Especially, I would like to thank Miss Sarah Cordery, for being an important person who taught me analytical techniques and for her excellent technical help in the past three years.

I thank all the volunteers for their participation in the experiments and their patience. Thanks also to University of Bath for financial support.

Finally, I thank my family, especially my mum Qingyun, for their moral support and my boyfriend, Jia, for his encouragement at all time.

Abstract

Atopic dermatitis (AD) is one of the most common inflammatory skin diseases. The cause of AD is multifactoral and it is affected by both genetic and environmental factors. Of all the causes of potential barrier defects, the lowered amino-acid derived natural moisturizing factor (NMF) in the stratum corneum (SC), especially associated with a known filaggrin mutation, shows the strongest link to AD. As a result, quantification of NMF in the SC in both healthy and compromised SC is the principal aim of this thesis.

Because tape stripping is a key technique used to harvest the SC, a novel imaging method to measure the amount of SC per tape strip was validated. This method offers rapid, simple and reproducible SC quantification. It shows good correlation with existing gravimetric and infrared absorption methods and may provide a better standard method in the future.

The tape-stripping extraction of NMF showed an abundant SC 'reservoir' of the constituents in healthy skin. Iontophoretic extraction of NMF was highly dependant upon molecular properties, particularly charge and concentration. In general, charged NMF constituents were easily extracted by reverse iontophoresis, whereas iontophoresis only offered modest enhancement of zwitterionic species.

Quantification of NMF at different body sites, specifically forehead and forearm, showed similar profiles. However, forehead SC was thinner, and in general contained a lower total amount of NMF and less-ordered lipids. Forehead SC may therefore be considered a less competent barrier.

A 3-week application of 0.1% w/v sodium lauryl sulphate (SLS) to healthy volunteers was used to model damaged skin similar to that in AD and chronic irritant contact dermatitis. The SC barrier post-treatment showed significantly reduced NMF, substantial lipid disordering, and the presence of immature corneocytes. The methods employed were sufficiently sensitive to detect these changes. In particular, the NMF components present at high levels in the SC may be useful, potential markers for skin 'health' and for its resistance to irritant chemicals.

List of abbreviations

AAs	Amino acids
AD	Atopic dermatitis
ATR-FTIR	Attenuated total reflectance-fourier transform infrared spectroscopy
CE	Cornified envelope
DPK	Dermatopharmacokinetic
ICD	Irritant contact dermatitis
IgE	Immunoglobulin E
KIF	Keratin intermediate filament
KLK	Kallikrein
LCMS	Liquid chromatography mass spectrometry
LEKTI	Lymphoepithelial Kazal-type 5 serine protease inhibitor
NMF	Natural moisturising factor
NOS	Nitric oxide synthase
NS	Netherton syndrome
PAD	Peptidylarginine deiminases
PCA	Pyrrolidone carboxylic acid
SC	Stratum corneum
SLS	Sodium lauryl sulphate
TEWL	Transepidermal water loss
UA	Urocanic acid

Chapter 1: Stratum corneum competence and atopic dermatitis

Abstract

Atopic dermatitis (AD) is one of the most common inflammatory skin diseases. The cause of AD is multifactoral and it is affected by both genetic and environmental factors. It is believed that an impaired barrier function is crucial in the development of AD. In this chapter, structural changes of the stratum corneum (SC) observed in AD, that may lead to comprised barrier function, are explained.

Out of all the causes of potential barrier defects, lowered amino-acid derived natural moisturizing factors (NMF) in the SC, especially those associated with filaggrin mutation, show the strongest links to AD. As a result, quantification of NMF in the SC in both healthy and comprised SC is the main aim of this thesis.

The ultimate goal of this project is to characterize skin barrier function using different bioengineering methods that may underpin a non-invasive technology to identify infants with predisposition to a defective skin barrier.

1. Introduction

1.1 Atopic dermatitis (AD)

Atopic dermatitis (AD) or eczema is the most common childhood inflammatory skin disease [1]. It often begins in infancy or early childhood, with ~90% of cases appearing in the first 5 years of life. The hallmarks of AD are a chronic, relapsing form of skin inflammation, an impaired barrier function that causes dry skin and, in a more severe form, increased immunoglobulin E (IgE) levels, reflecting sensitization to allergens.

Patients with eczema report lower quality of life than that of the general population [1]. The sleeplessness associated with itching affects over 60% of children [1-2]. Lack of sleep affects the whole family and leads to poor performance at school and work. In addition to the physiological difficulties, children with AD have higher rates of psychological abnormalities, including behavioural problems, clinginess and fearfulness, while mothers have reported a decrease in employment outside the home, poor social support and stress about parenting [3]. Compared to other chronic childhood diseases, parents rated eczema as worse for children than having insulin dependent diabetes and the direct financial cost in caring for a child with moderate to severe eczema is higher than that for the average child with asthma, and is similar to that for diabetes [4].

In comparison to the difficulties in managing the chronic disease, the treatment of mild and moderate eczema is simple. It is based on daily application of emollients, with or without antibacterial ingredients, accompanied by symptomatic anti-inflammatory therapy consisting of topical glucocorticosteroids or topical calcineurin inhibitors on an 'as needed' basis [5]. Although systemic treatments are required for severe diseases, most patients are able to control the disease with simple regimes.

1.1.1 Development of AD

Traditionally eczema has been divided into extrinsic AD characterised by an elevated IgE level and a non-IgE associated form called intrinsic AD. However, it is recognized that there is a transient form of AD with a low level of IgE or without any detectable sensitization but which develops increased levels of IgE and sensitization later on in life [6]. Some patients even go on to develop sensitisation to self-proteins or to skin bacteria [7]. Accordingly,

Bieber [8] hypothesised that three phases exist in the natural history of AD as shown in Figure 1.

Figure 1: Gene-gene and gene-environment interactions in natural history of AD (Redrawn from Bieber [8])

The initial phase is the development of non-atopic dermatitis with genetic mutations causing impaired barrier function. Then, atopic gene pre-disposition and environmental factors lead to sensitization and development of AD. Finally, scratching causes the release of self-proteins in skin and further skin barrier damage leads to autoallergic atopic dermatitis.

Figure 2: Skin barrier function in arbitrary units as a function of the age. (Redrawn from Cork [9])

Recently，an alternative hypothesis [9] (Figure 2) has been suggested for the early progression of AD. In children, who do not have a genetic pre-disposition to a defective skin barrier (green line), their condition is worse at birth and then improves with time. Most importantly, it is always above the threshold for the signs and symptoms of AD to be seen. However, children with a pre-disposition (blue and red lines) have this profile shifted downward by an amount which is dependent on the severity of the combined genetic mutations. In the majority of cases, the natural improvement of skin barrier function with age may be sufficient to achieve complete remission (blue line). The skin barrier profile can also be adjusted upwards by effective treatment, whereas undesirable environmental factors have the opposite effect. Several environmental factors have been associated with AD, including use of soaps and detergents, washing with hard water, and exposure to house dust mites and food allergens [9-13]. As those are modifiable factors, it follows that identification of children with a genetic pre-disposition may allow the undesirable environmental factors to be avoided or substantially reduced. Nevertheless, like the first scenario, the importance of genetic pre-disposition of impaired barrier function in the development of AD is highlighted.

1.1.2 The atopic march

The sequential development of the manifestations of AD during early childhood is often referred to as the atopic march. Several longitudinal studies [14-17] have provided evidence for the progression from AD to the development of asthma and allergic rhinitis. A more recent study [18] has demonstrated that early AD is associated with asthma; in particular, infants with eczema and wheeze have a marked loss of lung function and subsequently develop asthma at school age. The results suggest a distinct phenotype of AD leading to asthma. Since the identification of filaggrin gene mutations as an important risk factor for AD, several studies [19-21] have confirmed that AD patients with these mutations have increased risk of developing asthma and allergic rhinitis in the later years. Thus, by identifying this phenotype of AD associated with filaggrin mutations, prevention of asthma and allergic rhinitis may also be possible.

1.2 Structure of the skin

The skin is one of the largest organs of the body, and functions as a protective and regulatory barrier between the body and the external environment. As illustrated in Figure 3, it consists of two principal layers, the dermis and the epidermis, separated by the basal lamina.

The dermis is highly vascularised and includes dermal fibroblasts, nerve endings, sebaceous glands and sweat glands. It plays an important role in the regulation of temperature, pressure, pain, and provides nutritive and immune support to the epidermis [22].

Figure 3 is available to be downloaded from the following website:

http://shs.westport.k12.ct.us/forensics/04-fingerprints/skin_layers.gif

Figure 3: Structure of the skin [23]

The epidermis, the outer layer interacting with the environment, is the major protective layer. The stratified epidermis, which is essentially composed of keratinocytes, can be further divided into four distinct layers: stratum basale, stratum spinosum, stratum granulosum and stratum corneum (SC). The keratinocytes originate from epidermal stem cells in stratum basale and undergo continuous differentiation during the course of migration upwards through spinosum and granulosum layers. Finally, SC, the outermost layer of epidermis, is composed of corneocytes (terminally differentiated keratinocytes)

and intercellular lipid lamellae (predominately secreted from lamellar granules during the final differentiation of keratinocytes) [24-25]. With respect to the body's first line of defence against external assault by foreign substances, the SC is the most relevant.

1.2.1   Stratum corneum structure

The SC is the skin main barrier to the penetration of irritants and allergens. It consists of corneocytes, flattened dead cells endowed with a cornified envelope (CE), analogous to bricks, and the intercellular lipid lamellae acting as mortar. Corneocytes are also strongly bound to each other by corneodesmosomes, the intercellular junctions of the SC, providing a strong mechanical protection to the epidermis. Alterations of the barrier causing increased water loss through the skin are the hallmark of AD. The alterations are complex and multifactorial.

1.2.2   Cornified envelopes (CE)

The CE is the final product of terminal differentiation of keratinocytes (KC); it is marked by the replacement of the KC plasma membrane with an insoluble protein layer [26] composed of loricrin, involucrin, filaggrin and small proline-rich proteins, which are cross-linked by transglutaminases.

The surface of the CE is coated with a monolayer of covalently bound ω-hydroxyceramides and fatty acids forming a lipid envelope, which by providing a hydrophobic surface is thought to play an essential role in the interaction with intercellular lipid matrix. The amount of protein-bound ω-hydroxyceramides in healthy epidermis comprises around 50% w/w of total protein-bound lipids, whereas this percentage decreases to 23-28% w/w in non-lesional areas and down to 10-25% w/w in affected areas in AD with a correlated increase in protein-bound ω-hydroxyl fatty acids [27] This change could generate a charged CE surface which may affect its interaction with intercellular lipid lamellae.

Recent research has also focused on corneocyte structure itself. The surface area of corneocytes is inversely correlated with transepidermal water loss (TEWL) [28-29], logical result of a longer pathlength for diffusion. A reduced corneocyte surface area in clinically asymptomatic skin in AD has indeed been reported [30-31]. Moreover, the identification of two distinct, so-called "fragile" (immature) and "rigid" (mature), corneocyte populations suggests a gradual modification of the corneocyte protein structure mediated by

transglutaminase [32-33]. Furthermore, immature corneocytes are detected in the surface SC of involved areas of AD, but not in uninvolved sites [34], highlighting at least in part the importance of incompletely mature corneocytes to impaired barrier function.

1.2.3   Stratum corneum lipid lamellae

Corneocytes are surrounded by lipid lamellae, composed of ceramides, cholesterol, fatty acids and cholesterol esters. These substances prevent the transepidermal loss of water and the penetration of exogenously applied materials [9]. As mentioned previously, the lipids are synthesized and stored in lamellar granules, which are then extruded into the extracellular space in the upper granular layer during cornification [25]. Disturbed maturation and delivery of the lamellar granules [35] and reduced levels of ceramides, especially ceramide 1 (also known as CER[EOS]), in AD have been reported [36-39]. This reduction in ceramides is, at least in part, a result of modified enzyme activities associated with ceramide production. In AD, prosaposin, a sphingolipid activator protein that facilitates the synthesis of ceramides is reduced [40] while, conversely, sphingomyelin deacylase, an enzyme that competes for ceramide precursors is over-expressed [41].

In recent years, ceramides, which constitute approximately 50% w/w of the SC lipids [42], have been the subject of most interest. In fact, 11 classes of ceramides have now been identified and named according to their fatty acid and sphingoid structures (Table 1). The average chain length of ceramides has been suggested as a possible marker of AD. As well as a reduced total ceramides level, ceramides profiling in AD patients showed an increase species with <40 total carbon atoms (e.g. CER[NS], CER[NDS], and CER[AS]), and a decrease in the level of larger species (>50 total carbon atoms, e.g. CER[NS], CER[NDS], CER[NH], CER[AS], and CER[AH]) [43].

SC barrier function is also influenced by lipid-packing, which appears to exist as a balance between orthorhombic (a solid crystalline state) and hexagonal (gel) states [44]. Orthorhombically packed lipids are required to produce a better barrier [45]. In patients with AD and lamellar ichthyosis, an decrease in orthorhombic packing has been found [46-47] and it is probably associated with a reduced level of CER[EOS], since the absence of this compound in lipid mixtures results in a predominantly hexagonal phase [48].

Fatty acid / Sphingoid	Non-hydroxy fatty acid [N]	α-Hydroxy fatty acid [A]	Esterified ω-hydroxy fatty acid [EO]
Dihydrosphingosine [DS]	CER[NDS]	CER[ADS]	Unidentified
Sphingosine [S]	CER[NS]	CER[AS]	CER[EOS]
6-Hydroxy sphingosine [H]	CER[NH]	CER[AH]	CER[EOH]
Phytosphingosine [P]	CER[NP]	CER[AP]	CER[EOP]

Table 1: Eleven classes ceramides identified in human stratum corneum [43]

1.2.4   Stratum corneum desquamation

The maintenance of SC formation and function lies in the balance between epidermal cell differentiation and desquamation events [49]. The latter is tightly controlled by a complex mixture of proteases and protease inhibitors, the action of which controls the integrity of corneodesmosomes. Various serine, cysteine, and aspartic acid proteases have been detected in the SC [50-52]. Among them, kallikrein (KLK) related serine peptidases are the key proteases, including KLK5 and KLK14 which contribute to the principal trypsin-like activity, while KLK7 accounts for the SC chymotrypsin-like activity [53]. The activated proteases target corneodesmosome proteins and are regulated by serine protease inhibitors, for example KLK7 is inhibited by secretory leukocyte protease inhibitor, elafin and lymphoepithelial Kazal-type 5 serine protease inhibitor (LEKTI); on the other hand, trypsin-like KLKs are only inhibited by LEKTI [54].

Epidermal KLKs are implicated in many protective physiological processes in human SC, as well in regulating skin desquamation. Their functions involve activating proinflammtory cytokines, e.g. IL-1β [55], regulating innate immune responses through cathlicidin activation [56], degradation of lipid processing enzymes [57] and modifying proteinase-activated receptor (PAR) activities, which in turn affects cell differentiation, proliferation and inflammation [58].

Given the importance of these proteases, most research has focused on their activity at different body sites and in diseased skin. The levels of KLK5 and another tryptase-like enzyme, but not KLK7, were found to be elevated in cheek compared to forearm [59]. Although a reduced activity of trypsin-like activity was described originally in non-eczematous AD skin [60], recent reports demonstrated an increase in serine protease activity in atopic skin [61-62], and the latter is consistent with an increase in multiple tissue kallikrein mRNAs in AD [63].

The most convincing evidence so far that established the link between excessive serine protease activity and impaired skin barrier function comes from the understanding of Netherton syndrome (NS). NS is a rare but severe form of ichthyosis caused by mutation in the SPINK5 gene, which encodes LEKTI [64]. For this reason, NS patients present with uncontrolled serine protease degradation of corneodesmosomes, implying that LEKTI plays a vital role in maintaining skin barrier function. However, the relevance of these findings to

AD is inconclusive. Two studies demonstrated significant association [65-66], which failed to be replicated [67]. In a more recent study, it was found that the SPINK5 mutation only associated when maternally inherited and was not a major contributor for AD [68]. This is probably because these studies only considered certain mutation polymorphisms; other variants may be of greater importance for eczema.

Nevertheless, exogenous proteases generated by house dust mites and *S. aureus* have been associated with AD exacerbation and may even trigger AD [69-71], further confirming the role of protease over-expression in weakening the skin barrier.

1.2.5 Epidermal pH

pH is defined as a negative decimal logarithm of the hydrogen ion activity in a solution [72]. Therefore, the nature of pH in the dense, lipid-, and protein-rich SC, which is largely devoid of water, remains to be defined. Nevertheless, the acidic character of skin's outer surface has been documented many years ago [73]. It was traditionally measured by glass electrodes [74-76]. Recently new high resolution microscopic techniques have been developed to probe the SC pH depth profile [77-78] and led to the understanding of "acid mantle" formation.

Two-photon fluorescence lifetime imaging has the ability to measure skin pH at both inter- and intra-corneocyte level [78]. It revealed the importance of a nonenergy-dependent sodium-proton exchanger (NHE1) in the generation of acidic extracellular domains of the lower SC [79]. In addition to NHE1, another two endogenous pathways have been identified as potential contributors of SC acidity: 1) secretory phospholiase A_2 ($sPLA_2$) generation of free fatty acids from phospholipids [80]; and 2) presence of acidic amino acid derivatives in SC [81], such as urocanic acid and pyrrolidone carboxylic acid.

The importance of skin's acidic character has been recognized as playing a crucial role in regulating several key protective functions of the skin, including permeability barrier homeostasis, SC integrity and cohesion [80, 82], antimicrobial defence [83] and cytokine activation [84-85]. The proposed mechanistic consequences of SC pH alteration is summarised in Figure 4. In order to explore the importance of SC pH, topical applications of superacids and superbases are used. By definition, superacids and superbases are at least an order of magnitude more acidic or more basic than 1N H_2SO_4 and 1N NaOH and their naphthalene structure favours absorption throughout the SC; they are therefore used to

manipulate SC pH even in very low concentrations [82]. Regular topical application of superacids successfully prevented emergence of murine atopic dermatitis and it thus highlighted the importance of the acidic SC in maintaining healthy skin barrier function [76].

Figure 4: Mechanistic consequences in response to change in SC pH (Redrawn from Hachem [82])

1.2.6   Stratum corneum natural moisturizing factor (NMF) and filaggrin

NMF and its origin

NMF (Table 2), found exclusively in the SC, is a collection of water-soluble, low molecular weight compounds, comprising approximately 20%-30% of corneocyte dry weight [86].

Table 2: Chemical composition of natural moisturizing factor (From Rawlings [86])

Compounds	Composition (% w/w)
Free amino acids	40
Pyrollidone carboxylic acid (PCA)	12
Lactate	12
Sugars	8.5
Urea	7
Chloride	6
Sodium	5
Potassium	4
Ammonia, uric acid, glucosamine and creatine	1.5
Calcium	1.5
Magnesium	1.5
Phosphate	0.5

Citrate and formate	0.5

NMF acts as extremely efficient humectants by absorbing moisture and then dissolving in its own water of hydration. It is believed to be critical in maintaining the hydration of the skin despite the desiccating action of the environment [87]. Some NMF components, such as urea, lactate and glycerol, are either partially secreted from sweat glands or derived from sebaceous glands. Their importance in skin hydration has long been recognized [88-92] and hence their presence in various commercially available moisturizing products. The presence of sugars in the SC is probably due to the release of glucose from glucosylceramides during the final processing of intercellular lipid lamellae [93] or as by-products released from the degradation of desmosomes and corneodesmosomes [94]. More recently, hyaluronic acid has also been considered be part of NMF [95] and suggested to participate in the epidermal response to barrier injury [96].

However, the majority of the NMF composes free amino acids, which are primarily derived from filaggrin. Filaggrin was first known as a keratin intermediate filament (KIF) associated protein that aggregated epidermal keratin filaments *in vitro* [97]. It is synthesized from profilaggrin (Figure 5), an approximately 500-kDa insoluble, highly basic, heavily phosphorylated, histidine-rich protein, consisting of 10 to 12 repeating filaggrin units [86, 98]. During the transition of the mature granular cell into a corneocyte, rapid dephosphorylation of pro-filaggrin occurs, yielding filaggrin (Figure 6) [86]. Filaggrin monomers, which do not persist beyond the two to three deepest layers of the SC, facilitate the aggregation of KIF and attach to KIF through the formation of salt bridges between positively-charged arginine and histidine residues on filaggrin and the negative charges on KIF [26]. As corneocytes proceed upwards through the SC, deiminiation and then complete proteolysis of filaggrin yields free amino acids and its derivatives, which are known collectively as the amino-acid-derived components of NMF (Figure 6).

Figure 5: Profilaggrin protein structure (Adapted from Sandilands et al [99]). Profilaggrin is expressed as a polyprotein that contains a variable number (10-12) of near-identical filaggrin repeats (blue circle), which are flanked on either side by partial, imperfect filaggrin repeats (light blue oval). Each repeat is separated by a linker. It also includes N-terminal and C-terminal domains (purple oval) at each end. The N-terminal domain can be subdivided into two distinct subdomains: the A domain (red) containing two Ca^{2+}-binding motifs and a cationic B domain (orange).

Figure 6: Processing of profilaggrin by currently identified proteases. Profilaggrin is synthesized and stored in keratohyalin granules in keratinocytes. During the formation of cornified envelope, profilaggrin is dephosphorylated and proteolytically processed into filaggrin monomers, which aid in the bundling of keratin intermediate filaments (KIF). Subsequently, filaggrin is deiminated, causing its release from keratin and allowing its degradation into free hygroscopic amino acids that act as components of NMF.

The functional effects of the amino-acid derived components of NMF on the SC have been studied. The primary role of NMF is to keep SC hydrated and the corneocytes that possess the highest concentration of NMF retain more water [86]. It is fascinating that, under extreme humidity conditions, the corneocytes take up free water and swell tremendously in the vertical direction (i.e., resulting mainly in an increase in cell thickness). However, the magnitude of this hydration is higher in the central region of the SC than that in the superficial and deeper regions [48, 100]. This observation is in excellent agreement with the concentration of amino-acid derived NMF, that appears to be maximal in the mid-SC [101]. The low level of NMF in the deeper SC is probably because little degradation of filaggrin is programmed in the well-hydrated conditions found here [102]; in contrast, daily washing likely leads to less NMF in the superficial SC. The absence of swelling in the deeper SC suggests that no free water is present thereby preventing dehydration of the adjacent viable epidermis. However, whether this is solely due to low NMF level cannot be unambiguously concluded, since it is also possible that the corneocytes in this region are simply less permeable to water. Nonetheless, by keeping the SC hydrated, NMF encourages critical biochemical events; most importantly, the activation of several proteases requires moisture for their functions that subsequently leads to the generation of NMF itself [86] .

Furthermore, the presence of free amino acids, especially zwitterionic and basic species, also provides specific ionic interactions with KIF, that are crucial to the maintenance of SC elasticity and its plasticization [103]. Moreover, trans-urocanic acid (t-UA), a deamination product of histidine, undergoes a photoisomerisation reaction under ultra-violet (UV) light to cis-urocanic acid (c-UA). This process helps to prevent UV damage and may contribute to UV light-induced immunosuppression [104-105].

Filaggrin and its degradation products have traditionally been thought to be inside the corneocytes, since transitional cells during cornification become filled with homogenous keratohyaline masses (associated with profilaggrin) and the immunoreactivity of filaggrin is detectable mainly in the cytoplasm. However, the presence of NMF in the intercellular space is evident. After incubation with water, water pools can be observed in the intercellular spaces [100, 106], possibly indicating the presence of osmolytes outside the corneocytes. The latter may be formed during corneodesmosomes breakdown and via concomitant leaching of osmolytes from corneocytes.

In addition, passive extraction of SC *in vivo* with water can extract extensive amounts quite rapidly which seems inconsistent with all the material being located intra-corneocyte [107]. This idea is supported by an observation of the corneocyte volume lost during final differentiation *in vivo* and that filaggrin-positive keratohyaline material, lysosomes, mitochondria, glycogen granules and parts of endoplasmic reticulum were extruded into intercellular spaces during the granular cell to corneocyte transition [108]. Accordingly, two types of NMF were proposed: 'internal' NMF, which is present in the SC, and 'external' NMF, which fills the intercellular spaces of living epidermis.

There could be another explanation for the intercellular NMF as illustrated in Figure 7. The immature corneocytes at the bottom of SC are not permeable to water, thus have low swelling properties even under extreme hydration. When corneocytes move upwards the surface of the SC, they become more permeable to water and NMF; the middle section of the SC hence has the highest swelling properties. Once the corneocytes reach the surface of the SC, they become fully permeable, and thus lose their swelling and barrier properties.

Surface-SC

Corneocytes become fully permeable leading to the loss of both water and NMF into the environment.

Mid-SC

Corneocytes become permeable to both water and NMF. Reduction in humidity initiates filaggrin degradation and hence the level of NMF inside the corneocytes increases. This in turn introduces SC swelling by attracting water into the corneocytes. On the other hand, NMF slowly diffuses into intercellular spaces owing to a concentration gradient.

Deeper-SC

Corneocytes are impermeable to water thereby preventing dehydration of adjacent viable epidermis. Little degradation of filaggrin occurs due to highly humid condition.

Figure 7: Possible changes in filaggrin degradation and corneocyte permeability during SC maturation.

Control of filaggrin processing

Filaggrin proteolysis is still a poorly understood process; it is intriguing to understand, for example, how SC is able to degrade filaggrin into free amino acids, while keeping other structural proteins, such as loricrin and keratin, intact. Pro-filaggrin enzymatic processing is carried out in several steps as illustrated in Figure 6.

However, the proteolysis of filaggrin may not primarily be kinetically controlled by enzymes, but rather by the water gradient existing in the SC [102]. Scott and Harding found that filaggrin was accumulated through the entire thickness of the SC during late foetal development in rat. It was only when the rats were exposed to a dryer environment immediately after birth, that normal proteolysis occurred. And this process could be blocked by maintaining a 100% humidity atmosphere. They also noticed that proteolysis took place only between 80 and 95% humidity in isolated stratum corneum *in vitro*. Likewise, they studied the effect of 10-day occlusion on filaggrin proteolysis and revealed that the filaggrin hydrolysis was dramatically blocked and a virtual absence of free amino acids in the SC. Instead, a more acidic variant of filaggrin was present throughout the SC, probably due to the activation of PADs to disassemble the filaggrin/keratin complex, a process that is independent of water gradient [109].

The breakdown of filaggrin designed by nature is such a delicate system. At deeper layer of the SC, filaggrin proteolysis is blocked by high hydration level and its attachment to KIF in order to prevent dehydration of the viable epidermis or to avoid osmotic damage to the newly formed immature corneocytes. It is only when at some point in the SC, where large reduction in water content occurs, the production of a large quantity of hygroscopic NMF happens and enables the SC to remain hydrated beyond this point.

Filaggrin mutation and its association with AD

Mutations in the gene coding for filaggrin cause a severe form of dry skin disease (ichtyosis vulgaris, IV) (Figure 8). Due to its similarity to AD, its association with AD was studied. Various mutations have been identified and it is up to now the strongest genetic pre-disposition associated with the development of AD [110-116]. All the mutations appear to involve truncation of the profilaggrin molecule. The truncated profilaggrin cannot be processed into filaggrin peptides [115].

Figure 8 is available to be downloaded from the following reference: Chen [116]

Figure 8: Histological features of patients with IV. All left panels show hematoxylin and eosin (H&E) staining and right panels show immunohistochemical staining with the 15C10 monoclonal antibody against filaggrin repeats in skin biopsies. (a) Keratohyalin granules are clearly visible in normal control skin after H&E staining. Immunohistochemical staining detects filaggrin repeats readily in 4-5 granular cell layers and throughout the stratum corneum. (b) The presence of a heterozygote 441delA/1249insG filaggrin mutation in IV patient leads to a barely detectable keratohyalin granules and filaggrin staining in the granular layer. (Taken from Chen [116])

Unsurprisingly, a reduced level of NMF has been associated with the filaggrin mutation [117] and has been implicated in the etiology of several dermatological disorders including IV, AD and allergic contact sensitization [118-120]. Moreover, an incapacity to process profilaggrin is also related to an abnormal skin phenotype, examples including the caspase-14 deficient mice which have reduced epidermal hydration and increased TEWL (transepidermal water loss) [121]; and premature degradation of profilaggrin is associated with altered keratinisation and keratin organisation within the SC [122]. Together these observations suggest that correct profilaggrin production and processing as well as NMF production are vital to the generation of a healthy epidermis and SC.

Filaggrin expression

The reduction of filaggrin expression is far more complex than simply genetic mutations. The most convincing evidence is that filaggrin expression was shown to be reduced by over-expression of T_h2 cytokines (e.g. IL-4 and IL-13) independent of filaggrin mutation [123]. Likewise, a decreased level of typical filaggrin derived NMF components were found as a global feature of moderate to severe AD [120]. It was, therefore, suggested that filaggrin genotype was the major determinant of NMF, with disease severity as a second modifier.

The modulation of filaggrin is affected by environmental factors and physical damage. Previous study on single dose hexadecane or UV radiation showed a loss of filaggrin expression in newly generated SC directly after insults, with a subsequent more rapid filaggrin synthesis 2-3 days after irritation [124]. Another similar experiment also reported a marked reduction in the SC amino acid level after three doses of hexadecane irritations in guinea pigs [125]. Physical damage, such as tape-striping ,was known to reduce the NMF components [126]. The effects of hydration level on the NMF recovery after tape-stripping were studied recently [127]. It demonstrated a higher NMF level in treated sites with no occlusion than the sites fully occluded, highlighting the importance of humidity on NMF synthesis.

Furthermore, underlying long-term illnesses may affect NMF production. Study with patients on hemodialysis showed a similar level of NMF to non-lesional AD skin, which is significantly lower than healthy controls [128]. Changes in NMF profile was also detected in aging and xerotic skin [118, 129-130]. However, these experiments only sampled the SC surface, where its NMF level may be affected by daily activities, such as washing or application of moisturizers.

Nevertheless, since mutation is not the sole attributing factor of NMF, measuring filaggrin degradation products (i.e., NMF components) in the SC is superior to genetic analysis of filaggrin mutations for the assessment of skin barrier function. Quantification of NMF components in the SC could identify people who either have filaggrin gene mutations or are incapable of catalysing the breakdown of filaggrin protein. If this quantification is possible in infants, then those with pre-disposed genetic mutations of impaired barrier function could be identified before the development of AD. Consequently, treatment with emollients and prevention of contact allergens in these infants could potentially prevent or delay the onset of AD and possibly reduce its severity. The measurement of NMF may also

be used as an investigational tool to evaluate either the intrinsic skin barrier function or barrier response to topical treatments.

1.3 Sampling the skin to assess skin barrier function

1.3.1 Non-invasive tape-stripping

The removal of sequential layers of the stratum corneum using adhesive tapes can be performed with minimum discomfort and relative ease *in vivo*, usually on the volar forearm of healthy volunteers. The procedure is painless and non-invasive, given that only dead cells (corneocytes) are removed. The method was first described by Pinkus [131] and since then it has become a standard method in dermatological research. Tape-stripping is used to evaluate the bioavailability and bioequivalence of topical drugs [132-133] or to produce a damaged skin barrier; e.g., prior to the application of an allergen [134]. However, it can also be used in conjunction with other quantification techniques to assess skin barrier function as described further below.

1.3.2 Transepidermal water loss (TEWL) measurement and SC thickness

The SC is the primary barrier for water penetration through the skin, and thus its removal increases TEWL. Fitting TEWL measurements, recorded as a function of repeated tape-stripping of the SC, to Fick's 1st law of diffusion, allows SC thickness to be estimated [135-136]. Measurement of SC thickness is a useful indicator of skin competency, and permits drug concentration profiles across the SC of different individuals to be normalised and directly compared.

1.3.3 Integrating the SC with attenuated total reflectance-fourier transform infrared spectroscopy (ATR-FTIR)

Figure 9: ATR-FTIR spectrometer scan forearm surface skin.

FTIR is an established and powerful tool to probe the molecular structure of materials [137-138]. ATR-FTIR (Figure 9) captures spectroscopic information noninvasively and has been particularly useful in investigating of the SC. However, the ATR-FTIR evanescent wave enters only a few microns from the crystal surface into the sample and hence only molecular vibrations from the most superficial layer of the sample are recorded. Therefore, repeated scanning with ATR-FTIR as a function of sequential tape-stripping is required to obtain a SC depth profile of a specific molecular species from the absorption spectra obtained.

A particularly studied feature of the IR spectrum of SC is methylene group vibrations from intercellular lipids [45, 139]. Organisation of the lipid lamellae is important in skin barrier function as mentioned before, and the vibrational frequency of these lipids produces a useful index of SC performance.

Principal component analysis is a multivariate technique that can be applied to a data set without preconceived assumptions about their properties [140]. Principal component analysis is a powerful tool to identify patterns and differences in complex datasets, such as a Raman or FTIR spectrum, by transforming the original information into new variables, so-called principal components, that describe most of the variability. The use of this method to analyse spectroscopic information from the skin has recently been explored [141]. Further,

using this approach in a pilot study, Raman spectra from infants with filaggrin-related atopic dermatitis has been analysed and used to identify disease development [142].

1.3.4 Measuring corneocyte maturity and surface area

The physical properties of corneocytes can be used to provide information on the immaturity and surface area. Extraction and staining of corneocytes collected on sequential tapes-strips non-invasively has been used as an indicator of barrier function [32, 143] and as a tool to assess the effects of topical treatment [144].

1.3.5 Extraction of tapes

The extraction and quantification of endogenous compounds removed on tape-strips offers a valuable "window" on SC performance. Combined with TEWL measurements, a concentration –depth profile can then be constructed. To date, lipids [145-146], cytokines [147] and NMF [148] have been quantified using this approach.

1.3.6 Benefits and limitations

Tape-stripping is easy to perform and relatively non-invasive. Although it may cause minor irritation, the renewal of only essentially dead cells means that the recovery of the skin barrier is rapid. The main drawback of this technique is the variability in the amount of SC removed by the tape-strips. For this reason, the quantity of SC on each tape must be quantified to express the mass of a compound extracted per unit 'volume' of the matrix. Traditionally, this has been done by weighing the tapes before and after stripping to obtain the weight of SC removed by difference. However, the weighing procedure is far from ideal. There are problems due to static electricity on the tapes, and uncertainties introduced by the uptake of formulation excipients, for example. Therefore, in chapter 2 of this thesis, a novel SC quantification method has been evaluated as an alternative to the weighing method in search of a better approach.

1.3.7 Transdermal reverse iontophoresis and passive diffusion for analyte extraction from the skin

Iontophoresis (Figure 9) is a different, essentially non-invasive method which can be used either to deliver or to extract substances across or from the skin. Iontophoresis promotes molecular transport via the application of a small current (≤0.5 mA/cm^2).

Figure 10：A schematic diagram illustrating reverse iontophoresis. A constant current is applied from a power source. Electromigration causes cationic (C$^+$, red arrow) compounds to be repelled from anode and drawn towards the cathode, while anonic (A$^-$, blue arrow) species are repelled from cathode and attracted towards the anode. Cationic (C$^+$, red arrow) and Neutral (yellow arrow) compounds are also drawn towards the cathode by electroosmosis. To a negligible extent, in most cases, passive diffusion (green arrow) contributes to the flux under both electrodes driven by the corresponding concentration gradient.

Three mechanisms contribute to the transport of a molecule across the skin during iontophoresis:

1) The interaction of charged molecules with the electrical field (electromigration).

2) The enhancement of molecular transport by current-induced solvent flow (electroosmosis).

3) Passive transdermal diffusion driven by the corresponding concentration gradient.

The total flux through the skin is the sum of these three contributions:

$J_{TOTAL} = J_{EM} + J_{EO} + J_P$ (eq. 1)

where J_{EM} represents the flux attributable to electromigration, J_{EO}, is the electroosmotic flux, and J_P is passive diffusion.

Electromigration describes the movement of ions under the influence of the applied electrical field so as to maintain electroneutrality across the skin. The speed of migration of an ion is determined by its physicochemical characteristics and the properties of the media through which it is moving [149-150]. The sum of individual ionic charges flowing through the skin must equal the electrical current supplied by the power source. This means that each ion competes to carry current across the skin with all other ions present in the system. The extent of the competition depends on the concentration, charge and mobility of all the ions present in the system. The transport number of the ion (x) of interest, represents the fraction of current carried by this species and is expressed as:

$$t_x = \frac{c_x z_x \mu_x}{\sum_i c_i z_i \mu_i}$$

(eq.2)

where c, z and μ refer, respectively, to the concentration, valence and mobility inside the skin of the ion of interest (x) and of the other competing ions (i). The transport number can also be deduced experimentally by measuring the ionic flux of the ion of interest, J_x:

$$J_x = \frac{I \cdot t_x}{F \cdot z_x}$$

(eq.3)

where I is the total current; F is Faraday's constant; and z_x is the valence of ion x.

Electroosmosis is current-induced solvent flow. At physiological pH, skin has an overall negative charge. Application of an electric field across a negatively charged membrane favours the movement of cations that are attempting to neutralize the membrane charge and thus give rise to its cation selectivity, and this induces a solvent flow from anode-to-cathode direction. Electroosmotic flow therefore enhances the transport of neutral and cationic compounds. As electrical mobility decreases with increasing molecular weight, electroosmosis is believed to be the dominant mechanism of transport for large molecules [151].

Passive diffusion of ions as a result of a concentration gradient during iontophoresis is negligible, compared to electromigration and electroosmosis. The symmetry of iontophoresis means that ions can be both delivered from the electrodes into and through

the skin, and extracted from the subdermal compartment to these electrodes (Figure 10). The latter is referred to as 'reverse iontophoresis', and can be used to monitor endogenous molecules or drugs present in the subdermal compartment in a non-invasive manner. The GlucoWatch Biographer (Figure 11), developed by Cygnus Inc, is the only device based on reverse iontophoresis that has been approved by the regulatory authorities, including the U.S. Food and Drug Administration. The device is capable of monitoring blood glucose in a continuous manner every 10 minutes for a period of up to 13 hours.

Figure 11 is available to be downloaded from the following reference: [152]

Figure 11: The GlucoWatch Biographer technology [152].

However, the GlucoWatch has not been a commercial success and is no longer in the market because of some important drawbacks associated with the system, including: the requirement for calibration via a conventional finger-stick blood glucose measurement [153], the presence of a 'skin reservoir' of glucose necessitating a 'warm-up' period of ~2hr before useful measurements can be made, local irritation, and an inability to function when the wearer is actively sweating [154].

The term of this thesis, however, the presence of NMF in the skin [148, 154-157] offers a potential opportunity for reverse iontophoresis to extract the various components quickly and reproducibly with little or no contamination (at least in the earlier samples) from molecules deeper in the skin or in the blood.

2. Project aim and organisation of the thesis

This project aims to characterize skin barrier function using different bioengineering methods to underpin a non-invasive technology to identify infants pre-disposed to atopic dermatitis (AD). Successful attainment of this objective would ensure emollient treatment could be started as soon as possible, and contact with allergens and detergents to be avoided. In this way, it would be possible to prevent or delay the onset of AD and possibly reduce the severity of the disease.

As loss-of-function mutations found in the filaggrin gene are the most significant genetic factors associated with AD, the main target of this project is to analyse the amount and consumption of NMF components in healthy and in damaged skin using tape-stripping and reverse iontophoresis. Various bioengineering methods, including, FTIR measurements and immunochemical staining, are also used to provide complementary assessment of skin barrier function. The ultimate goal is to identify a diagnostic tool with which to detect impaired skin barrier function.

As tape-stripping is a major technique to be employed in this thesis, Chapter 2 first evaluates and compares a novel imaging method against the traditional gravimetric approach to quantify the SC removed on the tapes.

Chapter 3 concerns the *in vivo* extraction of NMF from healthy human volunteers. The SC 'reservoir' of NMF is quantified and the potential of reverse iontophoresis as an extraction tool is evaluated.

In Chapter 4, *in vivo* extraction of NMF from both the forearm and forehead of the same volunteers is designated to characterise two anatomic regions at which SC barrier function is notably different. Differences in NMF composition and SC intercellular lipid order at the two sites are assessed.

Finally, repeated exposure of healthy volunteers to the irritant sodium lauryl sulphate (SLS) is used to model a damaged skin barrier that is similar to that present in AD and chronic irritant contact dermatitis (Chapter 5). The SC 'reservoir' of NMF is quantified with and without SLS-induced irritation. Other bioengineering methods are also used to characterize skin barrier function in the search for a better marker of SC 'health'.

3. Reference

1. Lewis-Jones S, *Quality of life and childhood atopic dermatitis: the misery of living with childhood eczema.* International Journal of Clinical Practice, 2006. **60**(8): p. 984-992.

2. Chamlin SL, Frieden IJ, Williams ML, and Chren M-M, *Effects of atopic dermatitis on young American children and their families.* Pediatrics, 2004. **114**(3): p. 607-611.

3. Daud L, Garralda M, and David T, *Psychosocial adjustment in preschool children with atopic eczema.* Arch Dis Child, 1993. **69**(6): p. 670-676.

4. Su JC, Kemp AS, Varigos GA, and Nolan TM, *Atopic eczema: its impact on the family and financial cost.* Arch Dis Child, 1997. **76**(2): p. 159-162.

5. Cezmi AA, Mabeccel A, Thomas B, Carsten B-J, Mark B, Philippe E, Qutayba H, Alexander K, Donald YML, Jasna L, Thomas AL, Antonella M, Natalija N, Thomas A, Lanny R, Annika S, Simons FER, Jonathan S, Kristiina T, Ulrich W, Stefan W, Thomas W, and Torsten Z, *Diagnosis and treatment of atopic dermatitis in children and adults: European Academy of Allergology and Clinical Immunology/American Academy of Allergy, Asthma and Immunology/PRACTALL Consensus Report.* The Journal of allergy and clinical immunology, 2006. **118**(1): p. 152-169.

6. Novembre E, Cianferoni A, Lombardi E, Bernardini R, Pucci N, and Vierucci A, *Natural history of "intrinsic" atopic dermatitis.* Allergy, 2001. **56**(5): p. 452-453.

7. Natalija N, Jean-Pierre A, and Thomas B, *Allergic hyperreactivity to microbial components: A trigger factor of intrinsic atopic dermatitis?* The Journal of allergy and clinical immunology, 2003. **112**(1): p. 215-216.

8. Bieber T, *Atopic dermatitis.* N Engl J Med, 2008. **358**(14): p. 1483-1494.

9. Cork MJ, Danby SG, Vasilopoulos Y, Hadgraft J, Lane ME, Moustafa M, Guy RH, MacGowan AL, Tazi-Ahnini R, and Ward SJ, *Epidermal barrier dysfunction in atopic dermatitis.* J Invest Dermatol, 2009. **129**(8): p. 1892-1908.

10. McNally NJ, Williams HC, and Phillips DR, *Atopic eczema and the home environment.* British Journal of Dermatology, 2001. **145**(5): p. 730-736.

11. McNally NJ, Williams HC, Phillips DR, Smallman-Raynor M, Lewis S, Venn A, and Britton J, *Atopic eczema and domestic water hardness.* The Lancet, 1998. **352**(9127): p. 527-531.

12. Tan BB, Weald D, Strickland I, and Freidmann PS, *Double-blind controlled trial of effect of housedust-mite allergen avoidance on atopic dermatitis.* The Lancet, 1996. **347**(8993): p. 15-18.

13. Hamami I and Marks R, *Abnormalities in clinically normal skin-a possible explanation of the'angry back syndrome'.* Clinical and Experimental Dermatology, 1988. **13**(5): p. 328-333.

14. Bergmann R, Edenharter G, Bergmann K, Forster J, Bauer C, Wahn V, Zepp F, and Wahn U, *Atopic dermatitis in early infancy predicts allergic airway disease at 5 years.* Clinical & Experimental Allergy, 1998. **28**(8): p. 965-970.

15. Gustafsson D, Sjöberg O, and Foucard T, *Development of allergies and asthma in infants and young children with atopic dermatitis - a prospective follow - up to 7 years of age.* Allergy, 2000. **55**(3): p. 240-245.

16. Rhodes HL, Sporik R, Thomas P, Holgate ST, and Cogswell JJ, *Early life risk factors for adult asthma: A birth cohort study of subjects at risk.* Journal of Allergy and Clinical Immunology, 2001. **108**(5): p. 720-725.

17. Rhodes HL, Thomas P, Sporik R, Holgate ST, and Cogswell JJ, *A birth cohort study of subjects at risk of atopy. Twenty-two-year follow-up of wheeze and atopic status.* Am. J. Respir. Crit. Care Med., 2002. **165**(2): p. 176-180.

18. Illi S, von Mutius E, Lau S, Nickel R, Grüber C, Niggemann B, Wahn U, and the Multicenter Allergy Study G, *The natural course of atopic dermatitis from birth to age 7 years and the association with asthma.* Journal of Allergy and Clinical Immunology, 2004. **113**(5): p. 925-931.

19. Weidinger S, O'Sullivan M, Illig T, Baurecht H, Depner M, Rodriguez E, Ruether A, Klopp N, Vogelberg C, Weiland SK, McLean WHI, von Mutius E, Irvine AD, and Kabesch M, *Filaggrin mutations, atopic eczema, hay fever, and asthma in children.* Journal of Allergy and Clinical Immunology, 2008. **121**(5): p. 1203-1209.

20. Palmer CNA, Ismail T, Lee SP, Terron-Kwiatkowski A, Zhao Y, Liao H, Smith FJD, McLean WHI, and Mukhopadhyay S, *Filaggrin null mutations are associated with*

increased asthma severity in children and young adults. Journal of Allergy and Clinical Immunology, 2007. **120**(1): p. 64-68.

21. Marenholz I, Nickel R, Rüschendorf F, Schulz F, Esparza-Gordillo J, Kerscher T, Grüber C, Lau S, Worm M, Keil T, Kurek M, Zaluga E, Wahn U, and Lee Y-A, *Filaggrin loss-of-function mutations predispose to phenotypes involved in the atopic march.* Journal of Allergy and Clinical Immunology, 2006. **118**(4): p. 866-871.

22. Menon GK, *New insights into skin structure: scratching the surface.* Advanced Drug Delivery Reviews, 2002. **54**(Supplement 1): p. S3-S17.

23. Lazaroff and Rollison. 2011 [cited 2011; Available from: http://shs.westport.k12.ct.us/forensics/04-fingerprints/skin_layers.gif.

24. Clive RH, *The stratum corneum: structure and function in health and disease.* Dermatologic Therapy, 2004. **17**(s1): p. 6-15.

25. Madison KC, *Barrier Function of the Skin: "La Raison d'Etre" of the Epidermis.* J Investig Dermatol, 2003. **121**(2): p. 231-241.

26. Candi E, Schmidt R, and Melino G, *The cornified envelope: a model of cell death in the skin.* Nat Rev Mol Cell Biol, 2005. **6**(4): p. 328-340.

27. Macheleidt O, Kaiser HW, and Sandhoff K, *Deficiency of epidermal protein-bound w-hydroxyceramides in atopic dermatitis.* 2002. **119**(1): p. 166-173.

28. Hadgraft J and Lane ME, *Transepidermal water loss and skin site: A hypothesis.* International Journal of Pharmaceutics, 2009. **373**(1-2): p. 1-3.

29. Machado M, Salgado TM, Hadgraft J, and Lane ME, *The relationship between transepidermal water loss and skin permeability.* International Journal of Pharmaceutics, 2010. **384**(1-2): p. 73-77.

30. Al-Jaberi H and Marks R, *Studies of the clinically uninvolved skin in patients with dermatitis.* British Journal of Dermatology, 1984. **111**(4): p. 437-443.

31. Watanabe M, Tagami H, Horii I, Takahashi M, and Kligman AM, *Functional Analyses of the Superficial Stratum Corneum in Atopic Xerosis.* Arch Dermatol, 1991. **127**(11): p. 1689-1692.

32. Hirao T, Denda M, and Takahashi M, *Identification of immature cornified envelopes in the barrier-impaired epidermis by characterization of their hydrophobicity and antigenicities of the components.* Experimental Dermatology, 2001. **10**(1): p. 35-44.

33. Hirao T, *Involvement of transglutaminase in ex vivo maturation of cornified envelopes in the stratum corneum.* International Journal of Cosmetic Science, 2003. **25**(5): p. 245-257.

34. Tetsuji H, Tadashi T, Izuho T, Hiromi K, Mikiko O, Motoji T, and Hachiro T, *Ratio of immature cornified envelopes does not correlate with parakeratosis in inflammatory skin disorders.* Experimental Dermatology, 2003. **12**(5): p. 591-601.

35. Fartasch M, Bassukas I, and Diepgen T, *Disturbed extruding mechanism of lamellar bodies in dry non-eczematous kin of atopics.* The British Journal of Dermatology, 1992. **127**(3): p. 221-227.

36. Imokawa G, Abe A, Jin K, Higaki Y, Kawashima M, and Hidano A, *Decreased Level of Ceramides in Stratum Corneum of Atopic Dermatitis: An Etiologic Factor in Atopic Dry Skin?* J Invest Dermatol, 1991. **96**(4): p. 523-526.

37. Nardo A, Wertz P, Giannetti A, and Seidenari S, *Ceramide and Cholesterol Composition of the Skin of Patients with Atopic Dermatitis.* Acta Derm Venereol, 1998. **78**: p. 27-30.

38. Yamamoto A, Serizawa S, Ito M, and Sato Y, *Stratum corneum lipid abnormalities in atopic dermatitis.* Archives of Dermatological Research, 1991. **283**(4): p. 219-223.

39. Matsumoto M, Umemoto N, Sugiura H, and Uehara M, *Difference in Ceramide Composition between ``Dry'' and ``Normal'' Skin in Patients with Atopic Dermatitis.* Acta Derm Venereol, 1998. **79**: p. 246-247.

40. Chang-Yi C, Kusuda S, Seguchi T, Takahashi M, Aisu K, and Tezuka T, *Decreased Level of Prosaposin in Atopic Skin.* J Invest Dermatol, 1997. **109**(3): p. 319-323.

41. Hara J, Higuchi K, Okamoto R, Kawashima M, and Imokawa G, *High-Expression of Sphingomyelin Deacylase is an Important Determinant of Ceramide Deficiency Leading to Barrier Disruption in Atopic Dermatitis.* J Invest Dermatol, 2000. **115**(3): p. 406-413.

42. Yardley HJ and Summerly R, *Lipid composition and metabolism in normal and diseased epidermis.* Pharmacology & Therapeutics, 1981. **13**(2): p. 357-383.

43. Ishikawa J, Narita H, Kondo N, Hotta M, Takagi Y, Masukawa Y, Kitahara T, Takema Y, Koyano S, Yamazaki S, and Hatamochi A, *Changes in the Ceramide Profile of Atopic Dermatitis Patients.* J Invest Dermatol, 2010.

44.   Bouwstra J, Gooris G, and Ponec M, *The Lipid Organisation of the Skin Barrier: Liquid and Crystalline Domains Coexist in Lamellar Phases.* Journal of Biological Physics, 2002. **28**(2): p. 211-223.

45.   Berthaud F and Boncheva M, *Correlation between the properties of the lipid matrix and the degrees of integrity and cohesion in healthy human Stratum corneum.* Experimental Dermatology, 2010. **20**(3): p. 255-262.

46.   Pilgram G, Vissers D, van der Meulen H, Pavel S, Lavrijsen S, Bouwstra J, and Koerten H, *Aberrant Lipid Organization in Stratum Corneum of Patients with Atopic Dermatitis and Lamellar Ichthyosis.* J Invest Dermatol, 2001. **117**(3): p. 710-717.

47.   Bouwstra JA and Ponec M, *The skin barrier in healthy and diseased state.* Biochimica et Biophysica Acta (BBA) - Biomembranes, 2006. **1758**(12): p. 2080-2095.

48.   Bouwstra JA, Gooris GS, Dubbelaar FER, and Ponec M, *Phase Behavior of Stratum Corneum Lipid Mixtures Based on Human Ceramides: The Role of Natural and Synthetic Ceramide 1.* J Invest Dermatol, 2002. **118**(4): p. 606-617.

49.   Egelrud T, *Purification and preliminary characterization of stratum corneum chymotryptic enzyme: a proteinase that may be involved in desquamation.* J Invest Dermatol, 1993. **101**(2): p. 200-204.

50.   Kishibe M, Bando Y, Terayama R, Namikawa K, Takahashi H, Hashimoto Y, Ishida-Yamamoto A, Jiang Y-P, Mitrovic B, Perez D, Iizuka H, and Yoshida S, *Kallikrein 8 is involved in skin desquamation in cooperation with other kallikreins.* J. Biol. Chem., 2007. **282**(8): p. 5834-5841.

51.   Horikoshi T, Igarashi S, Uchiwa H, Brysk H, and Brysk M, *Role of endogenous cathepsin D-like and chymotrypsin-like proteolysis in human epidermal desquamation.* British Journal of Dermatology, 1999. **141**(3): p. 453-459.

52.   Ekholm IE, Brattsand M, and Egelrud T, *Stratum corneum tryptic enzyme in normal epidermis: a missing link in the desquamation process ?* J Invest Dermatol, 2000. **114**(1): p. 56-63.

53.   Brattsand M, Stefansson K, Lundh C, Haasum Y, and Egelrud T, *A proteolytic cascade of kallikreins in the stratum corneum.* J Invest Dermatol, 2004. **124**(1): p. 198-203.

54.   Borgono CA, Michael IP, Komatsu N, Jayakumar A, Kapadia R, Clayman GL, Sotiropoulou G, and Diamandis EP, *A potential role for multiple tissue kallikrein*

serine proteases in epidermal desquamation. J. Biol. Chem., 2007. **282**(6): p. 3640-3652.

55.   Nylander-lundgvist E and Egelrud T, *Formation of active IL-1 beta from pro-IL-1 beta catalyzed by stratum corneum chymotryptic enzyme in vitro.* Acta Derm Venereol. , 1997. **77**(3): p. 203-206.

56.   Yamasaki K, Schauber J, Coda A, Lin H, Dorschner RA, Schechter NM, Bonnart C, Descargues P, Hovnanian A, and Gallo RL, *Kallikrein-mediated proteolysis regulates the antimicrobial effects of cathelicidins in skin.* The FASEB Journal, 2006. **20**(12): p. 2068-2080.

57.   Hachem J-P, Man M-Q, Crumrine D, Uchida Y, Brown BE, Rogiers V, Roseeuw D, Feingold KR, and Elias PM, *Sustained Serine Proteases Activity by Prolonged Increase in pH Leads to Degradation of Lipid Processing Enzymes and Profound Alterations of Barrier Function and Stratum Corneum Integrity.* J Invest Dermatol, 2005. **125**(3): p. 510-520.

58.   Oikonomopoulou K, Hansen KK, Saifeddine M, Vergnolle N, Tea I, Blaber M, Blaber SI, Scarisbrick I, Diamandis EP, and Hollenberg MD, *Kallikrein-mediated cell signalling: targeting proteinase-activated receptors (PARs).* Biological Chemistry, 2006. **387**(6): p. 817-824.

59.   Voegeli R, Rawlings A, Doppler S, Heiland J, and Schreier T, *Profiling of serine protease activities in human stratum corneum and detection of a stratum corneum tryptase-like enzyme.* International Journal of Cosmetic Science, 2007. **29**(3): p. 191-200.

60.   Tarroux R, Assalit MF, Licu D, Périé JJ, and Redoulès D, *Variability of Enzyme Markers during Clinical Regression of Atopic Dermatitis.* Skin Pharmacology and Physiology, 2002. **15**(1): p. 55-62.

61.   Voegeli R, Rawlings A, Breternitz M, Doppler S, Schreier T, and Fluhr J, *Increased stratum corneum serine protease activity in acute eczematous atopic skin.* British Journal of Dermatology, 2009. **161**(1): p. 70-77.

62.   Nahoko K, Kiyofumi S, Cynthia K, Amber CL, Saba K, Fumiaki S, Kazuhiko T, and Eleftherios PD, *Human tissue kallikrein expression in the stratum corneum and serum of atopic dermatitis patients.* Experimental Dermatology, 2007. **16**(6): p. 513-519.

63.   Komatsu N, Saijoh K, Toyama T, Ohka R, Otsuki N, Hussack G, Takehara K, and Diamandis EP, *Multiple tissue kallikrein mRNA and protein expression in normal skin and skin diseases.* British Journal of Dermatology, 2005. **153**(2): p. 274-281.

64.   Raghunath M, Tontsidou L, Oji V, Aufenvenne K, Schurmeyer-Horst F, Jayakumar A, Stander H, Smolle J, Clayman GL, and Traupe H, *SPINK5 and Netherton Syndrome: Novel Mutations, Demonstration of Missing LEKTI, and Differential Expression of Transglutaminases.* J Invest Dermatol, 2004. **123**(3): p. 474-483.

65.   Walley AJ, Chavanas S, Moffatt MF, Esnouf RM, Ubhi B, Lawrence R, Wong K, Abecasis GR, Jones EY, Harper JI, Hovnanian A, and Cookson W, *Gene polymorphism in Netherton and common atopic disease.* Nat Genet, 2001. **29**(2): p. 175-178.

66.   Nishio Y, Noguchi E, Shibasaki M, Kamioka M, Ichikawa E, Ichikawa K, Umebayashi Y, Otsuka F, and Arinami T, *Association between polymorphisms in the SPINK5 gene and atopic dermatitis in the Japanese.* Genes Immun, 2003. **4**(7): p. 515-517.

67.   Folster-Holst R, Stoll M, Koch WA, Hampe J, Christophers E, and Schreiber S, *Lack of association of SPINK5 polymorphisms with nonsyndromic atopic dermatitis in the population of Northern Germany.* British Journal of Dermatology, 2005. **152**(6): p. 1365-1367.

68.   Weidinger S, Baurecht H, Wagenpfeil S, Henderson J, Novak N, Sandilands A, Chen H, Rodriguez E, O'Regan GM, Watson R, Liao H, Zhao Y, Barker JNWN, Allen M, Reynolds N, Meggitt S, Northstone K, Smith GD, Strobl C, Stahl C, Kneib T, Klopp N, Bieber T, Behrendt H, Palmer CNA, Wichmann HE, Ring J, Illig T, McLean WHI, and Irvine AD, *Analysis of the individual and aggregate genetic contributions of previously identified serine peptidase inhibitor Kazal type 5 (SPINK5), kallikrein-related peptidase 7 (KLK7), and filaggrin (FLG) polymorphisms to eczema risk.* Journal of Allergy and Clinical Immunology, 2008. **122**(3): p. 560-568.e4.

69.   Nakamura T, Hirasawa Y, Takai T, Mitsuishi K, Okuda M, Kato T, Okumura K, Ikeda S, and Ogawa H, *Reduction of Skin Barrier Function by Proteolytic Activity of a Recombinant House Dust Mite Major Allergen Der f 1.* J Invest Dermatol, 2006. **126**(12): p. 2719-2723.

70.   Jeong SK, Kim HJ, Youm J-K, Ahn SK, Choi EH, Sohn MH, Kim K-E, Hong JH, Shin DM, and Lee SH, *Mite and Cockroach Allergens Activate Protease-Activated Receptor 2*

and Delay Epidermal Permeability Barrier Recovery. J Invest Dermatol, 2008. **128**(8): p. 1930-1939.

71. Hirasawa Y, Takai T, Nakamura T, Mitsuishi K, Gunawan H, Suto H, Ogawa T, Wang X-L, Ikeda S, Okumura K, and Ogawa H, *Staphylococcus aureus Extracellular Protease Causes Epidermal Barrier Dysfunction.* J Invest Dermatol, 2009. **130**(2): p. 614-617.

72. Buck R, Covington A, Baucke F, Brett C, Camoes M, Milton M, Mussini T, Naumann R, Pratt K, Spitzer P, and Wilson G, *Measurement of pH. Definition, standards,and procedures (IUPAC Recommendations 2002).* Pure Appl Chem, 2002. **74**(11): p. 2169-2200.

73. Draize JH, *The Determination of the pH of the Skin of Man and Common Laboratory Animals.* The Journal of Investigative Dermatology, 1942. **5**(2): p. 77-85.

74. Schirren C, *Does the glass electrode determine the same pH-values on the skin surface as the quinhydrone electrode?* J Invest Dermatol, 1955. **24**: p. 485-488.

75. Abe T, Mayuzumi J, Kikuchi N, and Arai S, *Seasonal variations in skin temperature, skin pH, evaporative water loss and skin surface lipid values on human skin.* Chem Pharm Bull, 1979. **28**(2): p. 387-392.

76. Hatano Y, Man M-Q, Uchida Y, Crumrine D, Scharschmidt TC, Kim EG, Mauro TM, Feingold KR, Elias PM, and Holleran WM, *Maintenance of an Acidic Stratum Corneum Prevents Emergence of Murine Atopic Dermatitis.* J Invest Dermatol, 2009. **129**(7): p. 1824-1835.

77. Kroll C, Herrmann W, Stößer R, Borchert H-H, and Mäder K, *Influence of Drug Treatment on the Microacidity in Rat and Human Skin—An Electron Spin Resonance Imaging Study.* Pharmaceutical Research, 2001. **18**(4): p. 525-530.

78. Hanson KM, Behne MJ, Barry NP, Mauro TM, Gratton E, and Clegg RM, *Two-Photon Fluorescence Lifetime Imaging of the Skin Stratum Corneum pH Gradient.* Biophysical journal, 2002. **83**(3): p. 1682-1690.

79. Behne MJ, Meyer JW, Hanson KM, Barry NP, Murata S, Crumrine D, Clegg RW, Gratton E, Holleran WM, Elias PM, and Mauro TM, *NHE1 Regulates the Stratum Corneum Permeability Barrier Homeostasis. Microenvironment acidification assessed with fluorescence lifetime imaging.* J. Biol. Chem., 2002. **277**(49): p. 47399-47406.

80. Fluhr JW, Kao J, Jain M, Ahn SK, Feingold KR, and Elias PM, *Generation of Free Fatty Acids from Phospholipids Regulates Stratum Corneum Acidification and Integrity.* J Invest Dermatol, 2001. **117**(1): p. 44-51.

81. Krien PM and Kermici M, *Evidence for the Existence of a Self-Regulated Enzymatic Process Within the Human Stratum Corneum -An Unexpected Role for Urocanic Acid.* J Invest Dermatol, 2000. **115**(3): p. 414-420.

82. Hachem J-P, Crumrine D, Fluhr J, Brown BE, Feingold KR, and Elias PM, *pH Directly Regulates Epidermal Permeability Barrier Homeostasis, and Stratum Corneum Integrity/Cohesion.* J Invest Dermatol, 2003. **121**(2): p. 345-353.

83. Elias P, *The skin barrier as an innate immune element.* Seminars in Immunopathology, 2007. **29**(1): p. 3-14.

84. Hachem J, Fowler A, Behne MJ, Fluhr J, Feingold KR, and Elias P, *Increased stratum corneum pH promotes activation and release of primary cytokines from the stratum corneum attributable to activation of serine proteases.* J Invest Dermatol, 2002. **119**: p. 258 (abstract).

85. Gunathilake R, Schurer NY, Shoo BA, Celli A, Hachem J-P, Crumrine D, Sirimanna G, Feingold KR, Mauro TM, and Elias PM, *pH-Regulated Mechanisms Account for Pigment-Type Differences in Epidermal Barrier Function.* J Invest Dermatol, 2009. **129**(7): p. 1719-1729.

86. Rawlings A and Harding C, *Moisturization and skin barrier function.* Dermatologic Therapy, 2004. **17**(s1): p. 43-48.

87. Levin J and Maibach H, *Human skin buffering capacity: an overview.* Skin Research and Technology, 2008. **14**(2): p. 121-126.

88. Lodén M, Andersson AC, Andersson C, Frödin T, Öman H, and Lindberg M, *Instrumental and dermatologist evaluation of the effect of glycerine and urea on dry skin in atopic dermatitis.* Skin Research and Technology, 2001. **7**(4): p. 209-213.

89. Nakagawa N, Sakai S, Matsumoto M, Yamada K, Nagano M, Yuki T, Sumida Y, and Uchiwa H, *Relationship Between NMF (Lactate and Potassium) Content and the Physical Properties of the Stratum Corneum in Healthy Subjects.* J Invest Dermatol, 2004. **122**(3): p. 755-763.

90. Choi EH, Man M-Q, Wang F, Zhang X, Brown BE, Feingold KR, and Elias PM, *Is Endogenous Glycerol a Determinant of Stratum Corneum Hydration in Humans?* J Invest Dermatol, 2005. **125**(2): p. 288-293.

91. Hara-Chikuma M and Verkman AS, *Aquaporin-3 functions as a glycerol transporter in mammalian skin.* Biol. Cell, 2005. **97**(7): p. 479-486.

92. Fluhr JW, Mao-Qiang M, Brown BE, Wertz PW, Crumrine D, Sundberg JP, Feingold KR, and Elias PM, *Glycerol Regulates Stratum Corneum Hydration in Sebaceous Gland Deficient (Asebia) Mice.* J Invest Dermatol, 2003. **120**(5): p. 728-737.

93. Holleran WM, Takagi Y, Imokawa G, Jackson S, Lee JM, and Elias PM, *beta-Glucocerebrosidase activity in murine epidermis: characterization and localization in relation to differentiation.* Journal of Lipid Research, 1992. **33**(8): p. 1201-9.

94. Walsh A and Chapman SJ, *Sugars protect desmosome and corneosome glycoproteins from proteolysis.* Archives of Dermatological Research, 1991. **283**(3): p. 174-179.

95. Sakai S, Yasuda R, Sayo T, Ishikawa O, and Inoue S, *Hyaluronan Exists in the Normal Stratum Corneum.* J Invest Dermatol, 2000. **114**(6): p. 1184-1187.

96. Maytin EV, Chung HH, and Seetharaman VM, *Hyaluronan Participates in the Epidermal Response to Disruption of the Permeability Barrier in Vivo.* Am J Pathol, 2004. **165**(4): p. 1331-1341.

97. Steinert PM, Cantieri JS, Teller DC, Lonsdale-Eccles JD, and Dale BA, *Characterization of a class of cationic proteins that specifically interact with intermediate filaments.* Proceedings of the National Academy of Sciences, 1981. **78**(7): p. 4097-4101.

98. Scott IR, Harding CR, and Barrett JG, *Histidine-rich protein of the keratohyalin granules: Source of the free amino acids, urocanic acid and pyrrolidone carboxylic acid in the stratum corneum.* Biochimica et Biophysica Acta (BBA) - General Subjects, 1982. **719**(1): p. 110-117.

99. Sandilands A, Sutherland C, Irvine AD, and McLean WHI, *Filaggrin in the frontline: role in skin barrier function and disease.* J Cell Sci, 2009. **122**(9): p. 1285-1294.

100. Bouwstra JA, Groenink HWW, Kempenaar JA, Romeijn SG, and Ponec M, *Water Distribution and Natural Moisturizer Factor Content in Human Skin Equivalents Are Regulated by Environmental Relative Humidity.* J Invest Dermatol, 2007. **128**(2): p. 378-388.

101. Caspers PJ, Lucassen GW, Carter EA, Bruining HA, and Puppels GJ, *In vivo confocal raman microspectroscopy of the skin: noninvasive determination of molecular concentration profiles.* J Invest Dermatol, 2001. **116**(3): p. 434-442.

102. Scott IR and Harding CR, *Filaggrin breakdown to water binding compounds during development of the rat stratum corneum is controlled by the water activity of the environment.* Developmental Biology, 1986. **115**(1): p. 84-92.

103. Jokura Y, Ishikawa S, Tokuda H, and Imokawa G, *Molecular Analysis of Elastic Properties of the Stratum Corneum by Solid-State 13C-Nuclear Magnetic Resonance Spectroscopy.* J Invest Dermatol, 1995. **104**(5): p. 806-812.

104. Walterscheid J, Nghiem D, Kazimi N, Nutt L, McConkey D, Norval M, and Ullrich S, *Cis-urocanic acid, a sunlight-induced immunosuppressive factor, activates immune suppression via the 5-HT$_{2A}$ receptor.* Proceedings of the National Academy of Sciences, 2006. **103**(46): p. 17420-17425.

105. McLoone P, Simics E, Barton A, Norval M, and Gibbs NK, *An action spectrum for the production of cis-urocanic acid in human skin in vivo.* J Invest Dermatol, 2005. **124**(5): p. 1071-1074.

106. Warner RR, Stone KJ, and Boissy YL, *Hydration Disrupts Human Stratum Corneum Ultrastructure.* J Invest Dermatol, 2003. **120**(2): p. 275-284.

107. Sylvestre JP, Bouissou C, Guy R, and Delgado-Charro MB, *Extraction and quantification of amino acids in human stratum corneum in vivo.* British Journal of Dermatology, 2010. **163**(3): p. 458-465.

108. Nguyen V, Ndoye A, Hall L, Zia S, Arredondo J, Chernyavsky A, Kist D, Zelickson B, Lawry M, and Grando S, *Programmed cell death of keratinocytes culminates in apoptotic secretion of a humectant upon secretagogue action of acetylcholine.* J Cell Sci, 2001. **114**(6): p. 1189-1204.

109. Harding CR and Scott I, *Alterations in the processing of human filaggrin following skin occlusion in vivo and in vitro.* Journal of investigative dermatology, 1993. **100**(4): p. 579.

110. Zhang X, Liu S, Chen X, Zhou B, Liu D, Lei G, Xiao X, Liu H, and Wang H, *Novel and recurrent mutations in the filaggrin gene in Chinese patients with ichthyosis vulgaris.* British Journal of Dermatology, 2010. **163**(1): p. 63-69.

111.   Cascella R, Cuzzola VF, Lepre T, Galli E, Moschese V, Chini L, Mazzanti C, Fortugno P, Novelli G, and Giardina E, *Full Sequencing of the FLG Gene in Italian Patients with Atopic Eczema: Evidence of New Mutations, but Lack of an Association.* J Invest Dermatol, 2011. **131**(4): p. 982-984.

112.   Muller S, Marenholz I, Lee Y, Sengler C, Zitnik S, Griffioen R, Meglio P, Wahn U, and Nickel R, *Association of filaggrin loss-of-function-mutations with atopic dermatitis and asthma in the Early Treatment of the Atopic Child (ETAC) population.* Pediatric Allergy and Immunology, 2009. **20**(4): p. 358-361.

113.   Sandilands A, O'Regan GM, Liao H, Zhao Y, Terron-Kwiatkowski A, Watson RM, Cassidy AJ, Goudie DR, Smith FJD, McLean WHI, and Irvine AD, *Prevalent and rare mutations in the gene encoding filaggrin cause ichthyosis vulgaris and predispose individuals to atopic dermatitis.* J Invest Dermatol, 2006. **126**(8): p. 1770-1775.

114.   Nomura T, Akiyama M, Sandilands A, Nemoto-Hasebe I, Sakai K, Nagasaki A, Palmer CNA, Smith FJD, McLean WHI, and Shimizu H, *Prevalent and rare mutations in the gene encoding filaggrin in Japanese patients with ichthyosis vulgaris and atopic dermatitis.* J Invest Dermatol, 2008. **129**: p. 1302-1305.

115.   Brown SJ and Irvine AD, *Atopic eczema and the filaggrin story.* Seminars in Cutaneous Medicine and Surgery, 2008. **27**(2): p. 128-137.

116.   Chen H, Ho JCC, Sandilands A, Chan YC, Giam YC, Evans AT, Lane EB, and McLean WHI, *Unique and recurrent mutations in the filaggrin gene in Singaporean Chinese patients with ichthyosis vulgaris.* J Invest Dermatol, 2008. **128**(7): p. 1669-1675.

117.   Kezic S, Kemperman PMJH, Koster ES, de Jongh CM, Thio HB, Campbell LE, Irvine AD, McLean IWH, Puppels GJ, and Caspers PJ, *Loss-of-Function mutations in the filaggrin gene lead to reduced level of natural moisturizing factor in the stratum corneum.* J Invest Dermatol, 2008. **128**(8): p. 2117-2119.

118.   Takahashi M and Tezuka T, *The content of free amino acids in the stratum corneum is increased in senile xerosis.* Archives of Dermatological Research, 2004. **295**(10): p. 448-452.

119.   Novak N, Baurecht H, Schafer T, Rodriguez E, Wagenpfeil S, Klopp N, Heinrich J, Behrendt H, Ring J, Wichmann E, Illig T, and Weidinger S, *Loss-of-function mutations in the filaggrin gene and allergic contact sensitization to nickel.* J Invest Dermatol, 2007. **128**(6): p. 1430-1435.

120. Kezic S, O'Regan GM, Yau N, Sandilands A, Chen H, Campbell LE, Kroboth K, Watson R, Rowland M, Irwin McLean WH, and Irvine AD, *Levels of filaggrin degradation products are influenced by both filaggrin genotype and atopic dermatitis severity.* Allergy, 2011: p. 934-940.

121. Denecker G, Ovaere P, Vandenabeele P, and Declercq W, *Caspase-14 reveals its secrets.* J. Cell Biol., 2008. **180**(3): p. 451-458.

122. Ginger R, Blachford S, Rowland J, Rowson M, and Harding C, *Filaggrin repeat number polymorphism is associated with a dry skin phenotype.* Archives of Dermatological Research, 2005. **297**(6): p. 235-241.

123. Howell MD, Kim BE, Gao P, Grant AV, Boguniewicz M, DeBenedetto A, Schneider L, Beck LA, Barnes KC, and Leung DYM, *Cytokine modulation of atopic dermatitis filaggrin skin expression.* Journal of Allergy and Clinical Immunology, 2009. **124**(3, Supplement 2): p. R7-R12.

124. Scott IR, *Alterations in the Metabolism of Filaggrin in the Skin After Chemical- and Ultraviolet-Induced Erythema.* J Invest Dermatol, 1986. **87**(4): p. 460-465.

125. Rossmiller JD and Hoekstra WG, *Hexadecane-Induced Hyperkeratinization of Guinea Pig Skin.* The Journal of Investigative Dermatology, 1966. **47**(1): p. 44-48.

126. Denda M, Hori J, Koyama J, Yoshida S, Nanba R, Takahashi M, Horii I, and Yamamoto A, *Stratum corneum sphingolipids and free amino acids in experimentally-induced scaly skin.* Archives of Dermatological Research, 1992. **284**(6): p. 363-367.

127. Visscher M, Robinson M, and Wickett R, *Stratum corneum free amino acids following barrier perturbation and repair.* International Journal of Cosmetic Science, 2011. **33**(1): p. 80-89.

128. Takahashi M and Ikezawa Z, *Dry skin in atopic dermatitis and patients on hemodialysis.* Dry skin and moisturizers:chemistry and function. 1999: Informa healthcare.

129. Horii I, Nakayama Y, Obata M, and Tagami H, *Stratum corneum hydration and amino acid content in xerotic skin.* British Journal of Dermatology, 1989. **121**(5): p. 587-592.

130. Jacobson TM, Yuksel KU, Geesin JC, Gordon JS, Lane AT, and Gracy RW, *Effects of Aging and Xerosis on the Amino Acid Composition of Human Skin.* J Invest Dermatol, 1990. **95**(3): p. 296-300.

131. Pinkus H, *Examination of the epidermis by the strip method.* The Journal of Investigative Dermatology, 1952. **19**(6): p. 431-447.

132. Alberti I, Kalia YN, Naik A, and Guy RH, *Assessment and prediction of the cutaneous bioavailability of topical terbinafine, in vivo, in man.* Pharmaceutical Research, 2001. **18**(10): p. 1472-1475.

133. Shah VP, Flynn GL, Yacobi A, Maibach HI, Bon C, Fleischer NM, Franz TJ, Kaplan SA, Kawamoto J, Lesko LJ, Marty J-P, Pershing LK, Schaefer H, Sequeira JA, Shrivastava SP, Wilkin J, and Williams RL, *Bioequivalence of topical dermatological dosage forms-methods of evaluation of bioequivalence.* Pharmaceutical Research, 1998. **15**(2): p. 167-171.

134. Kondo H, Ichikawa Y, and Imokawa G, *Percutaneous sensitization with allergens through barrier-disrupted skin elicits a Th2-dominant cytokine response.* European Journal of Immunology, 1998. **28**(3): p. 769-779.

135. Russell LM, Wiedersberg S, and Delgado-Charro MB, *The determination of stratum corneum thickness An alternative approach.* European Journal of Pharmaceutics and Biopharmaceutics, 2008. **69**(3): p. 861-870.

136. Pirot F, Berardesca E, Kalia YN, Singh M, Maibach HI, and Guy RH, *Stratum Corneum Thickness and Apparent Water Diffusivity: Facile and Noninvasive Quantitation In Vivo.* Pharmaceutical Research, 1998. **15**(3): p. 492-494.

137. Obata Y, Utsumi S, Watanabe H, Suda M, Tokudome Y, Otsuka M, and Takayama K, *Infrared spectroscopic study of lipid interaction in stratum corneum treated with transdermal absorption enhancers.* International Journal of Pharmaceutics, 2010. **389**(1-2): p. 18-23.

138. Jain AK, Thomas NS, and Panchagnula R, *Transdermal drug delivery of imipramine hydrochloride.: I. Effect of terpenes.* Journal of Controlled Release, 2002. **79**(1-3): p. 93-101.

139. Bommannan D, Potts RO, and Guy RH, *Examination of Stratum Corneum Barrier Function In Vivo by Infrared Spectroscopy.* J Invest Dermatol, 1990. **95**(4): p. 403-408.

140. Krafft C, Steiner G, Beleites C, and Salzer R, *Disease recognition by infrared and Raman spectroscopy.* Journal of Biophotonics, 2009. **2**(1-2): p. 13-28.

141. Greve TM, Andersen KB, and Nielsen OF, *ATR-FTIR, FT-NIR and near-FT-Raman spectroscopic studies of molecular composition in human skin in vivo and pig ear skin in vitro.* Spectroscopy, 2008. **22**(6): p. 437-457.

142. González FJ, Alda J, Moreno-Cruz B, Martínez-Escanamé M, Ramírez-Elías MG, Torres-Álvarez B, and Moncada B, *Use of Raman spectroscopy for the early detection of filaggrin-related atopic dermatitis.* Skin Research and Technology, 2011. **17**(1): p. 45-50.

143. Kunii T, Hirao T, Kikuchi K, and Tagami H, *Stratum corneum lipid profile and maturation pattern of corneocytes in the outermost layer of fresh scars: the presence of immature corneocytes plays a much more important role in the barrier dysfunction than do changes in intercellular lipids.* British Journal of Dermatology, 2003. **149**(4): p. 749-756.

144. Mohammed D, Matts PJ, Hadgraft J, and Lane ME, *Influence of Aqueous Cream on corneocyte size, maturity, skin protease activity, protein content and Trans-Epidermal Water Loss.* British Journal of Dermatology, 2011. **164**(6): p. 1304-1310.

145. Weerheim A and Ponec M, *Determination of stratum corneum lipid profile by tape stripping in combination with high-performance thin-layer chromatography.* Archives of Dermatological Research, 2001. **293**(4): p. 191-199.

146. Popa I, Thuy L, Colsch B, Pin D, Gatto H, Haftek M, and Portoukalian J, *Analysis of free and protein-bound ceramides by tape stripping of stratum corneum from dogs.* Archives of Dermatological Research, 2010. **302**(9): p. 639-644.

147. De Jongh CM, Verberk MM, Spiekstra SW, Gibbs S, and Kezic S, *Cytokines at different stratum corneum levels in normal and sodium lauryl sulphate-irritated skin.* Skin Research and Technology, 2007. **13**(4): p. 390-398.

148. Sylvestre JP, Bouissou CC, Guy RH, and Delgado-Charro MB, *Extraction and quantification of amino acids in human stratum corneum in vivo.* British Journal of Dermatology, 2010. **163**(3): p. 458-465.

149. Phipps J and Gyory JR, *Transdermal ion migration.* Advanced Drug Delivery Reviews, 1992. **9**(2-3): p. 137-176.

150. Leboulanger B, Guy RH, and Delgado-Charro MB, *Reverse iontophoresis for non-invasive transdermal monitoring.* Physiological Measurement, 2004. **25**(3): p. R35.

151. Guy RH, Kalia YN, Delgado-Charro MB, Merino V, López A, and Marro D, *Iontophoresis: electrorepulsion and electroosmosis.* Journal of Controlled Release, 2000. **64**(1-3): p. 129-132.

152. Russell OP, Janet AT, and Michael JT, *Glucose monitoring by reverse iontophoresis.* Diabetes/Metabolism Research and Reviews, 2002. **18**(S1): p. S49-S53.

153. Sieg A, Guy RH, and Delgado-Charro MB, *Noninvasive glucose monitoring by reverse iontophoresis in vivo: application of the internal standard concept.* Clin Chem, 2004. **50**(8): p. 1383-1390.

154. Sieg A, Guy RH, and Delgado-Charro MB, *Simultaneous extraction of urea and glucose by reverse iontophoresis in vivo.* Pharmaceutical Research, 2004. **21**(10): p. 1805-1810.

155. Nixon S, Sieg A, Delgado-Charro MB, and Guy RH, *Reverse iontophoresis of L-lactate: In vitro and in vivo studies.* Journal of Pharmaceutical Sciences, 2007. **96**(12): p. 3457-3465.

156. Wascotte V, Caspers P, de Sterke J, Jadoul M, Guy R, and Préat V, *Assessment of the "skin reservoir" of urea by confocal raman microspectroscopy and reverse iontophoresis in vivo.* Pharmaceutical Research, 2007. **24**(10): p. 1897-1901.

157. Sieg A, Jeanneret F, Fathi M, Hochstrasser D, Rudaz S, Veuthey J-L, Guy RH, and Delgado-Charro MB, *Extraction of amino acids by reverse iontophoresis in vivo.* European Journal of Pharmaceutics and Biopharmaceutics, 2009. **72**(1): p. 226-231.

Chapter 1: Stratum corneum competence and atopic dermatitis

Abstract

Atopic dermatitis (AD) is one of the most common inflammatory skin diseases. The cause of AD is multifactoral and it is affected by both genetic and environmental factors. It is believed that an impaired barrier function is crucial in the development of AD. In this chapter, structural changes of the stratum corneum (SC) observed in AD, that may lead to comprised barrier function, are explained.

Out of all the causes of potential barrier defects, lowered amino-acid derived natural moisturizing factors (NMF) in the SC, especially those associated with filaggrin mutation, show the strongest links to AD. As a result, quantification of NMF in the SC in both healthy and comprized SC is the main aim of this thesis.

The ultimate goal of this project is to characterize skin barrier function using different bioengineering methods that may underpin a non-invasive technology to identify infants with predisposition to a defective skin barrier.

1. Introduction

1.1 Atopic dermatitis (AD)

Atopic dermatitis (AD) or eczema is the most common childhood inflammatory skin disease [1]. It often begins in infancy or early childhood, with ~90% of cases appearing in the first 5 years of life. The hallmarks of AD are a chronic, relapsing form of skin inflammation, an impaired barrier function that causes dry skin and, in a more severe form, increased immunoglobulin E (IgE) levels, reflecting sensitization to allergens.

Patients with eczema report lower quality of life than that of the general population [1]. The sleeplessness associated with itching affects over 60% of children [1-2]. Lack of sleep affects the whole family and leads to poor performance at school and work. In addition to the physiological difficulties, children with AD have higher rates of psychological abnormalities, including behavioural problems, clinginess and fearfulness, while mothers have reported a decrease in employment outside the home, poor social support and stress about parenting [3]. Compared to other chronic childhood diseases, parents rated eczema as worse for children than having insulin dependent diabetes and the direct financial cost in caring for a child with moderate to severe eczema is higher than that for the average child with asthma, and is similar to that for diabetes [4].

In comparison to the difficulties in managing the chronic disease, the treatment of mild and moderate eczema is simple. It is based on daily application of emollients, with or without antibacterial ingredients, accompanied by symptomatic anti-inflammatory therapy consisting of topical glucocorticosteroids or topical calcineurin inhibitors on an 'as needed' basis [5]. Although systemic treatments are required for severe diseases, most patients are able to control the disease with simple regimes.

1.1.1 Development of AD

Traditionally eczema has been divided into extrinsic AD characterised by an elevated IgE level and a non-IgE associated form called intrinsic AD. However, it is recognized that there is a transient form of AD with a low level of IgE or without any detectable sensitization but which develops increased levels of IgE and sensitization later on in life [6]. Some patients even go on to develop sensitisation to self-proteins or to skin bacteria [7]. Accordingly,

Bieber [8] hypothesised that three phases exist in the natural history of AD as shown in Figure 1.
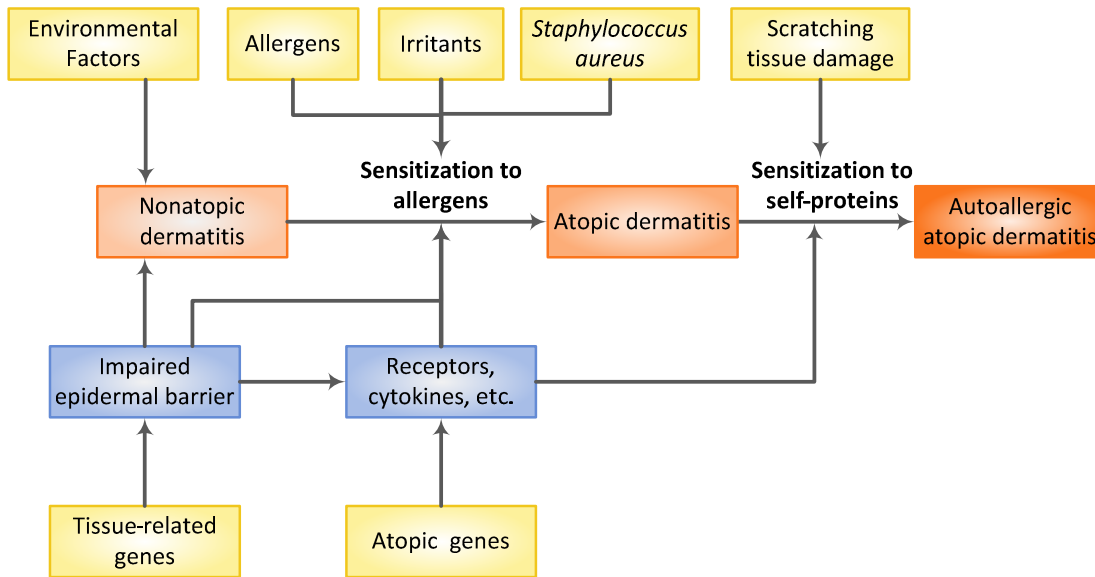

Figure 1: Gene-gene and gene-environment interactions in natural history of AD (Redrawn from Bieber [8])

The initial phase is the development of non-atopic dermatitis with genetic mutations causing impaired barrier function. Then, atopic gene pre-disposition and environmental factors lead to sensitization and development of AD. Finally, scratching causes the release of self-proteins in skin and further skin barrier damage leads to autoallergic atopic dermatitis.
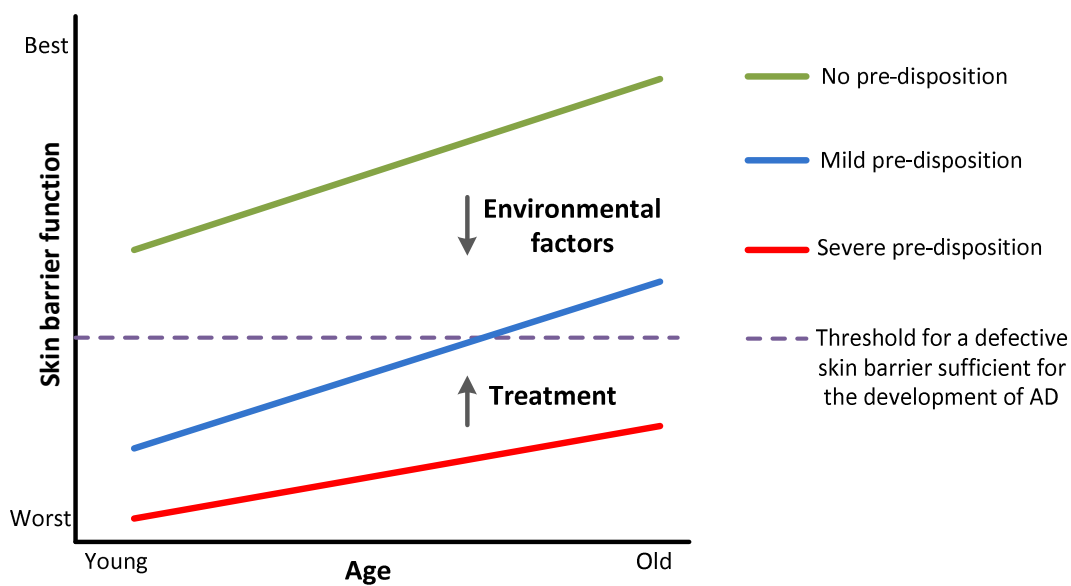

Figure 2: Skin barrier function in arbitrary units as a function of the age. (Redrawn from Cork [9])

Recently，an alternative hypothesis [9] (Figure 2) has been suggested for the early progression of AD. In children, who do not have a genetic pre-disposition to a defective skin barrier (green line), their condition is worse at birth and then improves with time. Most importantly, it is always above the threshold for the signs and symptoms of AD to be seen. However, children with a pre-disposition (blue and red lines) have this profile shifted downward by an amount which is dependent on the severity of the combined genetic mutations. In the majority of cases, the natural improvement of skin barrier function with age may be sufficient to achieve complete remission (blue line). The skin barrier profile can also be adjusted upwards by effective treatment, whereas undesirable environmental factors have the opposite effect. Several environmental factors have been associated with AD, including use of soaps and detergents, washing with hard water, and exposure to house dust mites and food allergens [9-13]. As those are modifiable factors, it follows that identification of children with a genetic pre-disposition may allow the undesirable environmental factors to be avoided or substantially reduced. Nevertheless, like the first scenario, the importance of genetic pre-disposition of impaired barrier function in the development of AD is highlighted.

1.1.2 The atopic march

The sequential development of the manifestations of AD during early childhood is often referred to as the atopic march. Several longitudinal studies [14-17] have provided evidence for the progression from AD to the development of asthma and allergic rhinitis. A more recent study [18] has demonstrated that early AD is associated with asthma; in particular, infants with eczema and wheeze have a marked loss of lung function and subsequently develop asthma at school age. The results suggest a distinct phenotype of AD leading to asthma. Since the identification of filaggrin gene mutations as an important risk factor for AD, several studies [19-21] have confirmed that AD patients with these mutations have increased risk of developing asthma and allergic rhinitis in the later years. Thus, by identifying this phenotype of AD associated with filaggrin mutations, prevention of asthma and allergic rhinitis may also be possible.

1.2 Structure of the skin

The skin is one of the largest organs of the body, and functions as a protective and regulatory barrier between the body and the external environment. As illustrated in Figure 3, it consists of two principal layers, the dermis and the epidermis, separated by the basal lamina.

The dermis is highly vascularised and includes dermal fibroblasts, nerve endings, sebaceous glands and sweat glands. It plays an important role in the regulation of temperature, pressure, pain, and provides nutritive and immune support to the epidermis [22].
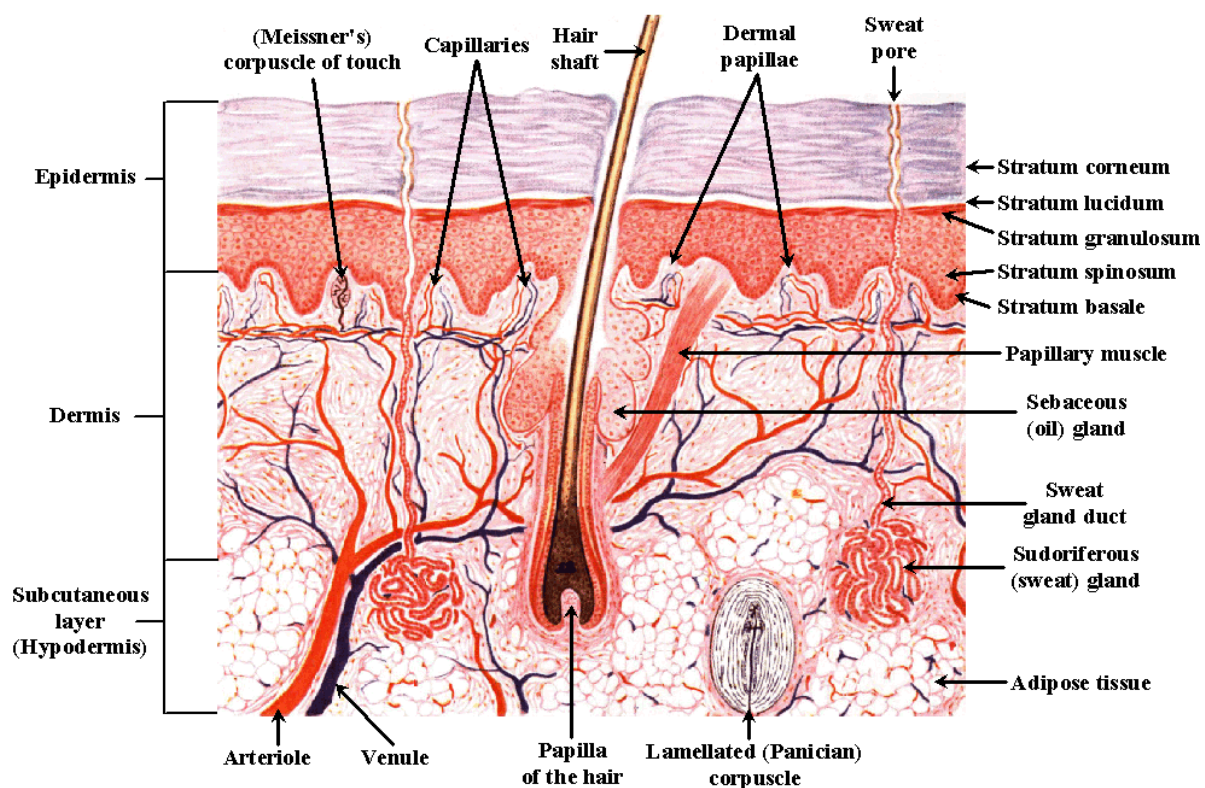
Figure 3: Structure of the skin [23]

The epidermis, the outer layer interacting with the environment, is the major protective layer. The stratified epidermis, which is essentially composed of keratinocytes, can be further divided into four distinct layers: stratum basale, stratum spinosum, stratum granulosum and stratum corneum (SC). The keratinocytes originate from epidermal stem cells in stratum basale and undergo continuous differentiation during the course of migration upwards through spinosum and granulosum layers. Finally, SC, the outermost layer of epidermis, is composed of corneocytes (terminally differentiated keratinocytes)

and intercellular lipid lamellae (predominately secreted from lamellar granules during the final differentiation of keratinocytes) [24-25]. With respect to the body's first line of defence against external assault by foreign substances, the SC is the most relevant.

1.2.1 Stratum corneum structure

The SC is the skin main barrier to the penetration of irritants and allergens. It consists of corneocytes, flattened dead cells endowed with a cornified envelope (CE), analogous to bricks, and the intercellular lipid lamellae acting as mortar. Corneocytes are also strongly bound to each other by corneodesmosomes, the intercellular junctions of the SC, providing a strong mechanical protection to the epidermis. Alterations of the barrier causing increased water loss through the skin are the hallmark of AD. The alterations are complex and multifactorial.

1.2.2 Cornified envelopes (CE)

The CE is the final product of terminal differentiation of keratinocytes (KC); it is marked by the replacement of the KC plasma membrane with an insoluble protein layer [26] composed of loricrin, involucrin, filaggrin and small proline-rich proteins, which are cross-linked by transglutaminases.

The surface of the CE is coated with a monolayer of covalently bound ω-hydroxyceramides and fatty acids forming a lipid envelope, which by providing a hydrophobic surface is thought to play an essential role in the interaction with intercellular lipid matrix. The amount of protein-bound ω-hydroxyceramides in healthy epidermis comprises around 50% w/w of total protein-bound lipids, whereas this percentage decreases to 23-28% w/w in non-lesional areas and down to 10-25% w/w in affected areas in AD with a correlated increase in protein-bound ω-hydroxyl fatty acids [27] This change could generate a charged CE surface which may affect its interaction with intercellular lipid lamellae.

Recent research has also focused on corneocyte structure itself. The surface area of corneocytes is inversely correlated with transepidermal water loss (TEWL) [28-29], logical result of a longer pathlength for diffusion. A reduced corneocyte surface area in clinically asymptomatic skin in AD has indeed been reported [30-31]. Moreover, the identification of two distinct, so-called "fragile" (immature) and "rigid" (mature), corneocyte populations suggests a gradual modification of the corneocyte protein structure mediated by

transglutaminase [32-33]. Furthermore, immature corneocytes are detected in the surface SC of involved areas of AD, but not in uninvolved sites [34], highlighting at least in part the importance of incompletely mature corneocytes to impaired barrier function.

1.2.3 Stratum corneum lipid lamellae

Corneocytes are surrounded by lipid lamellae, composed of ceramides, cholesterol, fatty acids and cholesterol esters. These substances prevent the transepidermal loss of water and the penetration of exogenously applied materials [9]. As mentioned previously, the lipids are synthesized and stored in lamellar granules, which are then extruded into the extracellular space in the upper granular layer during cornification [25]. Disturbed maturation and delivery of the lamellar granules [35] and reduced levels of ceramides, especially ceramide 1 (also known as CER[EOS]), in AD have been reported [36-39]. This reduction in ceramides is, at least in part, a result of modified enzyme activities associated with ceramide production. In AD, prosaposin, a sphingolipid activator protein that facilitates the synthesis of ceramides is reduced [40] while, conversely, sphingomyelin deacylase, an enzyme that competes for ceramide precursors is over-expressed [41].

In recent years, ceramides, which constitute approximately 50% w/w of the SC lipids [42], have been the subject of most interest. In fact, 11 classes of ceramides have now been identified and named according to their fatty acid and sphingoid structures (Table 1). The average chain length of ceramides has been suggested as a possible marker of AD. As well as a reduced total ceramides level, ceramides profiling in AD patients showed an increase species with <40 total carbon atoms (e.g. CER[NS], CER[NDS], and CER[AS]), and a decrease in the level of larger species (>50 total carbon atoms, e.g. CER[NS], CER[NDS], CER[NH], CER[AS], and CER[AH]) [43].

SC barrier function is also influenced by lipid-packing, which appears to exist as a balance between orthorhombic (a solid crystalline state) and hexagonal (gel) states [44]. Orthorhombically packed lipids are required to produce a better barrier [45]. In patients with AD and lamellar ichthyosis, an decrease in orthorhombic packing has been found [46-47] and it is probably associated with a reduced level of CER[EOS], since the absence of this compound in lipid mixtures results in a predominantly hexagonal phase [48].
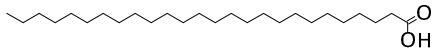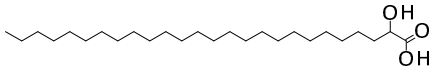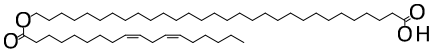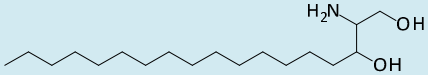
Fatty acid / Sphingoid	Non-hydroxy fatty acid [N]	α-Hydroxy fatty acid [A]	Esterified ω-hydroxy fatty acid [EO]
Dihydrosphingosine [DS]	CER[NDS]	CER[ADS]	Unidentified
Sphingosine [S]	CER[NS]	CER[AS]	CER[EOS]
6-Hydroxy sphingosine [H]	CER[NH]	CER[AH]	CER[EOH]
Phytosphingosine [P]	CER[NP]	CER[AP]	CER[EOP]

Table 1: Eleven classes ceramides identified in human stratum corneum [43]

1.2.4   Stratum corneum desquamation

The maintenance of SC formation and function lies in the balance between epidermal cell differentiation and desquamation events [49]. The latter is tightly controlled by a complex mixture of proteases and protease inhibitors, the action of which controls the integrity of corneodesmosomes. Various serine, cysteine, and aspartic acid proteases have been detected in the SC [50-52]. Among them, kallikrein (KLK) related serine peptidases are the key proteases, including KLK5 and KLK14 which contribute to the principal trypsin-like activity, while KLK7 accounts for the SC chymotrypsin-like activity [53]. The activated proteases target corneodesmosome proteins and are regulated by serine protease inhibitors, for example KLK7 is inhibited by secretory leukocyte protease inhibitor, elafin and lymphoepithelial Kazal-type 5 serine protease inhibitor (LEKTI); on the other hand, trypsin-like KLKs are only inhibited by LEKTI [54].

Epidermal KLKs are implicated in many protective physiological processes in human SC, as well in regulating skin desquamation. Their functions involve activating proinflammtory cytokines, e.g. IL-1β [55], regulating innate immune responses through cathlicidin activation [56], degradation of lipid processing enzymes [57] and modifying proteinase-activated receptor (PAR) activities, which in turn affects cell differentiation, proliferation and inflammation [58].

Given the importance of these proteases, most research has focused on their activity at different body sites and in diseased skin. The levels of KLK5 and another tryptase-like enzyme, but not KLK7, were found to be elevated in cheek compared to forearm [59]. Although a reduced activity of trypsin-like activity was described originally in non-eczematous AD skin [60], recent reports demonstrated an increase in serine protease activity in atopic skin [61-62], and the latter is consistent with an increase in multiple tissue kallikrein mRNAs in AD [63].

The most convincing evidence so far that established the link between excessive serine protease activity and impaired skin barrier function comes from the understanding of Netherton syndrome (NS). NS is a rare but severe form of ichthyosis caused by mutation in the SPINK5 gene, which encodes LEKTI [64]. For this reason, NS patients present with uncontrolled serine protease degradation of corneodesmosomes, implying that LEKTI plays a vital role in maintaining skin barrier function. However, the relevance of these findings to

AD is inconclusive. Two studies demonstrated significant association [65-66], which failed to be replicated [67]. In a more recent study, it was found that the SPINK5 mutation only associated when maternally inherited and was not a major contributor for AD [68]. This is probably because these studies only considered certain mutation polymorphisms; other variants may be of greater importance for eczema.

Nevertheless, exogenous proteases generated by house dust mites and *S. aureus* have been associated with AD exacerbation and may even trigger AD [69-71], further confirming the role of protease over-expression in weakening the skin barrier.

1.2.5 Epidermal pH

pH is defined as a negative decimal logarithm of the hydrogen ion activity in a solution [72]. Therefore, the nature of pH in the dense, lipid-, and protein-rich SC, which is largely devoid of water, remains to be defined. Nevertheless, the acidic character of skin's outer surface has been documented many years ago [73]. It was traditionally measured by glass electrodes [74-76]. Recently new high resolution microscopic techniques have been developed to probe the SC pH depth profile [77-78] and led to the understanding of "acid mantle" formation.

Two-photon fluorescence lifetime imaging has the ability to measure skin pH at both inter- and intra-corneocyte level [78]. It revealed the importance of a nonenergy-dependent sodium-proton exchanger (NHE1) in the generation of acidic extracellular domains of the lower SC [79]. In addition to NHE1, another two endogenous pathways have been identified as potential contributors of SC acidity: 1) secretory phospholiase A_2 ($sPLA_2$) generation of free fatty acids from phospholipids [80]; and 2) presence of acidic amino acid derivatives in SC [81], such as urocanic acid and pyrrolidone carboxylic acid.

The importance of skin's acidic character has been recognized as playing a crucial role in regulating several key protective functions of the skin, including permeability barrier homeostasis, SC integrity and cohesion [80, 82], antimicrobial defence [83] and cytokine activation [84-85]. The proposed mechanistic consequences of SC pH alteration is summarised in Figure 4. In order to explore the importance of SC pH, topical applications of superacids and superbases are used. By definition, superacids and superbases are at least an order of magnitude more acidic or more basic than 1N H_2SO_4 and 1N NaOH and their naphthalene structure favours absorption throughout the SC; they are therefore used to

manipulate SC pH even in very low concentrations [82]. Regular topical application of superacids successfully prevented emergence of murine atopic dermatitis and it thus highlighted the importance of the acidic SC in maintaining healthy skin barrier function [76].
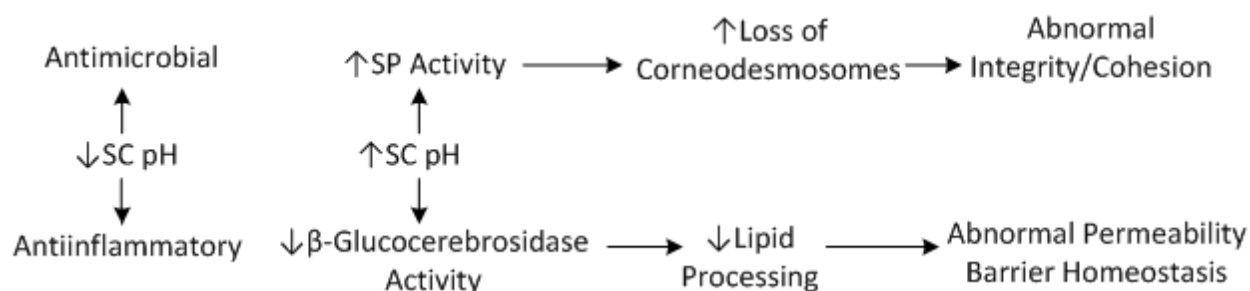

Figure 4: Mechanistic consequences in response to change in SC pH (Redrawn from Hachem [82])

1.2.6 Stratum corneum natural moisturizing factor (NMF) and filaggrin

<u>NMF and its origin</u>

NMF (Table 2), found exclusively in the SC, is a collection of water-soluble, low molecular weight compounds, comprising approximately 20%-30% of corneocyte dry weight [86].

Table 2: Chemical composition of natural moisturizing factor (From Rawlings [86])

Compounds	Composition (% w/w)
Free amino acids	40
Pyrollidone carboxylic acid (PCA)	12
Lactate	12
Sugars	8.5
Urea	7
Chloride	6
Sodium	5
Potassium	4
Ammonia, uric acid, glucosamine and creatine	1.5
Calcium	1.5
Magnesium	1.5
Phosphate	0.5

Citrate and formate	0.5

NMF acts as extremely efficient humectants by absorbing moisture and then dissolving in its own water of hydration. It is believed to be critical in maintaining the hydration of the skin despite the desiccating action of the environment [87]. Some NMF components, such as urea, lactate and glycerol, are either partially secreted from sweat glands or derived from sebaceous glands. Their importance in skin hydration has long been recognized [88-92] and hence their presence in various commercially available moisturizing products. The presence of sugars in the SC is probably due to the release of glucose from glucosylceramides during the final processing of intercellular lipid lamellae [93] or as by-products released from the degradation of desmosomes and corneodesmosomes [94]. More recently, hyaluronic acid has also been considered be part of NMF [95] and suggested to participate in the epidermal response to barrier injury [96].

However, the majority of the NMF composes free amino acids, which are primarily derived from filaggrin. Filaggrin was first known as a keratin intermediate filament (KIF) associated protein that aggregated epidermal keratin filaments *in vitro* [97]. It is synthesized from profilaggrin (Figure 5), an approximately 500-kDa insoluble, highly basic, heavily phosphorylated, histidine-rich protein, consisting of 10 to 12 repeating filaggrin units [86, 98]. During the transition of the mature granular cell into a corneocyte, rapid dephosphorylation of pro-filaggrin occurs, yielding filaggrin (Figure 6) [86]. Filaggrin monomers, which do not persist beyond the two to three deepest layers of the SC, facilitate the aggregation of KIF and attach to KIF through the formation of salt bridges between positively-charged arginine and histidine residues on filaggrin and the negative charges on KIF [26]. As corneocytes proceed upwards through the SC, deiminiation and then complete proteolysis of filaggrin yields free amino acids and its derivatives, which are known collectively as the amino-acid-derived components of NMF (Figure 6).
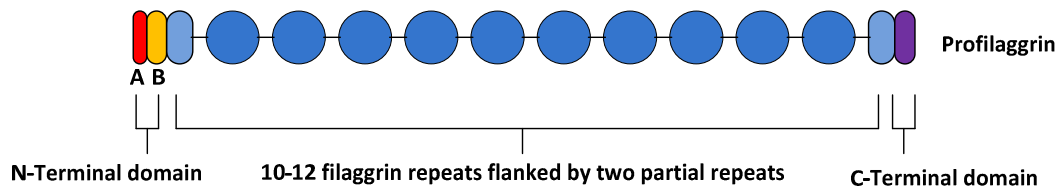
Figure 5: Profilaggrin protein structure (Adapted from Sandilands et al [99]). Profilaggrin is expressed as a polyprotein that contains a variable number (10-12) of near-identical filaggrin repeats (blue circle), which are flanked on either side by partial, imperfect filaggrin repeats (light blue oval). Each repeat is separated by a linker. It also includes N-terminal and C-terminal domains (purple oval) at each end. The N-terminal domain can be subdivided into two distinct subdomains: the A domain (red) containing two Ca^{2+}-binding motifs and a cationic B domain (orange).
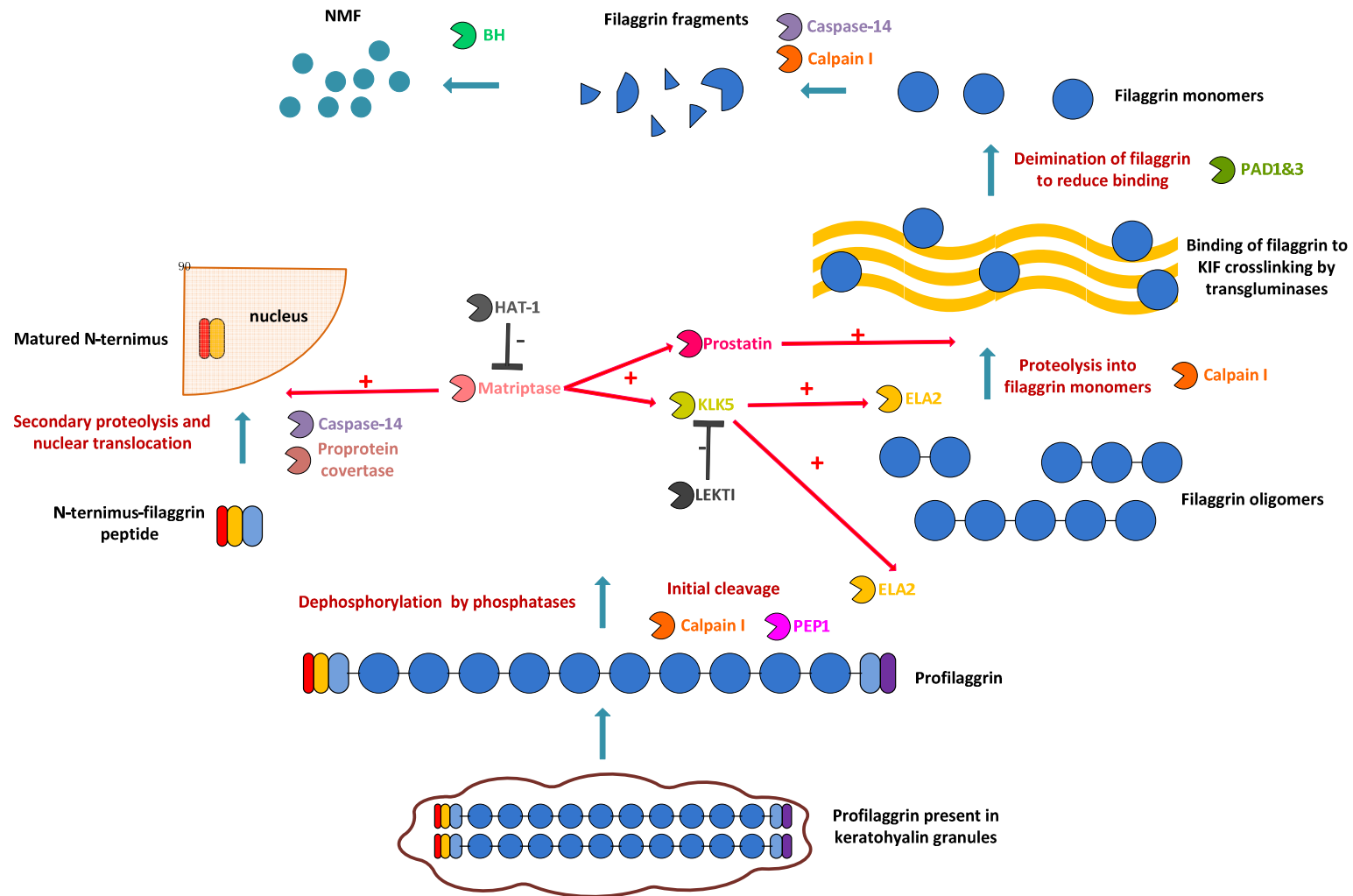
Figure 6: Processing of profilaggrin by currently identified proteases. Profilaggrin is synthesized and stored in keratohyalin granules in keratinocytes. During the formation of cornified envelope, profilaggrin is dephosphorylated and proteolytically processed into filaggrin monomers, which aid in the bundling of keratin intermediate filaments (KIF). Subsequently, filaggrin is deiminated, causing its release from keratin and allowing its degradation into free hygroscopic amino acids that act as components of NMF.

The functional effects of the amino-acid derived components of NMF on the SC have been studied. The primary role of NMF is to keep SC hydrated and the corneocytes that possess the highest concentration of NMF retain more water [86]. It is fascinating that, under extreme humidity conditions, the corneocytes take up free water and swell tremendously in the vertical direction (i.e., resulting mainly in an increase in cell thickness). However, the magnitude of this hydration is higher in the central region of the SC than that in the superficial and deeper regions [48, 100]. This observation is in excellent agreement with the concentration of amino-acid derived NMF, that appears to be maximal in the mid-SC [101]. The low level of NMF in the deeper SC is probably because little degradation of filaggrin is programmed in the well-hydrated conditions found here [102]; in contrast, daily washing likely leads to less NMF in the superficial SC. The absence of swelling in the deeper SC suggests that no free water is present thereby preventing dehydration of the adjacent viable epidermis. However, whether this is solely due to low NMF level cannot be unambiguously concluded, since it is also possible that the corneocytes in this region are simply less permeable to water. Nonetheless, by keeping the SC hydrated, NMF encourages critical biochemical events; most importantly, the activation of several proteases requires moisture for their functions that subsequently leads to the generation of NMF itself [86] .

Furthermore, the presence of free amino acids, especially zwitterionic and basic species, also provides specific ionic interactions with KIF, that are crucial to the maintenance of SC elasticity and its plasticization [103]. Moreover, trans-urocanic acid (t-UA), a deamination product of histidine, undergoes a photoisomerisation reaction under ultra-violet (UV) light to cis-urocanic acid (c-UA). This process helps to prevent UV damage and may contribute to UV light-induced immunosuppression [104-105].
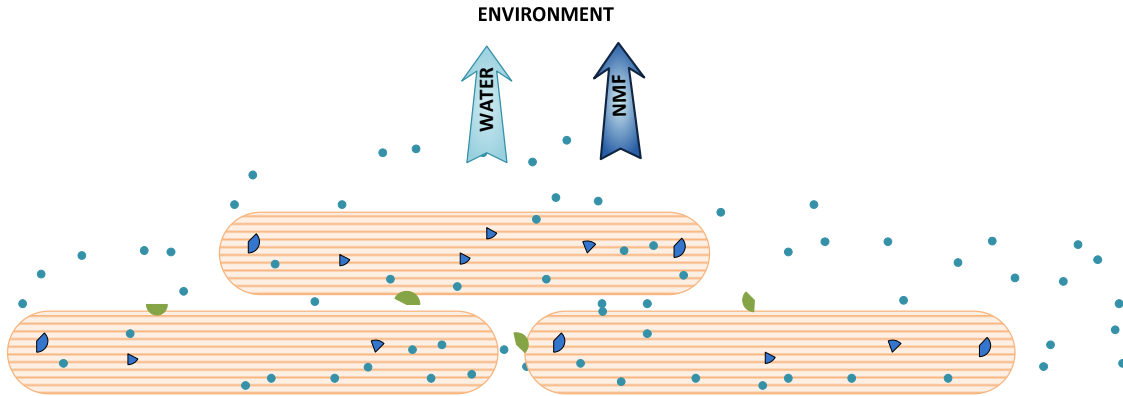
Filaggrin and its degradation products have traditionally been thought to be inside the corneocytes, since transitional cells during cornification become filled with homogenous keratohyaline masses (associated with profilaggrin) and the immunoreactivity of filaggrin is detectable mainly in the cytoplasm. However, the presence of NMF in the intercellular space is evident. After incubation with water, water pools can be observed in the intercellular spaces [100, 106], possibly indicating the presence of osmolytes outside the corneocytes. The latter may be formed during corneodesmosomes breakdown and via concomitant leaching of osmolytes from corneocytes.

In addition, passive extraction of SC *in vivo* with water can extract extensive amounts quite rapidly which seems inconsistent with all the material being located intra-corneocyte [107]. This idea is supported by an observation of the corneocyte volume lost during final differentiation *in vivo* and that filaggrin-positive keratohyaline material, lysosomes, mitochondria, glycogen granules and parts of endoplasmic reticulum were extruded into intercellular spaces during the granular cell to corneocyte transition [108]. Accordingly, two types of NMF were proposed: 'internal' NMF, which is present in the SC, and 'external' NMF, which fills the intercellular spaces of living epidermis.

There could be another explanation for the intercellular NMF as illustrated in Figure 7. The immature corneocytes at the bottom of SC are not permeable to water, thus have low swelling properties even under extreme hydration. When corneocytes move upwards the surface of the SC, they become more permeable to water and NMF; the middle section of the SC hence has the highest swelling properties. Once the corneocytes reach the surface of the SC, they become fully permeable, and thus lose their swelling and barrier properties.
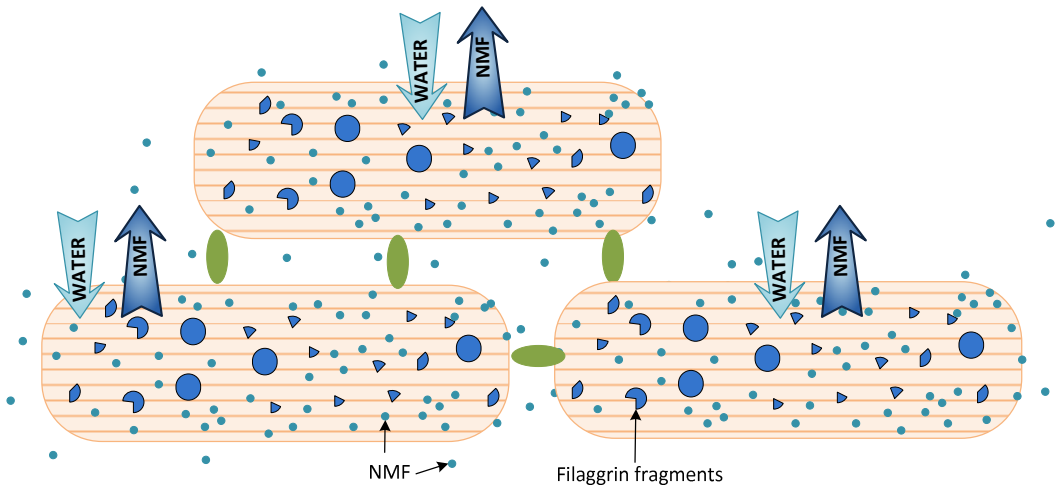
Surface-SC

Corneocytes become fully permeable leading to the loss of both water and NMF into the environment.

Mid-SC

Corneocytes become permeable to both water and NMF. Reduction in humidity initiates filaggrin degradation and hence the level of NMF inside the corneocytes increases. This in turn introduces SC swelling by attracting water into the corneocytes. On the other hand, NMF slowly diffuses into intercellular spaces owing to a concentration gradient.

Deeper-SC

Corneocytes are impermeable to water thereby preventing dehydration of adjacent viable epidermis. Little degradation of filaggrin occurs due to highly humid condition.
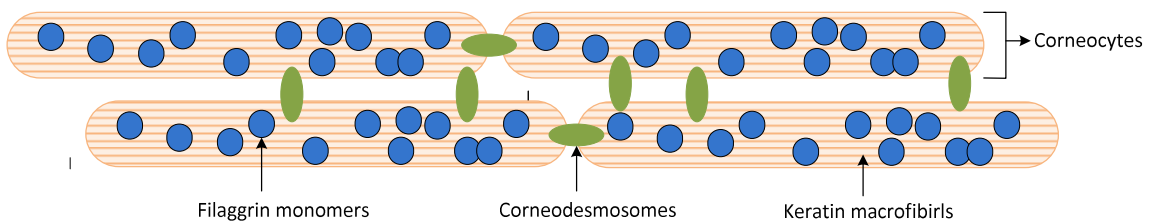

Figure 7: Possible changes in filaggrin degradation and corneocyte permeability during SC maturation.

Control of filaggrin processing

Filaggrin proteolysis is still a poorly understood process; it is intriguing to understand, for example, how SC is able to degrade filaggrin into free amino acids, while keeping other structural proteins, such as loricrin and keratin, intact. Pro-filaggrin enzymatic processing is carried out in several steps as illustrated in Figure 6.

However, the proteolysis of filaggrin may not primarily be kinetically controlled by enzymes, but rather by the water gradient existing in the SC [102]. Scott and Harding found that filaggrin was accumulated through the entire thickness of the SC during late foetal development in rat. It was only when the rats were exposed to a dryer environment immediately after birth, that normal proteolysis occurred. And this process could be blocked by maintaining a 100% humidity atmosphere. They also noticed that proteolysis took place only between 80 and 95% humidity in isolated stratum corneum *in vitro*. Likewise, they studied the effect of 10-day occlusion on filaggrin proteolysis and revealed that the filaggrin hydrolysis was dramatically blocked and a virtual absence of free amino acids in the SC. Instead, a more acidic variant of filaggrin was present throughout the SC, probably due to the activation of PADs to disassemble the filaggrin/keratin complex, a process that is independent of water gradient [109].

The breakdown of filaggrin designed by nature is such a delicate system. At deeper layer of the SC, filaggrin proteolysis is blocked by high hydration level and its attachment to KIF in order to prevent dehydration of the viable epidermis or to avoid osmotic damage to the newly formed immature corneocytes. It is only when at some point in the SC, where large reduction in water content occurs, the production of a large quantity of hygroscopic NMF happens and enables the SC to remain hydrated beyond this point.

Filaggrin mutation and its association with AD

Mutations in the gene coding for filaggrin cause a severe form of dry skin disease (ichtyosis vulgaris, IV) (Figure 8). Due to its similarity to AD, its association with AD was studied. Various mutations have been identified and it is up to now the strongest genetic pre-disposition associated with the development of AD [110-116]. All the mutations appear to involve truncation of the profilaggrin molecule. The truncated profilaggrin cannot be processed into filaggrin peptides [115].
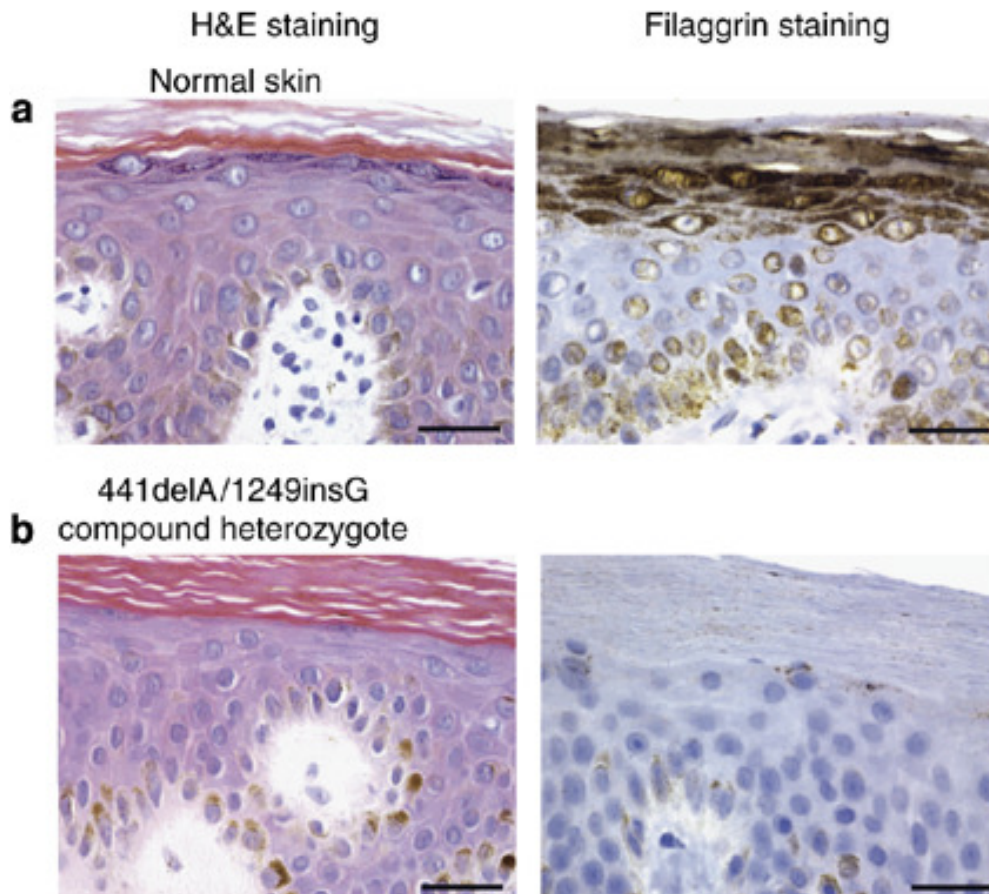
Figure 8: Histological features of patients with IV. All left panels show hematoxylin and eosin (H&E) staining and right panels show immunohistochemical staining with the 15C10 monoclonal antibody against filaggrin repeats in skin biopsies. (a) Keratohyalin granules are clearly visible in normal control skin after H&E staining. Immunohistochemical staining detects filaggrin repeats readily in 4-5 granular cell layers and throughout the stratum corneum. (b) The presence of a heterozygote 441delA/1249insG filaggrin mutation in IV patient leads to a barely detectable keratohyalin granules and filaggrin staining in the granular layer. (Taken from Chen [116])

Unsurprisingly, a reduced level of NMF has been associated with the filaggrin mutation [117] and has been implicated in the etiology of several dermatological disorders including IV, AD and allergic contact sensitization [118-120]. Moreover, an incapacity to process profilaggrin is also related to an abnormal skin phenotype, examples including the caspase-14 deficient mice which have reduced epidermal hydration and increased TEWL (transepidermal water loss) [121]; and premature degradation of profilaggrin is associated with altered keratinisation and keratin organisation within the SC [122]. Together these observations suggest that correct profilaggrin production and processing as well as NMF production are vital to the generation of a healthy epidermis and SC.

Filaggrin expression

The reduction of filaggrin expression is far more complex than simply genetic mutations. The most convincing evidence is that filaggrin expression was shown to be reduced by over-expression of T_h2 cytokines (e.g. IL-4 and IL-13) independent of filaggrin mutation [123]. Likewise, a decreased level of typical filaggrin derived NMF components were found as a global feature of moderate to severe AD [120]. It was, therefore, suggested that filaggrin genotype was the major determinant of NMF, with disease severity as a second modifier.

The modulation of filaggrin is affected by environmental factors and physical damage. Previous study on single dose hexadecane or UV radiation showed a loss of filaggrin expression in newly generated SC directly after insults, with a subsequent more rapid filaggrin synthesis 2-3 days after irritation [124]. Another similar experiment also reported a marked reduction in the SC amino acid level after three doses of hexadecane irritations in guinea pigs [125]. Physical damage, such as tape-striping ,was known to reduce the NMF components [126]. The effects of hydration level on the NMF recovery after tape-stripping were studied recently [127]. It demonstrated a higher NMF level in treated sites with no occlusion than the sites fully occluded, highlighting the importance of humidity on NMF synthesis.

Furthermore, underlying long-term illnesses may affect NMF production. Study with patients on hemodialysis showed a similar level of NMF to non-lesional AD skin, which is significantly lower than healthy controls [128]. Changes in NMF profile was also detected in aging and xerotic skin [118, 129-130]. However, these experiments only sampled the SC surface, where its NMF level may be affected by daily activities, such as washing or application of moisturizers.

Nevertheless, since mutation is not the sole attributing factor of NMF, measuring filaggrin degradation products (i.e., NMF components) in the SC is superior to genetic analysis of filaggrin mutations for the assessment of skin barrier function. Quantification of NMF components in the SC could identify people who either have filaggrin gene mutations or are incapable of catalysing the breakdown of filaggrin protein. If this quantification is possible in infants, then those with pre-disposed genetic mutations of impaired barrier function could be identified before the development of AD. Consequently, treatment with emollients and prevention of contact allergens in these infants could potentially prevent or delay the onset of AD and possibly reduce its severity. The measurement of NMF may also

be used as an investigational tool to evaluate either the intrinsic skin barrier function or barrier response to topical treatments.

1.3 Sampling the skin to assess skin barrier function

1.3.1   Non-invasive tape-stripping

The removal of sequential layers of the stratum corneum using adhesive tapes can be performed with minimum discomfort and relative ease *in vivo*, usually on the volar forearm of healthy volunteers. The procedure is painless and non-invasive, given that only dead cells (corneocytes) are removed. The method was first described by Pinkus [131] and since then it has become a standard method in dermatological research. Tape-stripping is used to evaluate the bioavailability and bioequivalence of topical drugs [132-133] or to produce a damaged skin barrier; e.g., prior to the application of an allergen [134]. However, it can also be used in conjunction with other quantification techniques to assess skin barrier function as described further below.

1.3.2   Transepidermal water loss (TEWL) measurement and SC thickness

The SC is the primary barrier for water penetration through the skin, and thus its removal increases TEWL. Fitting TEWL measurements, recorded as a function of repeated tape-stripping of the SC, to Fick's 1st law of diffusion, allows SC thickness to be estimated [135-136]. Measurement of SC thickness is a useful indicator of skin competency, and permits drug concentration profiles across the SC of different individuals to be normalised and directly compared.

1.3.3 Integrating the SC with attenuated total reflectance-fourier transform infrared spectroscopy (ATR-FTIR)
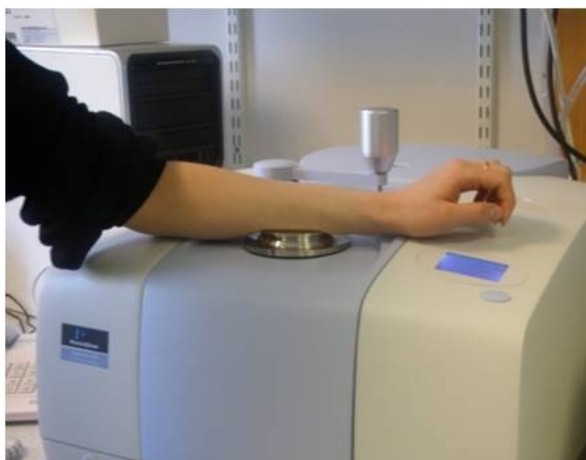

Figure 9: ATR-FTIR spectrometer scan forearm surface skin.

FTIR is an established and powerful tool to probe the molecular structure of materials [137-138]. ATR-FTIR (Figure 9) captures spectroscopic information noninvasively and has been particularly useful in investigating of the SC. However, the ATR-FTIR evanescent wave enters only a few microns from the crystal surface into the sample and hence only molecular vibrations from the most superficial layer of the sample are recorded. Therefore, repeated scanning with ATR-FTIR as a function of sequential tape-stripping is required to obtain a SC depth profile of a specific molecular species from the absorption spectra obtained.

A particularly studied feature of the IR spectrum of SC is methylene group vibrations from intercellular lipids [45, 139]. Organisation of the lipid lamellae is important in skin barrier function as mentioned before, and the vibrational frequency of these lipids produces a useful index of SC performance.

Principal component analysis is a multivariate technique that can be applied to a data set without preconceived assumptions about their properties [140]. Principal component analysis is a powerful tool to identify patterns and differences in complex datasets, such as a Raman or FTIR spectrum, by transforming the original information into new variables, so-called principal components, that describe most of the variability. The use of this method to analyse spectroscopic information from the skin has recently been explored [141]. Further,

using this approach in a pilot study, Raman spectra from infants with filaggrin-related atopic dermatitis has been analysed and used to identify disease development [142].

1.3.4 Measuring corneocyte maturity and surface area

The physical properties of corneocytes can be used to provide information on the immaturity and surface area. Extraction and staining of corneocytes collected on sequential tapes-strips non-invasively has been used as an indicator of barrier function [32, 143] and as a tool to assess the effects of topical treatment [144].

1.3.5 Extraction of tapes

The extraction and quantification of endogenous compounds removed on tape-strips offers a valuable "window" on SC performance. Combined with TEWL measurements, a concentration –depth profile can then be constructed. To date, lipids [145-146], cytokines [147] and NMF [148] have been quantified using this approach.

1.3.6 Benefits and limitations

Tape-stripping is easy to perform and relatively non-invasive. Although it may cause minor irritation, the renewal of only essentially dead cells means that the recovery of the skin barrier is rapid. The main drawback of this technique is the variability in the amount of SC removed by the tape-strips. For this reason, the quantity of SC on each tape must be quantified to express the mass of a compound extracted per unit 'volume' of the matrix. Traditionally, this has been done by weighing the tapes before and after stripping to obtain the weight of SC removed by difference. However, the weighing procedure is far from ideal. There are problems due to static electricity on the tapes, and uncertainties introduced by the uptake of formulation excipients, for example. Therefore, in chapter 2 of this thesis, a novel SC quantification method has been evaluated as an alternative to the weighing method in search of a better approach.

1.3.7 Transdermal reverse iontophoresis and passive diffusion for analyte extraction from the skin

Iontophoresis (Figure 9) is a different, essentially non-invasive method which can be used either to deliver or to extract substances across or from the skin. Iontophoresis promotes molecular transport via the application of a small current (≤0.5 mA/cm^2).
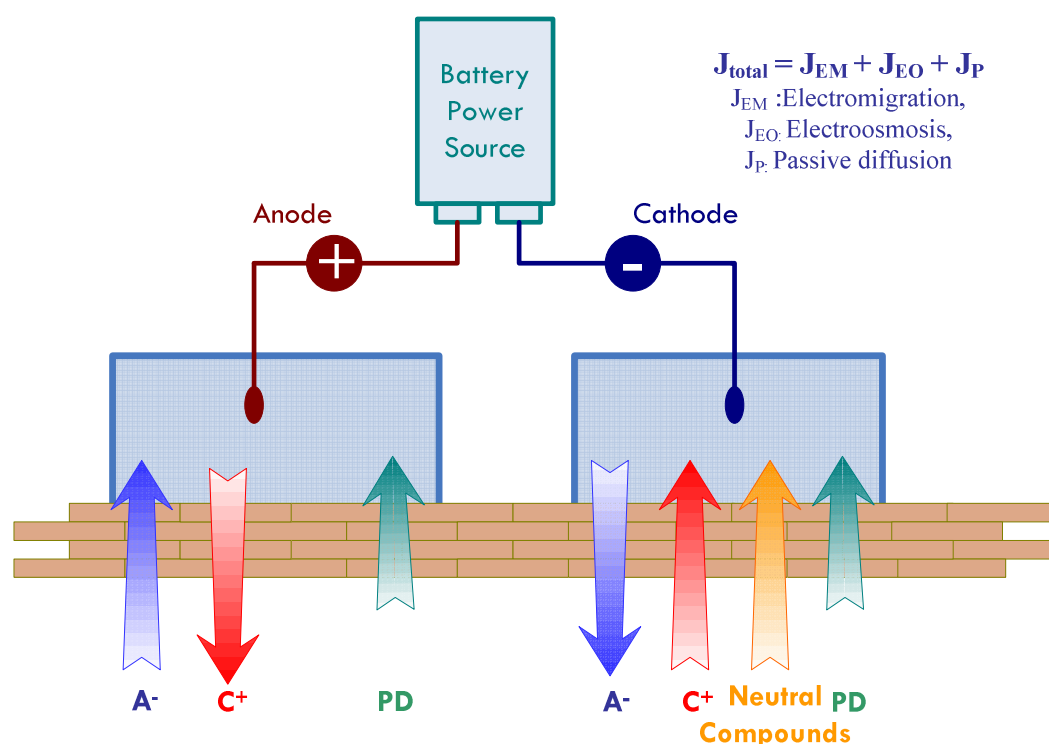

Figure 10：A schematic diagram illustrating reverse iontophoresis. A constant current is applied from a power source. Electromigration causes cationic (C$^+$, red arrow) compounds to be repelled from anode and drawn towards the cathode, while anonic (A$^-$, blue arrow) species are repelled from cathode and attracted towards the anode. Cationic (C$^+$, red arrow) and Neutral (yellow arrow) compounds are also drawn towards the cathode by electroosmosis. To a negligible extent, in most cases, passive diffusion (green arrow) contributes to the flux under both electrodes driven by the corresponding concentration gradient.

Three mechanisms contribute to the transport of a molecule across the skin during iontophoresis:

1) The interaction of charged molecules with the electrical field (electromigration).

2) The enhancement of molecular transport by current-induced solvent flow (electroosmosis).

3) Passive transdermal diffusion driven by the corresponding concentration gradient.

The total flux through the skin is the sum of these three contributions:

$J_{TOTAL} = J_{EM} + J_{EO} + J_P$ (eq. 1)

where J_{EM} represents the flux attributable to electromigration, J_{EO}, is the electroosmotic flux, and J_P is passive diffusion.

Electromigration describes the movement of ions under the influence of the applied electrical field so as to maintain electroneutrality across the skin. The speed of migration of an ion is determined by its physicochemical characteristics and the properties of the media through which it is moving [149-150]. The sum of individual ionic charges flowing through the skin must equal the electrical current supplied by the power source. This means that each ion competes to carry current across the skin with all other ions present in the system. The extent of the competition depends on the concentration, charge and mobility of all the ions present in the system. The transport number of the ion (x) of interest, represents the fraction of current carried by this species and is expressed as:

$$t_x = \frac{c_x z_x \mu_x}{\sum\limits_i c_i z_i \mu_i}$$ (eq.2)

where c, z and μ refer, respectively, to the concentration, valence and mobility inside the skin of the ion of interest (x) and of the other competing ions (i). The transport number can also be deduced experimentally by measuring the ionic flux of the ion of interest, J_x:

$$J_x = \frac{I \cdot t_x}{F \cdot z_x}$$ (eq.3)

where I is the total current; F is Faraday's constant; and z_x is the valence of ion x.

Electroosmosis is current-induced solvent flow. At physiological pH, skin has an overall negative charge. Application of an electric field across a negatively charged membrane favours the movement of cations that are attempting to neutralize the membrane charge and thus give rise to its cation selectivity, and this induces a solvent flow from anode-to-cathode direction. Electroosmotic flow therefore enhances the transport of neutral and cationic compounds. As electrical mobility decreases with increasing molecular weight, electroosmosis is believed to be the dominant mechanism of transport for large molecules [151].

Passive diffusion of ions as a result of a concentration gradient during iontophoresis is negligible, compared to electromigration and electroosmosis. The symmetry of iontophoresis means that ions can be both delivered from the electrodes into and through

the skin, and extracted from the subdermal compartment to these electrodes (Figure 10). The latter is referred to as 'reverse iontophoresis', and can be used to monitor endogenous molecules or drugs present in the subdermal compartment in a non-invasive manner. The GlucoWatch Biographer (Figure 11), developed by Cygnus Inc, is the only device based on reverse iontophoresis that has been approved by the regulatory authorities, including the U.S. Food and Drug Administration. The device is capable of monitoring blood glucose in a continuous manner every 10 minutes for a period of up to 13 hours.

Figure 11: The GlucoWatch Biographer technology [152].

However, the GlucoWatch has not been a commercial success and is no longer in the market because of some important drawbacks associated with the system, including: the requirement for calibration via a conventional finger-stick blood glucose measurement [153], the presence of a 'skin reservoir' of glucose necessitating a 'warm-up' period of ~2hr before useful measurements can be made, local irritation, and an inability to function when the wearer is actively sweating [154].

The term of this thesis, however, the presence of NMF in the skin [148, 154-157] offers a potential opportunity for reverse iontophoresis to extract the various components quickly and reproducibly with little or no contamination (at least in the earlier samples) from molecules deeper in the skin or in the blood.

2. Project aim and organisation of the thesis

This project aims to characterize skin barrier function using different bioengineering methods to underpin a non-invasive technology to identify infants pre-disposed to atopic dermatitis (AD). Successful attainment of this objective would ensure emollient treatment could be started as soon as possible, and contact with allergens and detergents to be avoided. In this way, it would be possible to prevent or delay the onset of AD and possibly reduce the severity of the disease.

As loss-of-function mutations found in the filaggrin gene are the most significant genetic factors associated with AD, the main target of this project is to analyse the amount and consumption of NMF components in healthy and in damaged skin using tape-stripping and reverse iontophoresis. Various bioengineering methods, including, FTIR measurements and immunochemical staining, are also used to provide complementary assessment of skin barrier function. The ultimate goal is to identify a diagnostic tool with which to detect impaired skin barrier function.

As tape-stripping is a major technique to be employed in this thesis, Chapter 2 first evaluates and compares a novel imaging method against the traditional gravimetric approach to quantify the SC removed on the tapes.

Chapter 3 concerns the *in vivo* extraction of NMF from healthy human volunteers. The SC 'reservoir' of NMF is quantified and the potential of reverse iontophoresis as an extraction tool is evaluated.

In Chapter 4, *in vivo* extraction of NMF from both the forearm and forehead of the same volunteers is designated to characterise two anatomic regions at which SC barrier function is notably different. Differences in NMF composition and SC intercellular lipid order at the two sites are assessed.

Finally, repeated exposure of healthy volunteers to the irritant sodium lauryl sulphate (SLS) is used to model a damaged skin barrier that is similar to that present in AD and chronic irritant contact dermatitis (Chapter 5). The SC 'reservoir' of NMF is quantified with and without SLS-induced irritation. Other bioengineering methods are also used to characterize skin barrier function in the search for a better marker of SC 'health'.

3. Reference

1.   Lewis-Jones S, *Quality of life and childhood atopic dermatitis: the misery of living with childhood eczema.* International Journal of Clinical Practice, 2006. **60**(8): p. 984-992.

2.   Chamlin SL, Frieden IJ, Williams ML, and Chren M-M, *Effects of atopic dermatitis on young American children and their families.* Pediatrics, 2004. **114**(3): p. 607-611.

3.   Daud L, Garralda M, and David T, *Psychosocial adjustment in preschool children with atopic eczema.* Arch Dis Child, 1993. **69**(6): p. 670-676.

4.   Su JC, Kemp AS, Varigos GA, and Nolan TM, *Atopic eczema: its impact on the family and financial cost.* Arch Dis Child, 1997. **76**(2): p. 159-162.

5.   Cezmi AA, Mabeccel A, Thomas B, Carsten B-J, Mark B, Philippe E, Qutayba H, Alexander K, Donald YML, Jasna L, Thomas AL, Antonella M, Natalija N, Thomas A, Lanny R, Annika S, Simons FER, Jonathan S, Kristiina T, Ulrich W, Stefan W, Thomas W, and Torsten Z, *Diagnosis and treatment of atopic dermatitis in children and adults: European Academy of Allergology and Clinical Immunology/American Academy of Allergy, Asthma and Immunology/PRACTALL Consensus Report.* The Journal of allergy and clinical immunology, 2006. **118**(1): p. 152-169.

6.   Novembre E, Cianferoni A, Lombardi E, Bernardini R, Pucci N, and Vierucci A, *Natural history of "intrinsic" atopic dermatitis.* Allergy, 2001. **56**(5): p. 452-453.

7.   Natalija N, Jean-Pierre A, and Thomas B, *Allergic hyperreactivity to microbial components: A trigger factor of intrinsic atopic dermatitis?* The Journal of allergy and clinical immunology, 2003. **112**(1): p. 215-216.

8.   Bieber T, *Atopic dermatitis.* N Engl J Med, 2008. **358**(14): p. 1483-1494.

9.   Cork MJ, Danby SG, Vasilopoulos Y, Hadgraft J, Lane ME, Moustafa M, Guy RH, MacGowan AL, Tazi-Ahnini R, and Ward SJ, *Epidermal barrier dysfunction in atopic dermatitis.* J Invest Dermatol, 2009. **129**(8): p. 1892-1908.

10.   McNally NJ, Williams HC, and Phillips DR, *Atopic eczema and the home environment.* British Journal of Dermatology, 2001. **145**(5): p. 730-736.

11. McNally NJ, Williams HC, Phillips DR, Smallman-Raynor M, Lewis S, Venn A, and Britton J, *Atopic eczema and domestic water hardness.* The Lancet, 1998. **352**(9127): p. 527-531.

12. Tan BB, Weald D, Strickland I, and Freidmann PS, *Double-blind controlled trial of effect of housedust-mite allergen avoidance on atopic dermatitis.* The Lancet, 1996. **347**(8993): p. 15-18.

13. Hamami I and Marks R, *Abnormalities in clinically normal skin-a possible explanation of the'angry back syndrome'.* Clinical and Experimental Dermatology, 1988. **13**(5): p. 328-333.

14. Bergmann R, Edenharter G, Bergmann K, Forster J, Bauer C, Wahn V, Zepp F, and Wahn U, *Atopic dermatitis in early infancy predicts allergic airway disease at 5 years.* Clinical & Experimental Allergy, 1998. **28**(8): p. 965-970.

15. Gustafsson D, Sjöberg O, and Foucard T, *Development of allergies and asthma in infants and young children with atopic dermatitis - a prospective follow - up to 7 years of age.* Allergy, 2000. **55**(3): p. 240-245.

16. Rhodes HL, Sporik R, Thomas P, Holgate ST, and Cogswell JJ, *Early life risk factors for adult asthma: A birth cohort study of subjects at risk.* Journal of Allergy and Clinical Immunology, 2001. **108**(5): p. 720-725.

17. Rhodes HL, Thomas P, Sporik R, Holgate ST, and Cogswell JJ, *A birth cohort study of subjects at risk of atopy. Twenty-two-year follow-up of wheeze and atopic status.* Am. J. Respir. Crit. Care Med., 2002. **165**(2): p. 176-180.

18. Illi S, von Mutius E, Lau S, Nickel R, Grüber C, Niggemann B, Wahn U, and the Multicenter Allergy Study G, *The natural course of atopic dermatitis from birth to age 7 years and the association with asthma.* Journal of Allergy and Clinical Immunology, 2004. **113**(5): p. 925-931.

19. Weidinger S, O'Sullivan M, Illig T, Baurecht H, Depner M, Rodriguez E, Ruether A, Klopp N, Vogelberg C, Weiland SK, McLean WHI, von Mutius E, Irvine AD, and Kabesch M, *Filaggrin mutations, atopic eczema, hay fever, and asthma in children.* Journal of Allergy and Clinical Immunology, 2008. **121**(5): p. 1203-1209.

20. Palmer CNA, Ismail T, Lee SP, Terron-Kwiatkowski A, Zhao Y, Liao H, Smith FJD, McLean WHI, and Mukhopadhyay S, *Filaggrin null mutations are associated with*

increased asthma severity in children and young adults. Journal of Allergy and Clinical Immunology, 2007. **120**(1): p. 64-68.

21. Marenholz I, Nickel R, Rüschendorf F, Schulz F, Esparza-Gordillo J, Kerscher T, Grüber C, Lau S, Worm M, Keil T, Kurek M, Zaluga E, Wahn U, and Lee Y-A, *Filaggrin loss-of-function mutations predispose to phenotypes involved in the atopic march.* Journal of Allergy and Clinical Immunology, 2006. **118**(4): p. 866-871.

22. Menon GK, *New insights into skin structure: scratching the surface.* Advanced Drug Delivery Reviews, 2002. **54**(Supplement 1): p. S3-S17.

23. Lazaroff and Rollison. 2011 [cited 2011; Available from: http://shs.westport.k12.ct.us/forensics/04-fingerprints/skin_layers.gif.

24. Clive RH, *The stratum corneum: structure and function in health and disease.* Dermatologic Therapy, 2004. **17**(s1): p. 6-15.

25. Madison KC, *Barrier Function of the Skin: "La Raison d'Etre" of the Epidermis.* J Investig Dermatol, 2003. **121**(2): p. 231-241.

26. Candi E, Schmidt R, and Melino G, *The cornified envelope: a model of cell death in the skin.* Nat Rev Mol Cell Biol, 2005. **6**(4): p. 328-340.

27. Macheleidt O, Kaiser HW, and Sandhoff K, *Deficiency of epidermal protein-bound w-hydroxyceramides in atopic dermatitis.* 2002. **119**(1): p. 166-173.

28. Hadgraft J and Lane ME, *Transepidermal water loss and skin site: A hypothesis.* International Journal of Pharmaceutics, 2009. **373**(1-2): p. 1-3.

29. Machado M, Salgado TM, Hadgraft J, and Lane ME, *The relationship between transepidermal water loss and skin permeability.* International Journal of Pharmaceutics, 2010. **384**(1-2): p. 73-77.

30. Al-Jaberi H and Marks R, *Studies of the clinically uninvolved skin in patients with dermatitis.* British Journal of Dermatology, 1984. **111**(4): p. 437-443.

31. Watanabe M, Tagami H, Horii I, Takahashi M, and Kligman AM, *Functional Analyses of the Superficial Stratum Corneum in Atopic Xerosis.* Arch Dermatol, 1991. **127**(11): p. 1689-1692.

32. Hirao T, Denda M, and Takahashi M, *Identification of immature cornified envelopes in the barrier-impaired epidermis by characterization of their hydrophobicity and antigenicities of the components.* Experimental Dermatology, 2001. **10**(1): p. 35-44.

33. Hirao T, *Involvement of transglutaminase in ex vivo maturation of cornified envelopes in the stratum corneum.* International Journal of Cosmetic Science, 2003. **25**(5): p. 245-257.

34. Tetsuji H, Tadashi T, Izuho T, Hiromi K, Mikiko O, Motoji T, and Hachiro T, *Ratio of immature cornified envelopes does not correlate with parakeratosis in inflammatory skin disorders.* Experimental Dermatology, 2003. **12**(5): p. 591-601.

35. Fartasch M, Bassukas I, and Diepgen T, *Disturbed extruding mechanism of lamellar bodies in dry non-eczematous kin of atopics.* The British Journal of Dermatology, 1992. **127**(3): p. 221-227.

36. Imokawa G, Abe A, Jin K, Higaki Y, Kawashima M, and Hidano A, *Decreased Level of Ceramides in Stratum Corneum of Atopic Dermatitis: An Etiologic Factor in Atopic Dry Skin?* J Invest Dermatol, 1991. **96**(4): p. 523-526.

37. Nardo A, Wertz P, Giannetti A, and Seidenari S, *Ceramide and Cholesterol Composition of the Skin of Patients with Atopic Dermatitis.* Acta Derm Venereol, 1998. **78**: p. 27-30.

38. Yamamoto A, Serizawa S, Ito M, and Sato Y, *Stratum corneum lipid abnormalities in atopic dermatitis.* Archives of Dermatological Research, 1991. **283**(4): p. 219-223.

39. Matsumoto M, Umemoto N, Sugiura H, and Uehara M, *Difference in Ceramide Composition between ``Dry'' and ``Normal'' Skin in Patients with Atopic Dermatitis.* Acta Derm Venereol, 1998. **79**: p. 246-247.

40. Chang-Yi C, Kusuda S, Seguchi T, Takahashi M, Aisu K, and Tezuka T, *Decreased Level of Prosaposin in Atopic Skin.* J Invest Dermatol, 1997. **109**(3): p. 319-323.

41. Hara J, Higuchi K, Okamoto R, Kawashima M, and Imokawa G, *High-Expression of Sphingomyelin Deacylase is an Important Determinant of Ceramide Deficiency Leading to Barrier Disruption in Atopic Dermatitis.* J Invest Dermatol, 2000. **115**(3): p. 406-413.

42. Yardley HJ and Summerly R, *Lipid composition and metabolism in normal and diseased epidermis.* Pharmacology & Therapeutics, 1981. **13**(2): p. 357-383.

43. Ishikawa J, Narita H, Kondo N, Hotta M, Takagi Y, Masukawa Y, Kitahara T, Takema Y, Koyano S, Yamazaki S, and Hatamochi A, *Changes in the Ceramide Profile of Atopic Dermatitis Patients.* J Invest Dermatol, 2010.

44.   Bouwstra J, Gooris G, and Ponec M, *The Lipid Organisation of the Skin Barrier: Liquid and Crystalline Domains Coexist in Lamellar Phases.* Journal of Biological Physics, 2002. **28**(2): p. 211-223.

45.   Berthaud F and Boncheva M, *Correlation between the properties of the lipid matrix and the degrees of integrity and cohesion in healthy human Stratum corneum.* Experimental Dermatology, 2010. **20**(3): p. 255-262.

46.   Pilgram G, Vissers D, van der Meulen H, Pavel S, Lavrijsen S, Bouwstra J, and Koerten H, *Aberrant Lipid Organization in Stratum Corneum of Patients with Atopic Dermatitis and Lamellar Ichthyosis.* J Invest Dermatol, 2001. **117**(3): p. 710-717.

47.   Bouwstra JA and Ponec M, *The skin barrier in healthy and diseased state.* Biochimica et Biophysica Acta (BBA) - Biomembranes, 2006. **1758**(12): p. 2080-2095.

48.   Bouwstra JA, Gooris GS, Dubbelaar FER, and Ponec M, *Phase Behavior of Stratum Corneum Lipid Mixtures Based on Human Ceramides: The Role of Natural and Synthetic Ceramide 1.* J Invest Dermatol, 2002. **118**(4): p. 606-617.

49.   Egelrud T, *Purification and preliminary characterization of stratum corneum chymotryptic enzyme: a proteinase that may be involved in desquamation.* J Invest Dermatol, 1993. **101**(2): p. 200-204.

50.   Kishibe M, Bando Y, Terayama R, Namikawa K, Takahashi H, Hashimoto Y, Ishida-Yamamoto A, Jiang Y-P, Mitrovic B, Perez D, Iizuka H, and Yoshida S, *Kallikrein 8 is involved in skin desquamation in cooperation with other kallikreins.* J. Biol. Chem., 2007. **282**(8): p. 5834-5841.

51.   Horikoshi T, Igarashi S, Uchiwa H, Brysk H, and Brysk M, *Role of endogenous cathepsin D-like and chymotrypsin-like proteolysis in human epidermal desquamation.* British Journal of Dermatology, 1999. **141**(3): p. 453-459.

52.   Ekholm IE, Brattsand M, and Egelrud T, *Stratum corneum tryptic enzyme in normal epidermis: a missing link in the desquamation process ?* J Invest Dermatol, 2000. **114**(1): p. 56-63.

53.   Brattsand M, Stefansson K, Lundh C, Haasum Y, and Egelrud T, *A proteolytic cascade of kallikreins in the stratum corneum.* J Invest Dermatol, 2004. **124**(1): p. 198-203.

54.   Borgono CA, Michael IP, Komatsu N, Jayakumar A, Kapadia R, Clayman GL, Sotiropoulou G, and Diamandis EP, *A potential role for multiple tissue kallikrein*

serine proteases in epidermal desquamation. J. Biol. Chem., 2007. **282**(6): p. 3640-3652.

55.   Nylander-lundgvist E and Egelrud T, *Formation of active IL-1 beta from pro-IL-1 beta catalyzed by stratum corneum chymotryptic enzyme in vitro.* Acta Derm Venereol. , 1997. **77**(3): p. 203-206.

56.   Yamasaki K, Schauber J, Coda A, Lin H, Dorschner RA, Schechter NM, Bonnart C, Descargues P, Hovnanian A, and Gallo RL, *Kallikrein-mediated proteolysis regulates the antimicrobial effects of cathelicidins in skin.* The FASEB Journal, 2006. **20**(12): p. 2068-2080.

57.   Hachem J-P, Man M-Q, Crumrine D, Uchida Y, Brown BE, Rogiers V, Roseeuw D, Feingold KR, and Elias PM, *Sustained Serine Proteases Activity by Prolonged Increase in pH Leads to Degradation of Lipid Processing Enzymes and Profound Alterations of Barrier Function and Stratum Corneum Integrity.* J Invest Dermatol, 2005. **125**(3): p. 510-520.

58.   Oikonomopoulou K, Hansen KK, Saifeddine M, Vergnolle N, Tea I, Blaber M, Blaber SI, Scarisbrick I, Diamandis EP, and Hollenberg MD, *Kallikrein-mediated cell signalling: targeting proteinase-activated receptors (PARs).* Biological Chemistry, 2006. **387**(6): p. 817-824.

59.   Voegeli R, Rawlings A, Doppler S, Heiland J, and Schreier T, *Profiling of serine protease activities in human stratum corneum and detection of a stratum corneum tryptase-like enzyme.* International Journal of Cosmetic Science, 2007. **29**(3): p. 191-200.

60.   Tarroux R, Assalit MF, Licu D, Périé JJ, and Redoulès D, *Variability of Enzyme Markers during Clinical Regression of Atopic Dermatitis.* Skin Pharmacology and Physiology, 2002. **15**(1): p. 55-62.

61.   Voegeli R, Rawlings A, Breternitz M, Doppler S, Schreier T, and Fluhr J, *Increased stratum corneum serine protease activity in acute eczematous atopic skin.* British Journal of Dermatology, 2009. **161**(1): p. 70-77.

62.   Nahoko K, Kiyofumi S, Cynthia K, Amber CL, Saba K, Fumiaki S, Kazuhiko T, and Eleftherios PD, *Human tissue kallikrein expression in the stratum corneum and serum of atopic dermatitis patients.* Experimental Dermatology, 2007. **16**(6): p. 513-519.

63.   Komatsu N, Saijoh K, Toyama T, Ohka R, Otsuki N, Hussack G, Takehara K, and Diamandis EP, *Multiple tissue kallikrein mRNA and protein expression in normal skin and skin diseases.* British Journal of Dermatology, 2005. **153**(2): p. 274-281.

64.   Raghunath M, Tontsidou L, Oji V, Aufenvenne K, Schurmeyer-Horst F, Jayakumar A, Stander H, Smolle J, Clayman GL, and Traupe H, *SPINK5 and Netherton Syndrome: Novel Mutations, Demonstration of Missing LEKTI, and Differential Expression of Transglutaminases.* J Invest Dermatol, 2004. **123**(3): p. 474-483.

65.   Walley AJ, Chavanas S, Moffatt MF, Esnouf RM, Ubhi B, Lawrence R, Wong K, Abecasis GR, Jones EY, Harper JI, Hovnanian A, and Cookson W, *Gene polymorphism in Netherton and common atopic disease.* Nat Genet, 2001. **29**(2): p. 175-178.

66.   Nishio Y, Noguchi E, Shibasaki M, Kamioka M, Ichikawa E, Ichikawa K, Umebayashi Y, Otsuka F, and Arinami T, *Association between polymorphisms in the SPINK5 gene and atopic dermatitis in the Japanese.* Genes Immun, 2003. **4**(7): p. 515-517.

67.   Folster-Holst R, Stoll M, Koch WA, Hampe J, Christophers E, and Schreiber S, *Lack of association of SPINK5 polymorphisms with nonsyndromic atopic dermatitis in the population of Northern Germany.* British Journal of Dermatology, 2005. **152**(6): p. 1365-1367.

68.   Weidinger S, Baurecht H, Wagenpfeil S, Henderson J, Novak N, Sandilands A, Chen H, Rodriguez E, O'Regan GM, Watson R, Liao H, Zhao Y, Barker JNWN, Allen M, Reynolds N, Meggitt S, Northstone K, Smith GD, Strobl C, Stahl C, Kneib T, Klopp N, Bieber T, Behrendt H, Palmer CNA, Wichmann HE, Ring J, Illig T, McLean WHI, and Irvine AD, *Analysis of the individual and aggregate genetic contributions of previously identified serine peptidase inhibitor Kazal type 5 (SPINK5), kallikrein-related peptidase 7 (KLK7), and filaggrin (FLG) polymorphisms to eczema risk.* Journal of Allergy and Clinical Immunology, 2008. **122**(3): p. 560-568.e4.

69.   Nakamura T, Hirasawa Y, Takai T, Mitsuishi K, Okuda M, Kato T, Okumura K, Ikeda S, and Ogawa H, *Reduction of Skin Barrier Function by Proteolytic Activity of a Recombinant House Dust Mite Major Allergen Der f 1.* J Invest Dermatol, 2006. **126**(12): p. 2719-2723.

70.   Jeong SK, Kim HJ, Youm J-K, Ahn SK, Choi EH, Sohn MH, Kim K-E, Hong JH, Shin DM, and Lee SH, *Mite and Cockroach Allergens Activate Protease-Activated Receptor 2*

and Delay Epidermal Permeability Barrier Recovery. J Invest Dermatol, 2008. **128**(8): p. 1930-1939.

71. Hirasawa Y, Takai T, Nakamura T, Mitsuishi K, Gunawan H, Suto H, Ogawa T, Wang X-L, Ikeda S, Okumura K, and Ogawa H, *Staphylococcus aureus Extracellular Protease Causes Epidermal Barrier Dysfunction.* J Invest Dermatol, 2009. **130**(2): p. 614-617.

72. Buck R, Covington A, Baucke F, Brett C, Camoes M, Milton M, Mussini T, Naumann R, Pratt K, Spitzer P, and Wilson G, *Measurement of pH. Definition, standards,and procedures (IUPAC Recommendations 2002).* Pure Appl Chem, 2002. **74**(11): p. 2169-2200.

73. Draize JH, *The Determination of the pH of the Skin of Man and Common Laboratory Animals.* The Journal of Investigative Dermatology, 1942. **5**(2): p. 77-85.

74. Schirren C, *Does the glass electrode determine the same pH-values on the skin surface as the quinhydrone electrode?* J Invest Dermatol, 1955. **24**: p. 485-488.

75. Abe T, Mayuzumi J, Kikuchi N, and Arai S, *Seasonal variations in skin temperature, skin pH, evaporative water loss and skin surface lipid values on human skin.* Chem Pharm Bull, 1979. **28**(2): p. 387-392.

76. Hatano Y, Man M-Q, Uchida Y, Crumrine D, Scharschmidt TC, Kim EG, Mauro TM, Feingold KR, Elias PM, and Holleran WM, *Maintenance of an Acidic Stratum Corneum Prevents Emergence of Murine Atopic Dermatitis.* J Invest Dermatol, 2009. **129**(7): p. 1824-1835.

77. Kroll C, Herrmann W, Stößer R, Borchert H-H, and Mäder K, *Influence of Drug Treatment on the Microacidity in Rat and Human Skin—An Electron Spin Resonance Imaging Study.* Pharmaceutical Research, 2001. **18**(4): p. 525-530.

78. Hanson KM, Behne MJ, Barry NP, Mauro TM, Gratton E, and Clegg RM, *Two-Photon Fluorescence Lifetime Imaging of the Skin Stratum Corneum pH Gradient.* Biophysical journal, 2002. **83**(3): p. 1682-1690.

79. Behne MJ, Meyer JW, Hanson KM, Barry NP, Murata S, Crumrine D, Clegg RW, Gratton E, Holleran WM, Elias PM, and Mauro TM, *NHE1 Regulates the Stratum Corneum Permeability Barrier Homeostasis. Microenvironment acidification assessed with fluorescence lifetime imaging.* J. Biol. Chem., 2002. **277**(49): p. 47399-47406.

80. Fluhr JW, Kao J, Jain M, Ahn SK, Feingold KR, and Elias PM, *Generation of Free Fatty Acids from Phospholipids Regulates Stratum Corneum Acidification and Integrity.* J Invest Dermatol, 2001. **117**(1): p. 44-51.

81. Krien PM and Kermici M, *Evidence for the Existence of a Self-Regulated Enzymatic Process Within the Human Stratum Corneum -An Unexpected Role for Urocanic Acid.* J Invest Dermatol, 2000. **115**(3): p. 414-420.

82. Hachem J-P, Crumrine D, Fluhr J, Brown BE, Feingold KR, and Elias PM, *pH Directly Regulates Epidermal Permeability Barrier Homeostasis, and Stratum Corneum Integrity/Cohesion.* J Invest Dermatol, 2003. **121**(2): p. 345-353.

83. Elias P, *The skin barrier as an innate immune element.* Seminars in Immunopathology, 2007. **29**(1): p. 3-14.

84. Hachem J, Fowler A, Behne MJ, Fluhr J, Feingold KR, and Elias P, *Increased stratum corneum pH promotes activation and release of primary cytokines from the stratum corneum attributable to activation of serine proteases.* J Invest Dermatol, 2002. **119**: p. 258 (abstract).

85. Gunathilake R, Schurer NY, Shoo BA, Celli A, Hachem J-P, Crumrine D, Sirimanna G, Feingold KR, Mauro TM, and Elias PM, *pH-Regulated Mechanisms Account for Pigment-Type Differences in Epidermal Barrier Function.* J Invest Dermatol, 2009. **129**(7): p. 1719-1729.

86. Rawlings A and Harding C, *Moisturization and skin barrier function.* Dermatologic Therapy, 2004. **17**(s1): p. 43-48.

87. Levin J and Maibach H, *Human skin buffering capacity: an overview.* Skin Research and Technology, 2008. **14**(2): p. 121-126.

88. Lodén M, Andersson AC, Andersson C, Frödin T, Öman H, and Lindberg M, *Instrumental and dermatologist evaluation of the effect of glycerine and urea on dry skin in atopic dermatitis.* Skin Research and Technology, 2001. **7**(4): p. 209-213.

89. Nakagawa N, Sakai S, Matsumoto M, Yamada K, Nagano M, Yuki T, Sumida Y, and Uchiwa H, *Relationship Between NMF (Lactate and Potassium) Content and the Physical Properties of the Stratum Corneum in Healthy Subjects.* J Invest Dermatol, 2004. **122**(3): p. 755-763.

90.   Choi EH, Man M-Q, Wang F, Zhang X, Brown BE, Feingold KR, and Elias PM, *Is Endogenous Glycerol a Determinant of Stratum Corneum Hydration in Humans?* J Invest Dermatol, 2005. **125**(2): p. 288-293.

91.   Hara-Chikuma M and Verkman AS, *Aquaporin-3 functions as a glycerol transporter in mammalian skin.* Biol. Cell, 2005. **97**(7): p. 479-486.

92.   Fluhr JW, Mao-Qiang M, Brown BE, Wertz PW, Crumrine D, Sundberg JP, Feingold KR, and Elias PM, *Glycerol Regulates Stratum Corneum Hydration in Sebaceous Gland Deficient (Asebia) Mice.* J Invest Dermatol, 2003. **120**(5): p. 728-737.

93.   Holleran WM, Takagi Y, Imokawa G, Jackson S, Lee JM, and Elias PM, *beta-Glucocerebrosidase activity in murine epidermis: characterization and localization in relation to differentiation.* Journal of Lipid Research, 1992. **33**(8): p. 1201-9.

94.   Walsh A and Chapman SJ, *Sugars protect desmosome and corneosome glycoproteins from proteolysis.* Archives of Dermatological Research, 1991. **283**(3): p. 174-179.

95.   Sakai S, Yasuda R, Sayo T, Ishikawa O, and Inoue S, *Hyaluronan Exists in the Normal Stratum Corneum.* J Invest Dermatol, 2000. **114**(6): p. 1184-1187.

96.   Maytin EV, Chung HH, and Seetharaman VM, *Hyaluronan Participates in the Epidermal Response to Disruption of the Permeability Barrier in Vivo.* Am J Pathol, 2004. **165**(4): p. 1331-1341.

97.   Steinert PM, Cantieri JS, Teller DC, Lonsdale-Eccles JD, and Dale BA, *Characterization of a class of cationic proteins that specifically interact with intermediate filaments.* Proceedings of the National Academy of Sciences, 1981. **78**(7): p. 4097-4101.

98.   Scott IR, Harding CR, and Barrett JG, *Histidine-rich protein of the keratohyalin granules: Source of the free amino acids, urocanic acid and pyrrolidone carboxylic acid in the stratum corneum.* Biochimica et Biophysica Acta (BBA) - General Subjects, 1982. **719**(1): p. 110-117.

99.   Sandilands A, Sutherland C, Irvine AD, and McLean WHI, *Filaggrin in the frontline: role in skin barrier function and disease.* J Cell Sci, 2009. **122**(9): p. 1285-1294.

100.   Bouwstra JA, Groenink HWW, Kempenaar JA, Romeijn SG, and Ponec M, *Water Distribution and Natural Moisturizer Factor Content in Human Skin Equivalents Are Regulated by Environmental Relative Humidity.* J Invest Dermatol, 2007. **128**(2): p. 378-388.

101. Caspers PJ, Lucassen GW, Carter EA, Bruining HA, and Puppels GJ, *In vivo confocal raman microspectroscopy of the skin: noninvasive determination of molecular concentration profiles.* J Invest Dermatol, 2001. **116**(3): p. 434-442.

102. Scott IR and Harding CR, *Filaggrin breakdown to water binding compounds during development of the rat stratum corneum is controlled by the water activity of the environment.* Developmental Biology, 1986. **115**(1): p. 84-92.

103. Jokura Y, Ishikawa S, Tokuda H, and Imokawa G, *Molecular Analysis of Elastic Properties of the Stratum Corneum by Solid-State 13C-Nuclear Magnetic Resonance Spectroscopy.* J Invest Dermatol, 1995. **104**(5): p. 806-812.

104. Walterscheid J, Nghiem D, Kazimi N, Nutt L, McConkey D, Norval M, and Ullrich S, *Cis-urocanic acid, a sunlight-induced immunosuppressive factor, activates immune suppression via the 5-HT$_{2A}$ receptor.* Proceedings of the National Academy of Sciences, 2006. **103**(46): p. 17420-17425.

105. McLoone P, Simics E, Barton A, Norval M, and Gibbs NK, *An action spectrum for the production of cis-urocanic acid in human skin in vivo.* J Invest Dermatol, 2005. **124**(5): p. 1071-1074.

106. Warner RR, Stone KJ, and Boissy YL, *Hydration Disrupts Human Stratum Corneum Ultrastructure.* J Invest Dermatol, 2003. **120**(2): p. 275-284.

107. Sylvestre JP, Bouissou C, Guy R, and Delgado-Charro MB, *Extraction and quantification of amino acids in human stratum corneum in vivo.* British Journal of Dermatology, 2010. **163**(3): p. 458-465.

108. Nguyen V, Ndoye A, Hall L, Zia S, Arredondo J, Chernyavsky A, Kist D, Zelickson B, Lawry M, and Grando S, *Programmed cell death of keratinocytes culminates in apoptotic secretion of a humectant upon secretagogue action of acetylcholine.* J Cell Sci, 2001. **114**(6): p. 1189-1204.

109. Harding CR and Scott I, *Alterations in the processing of human filaggrin following skin occlusion in vivo and in vitro.* Journal of investigative dermatology, 1993. **100**(4): p. 579.

110. Zhang X, Liu S, Chen X, Zhou B, Liu D, Lei G, Xiao X, Liu H, and Wang H, *Novel and recurrent mutations in the filaggrin gene in Chinese patients with ichthyosis vulgaris.* British Journal of Dermatology, 2010. **163**(1): p. 63-69.

111. Cascella R, Cuzzola VF, Lepre T, Galli E, Moschese V, Chini L, Mazzanti C, Fortugno P, Novelli G, and Giardina E, *Full Sequencing of the FLG Gene in Italian Patients with Atopic Eczema: Evidence of New Mutations, but Lack of an Association.* J Invest Dermatol, 2011. **131**(4): p. 982-984.

112. Muller S, Marenholz I, Lee Y, Sengler C, Zitnik S, Griffioen R, Meglio P, Wahn U, and Nickel R, *Association of filaggrin loss-of-function-mutations with atopic dermatitis and asthma in the Early Treatment of the Atopic Child (ETAC) population.* Pediatric Allergy and Immunology, 2009. **20**(4): p. 358-361.

113. Sandilands A, O'Regan GM, Liao H, Zhao Y, Terron-Kwiatkowski A, Watson RM, Cassidy AJ, Goudie DR, Smith FJD, McLean WHI, and Irvine AD, *Prevalent and rare mutations in the gene encoding filaggrin cause ichthyosis vulgaris and predispose individuals to atopic dermatitis.* J Invest Dermatol, 2006. **126**(8): p. 1770-1775.

114. Nomura T, Akiyama M, Sandilands A, Nemoto-Hasebe I, Sakai K, Nagasaki A, Palmer CNA, Smith FJD, McLean WHI, and Shimizu H, *Prevalent and rare mutations in the gene encoding filaggrin in Japanese patients with ichthyosis vulgaris and atopic dermatitis.* J Invest Dermatol, 2008. **129**: p. 1302-1305.

115. Brown SJ and Irvine AD, *Atopic eczema and the filaggrin story.* Seminars in Cutaneous Medicine and Surgery, 2008. **27**(2): p. 128-137.

116. Chen H, Ho JCC, Sandilands A, Chan YC, Giam YC, Evans AT, Lane EB, and McLean WHI, *Unique and recurrent mutations in the filaggrin gene in Singaporean Chinese patients with ichthyosis vulgaris.* J Invest Dermatol, 2008. **128**(7): p. 1669-1675.

117. Kezic S, Kemperman PMJH, Koster ES, de Jongh CM, Thio HB, Campbell LE, Irvine AD, McLean IWH, Puppels GJ, and Caspers PJ, *Loss-of-Function mutations in the filaggrin gene lead to reduced level of natural moisturizing factor in the stratum corneum.* J Invest Dermatol, 2008. **128**(8): p. 2117-2119.

118. Takahashi M and Tezuka T, *The content of free amino acids in the stratum corneum is increased in senile xerosis.* Archives of Dermatological Research, 2004. **295**(10): p. 448-452.

119. Novak N, Baurecht H, Schafer T, Rodriguez E, Wagenpfeil S, Klopp N, Heinrich J, Behrendt H, Ring J, Wichmann E, Illig T, and Weidinger S, *Loss-of-function mutations in the filaggrin gene and allergic contact sensitization to nickel.* J Invest Dermatol, 2007. **128**(6): p. 1430-1435.

120. Kezic S, O'Regan GM, Yau N, Sandilands A, Chen H, Campbell LE, Kroboth K, Watson R, Rowland M, Irwin McLean WH, and Irvine AD, *Levels of filaggrin degradation products are influenced by both filaggrin genotype and atopic dermatitis severity.* Allergy, 2011: p. 934-940.

121. Denecker G, Ovaere P, Vandenabeele P, and Declercq W, *Caspase-14 reveals its secrets.* J. Cell Biol., 2008. **180**(3): p. 451-458.

122. Ginger R, Blachford S, Rowland J, Rowson M, and Harding C, *Filaggrin repeat number polymorphism is associated with a dry skin phenotype.* Archives of Dermatological Research, 2005. **297**(6): p. 235-241.

123. Howell MD, Kim BE, Gao P, Grant AV, Boguniewicz M, DeBenedetto A, Schneider L, Beck LA, Barnes KC, and Leung DYM, *Cytokine modulation of atopic dermatitis filaggrin skin expression.* Journal of Allergy and Clinical Immunology, 2009. **124**(3, Supplement 2): p. R7-R12.

124. Scott IR, *Alterations in the Metabolism of Filaggrin in the Skin After Chemical- and Ultraviolet-Induced Erythema.* J Invest Dermatol, 1986. **87**(4): p. 460-465.

125. Rossmiller JD and Hoekstra WG, *Hexadecane-Induced Hyperkeratinization of Guinea Pig Skin.* The Journal of Investigative Dermatology, 1966. **47**(1): p. 44-48.

126. Denda M, Hori J, Koyama J, Yoshida S, Nanba R, Takahashi M, Horii I, and Yamamoto A, *Stratum corneum sphingolipids and free amino acids in experimentally-induced scaly skin.* Archives of Dermatological Research, 1992. **284**(6): p. 363-367.

127. Visscher M, Robinson M, and Wickett R, *Stratum corneum free amino acids following barrier perturbation and repair.* International Journal of Cosmetic Science, 2011. **33**(1): p. 80-89.

128. Takahashi M and Ikezawa Z, *Dry skin in atopic dermatitis and patients on hemodialysis*. Dry skin and moisturizers:chemistry and function. 1999: Informa healthcare.

129. Horii I, Nakayama Y, Obata M, and Tagami H, *Stratum corneum hydration and amino acid content in xerotic skin.* British Journal of Dermatology, 1989. **121**(5): p. 587-592.

130. Jacobson TM, Yuksel KU, Geesin JC, Gordon JS, Lane AT, and Gracy RW, *Effects of Aging and Xerosis on the Amino Acid Composition of Human Skin.* J Invest Dermatol, 1990. **95**(3): p. 296-300.

131. Pinkus H, *Examination of the epidermis by the strip method.* The Journal of Investigative Dermatology, 1952. **19**(6): p. 431-447.

132. Alberti I, Kalia YN, Naik A, and Guy RH, *Assessment and prediction of the cutaneous bioavailability of topical terbinafine, in vivo, in man.* Pharmaceutical Research, 2001. **18**(10): p. 1472-1475.

133. Shah VP, Flynn GL, Yacobi A, Maibach HI, Bon C, Fleischer NM, Franz TJ, Kaplan SA, Kawamoto J, Lesko LJ, Marty J-P, Pershing LK, Schaefer H, Sequeira JA, Shrivastava SP, Wilkin J, and Williams RL, *Bioequivalence of topical dermatological dosage forms-methods of evaluation of bioequivalence.* Pharmaceutical Research, 1998. **15**(2): p. 167-171.

134. Kondo H, Ichikawa Y, and Imokawa G, *Percutaneous sensitization with allergens through barrier-disrupted skin elicits a Th2-dominant cytokine response.* European Journal of Immunology, 1998. **28**(3): p. 769-779.

135. Russell LM, Wiedersberg S, and Delgado-Charro MB, *The determination of stratum corneum thickness An alternative approach.* European Journal of Pharmaceutics and Biopharmaceutics, 2008. **69**(3): p. 861-870.

136. Pirot F, Berardesca E, Kalia YN, Singh M, Maibach HI, and Guy RH, *Stratum Corneum Thickness and Apparent Water Diffusivity: Facile and Noninvasive Quantitation In Vivo.* Pharmaceutical Research, 1998. **15**(3): p. 492-494.

137. Obata Y, Utsumi S, Watanabe H, Suda M, Tokudome Y, Otsuka M, and Takayama K, *Infrared spectroscopic study of lipid interaction in stratum corneum treated with transdermal absorption enhancers.* International Journal of Pharmaceutics, 2010. **389**(1-2): p. 18-23.

138. Jain AK, Thomas NS, and Panchagnula R, *Transdermal drug delivery of imipramine hydrochloride.: I. Effect of terpenes.* Journal of Controlled Release, 2002. **79**(1-3): p. 93-101.

139. Bommannan D, Potts RO, and Guy RH, *Examination of Stratum Corneum Barrier Function In Vivo by Infrared Spectroscopy.* J Invest Dermatol, 1990. **95**(4): p. 403-408.

140. Krafft C, Steiner G, Beleites C, and Salzer R, *Disease recognition by infrared and Raman spectroscopy.* Journal of Biophotonics, 2009. **2**(1-2): p. 13-28.

141. Greve TM, Andersen KB, and Nielsen OF, *ATR-FTIR, FT-NIR and near-FT-Raman spectroscopic studies of molecular composition in human skin in vivo and pig ear skin in vitro.* Spectroscopy, 2008. **22**(6): p. 437-457.

142. González FJ, Alda J, Moreno-Cruz B, Martínez-Escanamé M, Ramírez-Elías MG, Torres-Álvarez B, and Moncada B, *Use of Raman spectroscopy for the early detection of filaggrin-related atopic dermatitis.* Skin Research and Technology, 2011. **17**(1): p. 45-50.

143. Kunii T, Hirao T, Kikuchi K, and Tagami H, *Stratum corneum lipid profile and maturation pattern of corneocytes in the outermost layer of fresh scars: the presence of immature corneocytes plays a much more important role in the barrier dysfunction than do changes in intercellular lipids.* British Journal of Dermatology, 2003. **149**(4): p. 749-756.

144. Mohammed D, Matts PJ, Hadgraft J, and Lane ME, *Influence of Aqueous Cream on corneocyte size, maturity, skin protease activity, protein content and Trans-Epidermal Water Loss.* British Journal of Dermatology, 2011. **164**(6): p. 1304-1310.

145. Weerheim A and Ponec M, *Determination of stratum corneum lipid profile by tape stripping in combination with high-performance thin-layer chromatography.* Archives of Dermatological Research, 2001. **293**(4): p. 191-199.

146. Popa I, Thuy L, Colsch B, Pin D, Gatto H, Haftek M, and Portoukalian J, *Analysis of free and protein-bound ceramides by tape stripping of stratum corneum from dogs.* Archives of Dermatological Research, 2010. **302**(9): p. 639-644.

147. De Jongh CM, Verberk MM, Spiekstra SW, Gibbs S, and Kezic S, *Cytokines at different stratum corneum levels in normal and sodium lauryl sulphate-irritated skin.* Skin Research and Technology, 2007. **13**(4): p. 390-398.

148. Sylvestre JP, Bouissou CC, Guy RH, and Delgado-Charro MB, *Extraction and quantification of amino acids in human stratum corneum in vivo.* British Journal of Dermatology, 2010. **163**(3): p. 458-465.

149. Phipps J and Gyory JR, *Transdermal ion migration.* Advanced Drug Delivery Reviews, 1992. **9**(2-3): p. 137-176.

150. Leboulanger B, Guy RH, and Delgado-Charro MB, *Reverse iontophoresis for non-invasive transdermal monitoring.* Physiological Measurement, 2004. **25**(3): p. R35.

151. Guy RH, Kalia YN, Delgado-Charro MB, Merino V, López A, and Marro D, *Iontophoresis: electrorepulsion and electroosmosis.* Journal of Controlled Release, 2000. **64**(1-3): p. 129-132.

152. Russell OP, Janet AT, and Michael JT, *Glucose monitoring by reverse iontophoresis.* Diabetes/Metabolism Research and Reviews, 2002. **18**(S1): p. S49-S53.

153. Sieg A, Guy RH, and Delgado-Charro MB, *Noninvasive glucose monitoring by reverse iontophoresis in vivo: application of the internal standard concept.* Clin Chem, 2004. **50**(8): p. 1383-1390.

154. Sieg A, Guy RH, and Delgado-Charro MB, *Simultaneous extraction of urea and glucose by reverse iontophoresis in vivo.* Pharmaceutical Research, 2004. **21**(10): p. 1805-1810.

155. Nixon S, Sieg A, Delgado-Charro MB, and Guy RH, *Reverse iontophoresis of L-lactate: In vitro and in vivo studies.* Journal of Pharmaceutical Sciences, 2007. **96**(12): p. 3457-3465.

156. Wascotte V, Caspers P, de Sterke J, Jadoul M, Guy R, and Préat V, *Assessment of the "skin reservoir" of urea by confocal raman microspectroscopy and reverse iontophoresis in vivo.* Pharmaceutical Research, 2007. **24**(10): p. 1897-1901.

157. Sieg A, Jeanneret F, Fathi M, Hochstrasser D, Rudaz S, Veuthey J-L, Guy RH, and Delgado-Charro MB, *Extraction of amino acids by reverse iontophoresis in vivo.* European Journal of Pharmaceutics and Biopharmaceutics, 2009. **72**(1): p. 226-231.

Chapter 2: Evaluation of SC quantification methods in dermatopharmacokinetics

Abstract

Purpose:

An objective method to assess the rate and extent of drug permeation through the skin from topical formulations is required for bioequivalence purposes. Tape stripping the stratum corneum (SC) with adhesive tapes has emerged as a promising technique. When tapes are analysed individually, drug penetration profiles through the SC maybe constructed. To create such profiles, the amount of SC per tape must be measured. In this chapter, three methods to quantify the SC amount removed on each tape are compared: the gravimetric approach, infrared densitometry and a novel imagine technique.

Methods:

After tape-stripping human subjects, the SC amount per tape was determined gravimetrically and optically by both infrared densitometry and a novel imaging technique. A comparison between different techniques was made on samples collected at different times of the year, different body sites and using different adhesive tapes.

Results:

An excellent linear correlation between the infrared densitometry and imaging methods was observed, confirming that the latter technique primarily evaluates the amount of SC via its protein content; the greyscale measurement obtained may be converted, therefore, to a mass of protein per unit area of SC. A significant linear correlation between the imaging and gravimetric techniques was also obtained. The imaging approach was more reproducible than the gravimetric method. Despite variation between subjects and at different times of the year, the imaging approach was able to predict SC weight in reasonable agreement with the gravimetric method. Furthermore, the imaging method means is not sensitive to sebaceous lipids and is therefore more reliable when used to quantify SC thickness at skin sites where high levels of sebaceous lipids are found (e.g., forehead).

Conclusion:

The novel imaging method is a fast, simple and reproducible technique for the convenient quantification of SC on tape-strips, and correlates well with measurements made using the

gravimetric approach and infrared densitometry. The imaging approach, with further validation, may offer a better standard method for SC quantification in the future.

1. Introduction

Assessment of bioequivalence is essential for the licensing of generic drug products. For oral medication, bioavailability is typically defined by the rate and extent at which a drug reaches the general circulation. However, dermatological drug products are designed to exert a local effect with minimal systemic uptake. Therefore, systemic availability may not reflect local cutaneous bioavailability and drug levels should ideally be sampled, therefore, within the skin.

1.1 Need for accurate SC measurements

Since the stratum corneum (SC) is the considered to be the principal barrier to drug penetration, it may be assumed that drug levels in this membrane post-application of a drug-containing formulation should be correlated with those in the underlying tissues, and, perhaps, even in the blood stream [1]. Tape stripping involves sequential removal of layers of the SC with adhesive tapes upon which the drug concentration as a function of position within the SC may be assessed. The SC concentration-time profiles obtained by tape-stripping can be used to derive dermatopharmacokinetic (DPK) parameters.

However, removal of SC by tape-stripping is variable. The inconsistency is introduced by different operators, tape adhesiveness, variable pressure of tape application to the skin, SC cohesiveness and even the rate at which the tape is removed. Therefore, it is essential to measure the amount of the SC removed on each tape to relate the mass of drug extracted to a 'volume' of the matrix. The depth within the SC sampled by each successive tape strip can then be estimated.

1.2 Current methodology

Traditionally, each tape-strip is weighed before and after SC removal to determine the amount of tissue removed from the difference. The mass of SC removed on a tape-strip (M_{SC}) is related to the corresponding thickness (l) of the barrier by Eq.1:

$$M_{SC} = \rho_{SC} \, A \, l \qquad\qquad \text{(eq.1)}$$

where A is the SC area stripped and ρ_{SC} is its density (reported to be $1g/cm^3$,[2]). By performing concomitant measurements of transepidermal water loss (TEWL) during the tape-stripping process at an adjacent site, an estimate for the total SC thickness can be obtained [3]. However, the weighing procedure is far from ideal. The measured masses may be misleading due to static electricity on the tapes, the uptake of formulation excipients, etc.

Progress has been made in the evaluation of SC mass removed on each tape. Since ~80% of the SC mass is protein, primarily keratin [4], a protein assay is logically a useful approach to quantify SC on tape strips. A linear correlation between the SC amount determined by protein assay after extraction and the quantity of SC weight on each tape strip has been reported [5-6]. However, because of the procedure involved in the protein assay, it is not always possible to quantify the drug in the same SC sample, the analytical and stability problems being incompatible [5].

The difficulty has been circumvented by the introduction of optical methodology whereby the absorbance and scattering caused by SC on a tape-strip is determined at a specific (typically UV or visible) wavelength and has then been calibrated against the protein assay. Pseudo-absorption measurements at 430 nm resulted in an r^2 of 0.75 when used in this way [7]. However, the instrument used was expensive, non-portable and the handling of tape-strips in the measurement zone was difficult. More recently, an even better linear correlation ($r^2=0.85$) with SC protein has been obtained with the absorbance of SC on the tape-strip at ~850nm [8]. In this case, a compact, infrared densitometer was used in conjunction with specific D-Squame$^{®}$ tapes. The use of these pre-cut tapes restricts the shape and size of tape-stripping sites, and prevents other, cheaper, commercially available tapes being employed.

Here, a different optical method has been used, with which high resolution images have been taken under controlled conditions. The images are quantified by greyscale values which may be measured and analysed.

According to the Beer-lambert Law, the optical absorbance of a sample (Abs) is given by:

$$Abs = -Log\ (I/I_0) = \alpha l \qquad\qquad (eq.2)$$

where I_0 and I are the intensities of the incident, and transmitted light, respectively, α is the

absorption coefficient of the sample and l is the path length of the light through it.

The greyscale values of tapes which have been used to strip the SC reflect the manner in which light transmission through the tape is attenuated by the tissue. Hence,

$$Abs_{SC} = -Log (G_{SC}/G_{tape}) = \alpha_{SC}l \qquad (eq.3)$$

where G_{SC} is the mean greyscale value of tape onto which SC has been stripped, G_{tape} is the mean greyscale value of a blank tape, and α_{SC} is the absorption coefficient of the SC, l is the thickness of the corneocytes on the tape.

2. Material and methods

2.1 Materials

Three different tapes were compared: (a) D-Squame$^®$ disks (Cuderm Corporation, Dallas, TX, USA) with a diameter of 2.2 cm and an area of 3.8 cm^2 were used in the infrared densitometer measurements; (b) Scotch® Book tape 845(3M, St Paul, MN), 2.5x4 cm^2; and (c) Permacel J-LAR ® clear to the core tape (Permacel, Wisconsin, USA), 2.5x3.5 cm^2. All tapes were stored in covered trays and were used in both the gravimetric and imaging methods for quantification of the SC.

2.2 Subjects

Ethical approval was granted by the University of Bath Research Ethics Committee for Health and written, informed consent was obtained from all subjects. No volunteers had any history of dermatological disease, and restrained from recent topical formulation use. Details of the volunteers who participated in different parts of the study are summarised in Table 1.

Table 1: Volunteer details in each study.

Experiment Series	Number of volunteers	Time of year	Age (years)	Tape Used
1	12	Sept	24-42	D-Squame® disks
2	6	July & Aug	25-31	Scotch® Book tape 845
3a	6	May & June	25-30	Permacel J-LAR ®
3b	6 (same volunteers as experiment series 3a)	Jan & Feb	25-30	Permacel J-LAR ®
4	6	Jan -Mar	20-36	Permacel J-LAR ®

2.3 Tape stripping

For infrared densitometer measurements (Experiment Series 1), D-Squame® disks were applied to the skin under 225 g/cm^2 of pressure for 5 s. The device used to apply the pressure was supplied by the D-Squame® manufacturer. The sequential tape stripping (20 times) was performed on the mid ventral forearm. Tape-stripping using Scotch® Book tape 845 (Experiment Series 2) and Permacel J-LAR® tape (Experiment Series 4) was also performed on the ventral forearm. To examine the SC at different body sites, tape-stripping using Permacel J-LAR® tape was performed on the ventral forearm and on the forehead on two separate occasions (Experiment Series 3a&3b). ATR-FTIR spectra were recorded sequentially during tape-stripping to assess SC lipid content and organisation (Experiment series 3b).

The SC was progressively removed by the repeated application and removal of adhesive tape-strips. A template with a central hole (a 2x3 cm^2 square hole for Experiment Series 2, a 2x2 cm^2 square hole for Experiment Series 3 and a circle of 1.54 cm diameter for Experiment Series 4) was first affixed to the skin with self-adhesive medical tape (Curafix H, Lohmann & Rauscher,Rengsdorf, Germany) to ensure that all tape-strips were taken from exactly the same site. The tapes were applied with pressure from a weighted roller and then swiftly removed. TEWL measurements were recorded (AquaFlux V4.7, Biox Systems Ltd., London, UK) before and after each tape strip, and tape-stripping was stopped when TEWL reached 3-4 times the initial value, at which point approximately 75% of the SC had been removed [9].

2.4 Infrared densitometry

The pseudo-absorption of SC protein on the D-Squame® disks was determined using an infrared densitometer (Figure 1, SquameScan TM 850A®, Heiland electronic, Wetzlar, Germany). The disks were placed into a well, adhesive side up, exposing the measured area (1.8 cm^2, i.e., about 45% of the disk) of the densitometer. Prior to the experiment, the instrument was calibrated against a blank sample to read 0%.

Figure 1: The infrared densitometer SquameScan^{TM} 850A [8].

2.5 Gravimetric method

Tapes were stored for at least 12 hours before being weighed. Static electricity was discharged from the tapes prior to weighing (Figure 3, R50 discharging bar and ES50 power supply, Eltex Elektrostatik GmbH, Weil am Rhein, Germany). The tapes were weighed, before and after stripping, using a microbalance with precision of 0.1 μg (Sartorius SE-2F, Sartorius AG, Goettingen, Germany). The mass difference between two weights was taken as the mass of SC removed on the tape-strip.
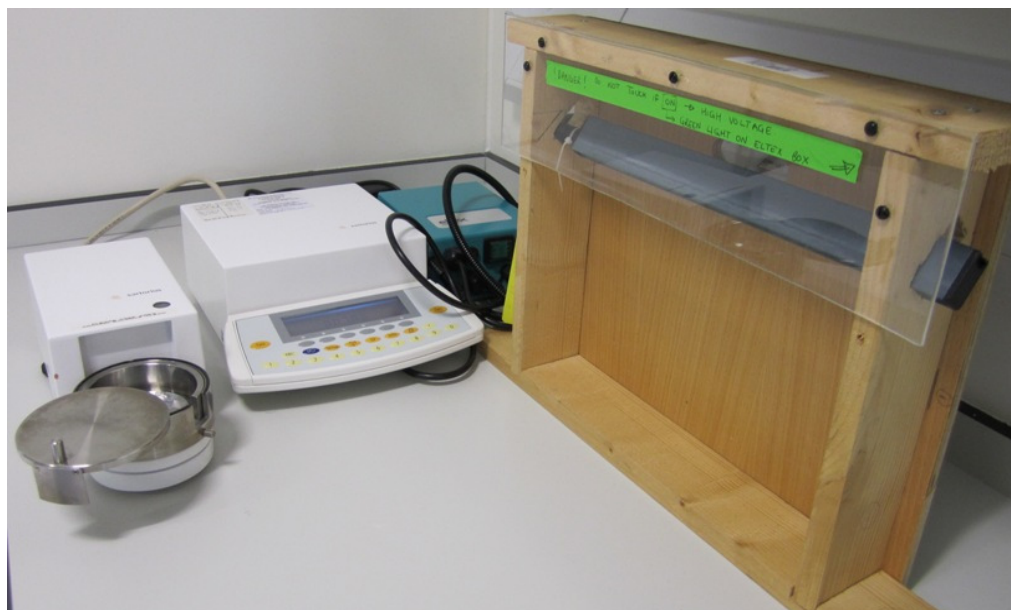
Figure 2: Sartorius balance and discharging bar

2.6 Imaging method

The tapes were also photographed using a Coolscan V slide scanner (Nikon UK Limited, Kingston upon Thames, UK) at a resolution of 4000 pixels per inch (157.5 pixels/mm) according to the method described by Russell [10]. The tape-striped area was cropped in the centre of each image and subjected to a full scan. The images were analysed by ImageJ (Rasband,W.S., U.S. National Institutes of Health, Bethesda, Maryland, USA; freeware from http://rsb.info.nih.gov/ij/) to obtain mean greyscale values. Each image was assigned an overall greyscale value (16 bit) in the range 0-64608, where 0 and 64608 represent black and white, respectively. The mean greyscale over all pixels was calculated by ImageJ; the average mean greyscale obtained from six blank tapes served as the control.

Figure 3: Nikon Coolscan V with slide feeder.

2.7 Attenuated total reflectance-fourier transform infrared spectroscopy (ATR-FTIR) measurements

Equipment

A PerkinElmer (Waltham, Massachusetts, USA) Spectrum 100 FT-IR spectrometer was used to record the *in vivo* measurements. The spectrometer was equipped with a universal, single-bounce ATR accessory with a round diamond crystal (2mm diameter).

Experiments

In Experiment Series 3b, the skin site (either forearm or forehead) was cleaned gently with an alcohol wipe and three IR spectra (16 scans each) were recorded. The SC was then progressively removed by the repeated application and removal of adhesive tape-strips. On the forearm, 3 replicate IR spectra were recorded after removing each of the first 6 tapes, and then after every other tape thereafter. On the forehead, 3 replicate IR spectra were recorded after removing each tape.

Spectral analysis

FTIR spectra were collected in the frequency range 4000-400 cm^{-1}. The frequency of the asymmetric (~2920cm^{-1}) and symmetric (~2850cm^{-1}) CH$_2$ stretching absorbances were determined from the first-order derivative of the spectrum using Spectrum^{TM} Express software. The normalised areas under both lipid stretching absorbances were calculated as previously described [11].

2.8 Statistics

All statistical tests, as detailed in the results below, were performed with Prism® version 5 (GraphPad Software, CA, USA).

3. Results

3.1 Correlation between greyscale and infrared densitometry

Infrared densitometry measures absorbance as the percentage of incident light absorbed by the sample $((1-I/I_0) \times 100)$; for SC, 60-98% of the incident radiation passes through without absorption, A linear correlation between these measurements and the greyscale values from the imaging method may therefore be anticipated. The results in Figure 4 show that this is indeed the case.
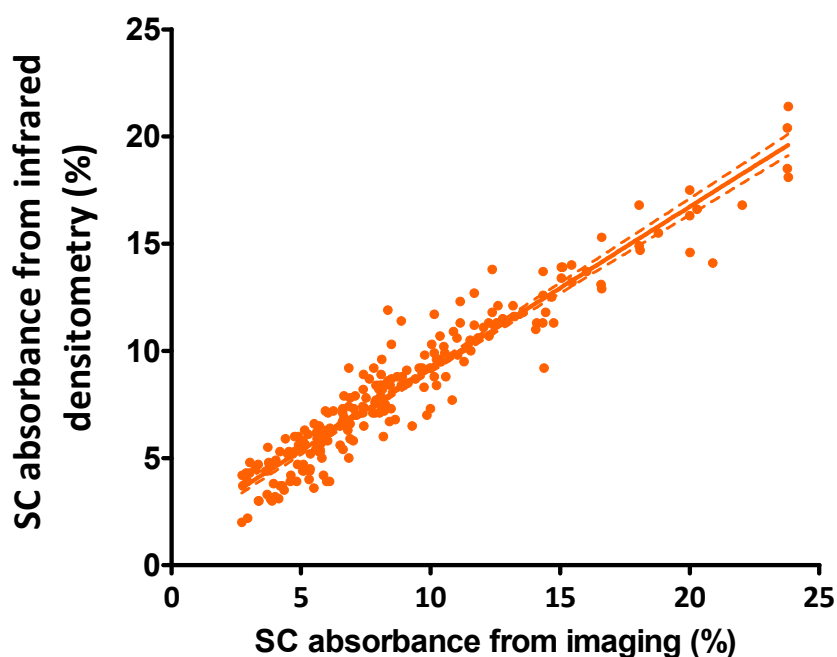
Figure 4: Linear regression of SC absorbance from infrared densitometry with that from imaging $(y=0.76x+1.56; r^2=0.91)$

The outcome, of course, is not surprising, since both methods measure light absorbance. The principal difference is the wavelength of the incident light, and this is reflected in a value of regression gradient which differs from 1. However, the excellent linearity of the regression means that the greyscale imaging method might also be used to derive the SC protein content.

3.2 Correlation between greyscale and weight on forearm.

The gravimetric and imaging methods were compared (Figure 5). All measurements were made within one day of tape-stripping.
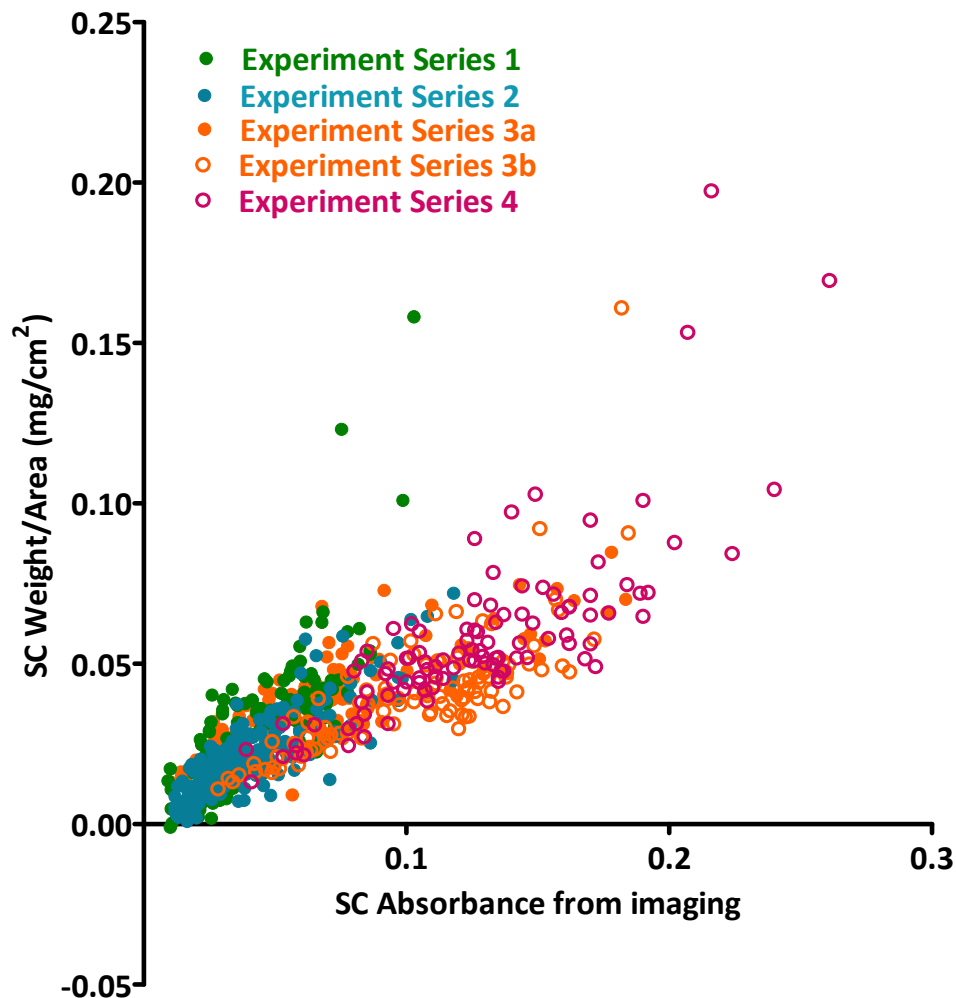
Figure 5: Correlation of SC quantification by weighing and imaging methods. The results from the different series of experiments performed are plotted together on the graph. A linearly significant correlation was found by a 2-tail Pearson's Correlation test ($R_{pearson}$ = 0.80, p<0.0001, n=801).

Seasonal changes affect tape-stripping

It is interesting to note that season affects tape-stripping in two different ways:

a) In the summer, the slope of SC weight per unit area versus absorbance is steeper than in winter, an effect apparent on both the forehead (Figure 6a) and forearm (Figure 6b). The precise reason for this observation is not known but suggests that the SC retains non-

absorbing materials more efficiently in the summer month.
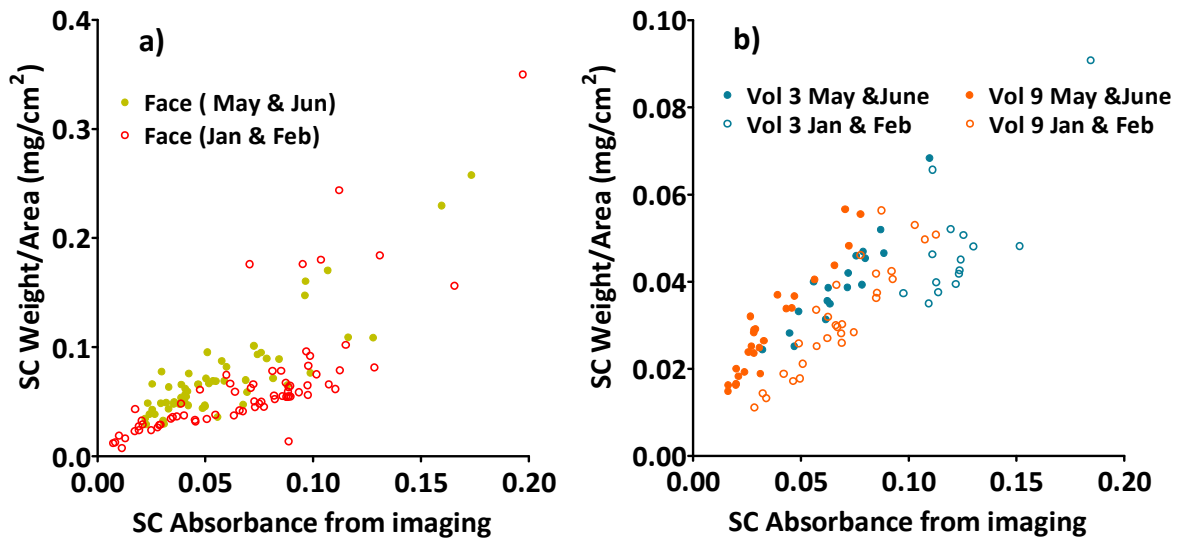
Figure 6: Seasonal changes affect the correlation between SC quantification by gravimetric and imaging methods at both forehead and forearm sites.

b) SC was more easily removed in the winter (Figure 6b). Using the same tape and the identical experiment method, most of the tapes removed more than 0.04mg/cm^2 SC in winter without any obvious dryness or skin flaking observed, while a much lower amount of SC was taken off in the warmer part of the year. The mean SC removed by an individual tape was 0.049 ± 0.025 mg/cm^2 in winter and 0.028 ± 0.018 mg/cm^2 at other times. This trend has also been reported by Voegeli et al [12], using infrared densitometery.

3.3 Prediction of SC weight removed using the imaging method on forearm skin.

Here, the potential to predict SC weight from greyscale measurements was examined. All the data points (n=678) obtained from healthy skin on the ventral forearm were randomly assigned to two groups: the first group (n=339) acted as a "training set" to develop a linear correlation. Six outliers with more than 0.15 mg/cm^2 of SC on the tapes were excluded. These outliers corresponded to the first tape removed during the stripping process and the exceptionally heavy weights observed may have been caused by contaminants present on

the skin surface. The subsequent correlation is summarised in Figure 7.
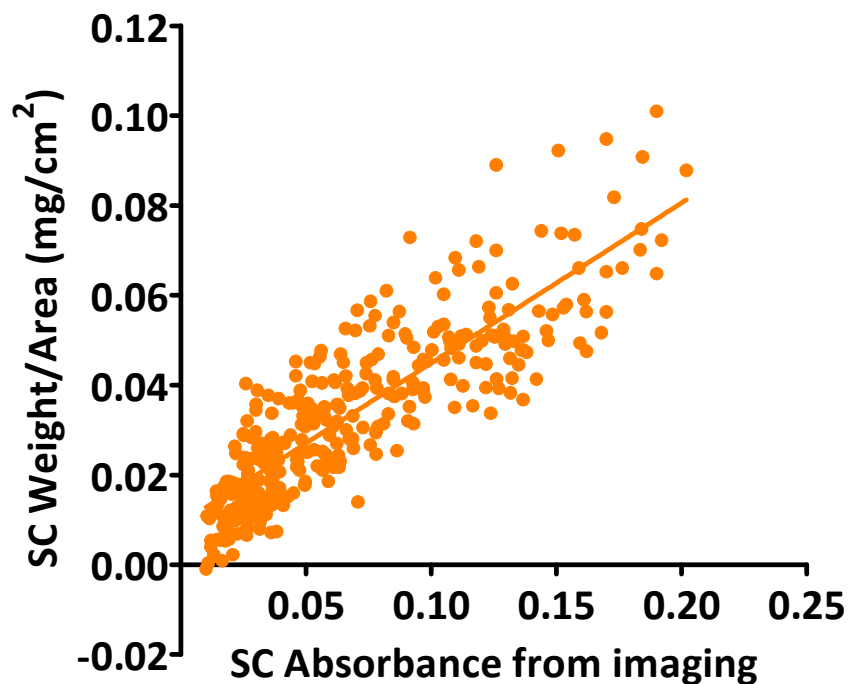
Figure 7: Overall linear regression of tape stripping data in the "training set": y= 0.36x + 0.01; r^2=0.73. 95% confidence intervals for the slope and intercept were 0.33-0.38 and 0.007-0.011, respectively.

Using the slope and intercept from the "training set" correlation, the SC weights on the other 339 tape-strips were then predicted and compared with the actual, experimentally determined values.
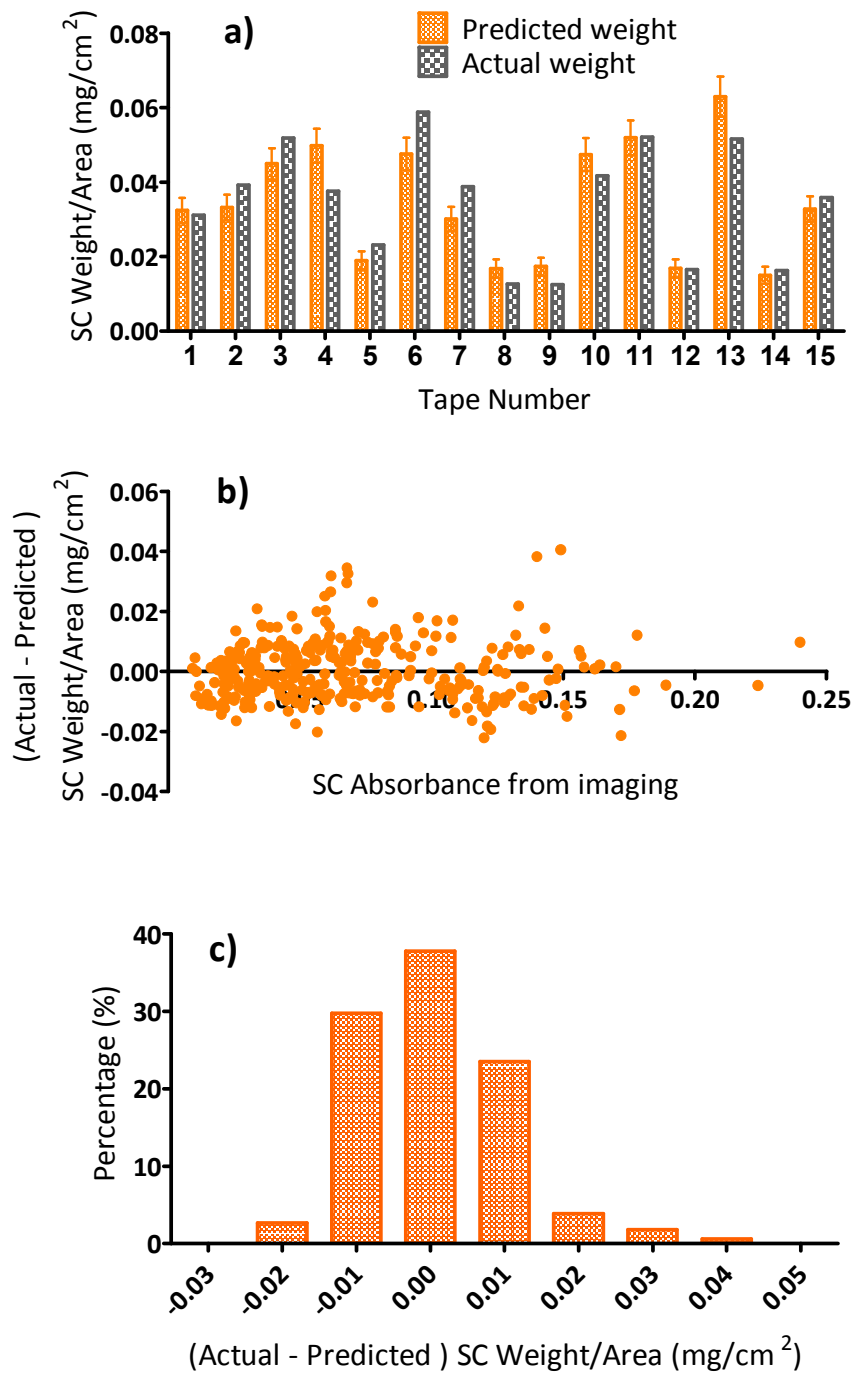
Figure 8: Comparison of predicted to actual SC weights on the "test" tape-strips (n=339): a) presented as a function of tape strip number for both predicted weight (mean ± 95% confidence interval) and actual weight; b) differences between actual and predicted values plotted as a function of SC absorbance determined by the greyscale imaging method; and c) in terms of a percentage distribution of the differences.

Figure 8a shows, as a function of tape-strip number, the agreement between actual and

predicted SC weights based on the correlation from the "training" data set. Good overlap is observed with no systemic over- or under- prediction. This is reinforced in Figure 8b and 8c which show that differences between actual and predicted weights, expressed in absolute terms, or as a percentage of distribution counts, were more or less normally distributed with respect to SC absorbance measurements and the amount of SC in the tapes.

The errors between the linear regression fitting and the experimentally determined weight in the remaining group (n=339) are calculated as:

Prediction error = "Actual Weight/A" – "Predicted Weight/A"   (eq.4)

The overall, mean (±SD) prediction error was 0.00116 ± 0.01279 mg/cm^2. It follows that there is potential for the greyscale imaging technique to be used to predict the amount of SC removed on a tape-strip.

3.4 Method Precision

In order to evaluate precision, both gravimetric and imaging methods were used to quantify the SC 5 times a day for 4 consecutive days on 15 tapes (Permacel J-LAR® tapes and D-Squame® disks).

<u>Gravimetric method precision</u>

These 15 tapes were weighed 5 times each day for 4 consecutive days without stripping. Figure 9a shows the deviations of single measurement from median weight of each tape. As expected the difference (0 ± 0.016mg) is normally distributed around zero.
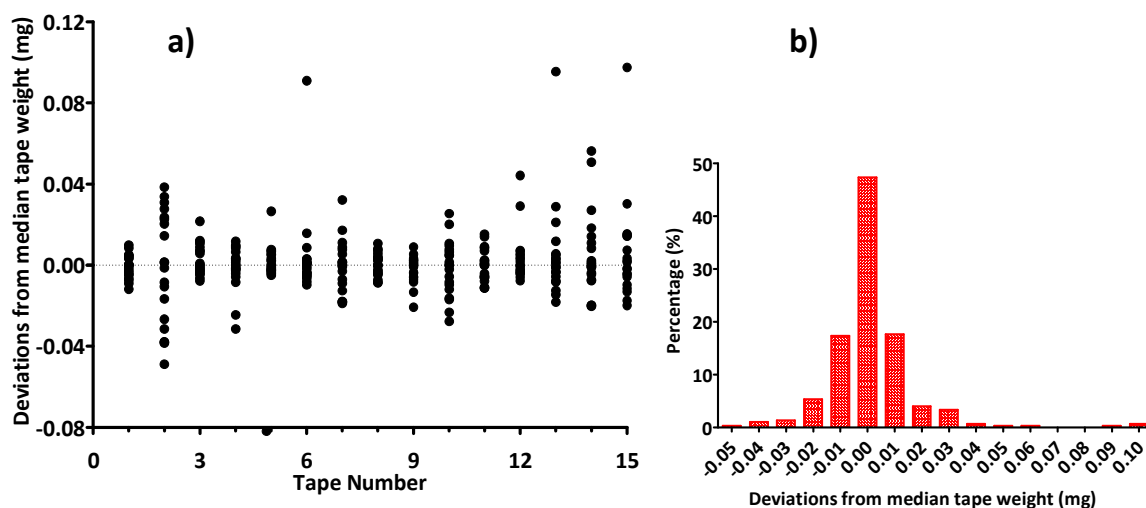
Figure 9: Error associated with balance (a) as a function of tape-strip number, and (b) in histogram form.

In analytical chemistry, limit of detection (LOD) is defined as 3 x standard deviation of the blank and the limit of quantification (LOQ) is defined as 10 x standard deviation of the blank. Thus the LOD and LOQ for the balance is 0.048 mg, 0.16 mg respectively. However, the gravimetric method requires two measurements. From a statistical point of view, there are two totally mutually independent events each with a variance. Therefore, the variance of the gravimetric measurement is twice the variance of the balance. The actual standard deviation of the gravimetric method is thereby $\sqrt{2}SD_{blank}$, and LOD and LOQ of gravimetric method is 0.068mg, 0.226mg respectively (Table 2).

Imaging method precision

The same tapes were optically assessed using the Coolscan slide scanner on 5 separate occasions a day for 4 consecutive days after stripping. ImageJ was then used to obtain a mean greyscale value. The corresponding control greyscale value (G_0) was determined by scanning six blank tapes in the same way. The absorbance error is 0.0000 ± 0.0012 (Figure 10), and could be converted into mg/cm^2 (Table 2) using the model developed above. The imaging method was very precise with very low errors compared to the gravimetric method.
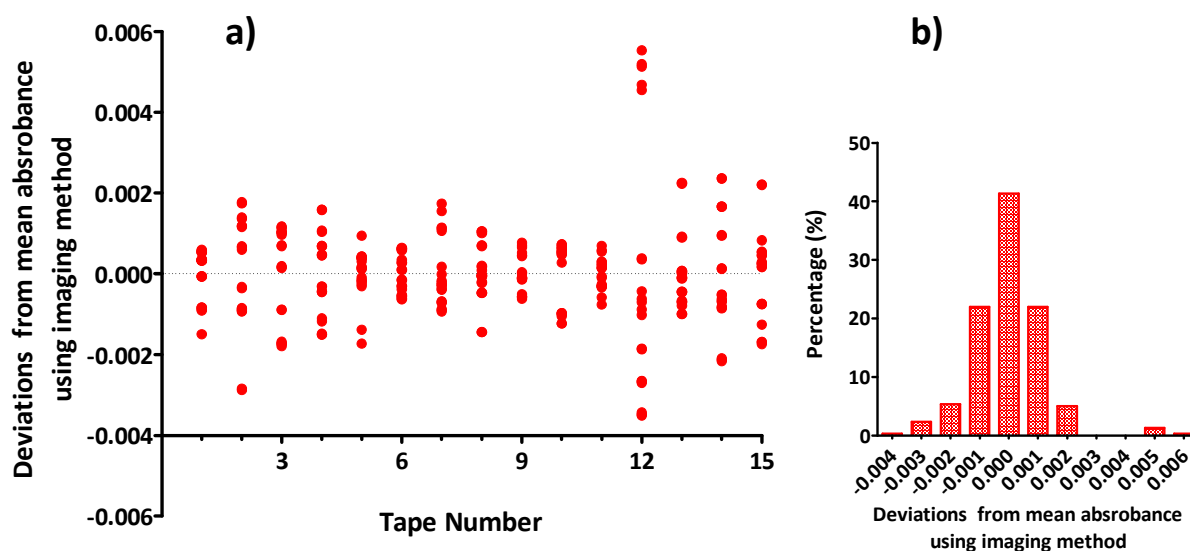
Figure 10: Error associated with the imaging method (a) as a function of tape-strip number, and (b) in histogram form.

Comparing the limits of detection (LOD) and quantification (LOQ) of two method

Table 2: Limits of detection (LOD) and quantification (LOQ) of imaging and gravimetric methods.

	Imaging		Gravimetric	
	Spring/Summer	Winter	Spring/Summer	Winter
LOD	0.00105 mg/cm^2	0.00105 mg/cm^2	0.068 mg	0.068 mg
LOQ	0.00349 mg/cm^2	0.00349 mg/cm^2	0.226 mg	0.226 mg
Average SC removed (mg/cm^2)	0.028	0.049	0.028	0.049
Tape-stripping area required to achieve LOD (cm^2)	-	-	2.43	1.39
Tape-stripping area required to achieve LOQ (cm^2)	-	-	8.07	4.61

The imaging method was more reproducible, with an LOQ much lower than the average amount of SC removed. In contrast, the gravimetric method was inherited with larger error meaning that greater area of SC need to be stripped to overcome the variability; clearly, such large area may not always be feasible in all experimental situations.

3.5 Percentage error of different methods

Assuming normally distributed data, the percentage error (%) of a particular method equals $\{(100 \times 1.96 \times SD)/\bar{x}\}$ where SD and $\bar{x}$ are the standard deviation and mean of the population, respectively.

Table 3: Errors accounted with the different methods

Mean tape-stripping area (cm^2)	3.95	
Mean SC weight (mg)	0.035 ± 0.022	
Prediction error (mg/cm^2)	0.00116 ± 0.01279	283%
Gravimetric method error (mg)	0 ± 0.0226	127%
Imaging method error (mg/cm^2)	0 ± 0.00066	14.8%

Table 3 reveals large percentage errors and a more detailed analysis is required to understand their origin.

a) Equipment error

Repeated measurements on the same tape-strips with the balance and scanner employed in this work clearly demonstrate the greater error introduced by the former compared to the latter. In validating new method (i.e., imaging) against the gravimetric approach, it follows that the prediction model derived necessarily incorporates the inherently poorer reproducibility of the gravimetric technique.

b) Intrinsic variability of the samples

As the principal light absorbing components in the skin are keratin [8] and melanin the imaging method primarily reports on the amount of protein present. In contrast, the

gravimetric technique measures not only protein, but also the presence of lipids and other substances, which absorb minimally. These differences result in inter-subject variability (Figure 11a) and to quite noticeable seasonal effects (Figure 11b). Thus it may be sensible to use a calibration specific for a particular time of year, and to pay careful attention when integrating anatomic sites (such as the forehead) when the lipid weight fraction of the SC is relatively high. This point is described below.
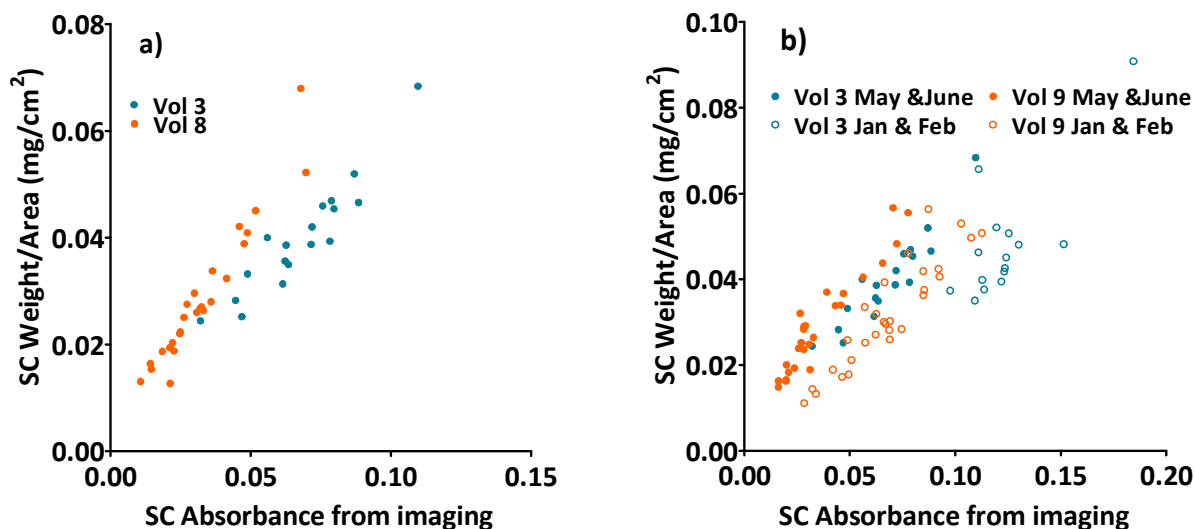
Figure 11: Intrinsic variability between subjects (a) and at different times of the year (b)

c) Error as a function of tape-stripping area

Establishment of a predictive model for the imaging measurement of SC amount removed by tape-stripping is more accurate when collaborated against the gravimetric approach using larger tape-strip areas. Extrapolation to smaller areas can then be undertaken with greater confidence.

3.6 Imaging method better quantifies SC on the forehead

Figure 12 compares gravimetric and imaging method to quantify SC removed from the forearm and forehead. The apparent weight of material from the forehead (at a particular greyscale value) was consistently greater than that from the forearm, an anomalous outcome given that the SC on the forehead is generally recognised to be thinner than that

at most other body sites. The logical interpretation of this observation is that the copious amount of sebaceous lipids secreted on the forehead are significantly contributing to the apparent SC weight measured gravimetrically but that these lipids are "transparent" to the imaging method. Indeed, TEWL measurements confirm this analysis, the value on the forehead being double that on the forearm (Table 5). Consistent with these measurements is that, on average, 21 tape-strip had to be removed from the forearm to provoke in 3-4 fold increase in TEWL, while only 11 were needed on the forehead (Table 5).
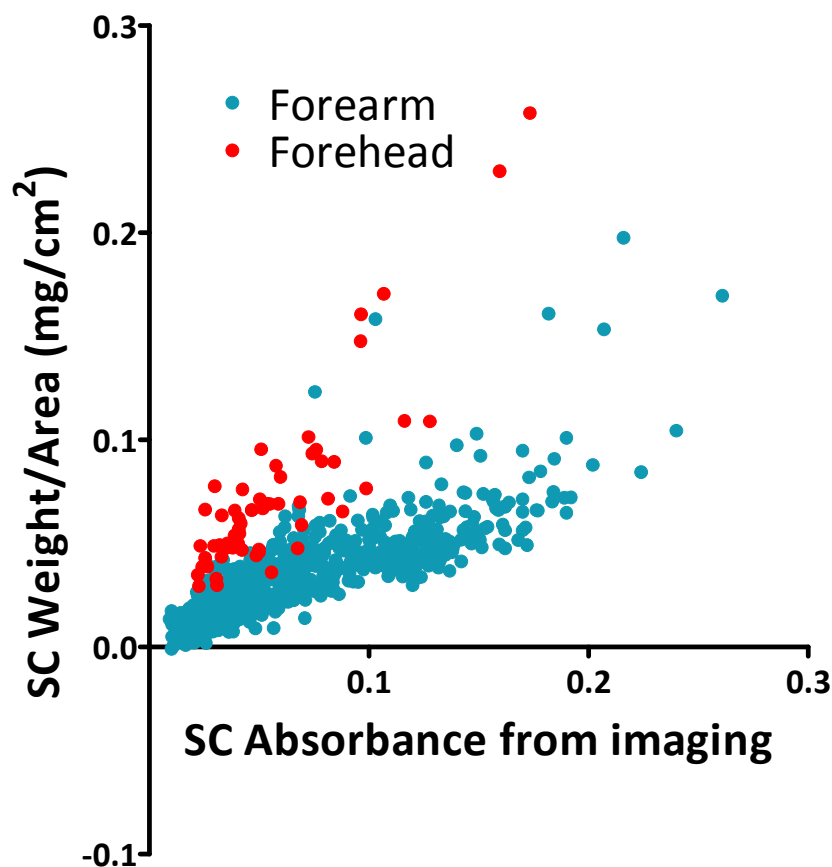
Figure 12: Correlation of SC measurements by weighing and imaging methods on both forearm and forehead.

Thickness of SC on forearm and forehead

When the gravimetric and imaging data were used to determine SC thickness on the forearm, there was complete agreement (see Table 4). In contrast, the imaging method assessed SC thickness on the forehead to be approximately 50% of that on the forearm (whereas the gravimetric approach found no difference) (Table 4). The individual data are summarised in Figure 13a. The gravimetrically determined SC weights removed are shown

in Figure 13b and reveal a very significant difference in particular is the amounts removed from the forehead and forearm on the first tape-strip (p=0.0015, 2-tailed t-test), again strongly implicating the substantial presence of sebaceous lipids.

Table 4: TEWL results and estimated apparent SC thickness (mean ± SD) on forehead and forearm.

	Forearm		Forehead	
Initial TEWL (mg/cm^2/h)	11. 6±2.3		20.2±4.8	
Tapes required to reach ~3-4X initial TEWL	21		11	
	Gravimetric	Imaging	Gravimetric	Imaging
Predicted SC thickness (µm)	9.6±2.7	8.9±2.5	9.4±1.9	4.5±1.0
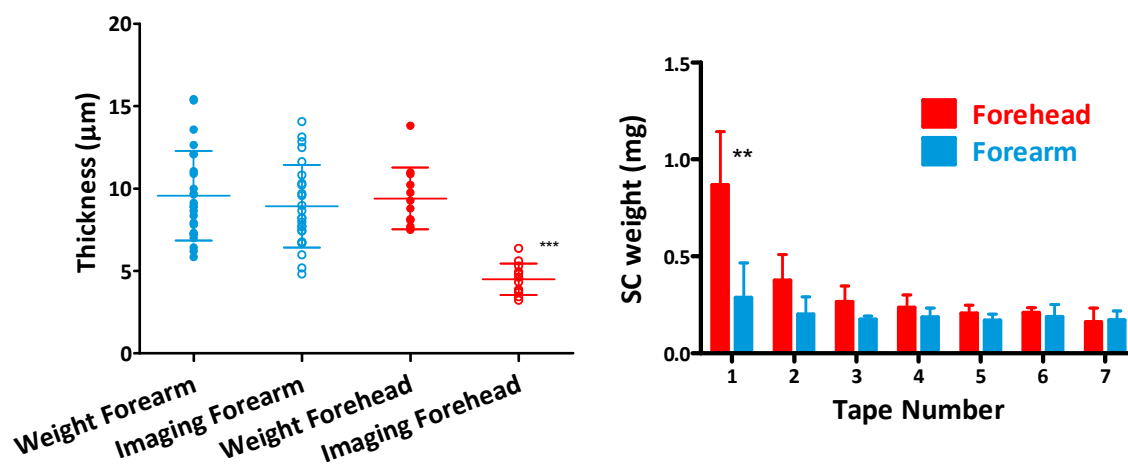
Figure 13: a) Predicted SC thickness from gravimetric and imaging methods on forearm and forehead. The forehead SC thickness measured by imaging method is significantly different from all others (P<0.0001, 1-way ANOVA followed by Bonferroni's multiple comparison test). b) Weights (mean± SD) of SC removed as a function of tape-strip number on forehead and forearm. The weight SC removed from the forehead on the front tape is significantly greater (p=0.0015, 2-tailed unpaired t test) than that from the forearm.

IR absorbance of lipids (CH$_2$ stretching absorbance)

To confirm the interference of sebaceous lipids in the gravimetric method, IR spectra were taken while tape-stripping the two sampling sites. FTIR spectroscopy has been used to report on biomembrane lipid ordering through the C-H stretching absorbance from the

methylene groups of the lipid acyl chains. The CH_2 stretching absorbance undergoes a blue shift, i.e., a shift to higher wavenumber, when the degree of lipid disorder increases.

Figure 14 shows that both asymmetric (~2920cm^{-1}) and symmetric (~2850cm^{-1}) CH_2 stretching absorbances occurred at higher wavenumbers at the skin surface (i.e., before tape-stripping) at both skin sites a feature which has been attributed to the contribution of sebaceous lipids [11]. Both CH_2 stretching absorbance frequencies pre-tape-stripping are significantly greater than those after removal of SC ($p<0.0001$, repeated measure one-way ANOVA followed by Bonferroni's multiple comparison test). SC lipids on the forehead were much less ordered than those on the forearm both at the surface and throughout the SC ($p<0.0001$, paired t-test).

The normalised area under the lipid peaks (Figure 14c) were calculated as previously described [11], and suggested a higher amount of lipid on the forehead, especially near the surface. The difference between forehead and forearm was significant (repeated measure one-way ANOVA followed by Bonferroni's multiple comparison test ($p<0.0001$)).

In addition, as demonstrated in Figure 15, a significant correlation ($p<0.0001$, Spearman correlation test) was found between lipid amount on the forehead determined spectroscopically and the weight of SC on the corresponding tape-strips. This provides further proof that the gravimetric method is not a useful tool with which measure the amount of SC on the forehead removed by tape-stripping. In contrast, the imaging method, as described above is not sensitive to the sebaceous lipid contamination and successfully reveals that forehead SC is indeed thinner than that on the forearm.
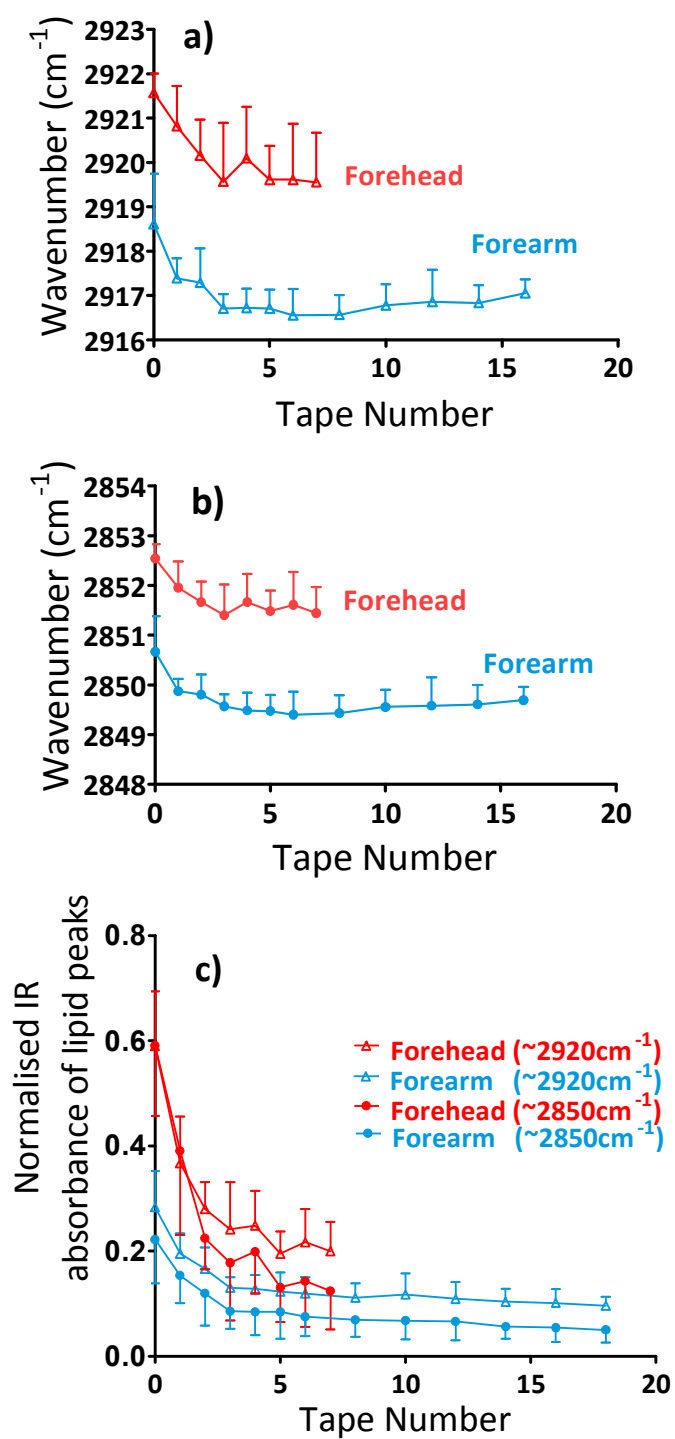
Figure 14: (a) CH_2 asymmetric (~2920cm^{-1}) and (b) symmetric (~2850cm^{-1}) stretching absorbances as a function of tape-strip number (mean ± SD, n=6). (c) Normalised areas under the CH_2 asymmetric and symmetric stretching absorbances as a function of tape-strip number (mean ± SD; n=6)
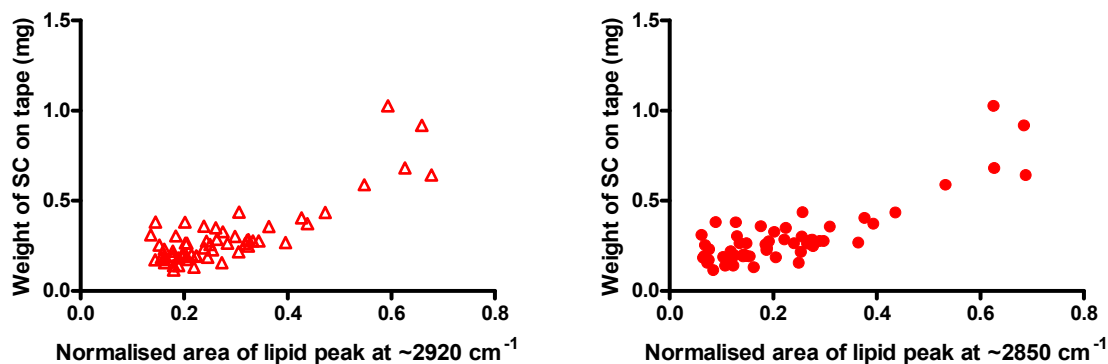
Figure 15: Correlation of SC weights removed on tape-strips, with normalised areas under the C-H absorbance (at ~2920cm^{-1} and 2850cm^{-1}) determined by FTIR. Both correlations are significant (p<0.0001, 2-tail) with non-parametric Spearman correlation coefficients of 0.62 and 0.65, respectively.

4. Time investment

The gravimetric method is the most costly in terms of time. Each tape has to be weighed twice and static charges on the tapes must be eliminated. The overall time required is variable but averages out at about 3-4 minutes per tape. Imaging and infrared spectrometry are faster, requiring 1-2 minutes for each tape. A sample image taken by the novel imaging method is shown below.
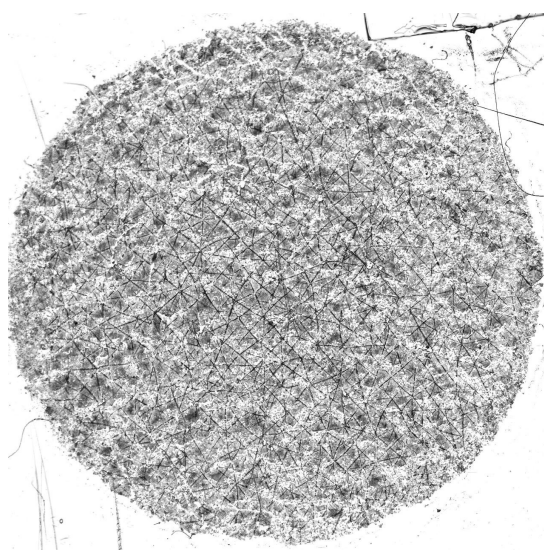
Figure 16: A sample image of the tape taken from Nikon scanner.

5. Conclusions

A novel imaging method, with which to quantify SC, is introduced that is fast, simple, reproducible and with a good signal to noise ratio. The technique correlates well with measurements made using other techniques, such as gravimetric approach and infrared densitometry [8] .

Correlation with infrared densitometry confirms that the imaging approach primarily evaluates the amount of SC via its protein content; the greyscale measurement may be converted, therefore, with a mass of protein per unit area of SC.

The feature of the imaging method means that it is not subject to interference or artefact when attempting to quantify SC thickness at skin sites where high levels of sebaceous lipids are found (e.g., on the forehead) and which can contribute significantly to the apparent SC weight removed by tape-stripping. The imaging approach, with further validation, may offer a better standard method for SC quantification in the future.

6. Reference

1. Herkenne C, Alberti I, Naik A, Kalia Y, Mathy F-X, Préat V, and Guy R, *In vivo methods for the assessment of topical drug bioavailability.* Pharmaceutical Research, 2008. **25**(1): p. 87-103.

2. Anderson RL and Cassidy JM, *Variations in physical dimensions and chemical composition of human stratum corneum.* J Invest Dermatol, 1973. **61**(1): p. 30-32.

3. Russell LM, Wiedersberg S, and Delgado-Charro MB, *The determination of stratum corneum thickness An alternative approach.* European Journal of Pharmaceutics and Biopharmaceutics, 2008. **69**(3): p. 861-870.

4. Matoltsy AG and Balsamo CA, *A study of the components of the cornified epithelium of human skin.* The Journal of Biophysical and Biochemical Cytology, 1955. **1**(4): p. 339-360.

5. Dreher F, Modjtahedi BS, Modjtahedi SP, and Maibach HI, *Quantification of stratum corneum removal by adhesive tape stripping by total protein assay in 96-well microplates.* Skin Research and Technology, 2005. **11**(2): p. 97-101.

6. Dreher F, Arens A, Hostýnek J, Mudumba S, Ademola J, and Maibach H, *Colorimetric method for quantifying human Stratum corneum removed by adhesive-tape stripping.* Acta Derm Venereol, 1998. **78**(3): p. 186-189.

7. Bornkessel A, Flach M, Arens-Corell M, Elsner P, and Fluhr JW, *Functional assessment of a washing emulsion for sensitive skin: mild impairment of stratum corneum hydration, pH, barrier function, lipid content, integrity and cohesion in a controlled washing test.* Skin Research and Technology, 2005. **11**(1): p. 53-60.

8. Voegeli R, Heiland J, Doppler S, Rawlings AV, and Schreier T, *Efficient and simple quantification of stratum corneum proteins on tape strippings by infrared densitometry.* Skin Research and Technology, 2007. **13**(3): p. 242-251.

9. Kalia YN, Alberti I, Sekkat N, Curdy C, Naik A, and Guy RH, *Normalization of Stratum Corneum Barrier Function and Transepidermal Water Loss In Vivo.* Pharmaceutical Research, 2000. **17**(9): p. 1148-1150.

10. Russell L, *Dermato-pharmacokinetics: an approach to evaluate topical drug bioavailabilty*, in *Department of Pharmacy and Pharmacology*. 2008, University of Bath: Bath.

11.   Bommannan D, Potts RO, and Guy RH, *Examination of Stratum Corneum Barrier Function In Vivo by Infrared Spectroscopy.* J Invest Dermatol, 1990. **95**(4): p. 403-408.

12.   Voegeli R, Rawlings A, Doppler S, Heiland J, and Schreier T, *Profiling of serine protease activities in human stratum corneum and detection of a stratum corneum tryptase-like enzyme.* International Journal of Cosmetic Science, 2007. **29**(3): p. 191-200.

Chapter 3: Amino-acid-derived components of natural moisturising factor in human stratum corneum *in vivo* extraction and quantification following tape-stripping and reverse iontophoresis.

Abstract

Purpose:

To employ tape-stripping and reverse iontophoresis, two minimally invasive tools, for the extraction and subsequent analysis of natural moisturising factor (NMF) within human stratum corneum (SC) *in vivo*.

Methods:

NMF components were extracted from human SC (n= 6 healthy volunteers) following repetitive tape-stripping. To quantify the amount of skin on each tape, the tapes were both weighed and optically scanned. On a contralateral site, reverse iontophoresis and passive diffusion were used to extract NMF from the skin over a 4-hour period. All extracted samples were analysed by liquid chromatography mass spectrometry (LCMS) to identify and quantify the amounts of 21 components of NMF.

Results:

Charged NMF components were extensively extracted by reverse iontophoresis as compared to passive diffusion; in some cases, extraction from beyond the SC was achieved by electrotransport. In contrast, passive and reverse iontophoretic extraction of zwitterionic compounds in NMF did not deplete their SC reservoirs. The two methods used to quantify SC on the tape strips were in good agreement thereby permitting the concentration of NMF, in this tissue to be expressed in appropriate units.

Conclusion:

The results confirm that reverse iontophoresis is a useful minimally-invasive tool, with which to rapidly sample NMF in the SC. Charged components are so efficiently pulled to the surface that there is clearly the potential to draw this species from tissues and other compartments below the SC. For zwitterionic species (predominately amino acids), passive extraction is of similar efficiency to reverse iontophoresis. The essentially non-invasive techniques agree well with tape-stripping in terms of an estimation of the total quantities of many NMF components in the SC.

1. Introduction

Filaggrin is a key protein in the formation of stratum corneum (SC) barrier. A filaggrin mutation is strongly associated with atopic dermatitis (AD) [1-4]. Filaggrin expression is also essential for SC hydration, as it is the precursor protein for the amino-acid-derived components of the natural moisturizing factor (NMF), a complex mixture of low molecular weight humectants.

NMF components absorb atmospheric moisture and dissolve in their own water of hydration. By maintaining the SC hydration, NMF facilitates critical biochemical events including most importantly, the regulation of several corneocyte proteases that are intimately involved in the generation of NMF itself [5]. The majority of the NMF components are amino acids (AAs) derived from filaggrin, while others, such as pyrrolidone carboxylic acid (PCA), citrulline, ornithine and urea, represent further transformed AAs. Not surprisingly, lower levels of NMF have been associated with the filaggrin mutation [6] and implicated in the etiology of several dermatological disorders including ichthyosis vulgaris, atopic dermatitis and allergic contact sensitization [7-8]. However, the down-regulation of filaggrin protein and the subsequent reduction in NMF is also due to inflammation. AD is a T-cell-mediated skin disease, and the primary event is associated with activation of T_h2 cells. Filaggrin deficiency in AD patients can therefore be acquired in part by the overexpression of T_h2 cytokines [9]. Neverthless, measuring the amount of NMF in the skin should be a good indicator of filaggrin expression and by extrapolation the barrier function of skin. The approach may also prove helpful for the early diagnosis of the aforementioned skin disorders.

Furthermore, amino acids (AAs) are essential to life, and imbalance in their systemic levels, due to genetic defects or metabolic problems, may have serious consequences [10]. As a result, the development of tools that can monitor both the systemic and skin levels of AAs would be sensible. Reverse iontophoresis has been used to track non-invasively the levels of endogenous molecules present in the subdermal compartment. Application of the small iontophoretic current facilitates the transport of low molecular weight, polar molecules, such as AAs, across a membrane and this technique has been used in the GlucoWatch® Biographer to monitor blood glucose. Extraction of AAs from the skin using reverse iontophoresis *in vivo* in human has been reported and the presence of a 'skin reservoir' of

NMF components has been confirmed [11-12]. However, some NMF components, like PCA, citrulline and ornithine, which are major constituents of NMF [13], have not been previously studied using reverse iontophoresis.

The amounts of NMF in the skin are also quantified in this work following SC removal using tape-stripping. This procedure progressively removes the SC and allows the spatial distribution of NMF components to be revealed. Quantification of skin on each tape was determined by a traditional gravimetric method and with a novel imaging technique. Correlation between these two approaches was assessed.

In this work, the further application of reverse iontophoresis to determine the amino-acid-derived components of NMF in human SC *in vivo* is investigated. The specific aims were (1) to examine the correlation between NMF measured in SC tape strips and that extracted by passive diffusion and reverse iontophoresis; (2) to examine the extent to which the latter technique is also able to sample subdermal AA concentrations; and (3) to compare the gravimetric and imaging methods for quantifying the amount of SC removed by tape-stripping.

2. Materials and methods

2.1 Chemicals

Sodium azide, NFPA (perfluoropentanoic acid), silver (Ag) wire (>99.99% purity),AgCl (99.999%), acetonitrile and all L-amino acids acids(Asn, Ser, Gly, Asp, Cit, Orn, Gln, Glu, Thr, Ala, Pro, Val, Tyr, Met, Ile, Leu, His, Lys, Phe, Arg, and Trp) were purchased from Sigma-Aldrich Co. (Gillingham, UK). Glycine-D5, Serine-D3, Glutamine-D5 were purchased from Cambridge Isotope Laboratories (Andover,MA). Deionized water (resistivity ≥18.2 MΩ/cm^2) was used to prepare all aqueous solutions (Barnstead Nanopure Diamond^{TM}, Dubuque, IA).

2.2 Human subjects

Six healthy volunteers (1 male, 5 females, aged between 25 and 31 years) with no history of skin disease participated in the study, which was approved by the Bath Local Research Ethics Committee, and provided written consent. Experiments were performed on the ventral forearm. The skin surface was first cleaned gently by an isopropyl alcohol swab (Medi-Swab, Seton Healthcare Group plc, England).

2.3   Reverse iontophoresis extraction

Two glass cells (internal diameter of 1.6 cm , extraction surface 2 cm^2) separated by ~4 cm were fixed to the ventral forearm with silicone grease and medical grade tape (Curafix H, Lohmann & Rauscher,Rengsdorf, Germany). Both cells were filled with 1.6 ml of 20 mM ammonium chloride in 10mM ammonium bicarbonate buffer at pH ~6.7. A direct current of 0.6 mA (i.e., 0.3 mA/cm^2) was applied from a Phoresor II Auto (Iomed, Model No. PM850, Salt lake City, UT) via Ag/AgCl electrodes. The entire contents of the anode and cathode chambers were collected and replaced by an equal volume of extraction solution at 15 and 30 minutes and then every half-hour thereafter for a total extraction time of 4 hours. The collected samples were passed through a sterile syringe filter (Cronus, 0.45 μm, 4 mm diameter, SMI-LabHut Ltd, Gloucester, UK) and stored in the freezer at -20°C until analysis.

2.4   Passive diffusion extraction

One glass cell (internal diameter of 1.6 cm, extraction surface 2 cm^2) was adhered to the skin as before and was filled with 1.6 ml of the same extraction solution used in the reverse iontophoresis experiment. Samples were collected at 30 minutes and at 1 hour and then every hour thereafter for a total of 4 hours. Identical sample filtration and storage procedures were followed as described before.

2.5   Tape-stripping

Tape-stripping was performed on the opposite ventral forearm of the same subject. The SC was progressively removed by the repeated application and removal of adhesive tape-strips (Scotch Book Tape, 3M, St. Paul, MN). A template with a central square hole (2x3 cm) was first fixed to the skin with self-adhesive medical tape (Curafix H, Lohmann & Rauscher,Rengsdorf, Germany) to ensure that all tape-strips were taken from exactly the same site. The tapes (2.5x4 cm) were applied with pressure from a weighted roller and then swiftly removed. TEWL measurements were taken (AquaFlux V4.7, Biox Systems Ltd., London, UK) before and after each tape strip, and tape-stripping was stopped when TEWL reached 3-4 times the initial value, at which point approximately 75% of the SC had been removed [14]. NMF on the tape-strips was subsequently extracted with an aqueous solution of sodium azide (20 mg/l). The first and second tapes were extracted individually

into 0.8 ml of this solution, while the remaining tapes were extracted into a volume of 1.6 ml. The extracted solutions were filtered (Cronus, 0.45 µm, 4 mm diameter, SMI-LabHut Ltd, Gloucester, UK) and stored at -20°C until analysis.

2.6   Analysis of tapes

2.6.1 Weighing method

Tapes were cut and stored for at least 12 hours. Static electricity was then discharged from the tapes (R50 discharging bar and ES50 power supply from Eltex Elektrostatick GmbH, Weil am Rhein, Germany) before being weighed before and then after stripping on a 0.1 µg precision balance (Sartorius SE2-F, Epsom, UK). From the SC mass, the strip area (6 cm^2) and the SC density (1 g/cm^3), the thickness of the SC layer removed can be calculated:

$$\text{Thickness} = \text{Mass}/(\text{Area} \times \text{Density})$$

 Six blank tapes were also included in the weighing protocol to correct for any variability introduced by environmental or other factors.

2.6.2 Imaging method

The tapes were also photographed using a Coolscan slide scanner (Nikon UK Limited, Kingston upon Thames, US) at a resolution of 4000 pixels per inch (157.5 pixels/mm) according to a previously described method [15]. A crop of 3203x4720 pixels (approximately 2x3 cm) was centred over each image and scanned in full. The images were saved and analysed by ImageJ (Rasband,W.S., U.S. National Institutes of Health, Bethesda, Maryland, USA; freeware from http://rsb.info.nih.gov/ij/) to obtain mean greyscale values. Each image was assigned a greyscale value (G_{SC}) in the range 0-64608, where 0 and 64608 represent black and white respectively. The mean greyscale over all pixels was calculated by ImageJ. Six blank tapes provided the mean greyscale background (G_{blank}).   The SC absorbance (A_{SC}) was then calculated as:

1) $A_{SC} = -\log (G_{SC}/G_{blank})$

As the weight of SC (M_{SC}) on each tape had been quantified, the correlate A_{SC} and M_{SC} as described in Chapter 2:

2) $M_{SC} = 0.36x\ A_{SC} +0.009$

2.7   Analytical chemistry

LCMS was performed on a Shimadzu LCMS-2010EV with a single quadrupole and a dual ion source (containing both electrospray and atmospheric pressure chemical ionization). The MS was operated in positive ion mode with the ionspray voltage set at 1.5 kV. Nitrogen was used both as a nebulising and drying gas at a flow rate of 1.5 L/min with a heat block temperature of 480°C and curved desolvation line temperature of 230°C. The quadrupole was operated in the selected ion monitoring mode and protonated molecules $[M+H]^+$ (Table 1) were used for quantification

Table 1: Molecules for quantification

Molecules	Abbr.	$[M+H]^+$	Molecules	Abbr.	$[M+H]^+$
Alanine	Ala	90	Arginine	Arg	175
Asparagine	Asn	133	Aspartic acid	Asp	134
Citruline	Cit	176	Glutamic acid	Glu	148
Glutamine	Gln	147	glutamine-D5		152
Glycine	Gly	76	Glycine-D2		78
Histidine	His	156	Isoleucine	Ile	132
Leucine	Leu	132	Lysine	Lys	147
Methionine	Met	150	Ornithine	Orn	133
Phenylalanine	Phe	166	Proline	Pro	116
Pyrrolidone carboxylic acid	PCA	130	Taurine	Tau	126
Serine	Ser	106	Serine-D3		109
Theonine	Thr	120	Tryptophan	Try	205
Tyrosine	Tyr	182	Urea		61
Trans-urocanic acid	t-UA	139	Cis-urocanic acid	c-UA	139
Valine	Val	118			

Separation was carried out on a Gemini C18 column (50x4.6 mm, 3 μm, 110 A, Phenomenex, USA). All analyses were carried out at 40°C with a flow-rate of 0.3 ml/min. A gradient was

used with eluent A being a 20 mM nonafluoropentanoic acid (NFPA) solution and eluent B acetonitrile. The gradient elution started with 99:1(v/v) A:B for 5 minutes, followed by a linear change to 86:14(v/v) A:B over 9 minutes, then 86:14(v/v) for 5 minutes, and subsequently altered linearly to 64:36(v/v) over 14 mintues. The MS was then switched to negative ion mode with 20/80 (v/v) A:B for 3 minutes to wash the column and finally equilibrated for 20 minutes under the initial conditions.

2.8 Data analysis and statistics

The concentrations of amino-acid-derived components of NMF were expressed in terms of amount per mass of SC. The change in TEWL as a function of the amount of the SC removed was modelled using the baseline-corrected non-linear model [16] to determine the barrier thickness (H).

$$\text{TEWL} = B + \frac{DK\Delta C}{H - h}$$

where B is the baseline correction factor; D is the diffusion coefficient of water in the SC; K is the SC-viable tissue partition coefficient of water; ΔC is the water concentration gradient across the SC; and h is the cumulative thickness values of SC removed. Fitting the results to this equation allows the best estimates of B, ($DK\Delta C$) and H to be deduced.

Extraction fluxes were calculated by dividing the amounts removed during a sampling interval by the duration of that collection period. Amounts extracted were divided by the skin area and expressed in nmol cm^{-2}. Data manipulation and statistics were performed using Graph Pad Prism v. 5.01 (Graph Pad Software Inc., San Diego, CA, U.S.A.). When datasets were compared, the level of statistical significance was fixed at $P < 0.05$. All results were expressed as mean ± SD.

3. Results and discussion

3.1   Thickness of SC

An example of fitting the TEWL results to the barrier-corrected model using gravimetric and imaging methods to measure the amount of SC removed is shown in Figure 1 for one subject.
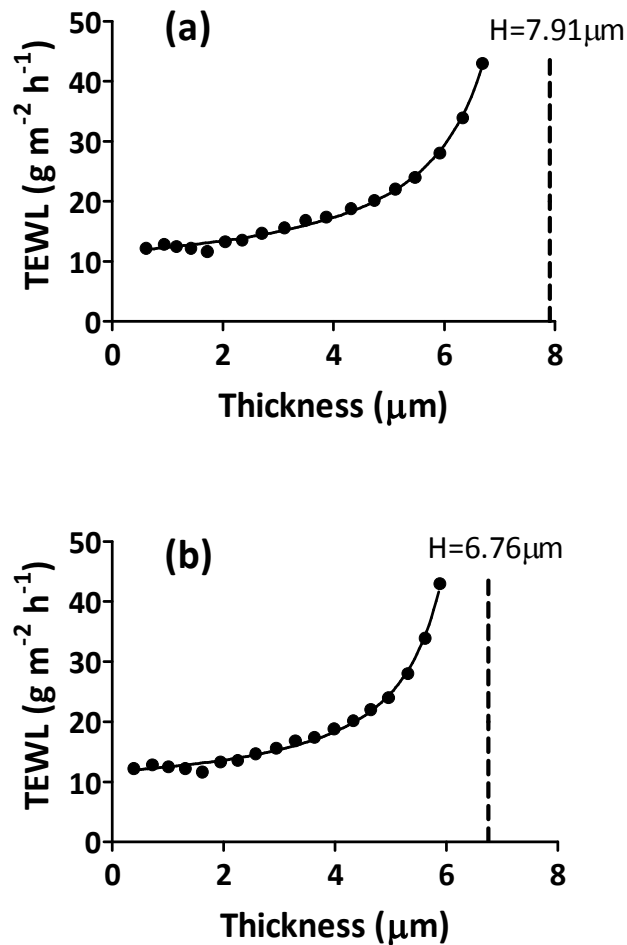
Figure 1: TEWL vs SC thickness for subject 1: (a) SC thickness determined gravimetrically, (b) SC thickness determined by imaging method.

The average SC thickness across all volunteers studied predicted by gravimetric and imaging methods were 7.5 ± 1.9µm and 6.2 ± 1.1µm, respectively. The difference is not significant (paired t-test, p=0.11).

3.2 Extraction of amino-acid-derived components of NMF

Twenty-one NMF components were successfully quantified. Other NMF components were detected but could not be quantified (methionine and taurine), while the chromatographic peaks of aspartic acid and asparagine either co-eluted with contaminant or suffered from severe ion suppression.

3.2.1 SC content determined by tape-stripping

The levels of each NMF component in *in vivo* SC tapes are shown in Table 2. The compounds extracted are separated into charged and zwiterionic species arranged in descending order of the amount present.

Table 2: Cumulative amounts (nmol/cm^2; mean ± SD; n=6) of NMF components extracted by tape-stripping, reverse iontophoresis and passive diffusion.

| Charged compounds				
Analytes	Tape-stripping	Passive diffusion	Anode	Cathode
PCA	129 ± 52	55 ± 29	231 ± 52	5.7 ± 1.6
Urocanic acid	32 ± 17	18 ± 11	98 ± 60	<LQL
Glutamic acid	12 ± 4	4.3 ± 3.3	54 ± 14	<LQL
Histidine	47± 16	17 ± 9	21 ± 12	78 ± 42
Ornithine	29 ± 19	12 ± 8	14 ± 11	68 ± 50
Arginine	20 ± 15	7.9 ± 4.3	3.5 ± 3.8	62 ± 32
Lysine	4.2 ± 6	1.1 ± 2.5	<LQL	33 ± 6
Zwitterions and Urea				
Analytes	Tape-stripping	Passive diffusion	Anode	Cathode
Serine	216 ± 60	98 ± 50	230 ± 94	178 ± 95
Glycine	118 ± 33	60 ± 28	141 ± 59	179 ± 42
Alanine	102 ± 51	40 ± 21	92 ± 20	99 ± 29
Threonine	62 ± 23	23 ± 12	49 ± 24	52 ± 19
Citruline	50 ± 15	23 ± 11	52 ± 23	46 ± 17
Valine	22 ± 9	8.7 ± 4.6	24 ± 12	21 ± 9
Proline	15 ± 5	7.5 ± 4.2	19 ± 11	17 ± 6
Tyrosine	12 ± 3	4.3 ± 2.1	12 ± 9	9.6 ± 3.9
Isoleucine	9.5 ± 3.8	3.7 ± 2.5	11 ± 6	8.9 ± 3.5
Leucine	7.3 ± 2.5	3.2 ± 2.2	9.3 ± 4.9	7.4 ± 2.8
Phenylalanine	4.9 ± 1.6	2.2 ± 1.5	6.3 ± 4.6	4.7 ± 2.3
Tryptophan	4.7 ± 1.7	1.8 ± 1.2	5.2 ± 4.3	2.7 ± 1.4
Glutamine	1.3 ± 0.7	0.4 ± 0.5	2.8 ± 2.0	1.6 ± 1.5
Urea	52 ± 38	64 ± 49	118 ± 56	107 ± 55
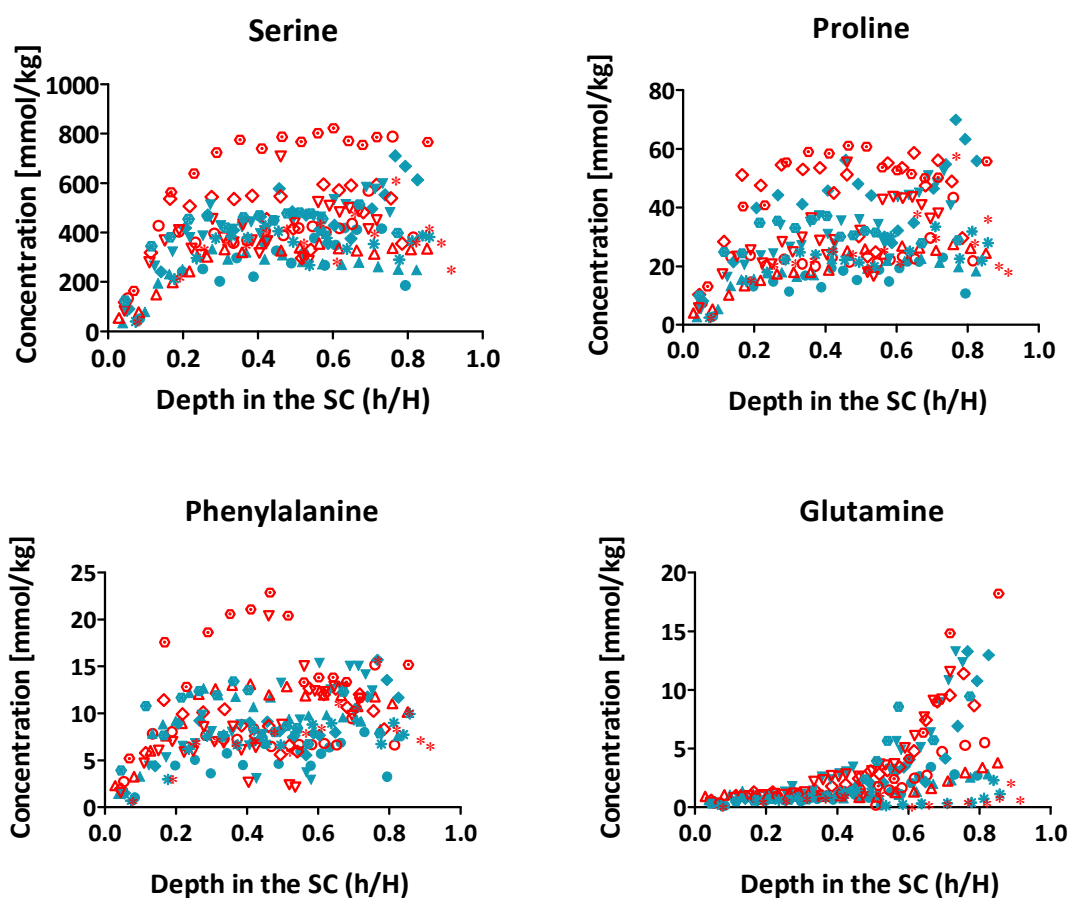
Figure 2: Concentration profiles of serine, proline, phenylalanine and glutamine as a function of position in the SC in 6 human volunteers determined using the gravimetric (cyan) and imaging methods (red).

Figure 2 illustrates typical concentration profiles as a function of position in the SC of serine (an AA abundantly present), proline (moderately abundant), phenylalanine and glutamine (present at low levels). Concentrations are given in mmol/kg. Distribution profiles of other NMFs components are listed in the Appendix 3.

There was good agreement between the results from the different methods used to quantify SC removed on each tape. The pattern of distribution of most of the NMF components is consistent, being negligible at the skin surface before increasing to relatively constant levels. The results concur with those in the literature [11, 17-18].

Glutamine (Figure 2) was the only NMF component which demonstrated a different pattern of distribution. It was nearly undetectable at the SC surface, but its concentration increased

dramatically in deeper layers. These could be the result of cyclization of free glutamine to form pyrrolidone carboxylic acid (PCA) progressively from the lower to the upper SC [19].
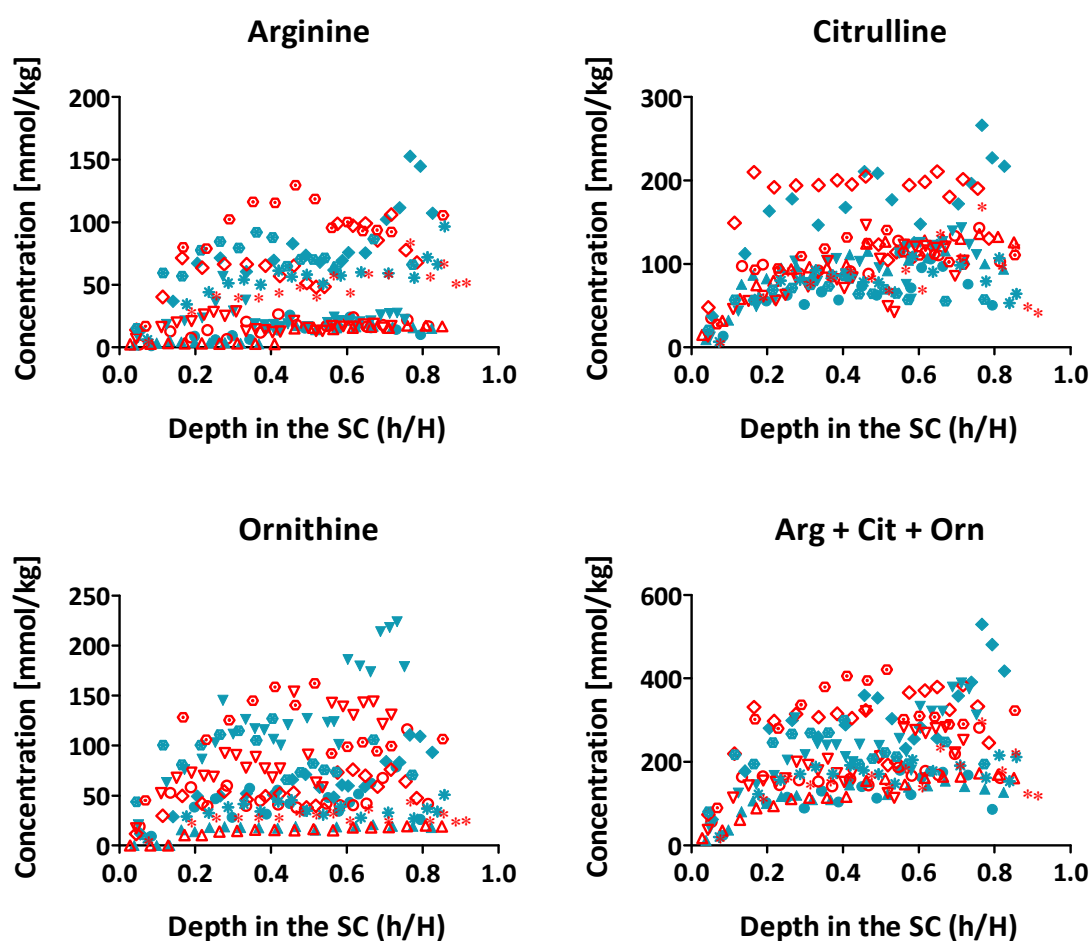
Figure 3: Concentration profiles of arginine, citrulline, ornithine and their sum as a function of position in the SC in 6 human volunteers determined using gravimetric (cyan) and imaging methods (red).

Individually, arginine, ornithine and citrulline showed large differences between volunteers, resulting in rather broad distributions (Figure 3). However, when the levels of these 3 compounds are summed (Arg + Cit + Orn), a more reproducible and similar distribution to that of the other NMF components is seen. It is known that ornithine is derived from the breakdown of arginine (by arginase-1), and that citrulline is the degradation product of arginine by nitric oxide synthase (NOS) [20] and peptidylarginine deiminases (PAD1 and PAD3) [21]. Thus, although the volunteers may have different levels of enzyme activity involved in the breakdown of arginine, the total concentration of the three species together

is relatively constant. The balance between the enzymes involved is important in controlling keratinocyte proliferation. Up-regulation of arginase-1 has been observed in the non-lesional skin of psoriasis patients such that decreased arginine and increased ornithine have been detected in the plasma of these individuals [22-23].

3.2.2 Extraction by reverse iontophoresis and passive diffusion

Figure 4 shows examples of the reverse iontophoretic and passive extraction of an acidic NMF component (PCA), a basic compound (histidine) and a zwitterion (serine). The corresponding extraction data of other NMF constituents are shown in Appendix 3.
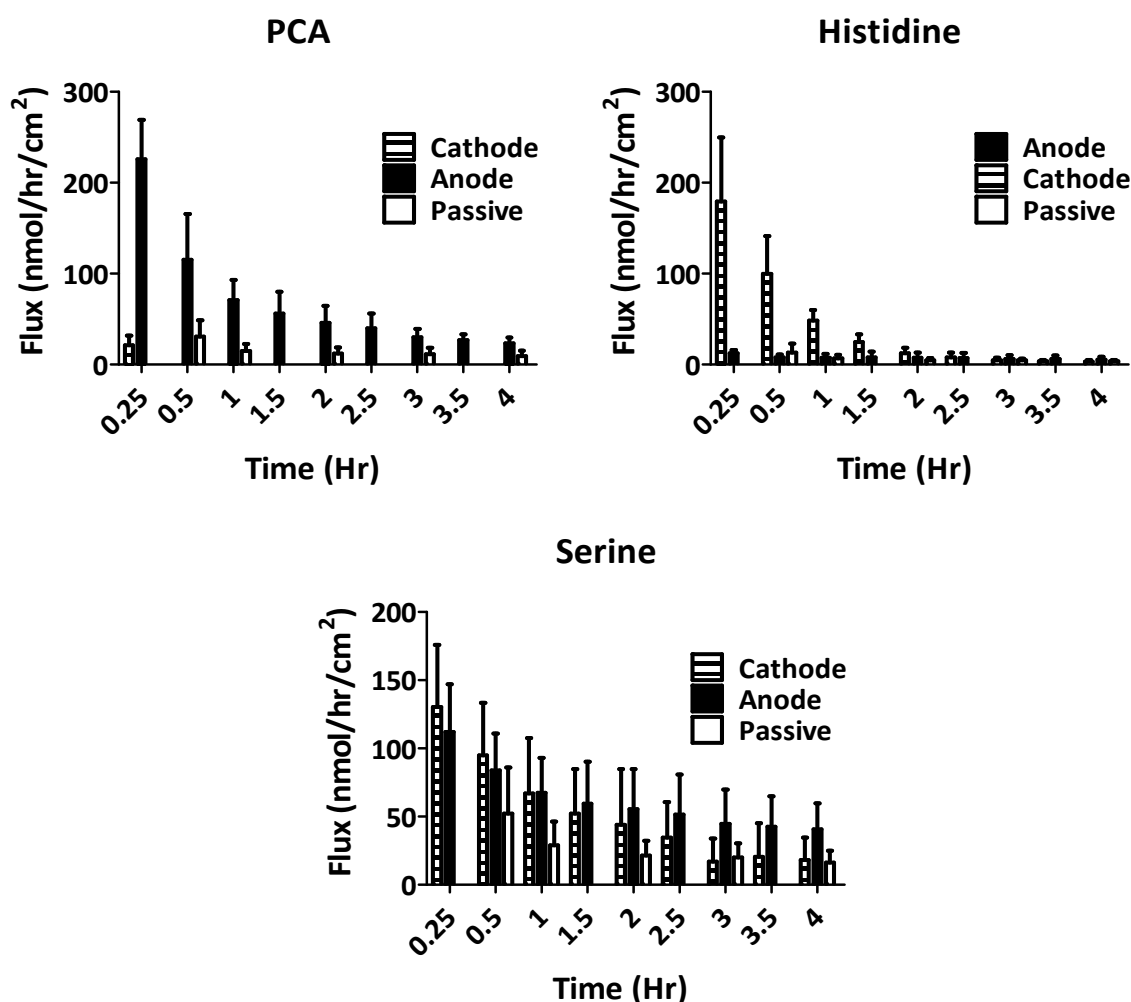
Figure 4: Reverse iontophoretic and passive extraction fluxes (mean ± SD) of PCA, histidine and serine *in vivo* in human volunteers (n=6) as a function of time.

The extraction of NMF components by reverse iontophoresis and passive diffusion can be separated into 3 groups:

a) Acidic compounds are negatively charged at physiological pH and are extracted predominantly at the anode. The extraction fluxes were similar with the initial flux being high but then decreasing rapidly over the first hour before stabilising. The amounts extracted at the cathode were minimal and, in some cases, like glutamic acid, below the LOQ.

b) Extraction of compounds positively charged at physiological pH was predominately at the cathode. The amounts detected at the anode and passively were minimal.

c) Zwitterions were, on the whole, similarly extracted to the anode and to the cathode. The amounts extracted by reverse iontophoresis were only moderately greater than those obtained passively.

3.3   Origins of NMF extracted

Table 2 compares the cumulative amounts of NMF components obtained from SC tape-stripping, reverse iontophoretic and passive extraction. The compounds can be separated into two groups:

1) Charged species (positively or negatively). Figure 5 shows two examples (PCA & Lysine); data for other NMF components are shown in the Appendix 3.
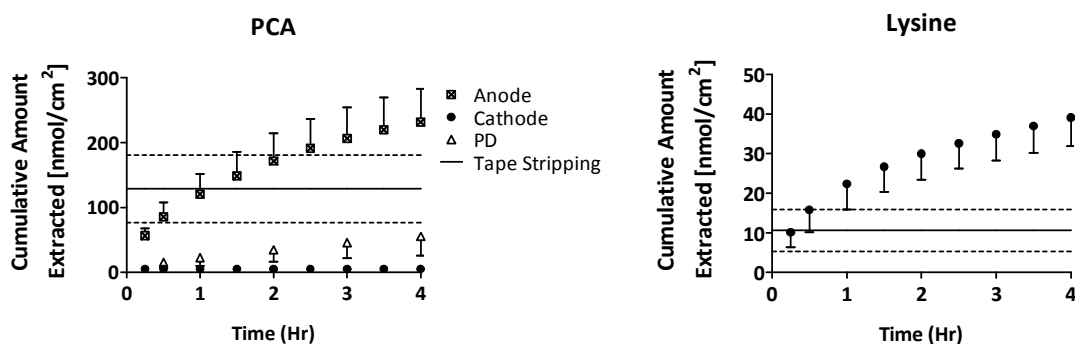
Figure 5: Cumulative amounts of PCA and lysine extracted (mean ± SD) by reverse iontophoresis and by passive diffusion as a function of time (n=6). The average quantities in the SC determined by tape-stripping are shown for comparison by the solid horizontal lines, with the ±SD indicated by the dashed lines.

Reverse iontophoresis is a very powerful technique to extract these molecules. By the end of 4 hours, extraction to the preferred electrode indicated that analytes were being sampled from beyond the SC. The extent to which this is the case depended on the properties of the molecule and its concentration in the SC. For example, PCA is present in large amounts in the SC, and the time taken to deplete this 'reservoir' is longer than that required for others, such as glutamic acid or lysine, which are present at lower levels.

2) Zwitterionic species and urea, the lowest molecular weight species. Figure 6 illustrates two examples (serine and proline) from this group.
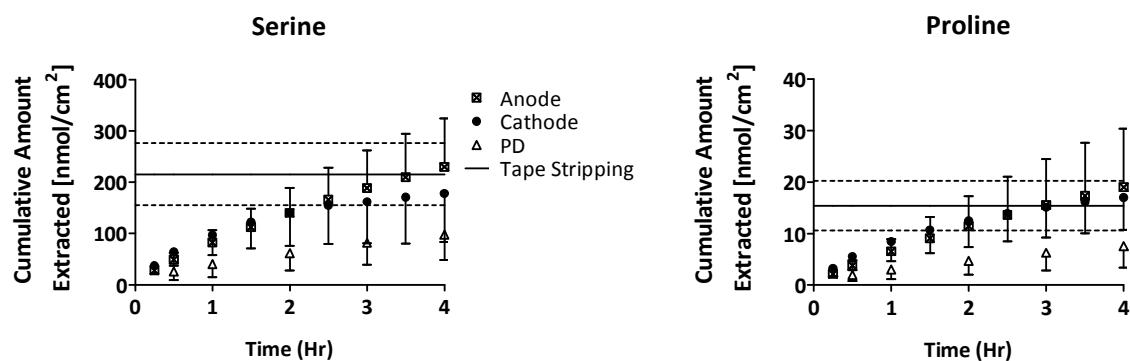
Figure 6: Cumulative amounts of serine and proline (mean ± SD) extracted by reverse iontophoresis and by passive diffusion as a function of time (n=6). The average quantities in the SC determined by tape-stripping are shown for comparison by the solid horizontal lines, with the ±SD indicated by the dashed lines.

For these compounds, reverse iontophoresis did not deplete the 'skin reservoir'. The quantities extracted by the reverse iontophoresis were higher than by passive diffusion, but much less to that seen for charged compounds.

Urea (molecular weight: 60) is very small, and is readily extracted by passive diffusion. However, as urea is also secreted in sweat onto the surface of the SC, the amounts extracted between subjects shows considerable variability.

4. Conclusions

There is an abundant amino-acid-derived NMF reservoir in the skin. Most NMF components are similarly distributed in the SC, their concentrations being relatively low near the surface, but increased and rather constant in the deeper SC. Reverse iontophoresis showed efficient extraction compared to passive diffusion of charged molecules, but only moderate enhancement with repeat to zwitterions. Two different methods for quantify of skin on the tapes were self-consistent.

5. Reference

1.   Muller S, Marenholz I, Lee Y, Sengler C, Zitnik S, Griffioen R, Meglio P, Wahn U, and Nickel R, *Association of filaggrin loss-of-function-mutations with atopic dermatitis and asthma in the Early Treatment of the Atopic Child (ETAC) population.* Pediatric Allergy and Immunology, 2009. **20**(4): p. 358-361.

2.   Nemoto-Hasebe I, Akiyama M, Nomura T, Sandilands A, McLean WHI, and Shimizu H, *Clinical Severity Correlates with Impaired Barrier in Filaggrin-Related Eczema.* J Invest Dermatol, 2008. **129**(3): p. 682-689.

3.   Nomura T, Akiyama M, Sandilands A, Nemoto-Hasebe I, Sakai K, Nagasaki A, Palmer CNA, Smith FJD, McLean WHI, and Shimizu H, *Prevalent and rare mutations in the gene encoding filaggrin in Japanese patients with ichthyosis vulgaris and atopic dermatitis.* J Invest Dermatol, 2008. **129**: p. 1302-1305.

4.   Brown SJ and Irvine AD, *Atopic eczema and the filaggrin story.* Seminars in Cutaneous Medicine and Surgery, 2008. **27**(2): p. 128-137.

5.   Rawlings A and Harding C, *Moisturization and skin barrier function.* Dermatologic Therapy, 2004. **17**(s1): p. 43-48.

6.   Kezic S, Kemperman PMJH, Koster ES, de Jongh CM, Thio HB, Campbell LE, Irvine AD, McLean IWH, Puppels GJ, and Caspers PJ, *Loss-of-Function mutations in the filaggrin gene lead to reduced level of natural moisturizing factor in the stratum corneum.* J Invest Dermatol, 2008. **128**(8): p. 2117-2119.

7.   Takahashi M and Tezuka T, *The content of free amino acids in the stratum corneum is increased in senile xerosis.* Archives of Dermatological Research, 2004. **295**(10): p. 448-452.

8.   Novak N, Baurecht H, Schafer T, Rodriguez E, Wagenpfeil S, Klopp N, Heinrich J, Behrendt H, Ring J, Wichmann E, Illig T, and Weidinger S, *Loss-of-function mutations in the filaggrin gene and allergic contact sensitization to nickel.* J Invest Dermatol, 2007. **128**(6): p. 1430-1435.

9.   Howell MD, Kim BE, Gao P, Grant AV, Boguniewicz M, DeBenedetto A, Schneider L, Beck LA, Barnes KC, and Leung DYM, *Cytokine modulation of atopic dermatitis*

filaggrin skin expression. Journal of Allergy and Clinical Immunology, 2009. **124**(3, Supplement 2): p. R7-R12.

10. Bender DA, *Amino acid metabolism*. Second ed. 1985, Chichester: John Wiley & Sons.

11. Sylvestre JP, Bouissou C, Guy R, and Delgado-Charro MB, *Extraction and quantification of amino acids in human stratum corneum in vivo.* British Journal of Dermatology, 2010. **163**(3): p. 458-465.

12. Sieg A, Jeanneret F, Fathi M, Hochstrasser D, Rudaz S, Veuthey J-L, Guy RH, and Delgado-Charro MB, *Extraction of amino acids by reverse iontophoresis in vivo.* European Journal of Pharmaceutics and Biopharmaceutics, 2009. **72**(1): p. 226-231.

13. Rawlings A and Matts P, *Stratum Corneum Moisturization at the Molecular Level : An Update in Relation to the Dry Skin Cycle.* J Invest Dermatol, 2005. **124**(6): p. 1099-1110.

14. Kalia YN, Alberti I, Sekkat N, Curdy C, Naik A, and Guy RH, *Normalization of Stratum Corneum Barrier Function and Transepidermal Water Loss In Vivo.* Pharmaceutical Research, 2000. **17**(9): p. 1148-1150.

15. Russell L, *Dermato-pharmacokinetics: an approach to evaluate topical drug bioavailabilty*, in *Department of Pharmacy and Pharmacology*. 2008, University of Bath: Bath.

16. Russell LM, Wiedersberg S, and Delgado-Charro MB, *The determination of stratum corneum thickness An alternative approach.* European Journal of Pharmaceutics and Biopharmaceutics, 2008. **69**(3): p. 861-870.

17. M. Egawa HT, *Comparison of the depth profiles of water and water-binding substances in the stratum corneum determined in vivo by Raman spectroscopy between the cheek and volar forearm skin: effects of age, seasonal changes and artificial forced hydration.* British Journal of Dermatology, 2008. **158**(2): p. 251-260.

18. Caspers PJ, Lucassen GW, Carter EA, Bruining HA, and Puppels GJ, *In vivo confocal raman microspectroscopy of the skin: noninvasive determination of molecular concentration profiles.* J Invest Dermatol, 2001. **116**(3): p. 434-442.

19. Barrett JG and Scott IR, *Pyrrolidone carboxylic acid synthesis in guinea pig epidermis.* J Investig Dermatol, 1983. **81**(2): p. 122-124.

20. Abeyakirthi S, Mowbray M, Van Overloop L, Wheatley P, Morris R, Declercq L, and Weller R, *O65. Arginase enzyme is overactive in non-lesional psoriatic skin.* Nitric Oxide, 2008. **19**(Supplement 1): p. 35-35.

21. Chavanas S, Méchin M-C, Nachat R, Adoue V, Coudane F, Serre G, and Simon M, *Peptidylarginine deiminases and deimination in biology and pathology: Relevance to skin homeostasis.* Journal of Dermatological Science, 2006. **44**(2): p. 63-72.

22. Schnorr O, Schuier M, Kagemann G, Wolf R, Walz M, Ruzicka T, Mayatepek E, Laryea M, Suschek CV, Kolb-Bachofen V, and Sies H, *Arginase-1 overexpression induces cationic amino acid transporter-1 in psoriasis.* Free Radical Biology and Medicine, 2005. **38**(8): p. 1073-1079.

23. Bruch-Gerharz D, Schnorr O, Suschek C, Beck K-F, Pfeilschifter J, Ruzicka T, and Kolb-Bachofen V, *Arginase 1 overexpression in psoriasis: limitation of inducible nitric oxide synthase activity as a molecular mechanism for keratinocyte hyperproliferation.* Am J Pathol, 2003. **162**(1): p. 203-211.

Chapter 4: Determination of amino acids in human forehead and forearm stratum corneum *in vivo* by tape-stripping and reverse iontophoresis.

Abstract

Purpose:

The goal of this project was to apply bioengineering methods to screen SC barrier function on the forehead and forearm of healthy volunteers using differences in lipid arrangement and in levels of natural moisturising factor (NMF) as potential markers.

Methods:

NMF components were extracted from the forearm and forehead of 6 healthy volunteers using reverse iontophoresis, passive diffusion and tape-stripping. The extracted samples were analysed by LCMS to identify and quantify the amounts of 21 NMF components. Transepidermal water loss (TEWL) measurements were taken before and after each tape-strip and the results were used to derive the SC thickness. The SC was also examined by attenuated total reflectance-Fourier transform infrared spectroscopy (ATR-FTIR) before and after each tape-strip to probe lipid quantity, composition and organisation at the two anatomic sites considered.

Results:

SC thickness on the forehead was significantly thinner than that on the forearm and TEWL values were correspondingly higher. The concentrations of most NMF components were similar at both sites but there was a lower total amount of NMF extracted from the forehead. However, those NMF components normally present in forearm SC in small quantities (e.g., glutamine and glutamic acid) were found in higher concentrations on the forehead and, as a result, were more easily extracted by passive diffusion and reverse iontophoresis. IR absorbance from both forearm and forehead SC at ~2850 cm^{-1} and 2920 cm^{-1} shifted to lower frequencies as tape-stripping progressed indicating that lipids near to the skin surface were relatively disordered, most probably due to the contribution from sebaceous constituents. This effect was much more marked on the forehead than on the forearm.

Conclusion:

The results confirm that forehead SC may be considered a less competent barrier than that on the forearm, as characterised by the presence of lesser amounts of NMF and less-ordered SC lipids.

1. Introduction

Natural moisturizing factor (NMF) is a collection of water-soluble, low-molecular-weight compounds found in the stratum corneum (SC). Functionally, it allows the SC to retain water against the dehydrating action of external environment and thus plays a key role in skin hydration [1]. NMF is composed primarily of free amino acids (AAs) and amino acids derivatives that are derived from filaggrin. Filaggrin is synthesized from profilaggrin, an approximately 500-kDa insoluble protein, consisting of 10 to 12 repeating filaggrin units [2-3]. During the transition of the mature granular cell into a corneocyte, rapid dephosphorylation of pro-filaggrin occurs, yielding filaggrin [3]. Filaggrin monomers facilitate the aggregation of keratin intermediate filaments (KIF). As corneocytes proceed upwards through the SC, deiminiation and complete proteolysis of filaggrin yields the components of NMF.

Presently, a filaggrin mutation is the strongest genetic risk factor for atopic dermatitis (AD) and ichthyosis vulgaris (IV) [4-7]. As a result of this mutation, lower levels of NMF are generated in atopic skin and this is thought to contribute to an impaired barrier function [8-9]. Furthermore, a reduced NMF level has also been reported in other abnormal dry and scaly skin [10-12]. Therefore, measuring the amount of NMF in the skin could be a good indicator of skin hydration and thus might be helpful in early diagnosis of these skin disorders.

Regional skin differences at various anatomical sites have been recognised [13]. For example, the SC on the face is thinner, and contains smaller corneocytes than that on the forearm. The surface area of facial corneocytes is smaller, resulting a shorter path-length for molecular transport and a noticeably higher permeability [14]. In addition, the face is one of the first body sites affected when atopic dermatitis (AD) develops and the ratio of fragile to mature corneocytes is higher here than on the inner upper arm [15]. Voegeli et al [16] have also demonstrated higher levels of desquamation-related proteases on the face. All these features are found in AD and it was highlighted, therefore, that the forearm and forehead skin of healthy volunteers might model the distinction between a competent SC and one pre-predisposed to AD.

The goal of this project, then, was to apply bioengineering techniques to evaluate SC barrier function on the face and forearm and to identify regional differences in barrier thickness, lipid arrangement and NMF quantity and composition.

2. Materials and methods

2.1 Chemicals

Sodium azide, NFPA (perfluoropentanoic acid), silver (Ag) wire (>99.99% purity), AgCl (99.999%), acetonitrile and all L-amino acids acids(Asn, Ser, Gly, Asp, Cit, Orn, Gln, Glu, Thr, Ala, Pro, Val, Tyr, Met, Ile, Leu, His, Lys, Phe, Arg, and Trp) were purchased from Sigma-Aldrich Co. (Gillingham, UK). Glycine-D5, Serine-D3, Glutamine-D5 were purchased from Cambridge Isotope Laboratories (Andover,MA). Deionised water (resistivity ≥ 18.2 MΩ/cm^2) was used to prepare all aqueous solutions (Barnstead Nanopure Diamond^{TM}, Dubuque, IA).

2.2 Human subjects

Six healthy volunteers (3 male, 3 female, aged between 25 and 31 years) with no history of skin disease participated in the study, which was approved by the Bath Local Research Ethics Committee, and provided written consent. Experiments were performed on the blemish-free site of ventral forearm and on the forehead on three separate occasions at least four weeks apart. The skin surfaces were first cleaned gently with an isopropyl alcohol swab (Medi-Swab, Seton Healthcare Group plc, England). Then, in the first component of the study, samples of NMF were obtained by passive extraction and by tape-stripping (at second, adjacent site). In the second part, sampling involved reverse iontophoresis at both sites. Finally, in a third aim of the study, tape-stripping was again performed on forehead and forearm with concomitant fourier transform infrared spectroscopy (FTIR) measurements focused specifically on the lipid organisations from the intercellular lipid domains. The facial skin should be examined before recruitment to ensure no obvious scarring is present in the sampling area, since scar tissue caused by acne may behave differently from normal skin.

2.3   Attenuated total reflectance-fourier transform infrared spectroscopy (ATR-FTIR)

2.3.1 Equipment

A PerkinElmer (Massachusetts,USA) Spectrum 100 FT-IR spectrometers was used to record the *in vivo* measurements. The spectrometer was equipped with a universal ATR accessory with a round diamond crystal (2 mm diameter). The single bounce top-plate was employed.

2.3.2 Experiments

Before any measurement, the skin site (either forearm or forehead) was cleaned with gentle alcohol wipe (Medi-Swab, Seton Healthcare Group plc, England). Three IR spectra with 16 scans each were then recorded. The SC was progressively removed by the repeated application and removal of adhesive tape-strips (Permacel J-LAR ® clear to the core tape, Permacel, Wisconsin, USA). On the forearm, 3 replicate IR spectra were recorded after removal of each tape for the first 6 strips and after every two tapes thereafter. On the forehead, 3 replicate spectra were recorded after each tape-strip.

2.3.3 Spectral analysis

FTIR spectra were collected in the frequency range 4000-400cm^{-1}. The peak frequency of the asymmetric (~2920cm^{-1}) and symmetric (~2850cm^{-1}) CH_2 stretching absorbances were obtained from the first-order derivatives using the Spectrum^{TM} Express software. The normalised areas under the CH_2 stretching absorbances were calculated as previously described [17].

2.4   Reverse iontophoretic extraction

Two glass cells (internal diameter 1.55 cm , extraction surface 1.89 cm^2) separated by ~4 cm were fixed to either the ventral forearm or the forehead of the subjects using silicone grease and medical grade tape (Curafix H, Lohmann & Rauscher,Rengsdorf, Germany). Both cells were filled with 1 ml of 20 mM ammonium chloride in 10 mM ammonium bicarbonate buffer at pH ~ 6.8. A direct current of 0.4 mA (i.e., 0.21 mA/cm^2) was applied from a Phoresor II Auto (Iomed, Model No. PM850, Salt lake City, UT) via Ag/AgCl electrodes. The entire contents of the anode and cathode chambers were collected and replaced by an equal volume of extraction solution after 15 and 30 minutes of iontophoresis and then every half-hour thereafter for a total extraction time of 3 hours. The collected samples were

passed through a sterile syringe filter (Cronus, 0.45 µm, 4 mm diameter, SMI-LabHut Ltd, Gloucester, UK) and stored in the freezer at -20°C until analysis.

2.5   Passive diffusion extraction

One glass cell (internal diameter 1.55 cm, extraction surface 1.89 cm^2) was adhered to the skin as before and was filled with 1 ml of the same extraction solution used in the reverse iontophoresis experiment. Samples were collected at 30 minutes and at 1 hour of passive extraction and then every hour thereafter for a total of 4 hours. Identical sample filtration and storage procedures were followed as described above.

2.6   Tape-stripping

Tape-stripping was performed on the ventral forearm and forehead of each subject. The SC was progressively removed by the repeated application and removal of adhesive tape-strips (Permacel J-LAR ® clear to the core tape). A template with a central square hole (2x2 cm) was first fixed to the skin with self-adhesive medical tape (Curafix H, Lohmann & Rauscher, Rengsdorf, Germany) to ensure that all tape-strips were taken from exactly the same site. The tapes (2.5x3 cm) were applied with pressure from a weighted roller and then swiftly removed. TEWL measurements were taken (AquaFlux V4.7, Biox Systems Ltd., London, UK) before and after each tape strip, and tape-stripping was stopped when TEWL reached 3-4 fold the initial value, at which point approximately 75% of the SC had been removed [18]. NMF in the SC removed on the tape-strips was subsequently extracted with an aqueous solution of sodium azide (20 mg/l). The first and second tapes were extracted individually into 0.5 ml of extraction solution, while the remaining tapes were extracted into 1 ml. The extracted solutions were filtered (Cronus, 0.45 µm, 4 mm diameter, SMI-LabHut Ltd, Gloucester, UK) and stored at -20°C until analysis.

2.7   Analysis of tapes

2.7.1   Weighing method

Tapes were prepared at least 12 hours before any experiment. Static electricity was discharged from the tapes prior to weighing (R50 discharging bar and ES50 power supply from Eltex Elektrostatick GmbH, Weil am Rhein, Germany). The tapes were weighed before

and after stripping on a 0.1 µg precision balance (Sartorius SE2-F, Epsom, UK) to determine the mass and hence by dividing the mass of SC removed. Dividing this mass by the strip area (4 cm^2) and by the SC density (1 g/cm^3), the thickness of the SC layer removed was calculated. Six blank tapes were weighed at the same time as the tapes used for SC stripping to correct for any variations due to environmental or other factors.

2.7.2 Imaging method

The tapes were also photographed using a Coolscan slide scanner (Nikon UK Limited, Kingston upon Thames, US) at a resolution of 4000 pixels per inch (157.5 pixels/mm) according to the method previously described [19]. A crop of approximately 2x2 cm was centred over each image and then scanned. The images were analysed by ImageJ (Rasband, W.S., U.S. National Institutes of Health, Bethesda, Maryland, USA; freeware from http://rsb.info.nih.gov/ij/) to obtain mean greyscale values. Each image was assigned a greyscale value in the range 0-64608, where 0 and 64608 represent black and white respectively. The mean greyscale over all pixels was calculated by ImageJ. As a control, mean greyscale of six blank tapes was determined. The SC absorbance (A_{SC}) was then calculated as:

1) A_{SC} = -log (G_{SC}/G_{blank})

As the weight of SC (M_{SC}) on each tape had been quantified, the correlate A_{SC} and M_{SC} as described in Chapter 2:

2) M_{SC} = 0.36x A_{SC} +0.009

2.8   Analytical analysis

LCMS   analysis was performed on a Shimadzu LCMS-2010EV with a single quadrupole and a dual ion source (containing both electrospray and atmospheric pressure chemical ionization). The MS was operated in positive ion mode with the ion spray voltage set at 1.5 kV. Nitrogen was used both as a nebulising and drying gas at a flow rate of 1.5 L/min with a heat block temperature of 480°C and curved desolvation line temperature of 230°C. The quadrupole was operated in the selected ion monitoring mode and protonated molecules [M+H]$^+$ (Table 1) were used for quantification.

Table 1: Molecules for quantification

Molecules	Abbr.	[M+H]$^+$	Molecules	Abbr.	[M+H]$^+$
Alanine	Ala	90	Arginine	Arg	175
Asparagine	Asn	133	Aspartic acid	Asp	134
Citruline	Cit	176	Glutamic acid	Glu	148
Glutamine	Gln	147	glutamine-D5		152
Glycine	Gly	76	Glycine-D2		78
Histidine	His	156	Isoleucine	Ile	132
Leucine	Leu	132	Lysine	Lys	147
Methionine	Met	150	Ornithine	Orn	133
Phenylalanine	Phe	166	Proline	Pro	116
Pyrrolidone carboxylic acid	PCA	130	Taurine	Tau	126
Serine	Ser	106	Serine-D3		109
Theonine	Thr	120	Tryptophan	Try	205
Tyrosine	Tyr	182	Urea		61
Trans-urocanic acid	t-UA	139	Cis-urocanic acid	c-UA	139
Valine	Val	118			

Separation was carried out on a Gemini C18 column (50x4.6 mm, 3 μm, 110 Å, Phenomenex, USA) at 40°C and a flow-rate of 0.3 ml/min. A gradient was used with eluent A comprising a 20 mM nonafluoropentanoic acid (NFPA) solution and eluent B acetonitrile. The gradient elution started with 99:1(v/v) A:B for 5 minutes, followed by a linear change to 86:14(v/v) A:B over 9 minutes, then 86:14(v/v) for 5 minutes, and subsequently altered linearly to 64:36(v/v) over 14 minutes. The MS was then switched to negative ion mode with 20/80 (v/v) A:B for 3 minutes to wash the column and finally equilibrated for 20 minutes under initial conditions.

2.9   Data analysis and statistics

Amino-acid-derived components of NMF in the SC were expressed in terms of amount per mass. The change in TEWL as a function of the amount of SC removed was modelled using the so-called baseline-corrected non-linear model [20] to obtain SC thickness using both the gravimetric and imaging methods. Extraction fluxes were calculated by dividing the amounts removed during a sampling interval by the duration of that collection period. Amounts extracted were divided by skin area and expressed in $nmol/cm^2$. Data manipulation and statistics were performed using Graph Pad Prism v. 5.01 (Graph Pad Software Inc., San Diego, CA, U.S.A.). When datasets were compared, the level of statistical significance was fixed at $P < 0.05$. All results were expressed as mean ± SD.

3. Results and discussion

3.1   Thickness of SC

Table 2 presents the average estimated SC thickness (n=6) on the forearm and forehead from the gravimetric and imaging experiments. The imaging method indicates a significantly thinner SC on forehead compared to the forearm (*** $p<0.001$, paired student t-test). The gravimetric approach, on the other hand, shows no apparent difference. The latter is, believed to be due to the significant contribution of sebum to the increased weight of the tape-strips (especially the most superficial -see Figure 1)

Table 2: Baseline TEWL reading and estimated SC thickness (n=6, mean ± SD) on the forehead and forearm determined by gravimetric and imaging methods.

	Forehead	Forearm
Initial TEWL (mg cm^{-2} hr^{-1})	19.9 ± 6.4	9.9 ± 1.5
SC thickness (μm) estimated by gravimetric method	9.4 ± 1.9	10.1 ± 2.6
SC thickness (μm) estimated by imaging technique	4.5 ± 1.0	9.9 ± 2.1
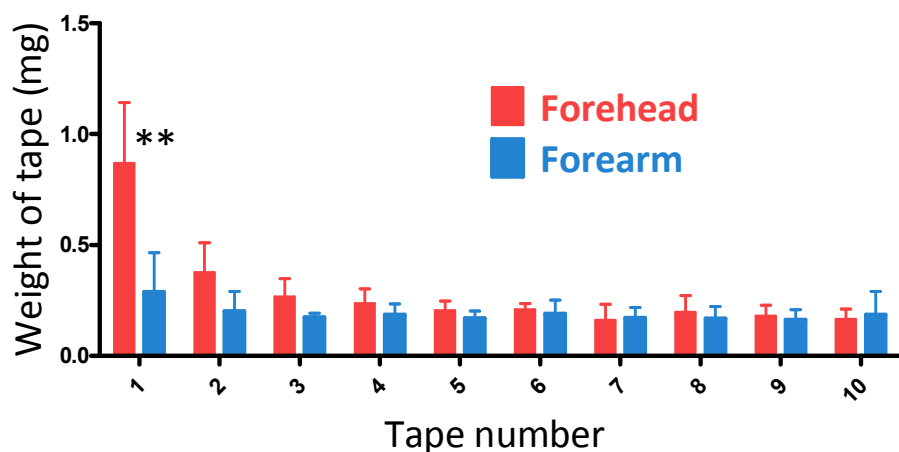
Figure 1: Weight (n=6, mean ± SD) of SC removed on consecutive tape strips on the forehead and forearm.

3.2   IR absorbance of lipids (CH$_2$ stretching absorbance)

IR spectroscopy has been used to report on biomembrane lipid ordering through the CH$_2$ stretching absorbances from the methylene groups of the lipid acyl chains. The CH$_2$ stretching absorbance undergoes a blue shift, i.e., a shift to a higher wavenumber, when the degree of lipid disorder increases.

As shown in Figure 2, the peak asymmetric (~2920cm^{-1}) and symmetric (~2850cm^{-1}) CH$_2$ stretching absorbances occurred at higher wavenumbers at the skin surface before tape-stripping. This is most probably due to the contribution from sebaceous constituents [17]. The CH$_2$ stretching frequencies at both sites before tape-stripping are significantly higher than those after tape-stripping (repeated measure one-way ANOVA followed by Bonferroni's Multiple Comparison Test, $p < 0.01$). Lipids on the forehead is much less ordered comparing to forearm due to much higher number of wavenumbers been detected through the SC (paired t-test $p < 0.0001$) .
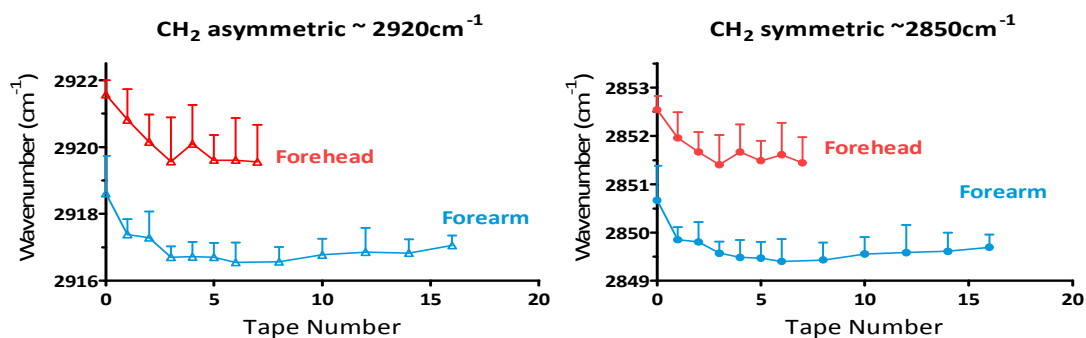
Figure 2: Peak CH_2 asymmetric (~2920cm^{-1}) and symmetric (~2850cm^{-1}) stretching frequencies as a function of tape-strip number (mean ± SD, n=6)

The normalised area under the CH_2 stretching absorbances in Figure 3 were calculated as previously described [17]. A significantly higher level of lipids on the forehead, especially at the surface, is suggested by these data. Repeated measure one-way ANOVA followed by Bonferroni's multiple comparison test ($p<0.01$).
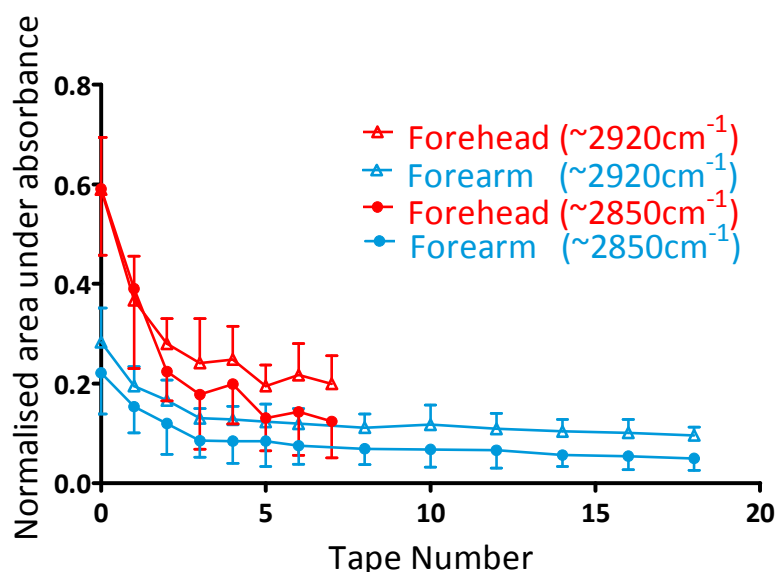
Figure 3: Normalised areas under the CH_2 asymmetric (~2920cm^{-1}) and symmetric (~2850cm^{-1}) stretching absorbances as a function of tape-strip number (mean ± SD, n=6)

Figure 4 illustrates the correlation between the spectroscopically estimated amounts of lipid on the forehead and the weight of SC on the corresponding tape-strip. These results imply that the significant amount of sebaceous lipid on the forehead constitutes importantly to the apparent SC weight on the tape-strip and indicates that, for this anatomic site, the gravimetric approach to determine SC thickness may not be reliable.

121
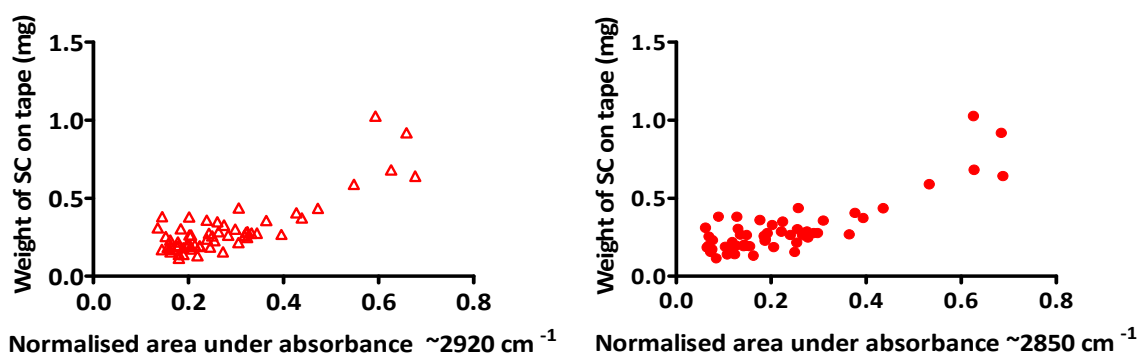
Figure 4: Correlation of the apparent SC weight removed on each tape-strip on the forehead with the normalised areas under the lipid peaks (at ~2920cm^{-1} and 2850cm^{-1}). Both correlations are significant (p<0.0001, 2 tails) with non-parametric Spearman correlation coefficients of r_s=0.6230 and r_s=0.6489, respectively.

3.3   Extraction of amino-acid-derived components of NMF

Twenty-one NMF components were successfully quantified. Other NMF components were detected but could not be quantified (methionine and taurine) while the chromatographic peaks of aspartic acid and asparagine either co-eluted with unknown contaminants or suffered from severe ion suppression.

3.3.1   SC content determined by tape-stripping

Figure 5 illustrates the concentration profile, as a function of SC depth, for serine (an abundantly present), threonine (moderately abundant), phenylalanine (present at low levels) and glutamine (similarly, less abundant) on both the forehead (red) and forearm (blue). As stated above, high sebum secretion on the forehead results in higher apparent weights of SC removed and the gravimetric method was not therefore used to calculate NMF component concentrations. Weights of SC removed on each tape were determined from the imaging technique (Equation 2) and individual NMF component concentrations were then plotted in terms of mmol per kg of SC removed. Distribution profiles of other NMF components are in the Appendix 4.
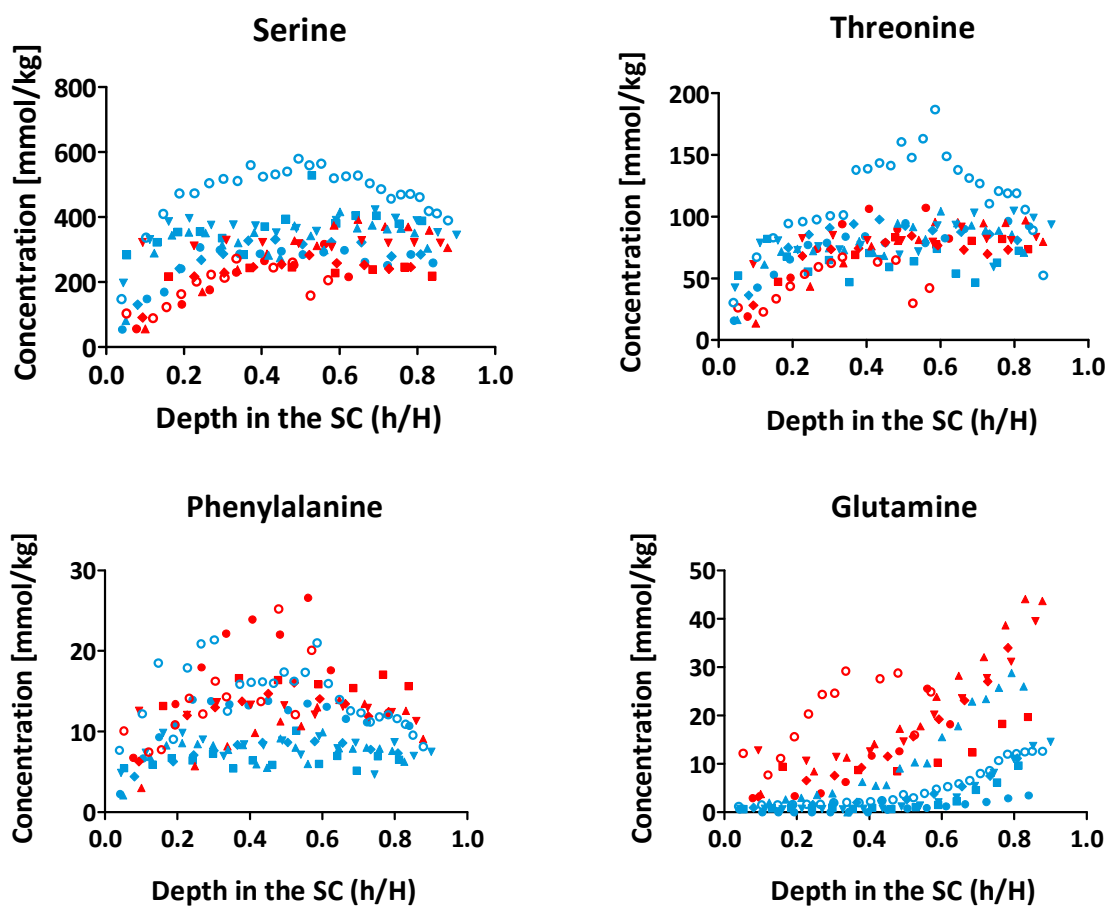
Figure 5: Concentration profiles of serine, threonine, phenylalanine and glutamine as a function of position in the SC on forehead (red) and forearm (blue) in 6 human volunteers.

In most cases, NMF components present at high concentration (e.g., serine) in the skin showed a trend of slightly higher levels on the forearm than on the forehead. For components of moderate concentration (e.g., threonine), similar amounts were found at both sites. However, the NMF constituents present at low concentration appeared at slightly higher levels on the forehead, especially glutamine and glutamic acid. These higher amounts may reflect a shorter time available for their transformation into pyrrolidone carboxylic acid (PCA) in a thinner SC [21]. Nevertheless, this transformation is still very efficient on the forehead, as shown by the relatively high amount of PCA present relative to glutamine. Because all the volunteers had healthy skin at both anatomic sites studied, wide differences in NMF levels are not expected.

3.3.2 Extraction by reverse iontophoresis and passive diffusion

Figure 6 presents examples of reverse iontophoretic and passive extraction of an acidic NMF component (PCA), a basic compound (lysine) and two zwitterions (serine and glutamine) from the forehead (red) and forearm (blue). Extraction of other NMF constituents are shown in the Appendix 4.
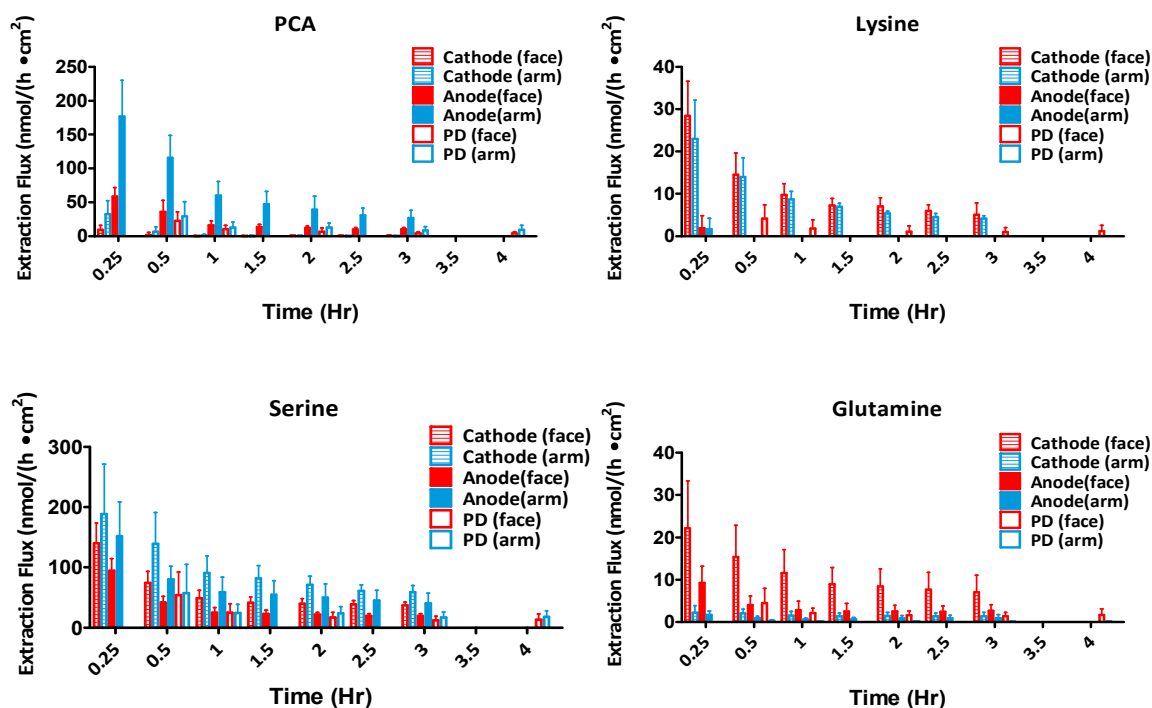
Figure 6: Reverse iontophoretic and passive extraction fluxes (mean ± SD) of an acidic NMF component (PCA), a basic constituent (lysine) and two zwitterions (serine and glutamine) *in vivo* in human volunteers (n=6) from forehead (red) and forearm (blue) skin as a function of time.

The extraction fluxes of all NMF components showed a similar pattern on both skin sites: the initial flux was high and then decreased rapidly over the first hour before stabilising in the later 2 hours.

The reverse iontophoretic and passive extraction of NMF components can be separated into 3 groups:

1) Acidic compounds are negatively charged in solution at physiological pH and were extracted predominantly at the anode. The amounts extracted at the cathode were minimal and, in most cases, below the LOQ. In Chapter 3, these compounds were considered unsuitable for quantification in the SC by reverse iontophoresis because of their extensive extraction from deeper compartment. However, as illustrated in Figure 6, the extraction of PCA on the forearm in the first hour is much higher than that on the forehead, suggesting the presence of a much larger reservoir of PCA in forearm SC. It follows that the initial amounts of charged compounds extracted may be a good indicator of levels in the SC.

2) Extraction of compounds that are positively charged at physiological pH took place mainly at the cathode. The amounts detected at the anode and by passive diffusion were minimal in comparison. As lysine was found only in low amounts in the SC at both sites, the extraction profiles are very similar on the forehead and forearm.

3) Zwitterions were similarly extracted to anode and cathode. Reverse iontophoresis only enhanced extraction by a modest extent, and little difference between forearm and forehead was observed. Glutamine was well extracted from forehead SC even though it was present in relatively low levels.

3.4   Origins of NMF extracted

The amounts of NMF recovered by SC tape-stripping are compared with reverse iontophoretic and passive extraction in Table 3.

Table 3: Cumulative amounts (nmol/cm^2; n=6; mean ± SD) of NMF components extracted in 3 hours by tape stripping, passive diffusion, and reverse iontophoresis (at anode and cathode).

Charged compounds								
Analytes	Tape-stripping		Passive diffusion		Anode		Cathode	
	Forehead	Forearm	Forehead	Forearm	Forehead	Forearm	Forehead	Forearm
PCA	54 ± 24	151 ± 48	29 ± 14	45 ± 27	93 ± 62	176 ± 52	3.9 ± 4.5	11.0 ± 6.6
Urocanic acid	13 ± 4	40 ± 22	8.1 ± 5.0	15 ± 14	9.5 ± 10.2	66 ± 29	5.0 ± 4.4	15.9 ± 26.7
Glutamic acid	18 ± 5	15 ± 8	13 ± 6	2.9 ± 1.7	59 ± 9	36 ± 15	1.8 ± 1.4	0.42 ± 0.5
Histidine	37 ± 15	64 ± 18	29 ± 12	14 ± 7	18 ± 6	31 ± 31	66 ± 22	88 ± 29
Ornithine	6.1 ± 5.2	23 ± 16	6.4 ± 5.1	3.3 ± 3.6	2.2 ± 2.5	5.2 ± 6.1	28 ± 19	59 ± 38
Arginine	25 ± 14	37 ± 31	18 ± 11	5.3 ± 7.1	8.3 ± 6.2	7.6 ± 7.6	63 ± 21	52 ± 33
Lysine	7.8 ± 3.3	12 ± 6	6.2 ± 6.0	<LQL	0.3 ± 0.7	0.4 ± 0.6	28 ± 7	24 ± 4
Zwitterions and Urea								
Analytes	Tape-stripping		Passive diffusion		Anode		Cathode	
	Forehead	Forearm	Forehead	Forearm	Forehead	Forearm	Forehead	Forearm
Serine	92 ± 33	283 ± 93	70 ± 35	86 ± 54	89 ± 15	202 ± 49	157 ± 31	264 ± 72
Glycine	44 ± 16	154 ± 46	37 ± 35	50 ± 30	46 ± 10	121 ± 31	73 ± 36	165 ± 49
Alanine	27 ± 7	98 ± 37	20 ± 8	31 ± 20	29 ± 8	66 ± 24	36 ± 15	69 ± 22
Threonine	26 ± 7	67 ± 22	16 ± 6	20 ± 12	17 ± 3	36 ± 13	26 ± 15	46 ± 14
Citruline	28 ± 5	71 ± 36	22 ± 14	22 ± 15	22 ± 11	38 ± 20	26 ± 13	46 ± 21
Valine	10 ± 2	26 ± 9	10 ± 4	9.6 ± 5.9	11 ± 2	16 ± 6	16 ± 5	17 ± 4
Proline	5.7 ± 1.7	18 ± 4	5.8 ± 2.7	5.6 ± 3.6	6.1 ± 2.3	12 ± 5	7.7 ± 3.7	12 ± 3
Tyrosine	7.9 ± 2.7	16 ± 5	5.6 ± 2.9	3.8 ± 2.4	8.1 ± 2.1	8.8 ± 5.0	10 ± 3	9.1 ± 2.4
Isoleucine	6.2 ± 0.9	14 ± 5	4.6 ± 2.4	3.2 ± 2.4	6.1 ± 1.7	7.7 ± 3.7	7.7 ± 2.4	7.1 ± 1.4
Leucine	8.1 ± 1.2	11 ± 5	7.4 ± 2.4	3.0 ± 1.5	8.7 ± 2.9	6.7 ± 3.0	10.9 ± 3.7	6.0 ± 1.3
Phenylalanine	5.1 ± 1.0	7.7 ± 3.5	4.5 ± 1.3	1.8 ± 1.3	5.3 ± 1.4	4.6 ± 1.9	6.3 ± 1.7	4.0 ± 0.8
Tryptophan	3.2 ± 1.0	6.6 ± 2.5	2.3 ± 1.3	1.6 ± 1.2	2.8 ± 1.0	3.4 ± 1.9	3.4 ± 1.0	2.8 ± 1.0
Glutamine	5.9 ± 2.0	3.3 ± 2.1	6.6 ± 3.8	0.4 ± 0.4	9.8 ± 5.4	2.9 ± 1.9	31 ± 13	4.6 ± 2.6
Urea	45 ± 27	93 ± 59	56 ± 35	66 ± 40	93 ± 62	105 ± 60	110 ± 37	122 ± 64

With the exception of glutamic acid, all charged species were present in higher amounts in forearm SC removed by tape-stripping; however, passive extraction sometimes showed the opposite result, e.g., for lysine passive extraction was clearly more efficient on the forehead. The higher amount found in forearm SC by tape-stripping almost certainly reflects the greater thickness of the barrier and the layer 'volume' from which NMF is being extracted. By contrast, the more facile and efficient passive extraction from the forehead indicates the weaker permeability barrier and more rapid diffusion of small solutes.

Reverse iontophoresis is a powerful tool with which to extract charged molecules. By the end of 3 hours, extraction to the preferred electrode was sampling analytes from beyond the SC (see Figure 7). The extent to which this is the case depends on the properties of the molecule and its concentration in the SC. For example, PCA is present in large amount in the SC, and the time taken to deplete this compound is therefore much longer than that required for others, such as lysine. However, because the systemic concentration of PCA is very low (2.16 ± 0.4 µM [22]), compared to that of essential amino acids (e.g., lysine, 100 - 300 µM [23]), the anodal extraction of PCA is largely affected once the skin reservoir has been depleted. It follows that PCA extraction by reverse iontophoresis may be a sensible strategy to probe skin barrier function.
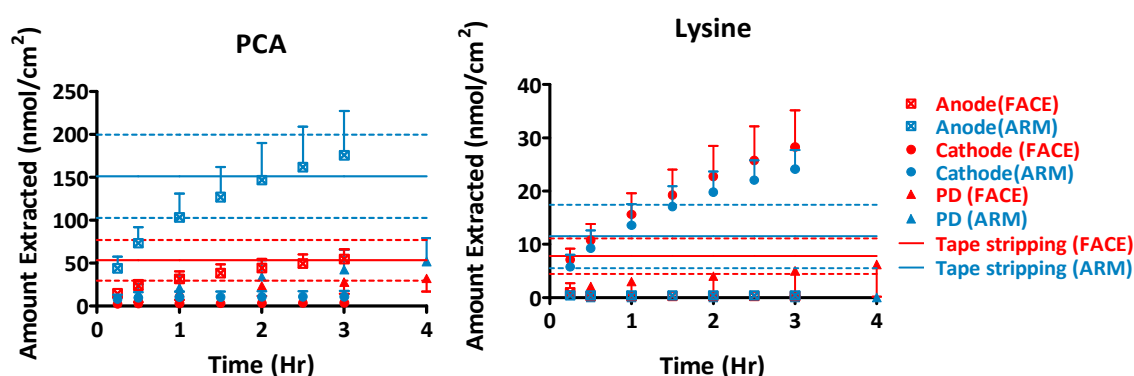
Figure 7: Cumulative amounts of PCA and lysine extracted (n=6; mean ± SD) by iontophoresis at both electrodes and by passive diffusion as a function of time from the forehead (red) and forearm (blue). The average quantities in the SC determined by tape-stripping are shown for comparison by the solid horizontal lines; with the ± SD indicated by dashed lines.

For the zwitterionic constituents of NMF, reverse iontophoresis could not deplete the amounts present in the 'SC reservoir' on the forearm by the end of 3 hours; in contrast, extraction from forehead SC was almost complete. The quantities extracted by reverse iontophoresis were, on the whole, higher than by passive diffusion, but not as dramatically different as seen for the charged compounds. Nevertheless, reverse iontophoresis improves the migration of the zwitterions significantly and higher extraction from the forearm has been observed.
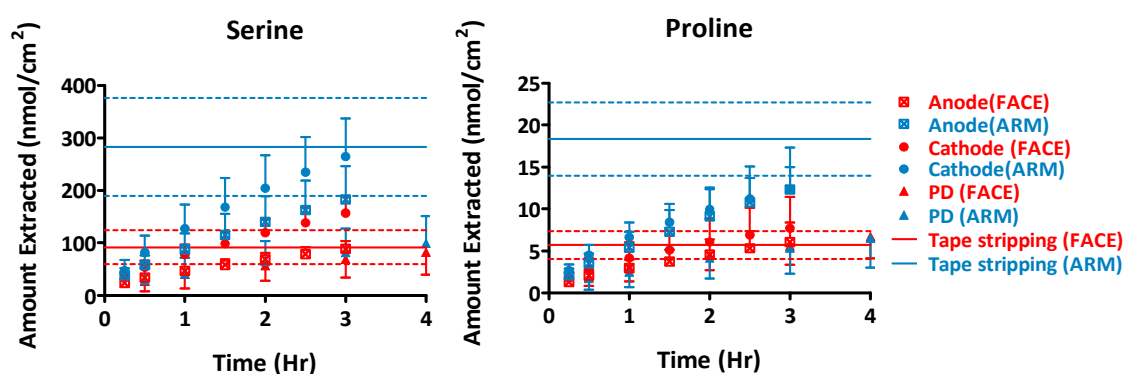
Figure 8: Cumulative amounts of serine and proline extracted (n=6; mean ± SD) by iontophoresis at both electrodes and by passive diffusion as a function of time from the forehead (red) and forearm (blue). The average quantities in the SC determined by tape-stripping are shown for comparison by the solid horizontal lines, with the ±SD indicated by dashed lines.

Urea (molecular weight: 60) is a small molecule, which readily permeates the skin. It is extracted efficiently by passive diffusion and, within 3 hours, the amount in the SC has been just about depleted. However, as urea is also secreted from sweat onto the surface of the SC, the amount extracted shows considerable variability between subjects.

4. Conclusions

These data demonstrate that an abundant amino-acid-derived NMF reservoir exists in forearm and forehead SC. Stratum corneum lipids on the forehead are more disordered, especially near the surface due to an extensive contribution of sebum. The concentrations

of amino-acid derived NMF components at both sites are similar. However, forehead SC is thinner and generally contains a lower total amount of NMF. Reverse iontophoresis efficiently extracted charged NMF components relative to passive diffusion. The initial extraction period predominately sampled NMF constituents in the SC. Moderate enhancement of the extraction of zwitterions components was observed with the quantities obtained being reflective of those in the SC.

5. Reference

1. Rawlings A and Matts P, *Stratum Corneum Moisturization at the Molecular Level : An Update in Relation to the Dry Skin Cycle.* J Invest Dermatol, 2005. **124**(6): p. 1099-1110.

2. Scott IR, Harding CR, and Barrett JG, *Histidine-rich protein of the keratohyalin granules: Source of the free amino acids, urocanic acid and pyrrolidone carboxylic acid in the stratum corneum.* Biochimica et Biophysica Acta (BBA) - General Subjects, 1982. **719**(1): p. 110-117.

3. Rawlings A and Harding C, *Moisturization and skin barrier function.* Dermatologic Therapy, 2004. **17**(s1): p. 43-48.

4. Muller S, Marenholz I, Lee Y, Sengler C, Zitnik S, Griffioen R, Meglio P, Wahn U, and Nickel R, *Association of filaggrin loss-of-function-mutations with atopic dermatitis and asthma in the Early Treatment of the Atopic Child (ETAC) population.* Pediatric Allergy and Immunology, 2009. **20**(4): p. 358-361.

5. Nomura T, Akiyama M, Sandilands A, Nemoto-Hasebe I, Sakai K, Nagasaki A, Palmer CNA, Smith FJD, McLean WHI, and Shimizu H, *Prevalent and rare mutations in the gene encoding filaggrin in Japanese patients with ichthyosis vulgaris and atopic dermatitis.* J Invest Dermatol, 2008. **129**: p. 1302-1305.

6. Nemoto-Hasebe I, Akiyama M, Nomura T, Sandilands A, McLean WHI, and Shimizu H, *Clinical Severity Correlates with Impaired Barrier in Filaggrin-Related Eczema.* J Invest Dermatol, 2008. **129**(3): p. 682-689.

7. Brown SJ and Irvine AD, *Atopic eczema and the filaggrin story.* Seminars in Cutaneous Medicine and Surgery, 2008. **27**(2): p. 128-137.

8. Kezic S, Kammeyer A, Calkoen F, Fluhr JW, and Bos JD, *Natural moisturizing factor components in the stratum corneum as biomarkers of filaggrin genotype: evaluation of minimally invasive methods.* British Journal of Dermatology, 2009. **161**(5): p. 1098-1104.

9. Kezic S, Kemperman PMJH, Koster ES, de Jongh CM, Thio HB, Campbell LE, Irvine AD, McLean IWH, Puppels GJ, and Caspers PJ, *Loss-of-Function mutations in the filaggrin gene lead to reduced level of natural moisturizing factor in the stratum corneum.* J Invest Dermatol, 2008. **128**(8): p. 2117-2119.

10. Horii I, Nakayama Y, Obata M, and Tagami H, *Stratum corneum hydration and amino acid content in xerotic skin.* British Journal of Dermatology, 1989. **121**(5): p. 587-592.

11. Takahashi M and Tezuka T, *The content of free amino acids in the stratum corneum is increased in senile xerosis.* Archives of Dermatological Research, 2004. **295**(10): p. 448-452.

12. Denda M, Hori J, Koyama J, Yoshida S, Nanba R, Takahashi M, Horii I, and Yamamoto A, *Stratum corneum sphingolipids and free amino acids in experimentally-induced scaly skin.* Archives of Dermatological Research, 1992. **284**(6): p. 363-367.

13. Ya-Xian Z, Suetake T, and Tagami H, *Number of cell layers of the stratum corneum in normal skin – relationship to the anatomical location on the body, age, sex and physical parameters* Archives of Dermatological Research, 1999. **291**: p. 555-559.

14. Machado M, Salgado TM, Hadgraft J, and Lane ME, *The relationship between transepidermal water loss and skin permeability.* International Journal of Pharmaceutics, 2010. **384**(1-2): p. 73-77.

15. Harding CR, Long S, Richardson J, Rogers J, Zhang Z, Bush A, and Rawlings AV, *The cornified cell envelope: an important marker of stratum corneum maturation in healthy and dry skin.* International Journal of Cosmetic Science, 2003. **25**(4): p. 157-167.

16. Voegeli R, Rawlings A, Doppler S, Heiland J, and Schreier T, *Profiling of serine protease activities in human stratum corneum and detection of a stratum corneum tryptase-like enzyme.* International Journal of Cosmetic Science, 2007. **29**(3): p. 191-200.

17. Aramaki J, Löffler C, Kawana S, Effendy I, Happle R, and Löffler H, *Irritant patch testing with sodium lauryl sulphate: interrelation between concentration and exposure time.* British Journal of Dermatology, 2001. **145**(5): p. 704-708.

18. Kalia YN, Alberti I, Sekkat N, Curdy C, Naik A, and Guy RH, *Normalization of Stratum Corneum Barrier Function and Transepidermal Water Loss In Vivo.* Pharmaceutical Research, 2000. **17**(9): p. 1148-1150.

19. Russell L, *Dermato-pharmacokinetics: an approach to evaluate topical drug bioavailabilty*, in *Department of Pharmacy and Pharmacology*. 2008, University of Bath: Bath.

20.   Russell LM, Wiedersberg S, and Delgado-Charro MB, *The determination of stratum corneum thickness An alternative approach.* European Journal of Pharmaceutics and Biopharmaceutics, 2008. **69**(3): p. 861-870.

21.   Barrett JG and Scott IR, *Pyrrolidone Carboxylic Acid Synthesis in Guinea Pig Epidermis.* J Invest Dermatol, 1983. **81**(2): p. 122-124.

22.   Wolfersberger MG and Tabachnik J, *Pyrrolidone carboxylic acid (pyroglutamic acid) in normal plasma.* Cellular and Molecular Life Sciences, 1973. **29**(3): p. 346-347.

23.   Kingsbury KJ, Kay L, and Hjelm M, *Contrasting plasma free amino acid patterns in elite athletes: association with fatigue and infection.* British Journal of Sports Medicine, 1998. **32**(1): p. 25-32.

Chapter 5: Assessment of skin barrier function following chronic exposure to sodium lauryl sulphate (SLS)

Abstract

Purpose:

Different bioengineering methods have been used to screen SC barrier function on sodium lauryl sulphate (SLS) treated and control forearm skin of healthy volunteers and to identify changes in corneocyte morphology, stratum corneum (SC) lipid organisation, and levels of natural moisturising factor (NMF) as markers of skin impairment.

Methods:

0.1% w/v SLS was applied to the ventral forearms of 7 healthy volunteers to provoke a compromised skin barrier. NMF components were extracted from the SLS-treated and from untreated, control sites using reverse iontophoresis and passive extraction, and by analysis of tape-strip samples. The quantities of 21 different components of NMF were identified and quantified by LCMS. Transepidermal water loss (TEWL) measurements were taken before and after every other tape-strip to determine SC thickness. The SC was examined post SLS-treatment by attenuated total reflectance-fourier transform infrared spectroscopy (ATR-FTIR). Lipid quantity and organisation were probed by recording spectra as a function of depth with the SC (assessed by repeated tape-stripping). The surface area and maturity of corneocytes removed by tape-stripping from the surface and deeper SC were also evaluated. Finally, on one volunteer, SC recovery 3, 7, 11, 15 days after the last SLS application was assessed.

Results:

SC thickness was significantly thinner post-SLS treatment and TEWL was correspondingly higher. The levels of most NMF components were reduced following chronic application of the surfactant. On the other hand, a few NMF constituents, which are normally present at low levels in normal skin, were either unchanged or higher after SLS application and were, as a result, more easily extracted by passive diffusion and reverse iontophoresis. The peak – CH_2 symmetric and asymmetric stretching absorbance frequencies were shifted to higher values following surfactant treatment indicating disordering of the SC intercellular lipids.

Changes in lipid packing from orthorhombic to hexagonal were also observed. Microscopic examination revealed that corneocytes from SLS-treated skin were less mature and had reduced surface area. In the one volunteer studied longitudinally, the SC had not recovered fully even 15 days after the final SLS application.

Conclusion:

The SC barrier was substantially impaired after chronic SLS application, showing significantly reduced NMF, substantial lipid disordering, and the presence of immature corneocytes.

1. Introduction

Repeated cutaneous exposure to particular chemicals is the leading cause of irritant contact dermatitis (ICD) [1] and of atopic dermatitis (AD) flares [2]. The 'irritation threshold' to the model irritant, sodium lauryl sulphate (SLS), has been suggested as an indicator of individual susceptibility to chronic ICD [3]; indeed, repeated exposure of healthy volunteers to a low concentration of SLS over 3 weeks has been used as a model for studying chronic ICD [4-5]. The development of ICD is not fully understood, but the symptoms are similar to AD: eczematous, inflamed skin lesions with pruritus in irritant-exposed areas and hyperkeratosis in chronic lesions. Present or past AD is also a predisposing factor for chronic ICD [6]. Moreover, repeated exposure to low concentrations of SLS increases the ratio of the cytokines IL-1RA to IL-1α, commonly found in cutaneous inflammation and chronic disorders such as AD [7]. Therefore, it was hypothesised that normal skin repeatedly exposed to a low concentration of SLS may be used to the model the distinction between a competent stratum corneum (SC) and a barrier compromised by AD.

The protein filaggrin plays an important role in the development of AD and its genetic-linked mutation is strongly associated the disease [8-11]. Filaggrin, an acronym for filament-aggregating protein, was first recognized as a keratin intermediate filament associated protein that aggregated epidermal keratin filaments *in vitro*. It is degraded in the SC into hygroscopic amino acids, which are known collectively as the amino-acid-derived components of natural moisturizing factor (NMF).

NMF, which is found exclusively in the SC, is a collection of water-soluble, low molecular weight compounds, comprising approximately 20-30% of corneocyte dry weight [12]. NMF components act as extremely efficient humectants by absorbing atmospheric moisture and dissolving in their own water of hydration. NMF is believed to be critical in maintaining the hydration of the skin despite the desiccating action of the environment [13]. However, NMF is much more important. By keeping the SC hydrated, NMF encourages critical biochemical events, most importantly, the regulation of several corneocyte proteases that are involved in the generation of NMF itself [12]. The majority of NMF components are derived from filaggrin. Not surprisingly, reduced NMF has been associated with the

filaggrin mutation [14] and has been implicated in the aetiology of several dermatological disorders including ichthyosis vulgaris, AD and allergic contact sensitization [15-16]. However, the down-regulation of filaggrin and thus a possible subsequent reduction in NMF, is not only due to genetic mutation but also to inflammation. AD is a T-cell-mediated skin disease, and the primary event is associated with T_h2 cell activation. Filaggrin deficiency in AD patients can therefore be acquired, at least in part, by the over-expression of T_h2 cytokines [17]. As a result, measuring the amount of NMF in the skin could be a good indicator of filaggrin expression and thus of the barrier function of the skin.

SLS is a common surfactant in soaps, shampoos, and skin care products and it is known to cause skin barrier damage. A repeated irritation test involving application of 0.1% w/v SLS for 6 hours a day, 4 days a week, for 3 weeks can imitate the skin damage caused by chronic contact with detergents [1]. Furthermore Torma [18] showed that, after a 24 hr application of 1% w/v SLS, filaggrin mRNA expression was strongly reduced already at 6 hours post-treatment, but that a major increase was detected after 4 days presumably indicating recovery of the skin barrier. However, because the high concentration of SLS used in this case was much higher than that encountered in real life, a 3-week exposure of healthy volunteers to a lower level of surfactant was thought to be a better model for producing eczematous-like skin. Measurements of TEWL throughout the application period indicated the extent to which the skin barrier had been damaged. Immediate removal of SC by tape-stripping post-exposure was not performed since passive extraction of these materials during SLS application may have occurred. For this reason, NMF components in the SC were sampled and quantified 3 days after the last exposure to SLS.

In addition to NMF quantification, the present study also examined the effects of SLS on other factors that may affect skin barrier function. Fourier-transform infrared spectroscopy (FTIR) is a well-known non-invasive technique with which to analyse skin lipid organisation *in vivo* [4]. Advantage is taken of the shallow penetration depth of infrared radiation into the skin by recording FTIR spectra during sequential tape-stripping to provide information on skin hydration and SC lipid arrangement throughout the SC. Moreover, corneocyte maturity and surface area have been measured using the SC tape-strip samples thereby allowing construction of rigid cornified envelopes to be assessed on another matter of SC barrier function [19].

The overall goal, therefore, was to apply different bioengineering methods to screen SC barrier function following prolonged SLS exposure and to explore the mechanisms by which damage to the skin occurs.

2. Materials and methods

2.1   Chemicals

Sodium azide, NFPA (perfluoropentanoic acid), silver (Ag) wire (>99.99% purity), AgCl (99.999%), acetonitrile, ethylenediaminetetraacetic acid (EDTA), Nile red, DL-dithiothreitol, Tris-HCl buffer, sodium dodecyl sulphate, monoclonal anti-involucrin antibody produced in mouse (clone SY5), FITC-labelled antimouse IgG, bovine serum albumin and all L-amino acids acids (Asn, Ser, Gly, Asp, Cit, Orn, Gln, Glu, Thr, Ala, Pro, Val, Tyr, Met, Ile, Leu, His, Lys, Phe, Arg, and Trp) were purchased from Sigma-Aldrich Co. (Gillingham, UK). Glycine-D5, Serine-D3, Glutamine-D5 were purchased from Cambridge Isotope Laboratories (Andover,MA). Perdeuterated sodium lauryl sulphate was purchased from Qmx laboratories (UK). Deionised water (resistivity ≥ 18.2 MΩ/cm^2) was used to prepare all aqueous solutions (Barnstead Nanopure Diamond^{TM}, Dubuque, IA).

2.2   Human subjects

Six healthy volunteers (2 male, 4 females, Caucasian and Asian subjects aged between 20 and 36 years) with no history of skin disease and no recent skin treatment participated in the main study, which was approved by the University of Bath research ethics approval committee, and provided written consent. On another female volunteer (27 years old, Asian subject), SLS recovery 3, 7, 11, 15 days after last SLS patch application was assessed. Soaps, detergents and moisturizers were not used on either arm during the experiment.

2.3   SLS treatment

1) Five sites on the left ventral forearm was exposed to a 0.1% w/v perdeuterated sodium lauryl sulphate solution (SLS, 250 µl, Qmx laboratories, UK), using a patch test chamber (Hilltop chamber of 25mm diameter and filter paper disc of 20 mm diameter), for 6 hours a day, 4 days a week, for 3 weeks as described in Table 1. The right ventral

forearm was used as control. The use of perdeuterated SLS permits its presence within the SC and its effect on endogenous skin lipids to be unambiguously resolved by infrared spectroscopy.

Table 1: SLS treatment protocol of the left forearms of the volunteers (n=6).

Week 1				Week 2				Week 3				Days after last patch application			
Tue	Wed	Thur	Fri	Tue	Wed	Thur	Fri	Tue	Wed	Thur	Fri	3	7	11	15
↑	↑	↑	↑	↑	↑	↑	↑	↑	↑	↑	↑	#			
*			*	*			*	*			*	Δ	Δ	Δ	Δ

↑ 6hr 0.1% w/v SLS patch application

* TEWL measurements

\# Main experiments (see Table 2)

Δ Recovery phase experiment (tape-stripping and FTIR, n=1)

2) Transepidermal water loss (TEWL) was measured at the treated and control sites on every Tuesday and Friday during the SLS treatment. The measurements were performed before patch application.

3) The SLS concentration was adjusted after day 4 and day 11 to mitigate against strong skin irritation reactions. If TEWL was >50 g m^{-2} h^{-1}, then the SLS concentration was halved. This was necessary for 1 week in two volunteers, one of whom also skipped the last patch application due to a strong erythematous reaction.

4) Six volunteers (n=6) participated in the main series of experiments 3 days after the final SLS application (Table 2). The skin sites on both arms were cleaned before any measurements with isopropyl alcohol wipes (Medi-Swab, Seton Healthcare Group plc, England) and allowed to dry completely.

5) One female volunteer participated in the recovery phase experiment which included tape stripping and FTIR measurements on day 3, 7, 11, 15 after the final SLS application.

Table 2: Experiment design on 3 days after the 3-week SLS treatment.

	Morning				Afternoon
	Site 1	Site 2	Site 3	Site 4	Site 5
Forearm , left **(SLS treated)**	Iontophoresis (Anode +)	Iontophoresis (Cathode -)	Passive extraction	Tape-stripped	Tape-stripped & FTIR
Forearm , right **(untreated control)**	Iontophoresis (Anode +)	Iontophoresis (Cathode -)	Passive extraction	Tape-stripped	Tape-stripped & FTIR

2.4   Reverse iontophoresis extraction

The iontophoretic system consisted of two glass cells (internal diameter 1.55 cm , extraction surface 1.89 cm^2), which were firmly attached to the forearm with silicon grease and held in place with medical adhesive tape (Curafix H, Lohmann & Rauscher,Rengsdorf, Germany). Silver-silver chloride (Ag/AgCl) electrodes were introduced via perforations in the plastic covers of the cells, which were filled with 1.6 ml of 20 mM ammonium chloride in 10 mM ammonium bicarbonate buffer at pH~ 6.8. A direct current of 0.4 mA (i.e., 0.21 mA/cm^2) was applied from a Phoresor II Auto (Iomed, Model No. PM850, Salt lake City, UT) via the Ag/AgCl electrodes. The entire contents of the anode and cathode chambers were collected and replaced by an equal volume of extraction solution at 15 and 30 minutes and then every half-hour thereafter for a total extraction time of 3 hours. The collected samples were passed through a sterile syringe filter (Cronus, 0.45 µm, 4 mm diameter, SMI-LabHut Ltd, Gloucester, UK) and stored in the freezer at -20°C until analysis.

2.5   Passive diffusion extraction

One glass cell (internal diameter 1.55 cm, extraction surface 1.89 cm^2) was adhered to the skin as above and was filled with 1 ml of the same extraction solution. Identical sampling, filtration and storage procedures were followed as before.

2.6   Tape-stripping

The SC was progressively removed by the repeated application and removal of adhesive tape-strips (Permacel J-LAR ® clear to the core tape, Permacel, Wisconsin, USA). A template with a round hole (diameter 1.54 cm) was first fixed to the skin with self-adhesive medical tape (Curafix H, Lohmann & Rauscher, Rengsdorf, Germany) to ensure that all tape-strips were taken from exactly the same site. The tapes (2.5 x 3 cm) were applied with pressure from a roller and then swiftly removed. TEWL measurements were taken (AquaFlux V4.7, Biox Systems Ltd., London, UK) before and after every other tape-strip, and tape-stripping was stopped when TEWL reached 3-4 fold the initial value, at which point approximately 75% of the SC had been removed [20].

Tape-strips removed from one site were used for analysis of corneocyte maturity and size, while those from another site were extracted with an aqueous solution of sodium azide (20 mg/l) which was subsequently analysed for NMF. Every two consecutive tapes were grouped and extracted into 1 ml of solution. The extracted solutions were filtered (Cronus, 0.45 μm, 4 mm diameter, SMI-LabHut Ltd, Gloucester, UK) and stored at -20°C until analysis.

2.7   Attenuated total reflectance-fourier transform infrared spectroscopy (ATR-FTIR) measurements

2.7.1 Equipment

A PerkinElmer (Massachusetts,USA) Spectrum 100 FT-IR spectrometers was used. The spectrometer was equipped with a universal ATR accessory with a round diamond crystal (2 mm diameter) and the single bounce top-plate was used.

2.7.2 Experiments

On both untreated and SLS-treated skin, two IR spectra with 200 scans each were recorded before tape-stripping and immediately after removing the 1st, 3rd, 5th, 15th and final tapes.

2.7.3 Spectral analysis

FTIR spectra were collected in the frequency range 4000-400cm^{-1}. To minimize the influence of the broad water peak at ~3300cm^{-1}, the peak frequencies of both asymmetric (~2920cm^{-1}) and symmetric (~2850cm^{-1}) CH_2 stretching absorbances were found following baseline-correction of the lipid absorption region (2990cm^{-1} − 2810cm^{-1}) and first-order

derivativisation (Spectrum[TM] Express software). The areas under both CH_2 stretching absorbances were calculated by their normalisation with respect to the combined areas of the amide I and II bands. Lipid organisation was assessed according to a published method [21]. Briefly, the second-derivative of the IR spectrum of the scissoring region ($1480cm^{-1}$ – $1460cm^{-1}$) were baseline-corrected and subsequently normalised to identical minima and maxima. The bandwith at 50% (FWHM) of the peak height was then calculated. Further chemometric analysis was performed using the computational package Matlab (The Mathworks Inc. Natick, MA, USA).

2.8   Corneocyte maturity and surface area

Corneocyte maturity was evaluated using a previously reported method [22]. Maturity was determined at the skin surface (first 2 tape-strips) and from the deepest SC layers sampled (last 3 tape-strips). Briefly, a corneocyte suspension was prepared by boiling and washing the tapes in a dissociation buffer consisting of 2% w/v sodium dodecyl sulphate, 20 mM dithiothreitol, 5 mM EDTA and 0.1 M Tris-HCl (pH 8.5) to remove soluble material. The resulting suspension was dropped onto a glass slide, air-dried and fixed in cold acetone (-30°C, 10min). The corneocytes were then exposed to anti-involucrin (1:100, clone SY5, Sigma) overnight, followed by staining with (a) FTIC-labelled antimouse IgG (1:100, Sigma) for two hours and (b) Nile red (3 µg/ml). Fluorescence images were then acquired at once using a microscope (Leica DMI 4000B, Wetzlar, Germany) equipped with a Leica DFC420C camera. Ratios of red to green pixels were quantified and analysed by ImageJ® (U.S. National Institutes of Health, Bethesda, Maryland, USA).

Corneocyte surface area (A) was also measured using ImageJ® and a mean value was calculated from 20 measured corneocytes from each sample.

2.9   Analysis of tapes

2.9.1   Weighing method

Tapes were equilibrated for at least 12 hours before being weighed. Static electricity was first discharged from the tapes (R50 discharging bar and ES50 power supply from Eltex Elektrostatick GmbH, Weil am Rhein, Germany), which were then weighed before and after stripping on a 0.1 µg precision balance (Sartorius SE2-F, Epsom, UK). The mass of SC

removed divided by the strip area (1.86 cm^2) and by the SC density (1 g/cm^3) allowed the thickness of the barrier layer on each tape to be calculated. Six blank tapes were weighed at the same time as those used for tape-stripping to correct for any variations due to environmental or other factors.

2.9.2 Imaging method

The tapes were photographed using a Coolscan slide scanner (Nikon UK Limited, Kingston upon Thames, US) at a resolution of 4000 pixels per inch (157.5 pixels/mm) as previously described [23]. A crop of approximately 2 x 2 cm was centred over each image. Images were analysed by ImageJ (U.S. National Institutes of Health, Bethesda, Maryland, USA) and a mean greyscale value for each was determined in the range 0-64608, where 0 and 64608 represent black and white respectively. The mean greyscale over all pixels was calculated by ImageJ. Six blank tapes provided the mean greyscale background (G_{blank}). The SC absorbance (A_{SC}) was then calculated as:

1) A_{SC} = -log (G_{SC}/G_{blank})

As the weight of SC (M_{SC}) on each tape had been quantified, the correlate A_{SC} and M_{SC} as described in Chapter 2:

2) M_{SC} = 0.36x A_{SC} +0.009

2.10   Analytical chemistry

LCMS was performed on a Shimadzu LCMS-2010EV with a single quadrupole and a dual ion source (containing both electrospray and atmospheric pressure chemical ionization). The MS was operated in positive ion mode with the ionspray voltage set at 1.5 kV. Nitrogen was used both as a nebulising and drying gas at a flow rate of 1.5 L/min with a heat block temperature of 480°C and curved desolvation line temperature of 230°C. The quadrupole was operated in the selected ion monitoring mode and protonated molecules [M+H]$^+$ (Table 3) were used for quantification

Table 3: Molecules for quantification

Molecules	Abbr.	[M+H]$^+$	Molecules	Abbr.	[M+H]$^+$
Alanine	Ala	90	Arginine	Arg	175
Asparagine	Asn	133	Aspartic acid	Asp	134
Citruline	Cit	176	Glutamic acid	Glu	148
Glutamine	Gln	147	glutamine-D5		152
Glycine	Gly	76	Glycine-D2		78
Histidine	His	156	Isoleucine	Ile	132
Leucine	Leu	132	Lysine	Lys	147
Methionine	Met	150	Ornithine	Orn	133
Phenylalanine	Phe	166	Proline	Pro	116
Pyrrolidone carboxylic acid	PCA	130	Taurine	Tau	126
Serine	Ser	106	Serine-D3		109
Theonine	Thr	120	Tryptophan	Try	205
Tyrosine	Tyr	182	Urea		61
Trans-urocanic acid	t-UA	139	Cis-urocanic acid	c-UA	139
Valine	Val	118			

Separation was carried out on a Gemini C18 column (50x4.6 mm, 3 µm, 110 Å, Phenomenex, USA). All analyses were carried out at 40°C with a flow-rate of 0.3 ml/min. A gradient was used with eluent A being a 20 mM nonafluoropentanoic acid (NFPA) solution and eluent B acetonitrile. The gradient elution started with 99:1(v/v) A:B for 5 minutes, followed by a linear change to 86:14(v/v) A:B over 9 minutes, then 86:14(v/v) for 5 minutes, and subsequently altered linearly to 64:36(v/v) over 14 minutes. The MS was then switched to negative ion mode with 20/80(v/v) A:B for 3 minutes to wash the column and finally equilibrated for 20 minutes under the initial conditions.

2.11   Data analysis and statistics

The concentrations of amino-acid-derived components of NMF were expressed in terms of amount per mass of SC. The change in TEWL as a function of the amount of the SC removed was modelled using the baseline-corrected non-linear model [24] to determine the barrier thickness (H).

$$\text{TEWL} = B + \frac{DK\Delta C}{H - h}$$

where B is the baseline correction factor; D is the diffusion coefficient of water in the SC; K is the SC-viable tissue partition coefficient of water; ΔC is the water concentration gradient across the SC; and h is the cumulative thickness values of SC removed. Fitting the results to this equation allows the best estimates of B, ($DK\Delta C$) and H to be deduced.

Extraction fluxes were calculated by dividing the amounts removed during a sampling interval by the duration of that collection period. Amounts extracted were divided by the skin area and expressed in $nmol/cm^2$. Data manipulation and statistics were performed using Graph Pad Prism v. 5.01 (Graph Pad Software Inc., San Diego, CA, U.S.A.). When datasets were compared, the level of statistical significance was fixed at $P < 0.05$. All results were expressed as mean ± SD.

3. Results and discussion

3.1 Skin reaction after 3 weeks SLS exposure
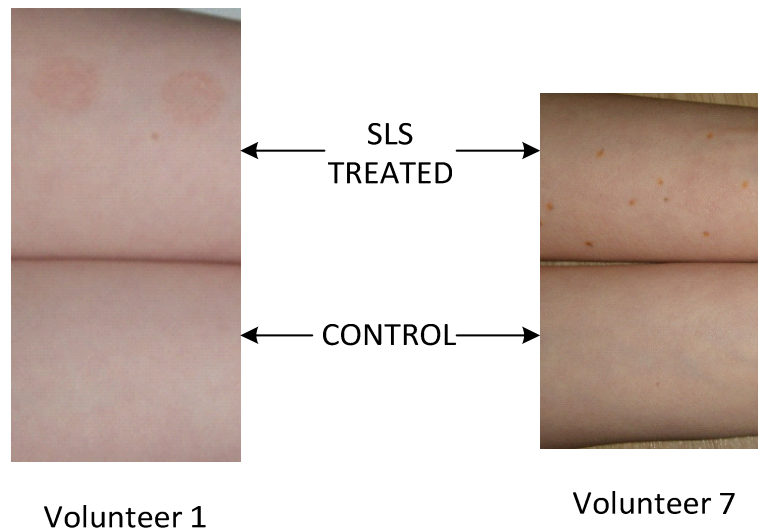
Figure 1: Skin reactions in volunteers 1 and 7 after 3 weeks of SLS exposure.

All volunteers but one (volunteer 7) developed dry, red patches at the site of SLS application. As described before [25-26], a large individual variation in response was observed. Some individuals developed redness in the first week, whereas volunteer 7 did not manifest clear, visible red patches after 3 weeks of SLS exposure.

3.2   TEWL after repeated SLS exposure

In two subjects, the SLS concentration was halved for 1 week due to a strong erythema appearing and a value of TEWL >50 g m^{-2} h^{-1}. One of these subjects also skipped the final patch application due once again to an intense erythematous reaction and TEWL>70 g m^{-2} h^{-1}. The same subjects showed skin reddening from the first week of SLS exposure, while most of the other subjects developed visible erythema only in the second or third week.
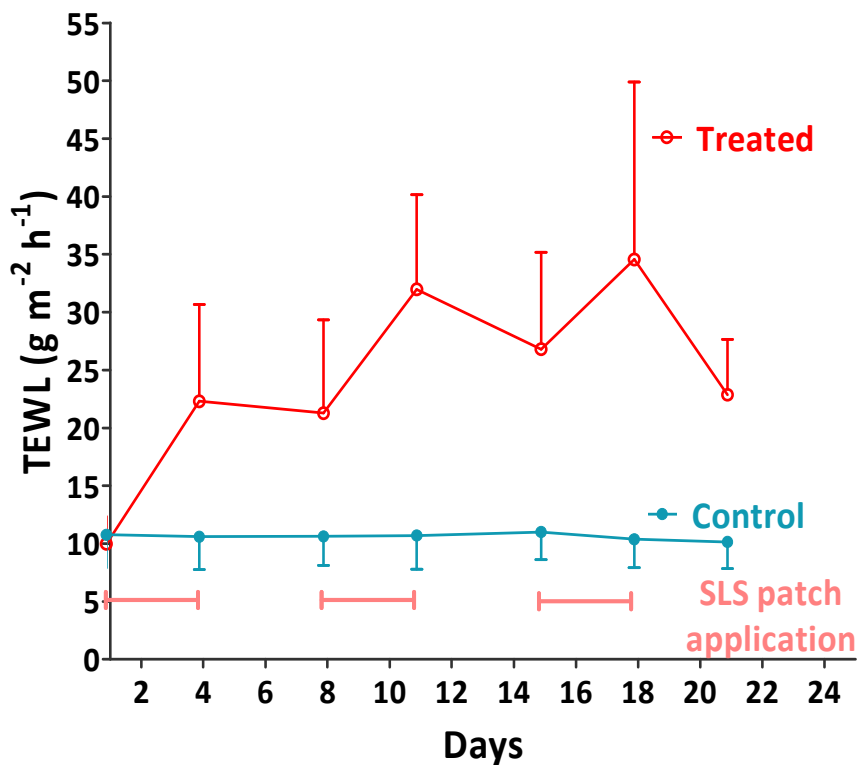
Figure 2: Transepidermal water loss (TEWL, mean ± SD, n=7) on SLS-treated and control sites during patch application and 3 days after the last patch application.

Figure 2 shows the mean change in TEWL during the SLS exposure period on both treated and control forearms. TEWL at the control site remained constant, while TEWL increased appreciably at site treated repeated with SLS. Partial recovery during the non-treatment days was apparent.

3.3 Corneocyte maturity
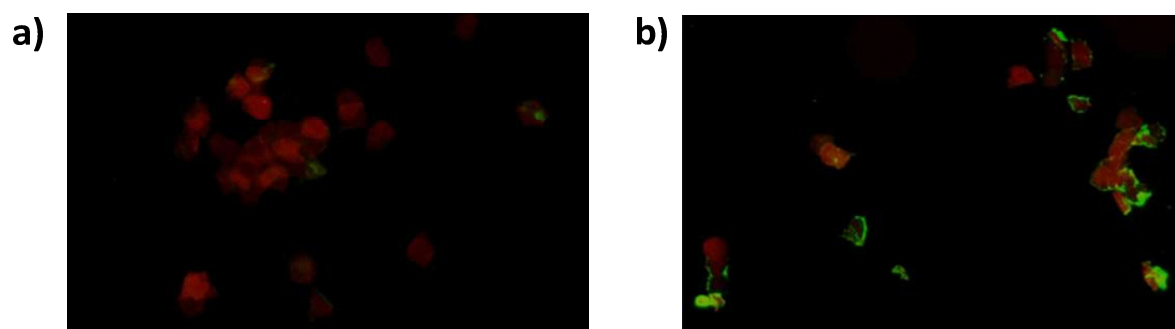
Figure 3: Sample microscopic images that contain primarily mature (a) or immature (b) corneocytes.
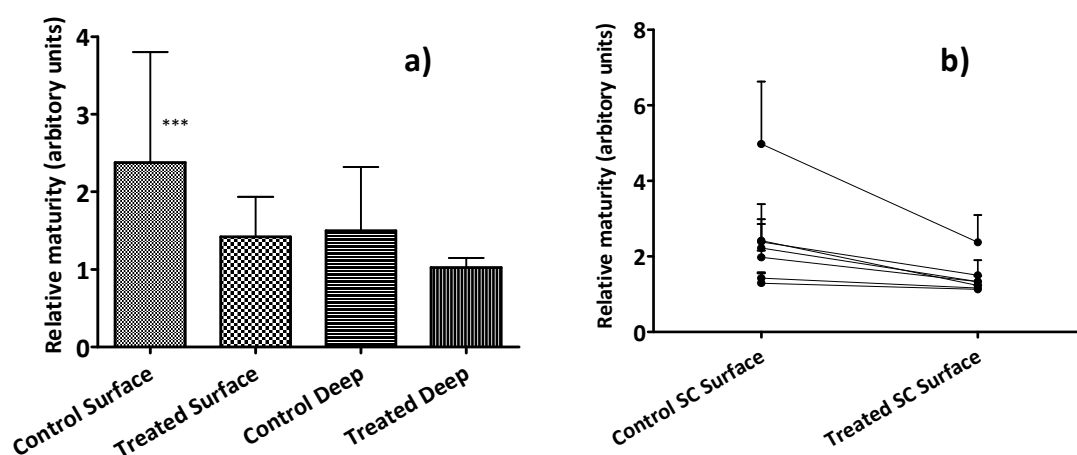
Figure 4: (a) Corneocyte maturity (appeared as the ratio of red/green pixels (see text), mean ± SD, n=7, 3 images per volunteer) on SLS-treated and control skin sites at the surface of and deep within the SC. (b) Corneocyte maturity of each individual on the surface of control and SLS-treated skin sites.

The maturity of corneocytes removed from control and treated sites (calculated as described previously [27]) is plotted in Figure 4a. A one-way ANOVA with Bonferroni's multiple comparison test demonstrated that the surface corneocytes from the control site showed significantly greater maturity than the other 3 sites (P<0.0001), between which there was no significant difference. Figure 4b illustrates individual changes in the maturity of surface corneocytes before and after SLS treatment. A clear decrease was seen in most volunteers. A similar result has been documented before; in that study, there were changes in corneocyte protein expression after a single 24-hours exposure to 1% w/v SLS exposure which was interpreted as an increased, premature synthesis of cornified cell envelope subsequent to the onset of irritation [18]. Likewise, corneocyte maturity was found to

decrease after 3 weeks of Aqueous Cream BP application [19]; it was suggested that SLS, which is present in this emollient at a concentration of 0.9% w/w, was the most likely causative agent of this effect.

3.4   Corneocyte surface area
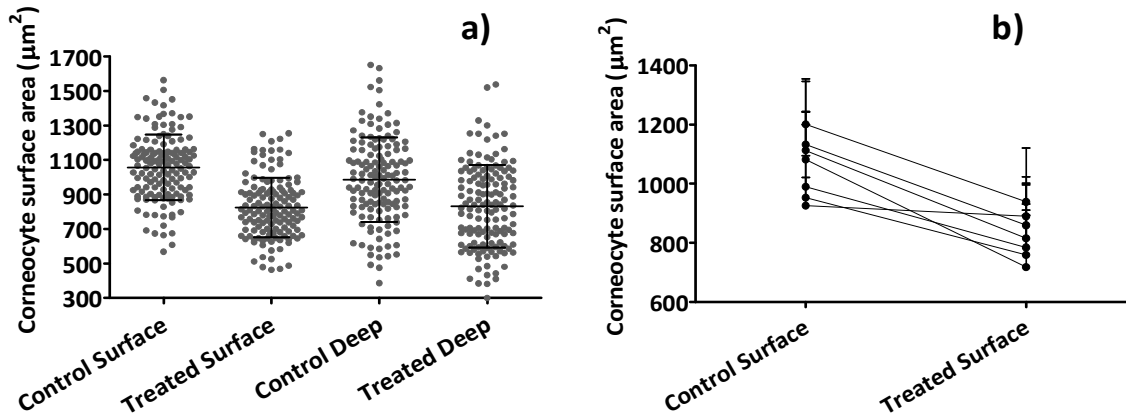
Figure 5: (a) Average corneocyte surface area (mean ± SD, n=7) on SLS-treated and control sites at the surface of and deep within the SC. (b) Average corneocyte surface area (mean ± SD) of each individual on the surface of control and SLS-treated skin sites.

Figure 5a shows the measured corneocyte surface area (n=7, mean ± SD) at different sites. The corneocyte surface area was significantly different (p<0.0001, one-way ANOVA). Bonferroni's multiple comparison post-test showed significant differences between SLS-treated and untreated, control sites at both SC surface and deeper layer. Figure 5b illustrates the changes in the area of surface corneocytes following SLS-treatment in each individual. With the exception of volunteer 7, who did not develop visible erythema even after 3 weeks of surfactant quantification, all volunteers showed a marked decrease in corneocyte surface area. The corneocyte surface area is believed to be inversely related to the turnover of the SC [28]; hence, the observed decrease in surface area indicates faster SC turnover rate after SLS-provoked irritation; an observation is consistent with previous work [29-30].

3.5   SC thickness
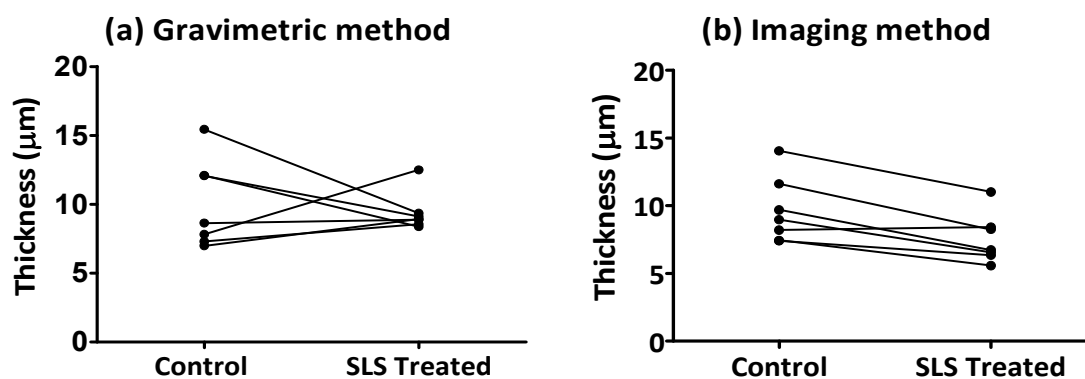
Figure 6: SC thickness predicted by gravimetric and imaging methods of control and SLS-treated skin. The SC thickness measured post SLS-treatment by the imaging method is significantly different from control (P=0.0052, paired t-test), whereas the gravimetric method did not identify change (p=0.655).

The SC thickness of control and SLS-treated skin was evaluated using the gravimetric and imaging methods. The latter approach indicated that the surfactant application significantly thinned the SC (p=0.0052, paired t-test), a result consistent with previous studies, which have shown that repeated application of Aqueous Cream BP led to a significant reduction in SC thickness [19, 31]. Precisely why the gravimetric technique had not revealed in similar pattern of behaviour is unclear; the low signal-to-noise ratio for this method, and the relatively small sample size, may be contributory factors.

3.6 SC Lipid quantity and organisation

IR spectroscopy can report on biomembrane lipid ordering through the C-H stretching absorbance frequencies from the methylene groups of the acyl chains. The CH_2 stretching absorbance undergoes a blue shift, i.e., a shift to higher wavenumber, when the degree of disorder of the lipid chains increases. As perdeuterated SLS was used in the present study, any changes in CH_2 stretching analysed reflect specifically the disorder in the endogenous SC lipids induced by the presence of the surfactant (i.e., there is no "contamination" of the CH_2 signal from the SLS itself) [32].
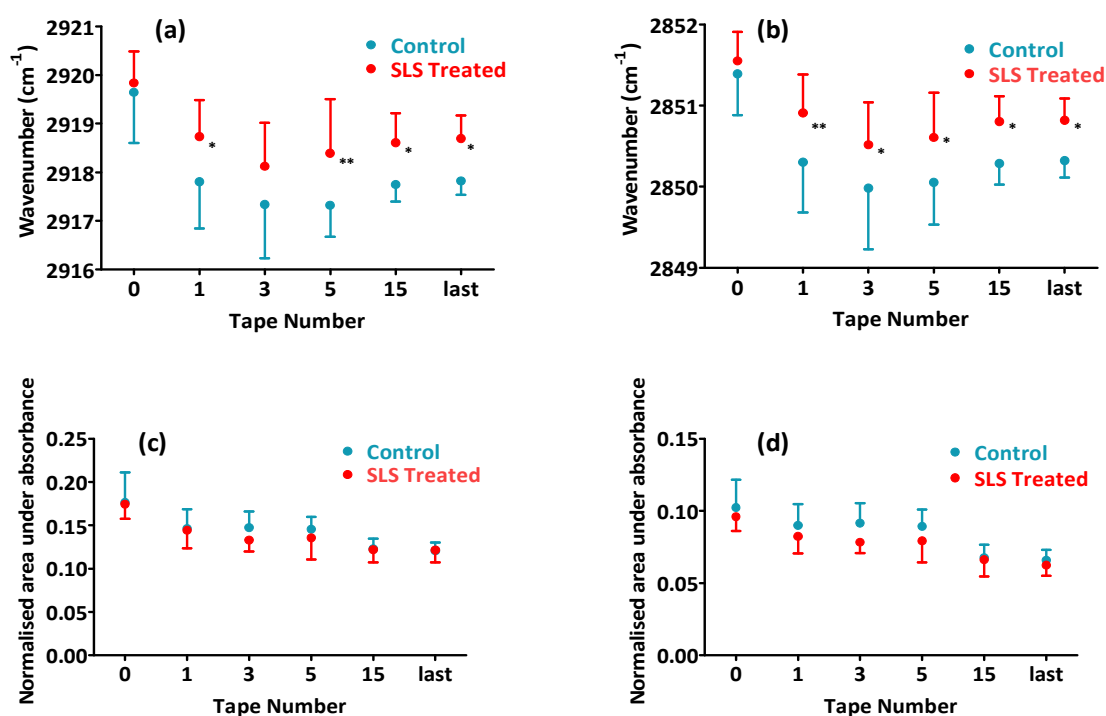
Figure 7: Peak frequencies (a,b) and normalised areas (c,d) under the CH_2 asymmetric ($\sim2920cm^{-1}$) (a,c) and symmetric ($\sim2850cm^{-1}$) (b,d) stretching absorbances as a function of tape-strip number (mean ± SD, n=7). Significant differences between SLS-treated and control sites are highlighted (* $p<0.05$, ** $p<0.01$, Bonferroni post-test).

Figure 7 (a,b) shows that the lipids were most highly disordered at the SC surface, probably due to the contribution of sebaceous constituents, and that SLS treatment did not offset this situation. However, deeper into the SC, the disordering of endogenous lipids following

SLS treatment was significant (repeated measure 2-way ANOVA with Bonferroni post-test: p=0.0007 for asymmetric CH_2 stretching; p=0.0012 for symmetric CH_2 stretching).

On the other hand, the areas under the CH_2 absorbance normalised against the combined area of both amide I and amide II peaks, did not change significantly following SLS treatment (p=0.372, asymmetric CH_2 stretching and p=0.058, symmetric CH_2 stretching by repeated measures two-way ANOVA with Bonferroni post-test), suggesting that no appreciable extraction of endogenous lipids had taken place.

Figure 8 can be downloaded from the following reference: Damien [21]

Figure 8: Temperature dependence lipid transition of FWHM spectra collected from excised human abdominal skin (mean ± SD, n=9). At low temperature, the skin was predominately orthorhombic packing and gradually changed to hexagonal packing with increasing temperature (Taken from Damien [21])

SC barrier function depends on intercellular lipid -packing which appears to involve a balance between orthorhombic (a solid crystalline state) and hexagonal structures (gel state) [33]. The orthorhombically -packed lipids provide the more formidable barrier. In patients with atopic dermatitis and lamellar ichthyosis which are characterised by poor barrier function, a decrease in orthorhombic packing has been found [34-35]. Recently, a new method to interpret the IR spectrum of SC *in vivo* demonstrated that TEWL was correlated with the extent of orthorhombic packing [21]. The method (illustrated by Figure 8) involves the measurement the CH_2 scissoring bandwith (full width at 50% peak height, FWHM).
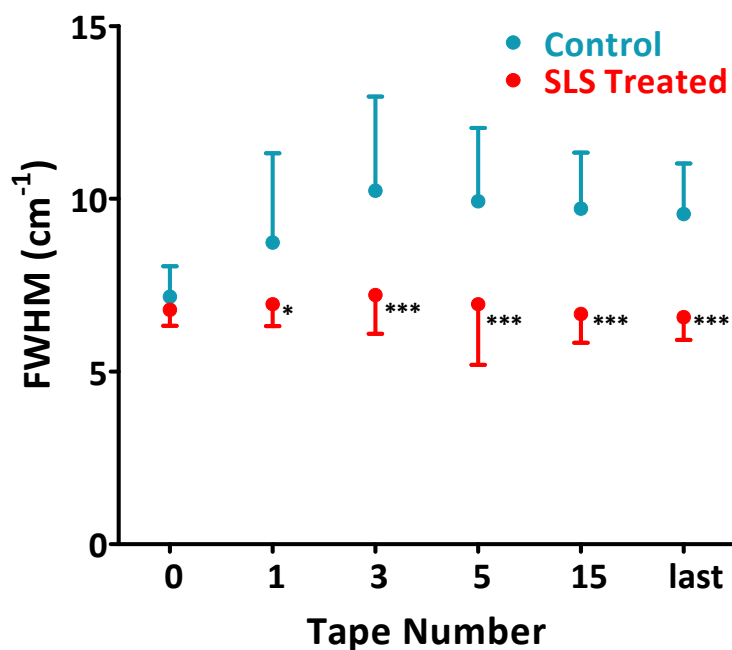
Figure 9: Average full width at 50% peak height (FWHM, cm^{-1}) as a function of tape-strip number (mean ± SD, n=7). The FWHM correlates with the extent of orthorhombic packing.

Here, using this technique, the depth profile of lateral lipid packing at control and SLS-treated skin sites was determined (Figure 9). At the SC surface, a high proportion of hexagonally packed lipids was observed at both sites, presumably due to the presence of sebum and consistent with earlier work [36]. However, in the deeper SC, the higher proportion of orthorhombic packing observed at the untreated control site was significantly reduced by the surfactant treatment, and the barrier now resembles to less efficient characteristics (P<0.0001, repeated measures two-way ANOVA with Bonferroni post-test).

In addition to its effects on SC lipids already discussed, SLS also affects lipogenesis [37]. Microscopic images of the skin after 24 hr treatment with 1% w/v or 48 hr application of 5% w/v SLS provoked spongiosis, alterations in lamella body secretion and lipid droplets inside the corneocytes [30, 38]. Further, quantification of SC lipids after 2 weeks application of 4% w/v SLS indicated a change in the composition of ceramides and cholesterol [39] and, most importantly, a decrease in long chain fatty-acids [39], which are essential for orthorhombic packing [33]. Nonetheless, even though a much lower concentration of SLS (0.1% w/v) was used in our study, disruption of lipid packing was clearly evident.

Given that SLS was applied under occlusion in this study, it is possible that perturbation of SC lipid lamellae may have been caused, at least in part, by hydration. It has been reported

hydration causes swelling of corneocytes, and formation of water pools within the intercellular lipids; separation of SC cells immediately after 24 hours of hydration has also been observed [40]. However, a more recent study has suggested that, even with such a long hydration time, the SC retained their cohesivity [41]. It was also shown that the balance between orthorhombic and hexagonal structures was only slightly affected by the level of SC hydration. Finally, distinct and prolonged changes in mRNA expression of enzymes involved in the synthesis of barrier lipids have been demonstrated after 24 hr 1% w/v SLS under occlusion. However, no significant changes were observed in the control experiment where skin was exposed to water alone, suggesting that hydration, per se has no major impact on lipid-metabolizing enzymes [29]. In any case, the experimental design of our work involved occlusion only for 6 hours per day, and allowed for a 48 hour 'relaxation' period at the end of 3 weeks treatment before any measurements were made. It is unlikely, therefore, that the effects observed may be attributable to SC hydration.

3.7   Principal component analysis of FTIR spectra

Principal component analysis is a multivariate technique that can be applied to a data set without any prior knowledge about grouping or trends in the information [42]. It is a powerful tool to identify patterns and differences in high-dimension data by transforming the original dataset into a set of new variables, or principal components (PCs), that describe most of the variability. PCs are calculated such that the first component accounts for the greatest variation in the data while subsequent components describe progressively decreasing amount of variance. Here, we explored whether IR spectral differences between treated and control sites could be identified using principal component analysis.

All spectra used in the analysis were collected subsequent to the removal of a first tape-strip to remove sebum and other contaminants on the surface of the skin. Because ATR-FTIR is very sensitive to the degree of skin contact with the reference crystal, the measured spectra are normalised before analysis. For this purpose, the intense amide II absorption band at 1540cm^{-1} was chosen as it is less sensitive to hydration, which increases as the SC is stripped to its lower levels, and to the effect of the O-H bending vibration that occurs at 1640cm^{-1} (which overlaps quite closely with the amide I absorbance). For the same reason, attention was focused specifically on the spectral range of 1550 to 650cm^{-1}. Finally, for

comparative purposes, an additional volunteer with a known history of atopic dermatitis (but with no obvious lesion at the time of measurement) was also included in the analysis.
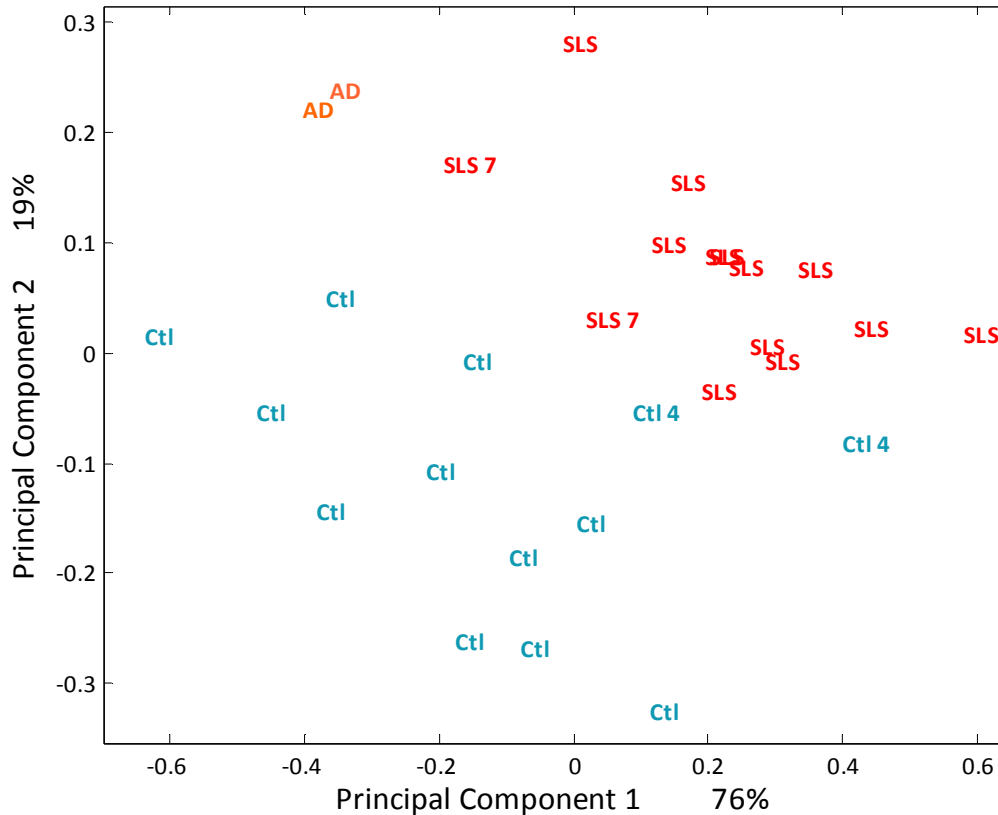
Figure 10: Scoreplot of PC1 vs PC2 for ATR-FTIR spectra taken from all volunteers. (Two spectra were obtained for each sampling site). Ctl: control forearm; Ctl 4: control forearm of volunteer 4; SLS: SLS treated forearm; SLS 7: SLS treated forearm of volunteer 7; AD: volunteer with history of atopic dermatitis.

Figure 10 shows that PC1 accounts for 76% of the variability observed in the data, while PC2 accounts for 19%. Notably, the control and SLS-treated spectral populations were clearly separated. In addition, the atopic volunteer fell very much into SLS-treated skin group even though no skin lesions were apparent at the time of sampling. Moreover, the control spectra of volunteer 4 for whom it was necessary to reduce the SLS concentration applied, and to skip the last surfactant application, due to a strong irritant response, fell at the borderline between the two populations suggesting an inherently weaker (a compromised) skin barrier even prior to the treatment. In contrast, the SLS-treated spectra of volunteer 7, whose barrier was least affected by the surfactant, also fell at the borderline, implying a resistive barrier to the effect of SLS.
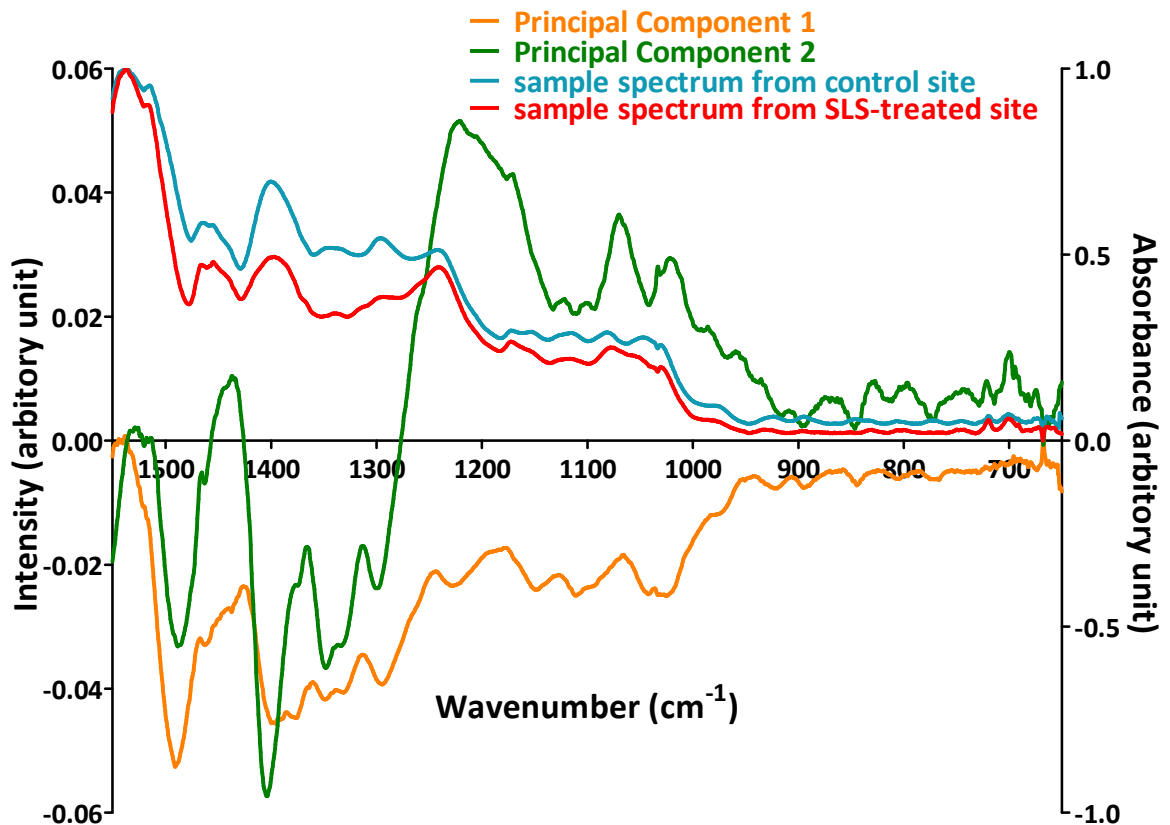
Figure 11: Representative IR spectra from control and SLS-treated skin (blue and red profiles, right-hand y-axis), and "relative intensiveness" attributed to PC1 and PC2 (orange and green profile, left-hand y-axis), as a function of frequency.

Figure 11 shows sample IR spectra from control and SLS-treated skin sites over the "fingerprint" frequency range 1500 – 700cm⁻¹. The general form of the spectra is similar with perhaps a smaller absorbance around 1400cm⁻¹ from SC that had been treated with surfactant (possibly indicating a loss of lipid and/or protein). This figure also shows, as a function of wavenumber, the relative "intensities" assigned to PC1 and PC2. The higher intensity at each frequency, the more important the wavenumber contributes towards the principle component.

3.8 Extraction of amino-acid-derived components of NMF

Twenty-one NMF components were successfully quantified. Other NMF components were detected but could not be quantified (methionine and taurine), while the chromatographic peaks of aspartic acid and asparagine either co-eluted with unknown contaminants or suffered from severe ion suppression.

3.8.1 SC content determined by tape-stripping

Figure 12 illustrates the concentration profile, a function of SC depth, for serine (an AA abundantly present), threonine (moderately abundant), phenylalanine (present at low levels) and glutamine (similarly, less abundant) on both the SLS-treated (red) and the control (blue) forearm. There was good agreement between the results from gravimetric (solid symbols) and imaging (open symbols) methods used to quantify SC removed on each tape as shown in previous chapters. Distribution profiles of other NMF components are in the Appendix 5.
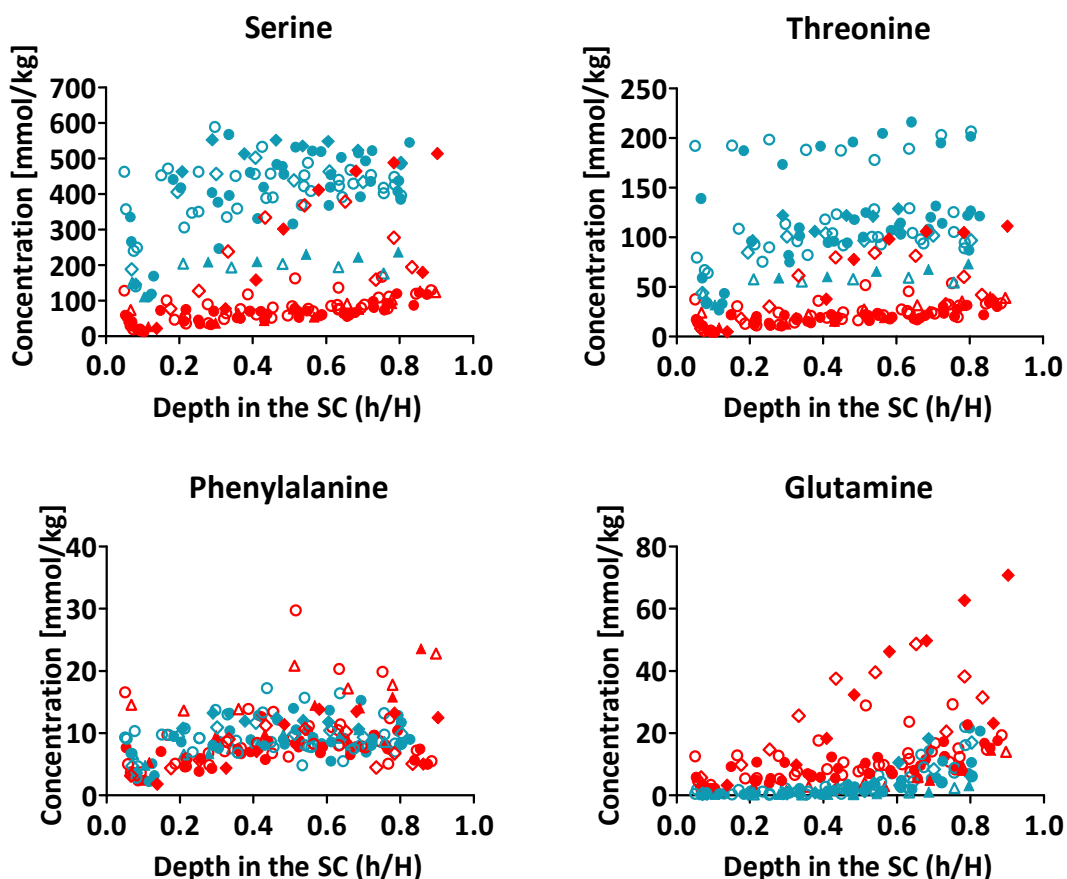
Figure 12: Concentration profiles of serine, threonine, phenylalanine and glutamine as a function of SC depth on SLS-treated (red) and untreated, control (blue) forearms (n=7, Volunteer 7: diamond; Volunteer 4: triangle; other volunteers: circles; gravimetric method: solid symbols; imaging method: open symbols).

After SLS treatment, the NMF components present at high or moderate concentration in the SC (e.g., serine and threonine) were dramatically reduced. Although each volunteer had different levels of NMF components on the control sites, the amounts after SLS-exposure reduced to much lower, similar values except for volunteer 7, whose barrier was least affected by the surfactant. In contrast, the lowest amount of NMF at the control site was observed in volunteer 4, for whom it was necessary to reduce the SLS concentration applied, and to skip the last surfactant application, due to a strong irritant response.

The reduced amount of NMF components may be caused by either an inability to process filaggrin or a reduced expression of filaggrin. The proteolysis of filaggrin is controlled by the water gradient existing in the SC [43]. Scott and Harding found that filaggrin accumulated

throughout the entire thickness of the SC during late foetal development in the rat, but that, only when the rats were exposed to a dryer environment immediately after birth, did normal proteolysis occur. This process could be blocked by maintaining the newborn rats in a 100% humidity atmosphere. Likewise, a 10-day occlusion dramatically blocked filaggrin proteolysis and caused a virtual absence of free amino acids in the SC [44]. However, because the experimental design of the research described in this chapter involved occlusion only for 6 hours per day, and allowed for a 48-hour 'relaxation' period at the end of 3 weeks treatment before any measurements were made, it seems unlikely that the effects observed may be attributed to the inhibition of filaggrin hydrolysis due to hydration.

The most likely cause of the dramatic reduction of NMF is believed to be decreased filaggrin gene expression. Microscopic images of punch biopsy specimens from human volunteers after 5% w/v SLS patch application for 48-hrs revealed the absence of keratohyalin granules [30], in which pro-filaggrin is normally present. Relatedly, a recent study showed that a 24-hour application of 1% w/v SLS, significantly reduced filaggrin mRNA 6 hours followed by a significant increase after 4 days; however, at the protein expression level, only the delayed increase was observed [18]. Our experiments, in contrast, exposed the volunteers to 0.1% w/v SLS for 3 weeks resulting, it would appear, in the inhibition of filaggrin mRNA production and a subsequent decrease in filaggrin protein expression.

The reduced level of NMF may also be a result of inflammation. By the end of 3 weeks, most volunteers had developed dry, erythematous, scaling skin at the treatment sites, indicative of an inflammatory response. It is known that T_h2 cytokines (IL-4 & IL-13) reduce filaggrin expression [17]. The fact that IL-4 was increased in healthy volunteers after a 6-72 hr exposure to 4% w/v SLS [45] suggests that this mechanism might also contribute to the lower level of NMF observed.

The NMF components present at low concentration in the SC (e.g., phenylalanine) were not affected by surfactant-treatment. Most of these NMF components are not major components of filaggrin protein [46]. Glutamine, on the other hand, is a major component of filaggrin, yet its presence in the SC is low. This may well be the result of cyclisation [47] to form pyrrolidone carboxylic acid (PCA), another main NMF constituent. The depth distribution profile of glutamine differs from the others; it is negligibly present at the SC

surface but then increases sharply in deeper layers, indicating that the transformation to PCA is very efficient. The slightly higher level of glutamine after SLS-irritation may reflect a higher SC turnover, and hence a shorter time available for the transformation to occur. On the other hand, the higher amount of glutamine may also be due to increased passive extraction caused by the weakened, SLS-treated skin barrier. In Chapter 4, glutamine was shown to be elevated in forehead SC again intimating that its level may inversely correlate with SC barrier function.
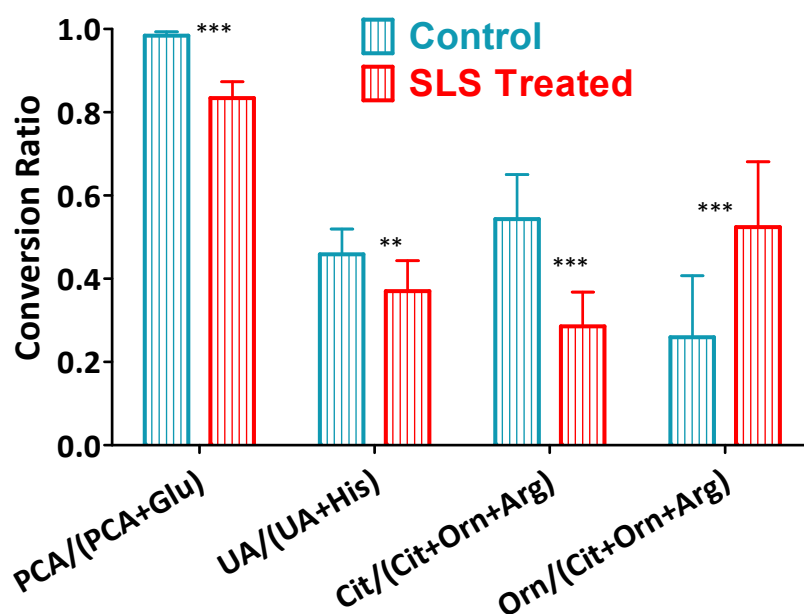
Figure 13: Conversion ratio of amino acid derivatives calculated from the cumulative amounts extracted by tape-stripping. Significant changes were detected for all derivatives (p<0.0001 for PCA, Cit and Orn; p=0.0036 for UA, paired t-test, n=7)

The generation of amino acid derivative was affected by surfactant treatment (Figure 13). It is known that trans-urocanic acid (t-UA) is synthesised from histidine by histidine ammonia-lyase [48]. Ornithine derives from the breakdown of arginine (Arg) by arginase, while citrulline (Cit) is the degradation product of arginine by nitric oxide synthase [49] and peptidylarginine deiminases (PAD1 and PAD3) [50-51]. Amino acid conversions (i.e., PCA/PCA+Glu, t-UA/t-UA+His, Cit/Arg+Cit+Orn) were significantly reduced after SLS-treatment, either because of a higher SC turnover rate and hence a shorter time available for the transformation, or due to reduced protease activities. Interestingly, the ratio Orn/Arg+Cit+Orn increased post-SLS treatment. This is typical of a highly proliferating SC.

For example, upregulation of arginase-1 has been seen in the non-lesional skin of psoriasis patients and, as a result, decreased arginine and increased ornithine have been detected in the plasma of these individuals [52-53]. Arginase has also been shown to be up-regulated after physical damage and its over-expression may retard wound healing by competing with nitric oxide synthase (NOS) for L-arginine [54]. While complete understanding of the role of arginases in the skin is not yet at hand, the changes seen in this amino acid's conversion is consistent with an earlier study involving a 24-hour application of 3% w/v SLS [55].

3.8.2   Extraction by reverse iontophoresis and passive diffusion

Figure 14 presents examples of reverse iontophoretic and passive extraction of an acidic NMF component (PCA), a basic compound (lysine) and two zwitterions (serine and glutamine) from the SLS-treated (red) and control (blue) forearms. Extraction of other NMF constituents is shown in the Appendix 5.
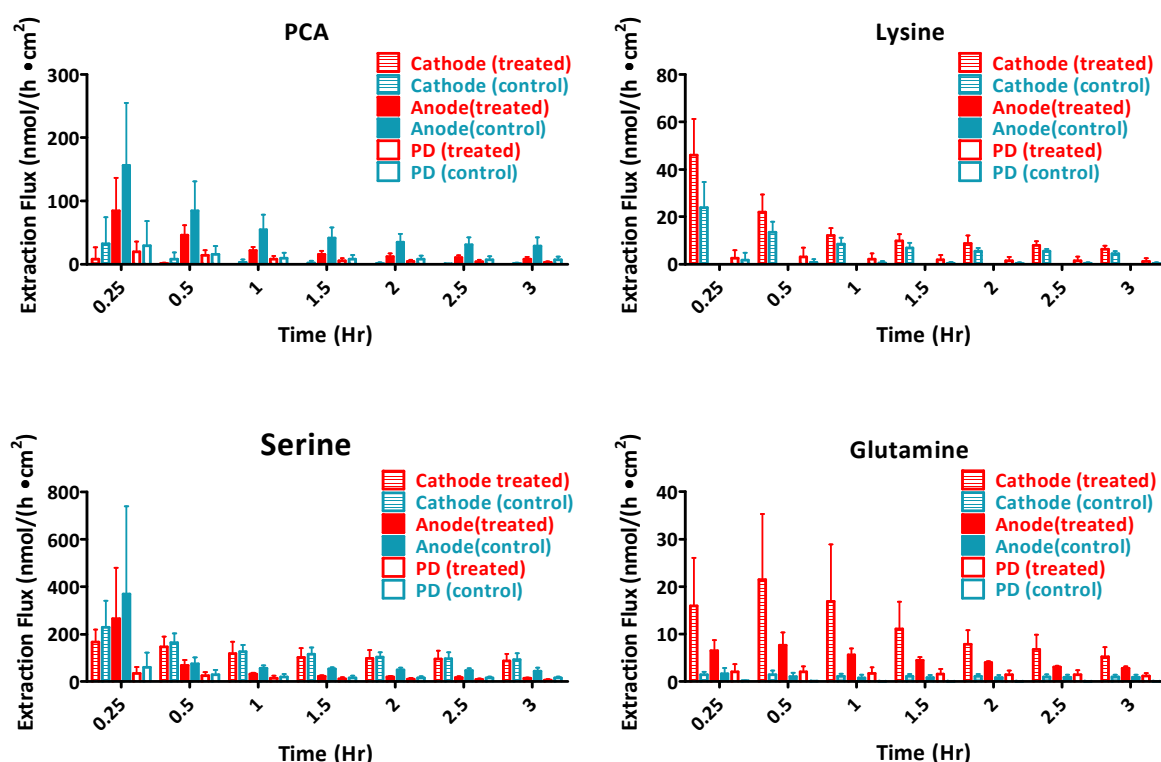
Figure 14: Reverse iontophoretic and passive extraction flux (mean ± SD) of an acidic NMF component (PCA), a basic constituent (lysine) and two zwitterions (serine and glutamine) *in vivo* in human volunteers (n=6) from the SLS-treated (red) and control (blue) forearms as a function of time.

The extraction fluxes of all NMF components showed a similar pattern: the initial flux was high and then decreased rapidly over the first hour before stabilising in the later 2 hours.

The reverse iontophoretic and passive extraction of NMF components can be separated into 3 groups:

1) Acidic compounds are negatively charged in solution at physiological pH and were extracted predominantly at the anode. The amounts extracted at the cathode were negligible and, in most cases, below the LOQ. In Chapter 3, these compounds were considered unsuitable for quantification in the SC by reverse iontophoresis because of their extensive extraction from deeper compartments. However, as illustrated in Figure 12, the extraction of PCA on the control site in the first hour was much higher than that on the SLS-treated site and its extraction was maintained at a higher rate even in the last 2 hours. This suggests the presence of a much larger SC reservoir of PCA in surfactant-exposed skin.

2) Extraction of compounds that were positively charged at physiological pH took place mainly at the cathode. The amounts detected at the anode and by passive diffusion were minimal in comparison. Given lysine was found in low amounts in the SC, but in high levels in plasma, the extraction profile was higher on the SLS-treated site suggesting a weakened SC barrier after irritation.

3) Zwitterions were similarly extracted to anode and cathode. Reverse iontophoresis only enhanced extraction by a modest extent and little differences between SLS-treated and control sites were observed. Although lower amounts of NMF components were observed after SLS-irritation, the weakened barrier inevitably facilitated the extraction of NMF components leading to negligible differences in iontophoretic extraction at both sites. The later extraction (>1.5hr) of these molecules may provide an indication of SC barrier function. Since, by then, the reservoir in the treated skin was depleted and extraction was correspondingly lower.

3.9 Origins of NMF extracted

The amounts of NMF components recovered by SC tape-stripping are compared with reverse iontophoretic and passive extractions in Table 4.

Table 4: Cumulative amounts (nmol/cm^2, mean ± SD; n=7) of NMF components extracted in 3 hours by passive diffusion, reverse iontophoresis (at anode and cathode; n=6) and by tape stripping (n=7).

Charged compounds								
Analytes	**Tape-stripping**		**Passive diffusion**		**Anode**		**Cathode**	
	SLS treated	**Control**	**SLS treated**	**Control**	**SLS treated**	**Control**	**SLS treated**	**Control**
PCA	25 ± 10	182 ± 85	21 ± 12	38 ± 22	56 ± 30	156 ± 66	2.1 ± 5.2	14 ± 17
Urocanic acid	13 ± 9	62 ± 35	10 ± 5	14 ± 8	32 ± 15	55 ± 19	4.7 ± 5.6	5.8 ± 5.9
Glutamic acid	18 ± 11	15 ± 4.2	10 ± 6	1.3 ± 0.9	51 ± 25	40 ± 10	1.2 ± 1.9	0.4 ± 0.7
Histidine	23 ± 18	69 ± 29	17 ± 8	12 ± 6	7.1 ± 3.7	22 ± 7	49 ± 8	72 ± 23
Ornithine	24 ± 27	39 ± 34	13 ± 7	5.3 ± 3.0	3.7 ± 3.2	10 ± 6	63 ± 11	41 ± 21
Arginine	6.1 ± 2.5	31 ± 22	4.7 ± 2.6	6.4 ± 5.6	0.6 ± 1.0	6.8 ± 4.3	36 ± 8	50 ± 25
Lysine	9.2 ± 3.9	14 ± 6	5.4 ± 6.5	1.6 ± 2.5	<LOQ	<LOQ	40 ± 10	25 ± 6
Zwitterions and Urea								
Analytes	**Tape-stripping**		**Passive diffusion**		**Anode**		**Cathode**	
	SLS treated	**Control**	**SLS treated**	**Control**	**SLS treated**	**Control**	**SLS treated**	**Control**
Serine	69 ± 65	307 ± 129	42 ± 22	64 ± 35	115 ± 73	238 ± 111	330 ± 110	366 ± 90
Glycine	34 ± 29	165 ± 69	28 ± 16	37 ± 18	53 ± 25	110 ± 27	105 ± 28	149 ± 44
Alanine	23 ± 17	132 ± 75	20 ± 12	23 ± 17	34 ± 16	70 ± 24	55 ± 22	79 ± 33
Threonine	19 ± 14	86 ± 51	12 ± 7	16 ± 9	15 ± 6	37 ± 10	38 ± 13	43 ± 18
Citruline	10 ± 3	81 ± 39	7.7 ± 5.3	17 ± 10	10 ± 5	41 ± 18	19 ± 7	46 ± 14
Valine	11 ± 6	29 ± 13	8.5 ± 4.9	6.3 ± 2.4	11 ± 5	17 ± 3	20 ± 5	16 ± 5
Proline	8.1 ± 4.8	23 ± 9	7.7 ± 4.5	4.8 ± 2.4	9.5 ± 4.5	14 ± 5	17 ± 5	14 ± 4
Tyrosine	9.3 ± 4.1	18 ± 6	5.1 ± 2.9	3.6 ± 1.7	7.0 ± 3.1	9.4 ± 1.9	13 ± 4	8.0 ± 2.2
Isoleucine	6.5 ± 3.4	13 ± 5	4.9 ± 3.7	2.3 ± 1.0	6.2 ± 3.3	7.3 ± 1.0	11 ± 5	6.4 ± 1.7
Leucine	11 ± 4	11 ± 4	7.2 ± 5.3	2.1 ± 0.7	12 ± 11	6.6 ± 1.2	16 ± 6	5.8 ± 1.1
Phenylalanine	6.2 ± 2.2	7.4 ± 2.9	3.9 ± 2.8	1.6 ± 0.7	5.3 ± 3.2	4.2 ± 1.2	9.3 ± 3.6	3.5 ± 0.5
Tryptophan	2.8 ± 1.5	6.4 ± 2.7	1.7 ± 0.9	1.4 ± 0.7	2.3 ± 1.1	3.8 ± 0.9	4.1 ± 1.2	2.9 ± 1.6
Glutamine	8.5 ± 8.0	2.8 ± 1.6	4.7 ± 2.9	0.2 ± 0.1	12 ± 5	2.9 ± 1.8	33 ± 18	3.3 ± 1.7
Urea	25 ± 10	62 ± 26	26 ± 10	33 ± 14	39 ± 16	101 ± 39	84 ± 34	93 ± 37

With the exception of glutamic acid, all charged species were present in higher amounts in the untreated SC removed by tape-stripping; however, passive extraction depended on the molecule; in some cases, extraction from the SLS-treated site was greater, e.g., lysine. The higher amounts found at the control sites almost certainly reflect the greater SC reservoir. In contrast, the sometimes more efficient passive extraction from the SLS-treated sites is indicative of a weakened barrier and the more rapid diffusion of small solutes.

Reverse iontophoresis is a powerful tool with which to extract charged molecules. By the end of 3 hours, extraction to the preferred electrode was sampling the analytes from beyond the SC (Figure 15). The extent to which this is the case depends on the properties of the molecule and its concentration in the SC. For example, PCA is present in large amount in the SC, and the time taken to deplete this compound is therefore much longer than that required for others, such as lysine. However, because the concentration of PCA in plasma is very low (2.16 $\pm$ 0.4 μM [56]), compared to that of essential amino acids (e.g., lysine 100 - 300 μM [57]), the anodal extraction of PCA is largely attenuated once the skin reservoir has been depleted.
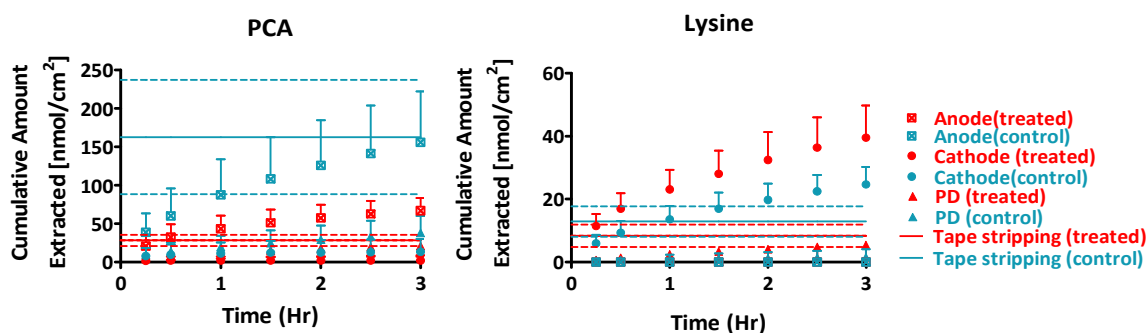
Figure 15: Cumulative amounts of PCA and lysine extracted (mean $\pm$ SD; n=6) by iontophoresis at both electrodes and by passive diffusion as a function of time from the SLS-treated (red) and untreated, control (blue) forearm. The average quantities in the SC determined by tape-stripping are shown for comparison by the solid horizontal lines, with the $\pm$SD indicated by dashed lines.

For the zwitterionic constituents of NMF, reverse iontophoresis could not deplete the amounts present in the 'SC reservoir' on the forearm by the end of 3 hours from the control site, but was able to extract from a deeper compartment at the SLS-treated sites. The

quantities extracted by reverse iontophoresis were, on the whole, higher than by passive diffusion, but not as dramatically different as seen for the charged compounds.
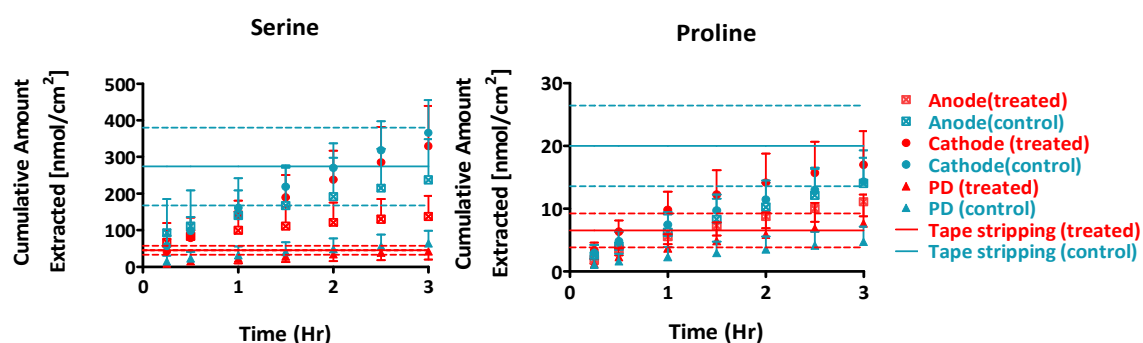
Figure 16: Cumulative amounts of serine and proline extracted (mean ± SD; n=6) by iontophoresis at both electrodes and by passive diffusion as a function of time from the SLS treated (red) and untreated, control (blue) forearms. The average quantities in the SC determined by tape-stripping are shown for comparison by the solid horizontal lines, with the ±SD indicated by dashed lines.

Urea (molecular weight: 60) is a small molecule, which readily permeates the skin. It is extracted efficiently by passive diffusion and, within 3 hours, the amount in the SC has been just about depleted on both sites. However, as urea is also secreted from sweat onto the surface of the SC, the amount extracted shows considerable variability between subjects.

4. Recovery phase

As shown in Figure 1, volunteer 7 had by far mildest reaction to SLS. There was no sign of erythema even after 3 weeks of SLS patch application. However, the effect of the surfactant on skin barrier function was evident, as demonstrated by an increased TEWL, less-ordered SC lipids and reduced NMF.

4.1 SC Lipids
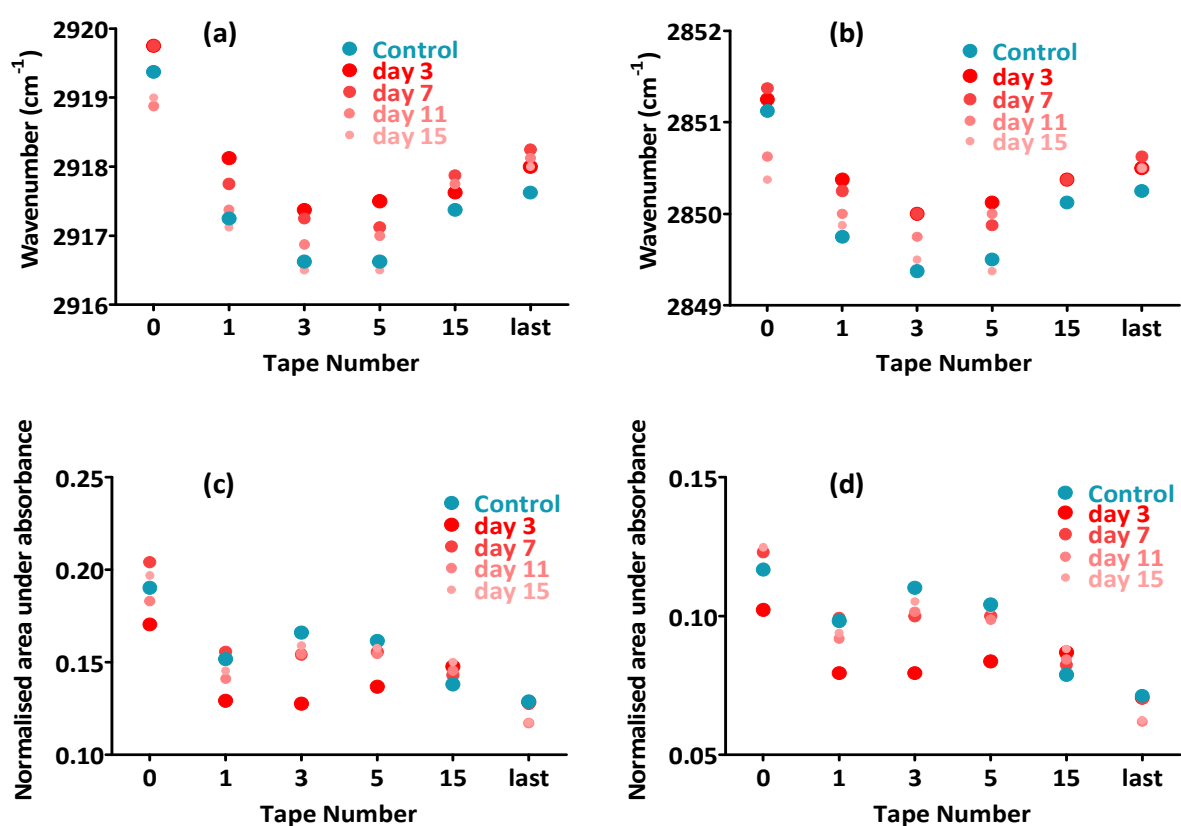
Figure 17: Peak frequencies (a,b) and normalised areas (c,d) under the CH_2 asymmetric (~2920cm^{-1}) (a,c) and symmetric (~2850cm^{-1}) (b,d) stretching absorbances as a function of tape-strip number from volunteer 7 on days 3,7,11 and 15 after the final SLS application.

Like the other volunteers studied, Figure 17 (a,b) shows that the lipids were most highly disordered at the SC surface, probably due to the contribution of sebaceous constituents, and that SLS treatment did not affect this situation. However, deeper into the SC, the

disordering of endogenous lipids following SLS treatment was evident, especially on day 3 after last SLS application. A comparable peak frequency to the control site was observed only after 15 days suggesting a prolonged disordering effect of SLS on lipid packing. On the 3rd day after the final patch application, the normalised areas under the CH_2 absorbances were reduced, but this difference was not observed on other days. However, the reduction on day 3 was not significant when data from other volunteers were grouped together (Figure 7). The fact that little difference was detected during recovery in comparison to the control site further confirms that no appreciable extraction of endogenous lipids, or induction of their synthesis, had taken place.
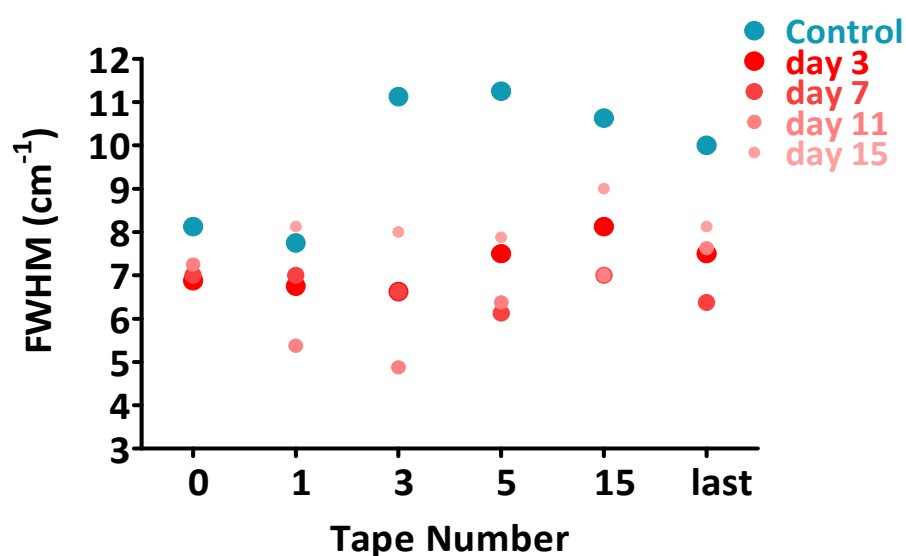
Figure 18: Full width at 50% peak height (FWHM, cm^{-1}) as a function of tape-strip number from volunteer 7 on day 3,7,11,15 after the final SLS patch application. The FWHM correlates with the extent of orthorhombic packing.

As observed in other volunteers, predominately hexagonal lipid packing was observed at the SC surface and in deeper layers even 15 days after the final SLS application. This is consistent with a previous study which concluded that an extended time was required to restore barrier function after SLS irritation [58]. This prolonged effect on lipid organisation suggests that the disturbance of lipid lamellae caused by SLS arises from the interruption of lipogenesis.

4.2 NMF recovery

A marked decrease in the NMF components present in high and moderate amounts (e.g., serine and citrulline) was observed in volunteer 7, but to a much less extent in comparison to other volunteers. During the two-week recovery period, most of these NMF constituents increased slowly from the deep layer of the SC to the surface and reached similar levels to the control site. This prolonged recovery could be due to either the facile loss of NMF constituents after SLS treatment due to a weakened barrier, or to a reduction in filaggrin synthesis meaning that NMF can only be replenished once new corneocytes differentiate with the correct level of filaggrin expression. Most NMF components that present at low levels (e.g., phenylalnine) did not change after treatment and during recovery; glutamine, however, increased after SLS treatment and then returned to normal during the recovery phase.
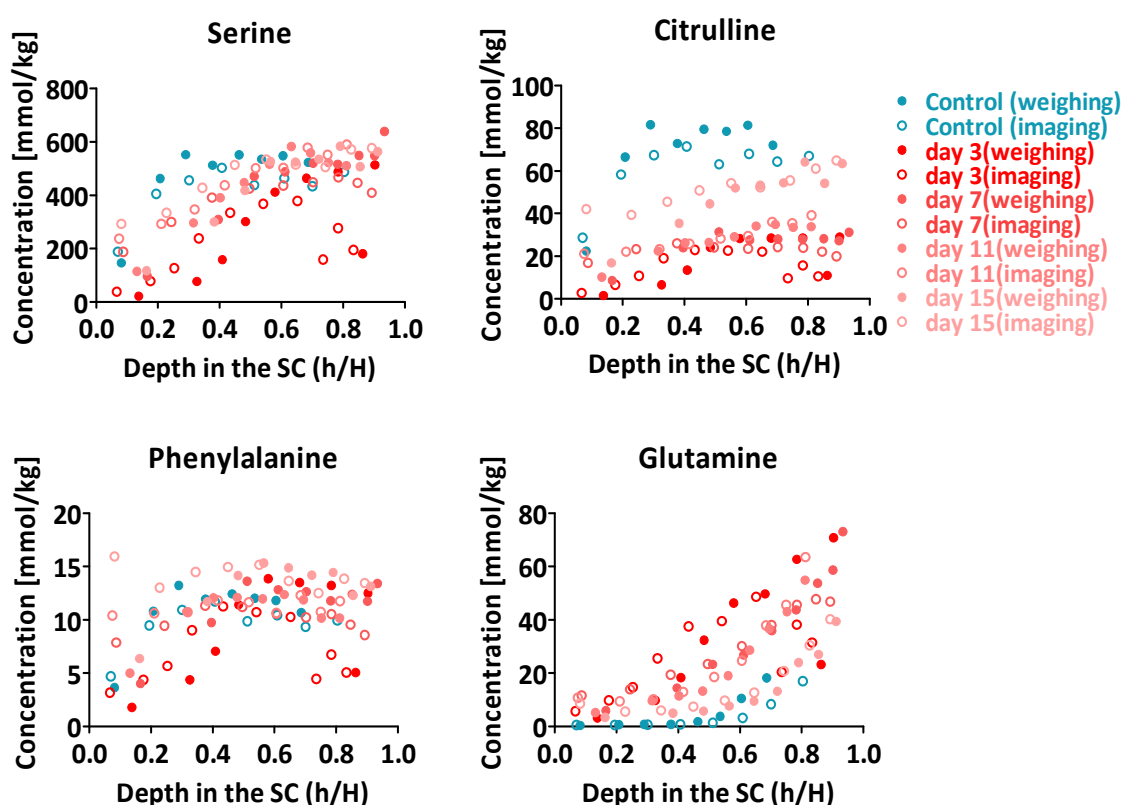
Figure 19: Concentration profiles of serine, citrulline, phenylalanine and glutamine as a function of position in the SC on SLS treated (red) and untreated, control (blue) forearms from volunteer 7 on day 3, 7, 11, 15 after the final SLS application (gravimetric method : solid circles, imaging method: open circles).

Amino acid derivatives (e.g. citrulline) recovered at a slower rate in comparison to essential amino acids. This is probably caused by a lower conversion ratio post-SLS treatment. Figure 20 indicates these changes. Similar to other volunteers, a decrease in PCA, UA and citrulline conversion was detected accompanied with an increase in ornithine synthesis.
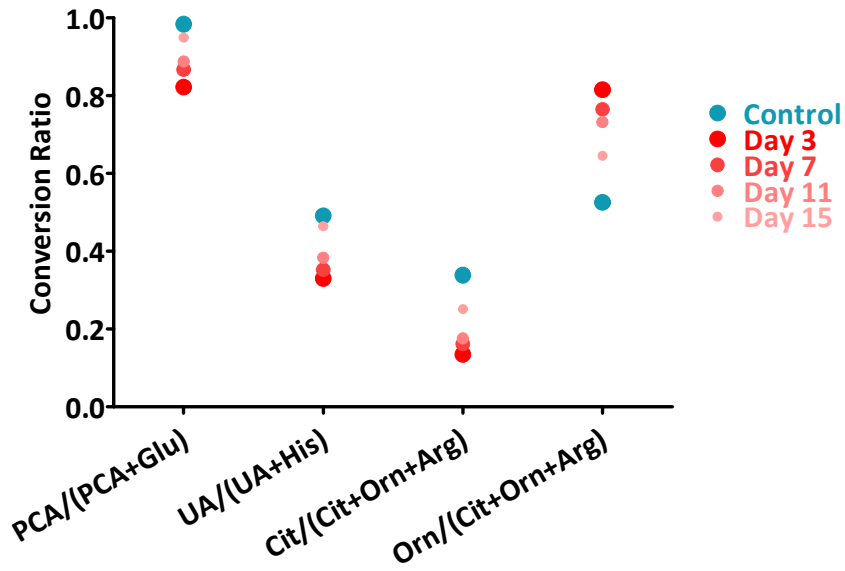
Figure 20: Conversion ratio of amino acid derivatives calculated from the cumulative amounts extracted by tape-stripping in volunteer 7 on days 3, 7, 11, 15 post SLS treatment.

.

5. Correlations of increased TEWL with different markers

To identify which markers may be most useful for the evaluation of skin barrier function, various parameters have been compared with either basal TEWL (i.e., TEWL measurements from the untreated, control site) or with the average TEWL increase after SLS treatment over the second and third week of exposure (ΔTEWL) using the Pearson correlation test (Table 5).

Table 5: Pearson correlation test results of various factors against either ΔTEWL or basal TEWL. NMF components were the cumulative amounts extracted from tape-strips at the control site. (ns: not significant, * : $p<0.05$, **: $p<0.01$)

	ΔTEWL	Basal TEWL
Basal TEWL	ns	
Cell maturity	ns	ns
SC thickness	*	ns
Surface area	ns	ns
Serine	**	*
Glycine	*	*
PCA	*	*
Arg+Cit+Orn	*	*
Histidine	*	**
Tyrosine	*	*

Small sample size and large individual variability may contribute to the lack of significant correlations between TEWL and the parameters describing corneocyte morphology. ΔTEWL was negatively correlated with SC thickness. The cumulative amount of some NMF components, normally present in high amounts in the SC, were significantly inversely correlated with both ΔTEWL and basal TEWL, and may serve, therefore, as potential markers for skin health and its resistance to irritants.

6. SLS damage to SC barrier
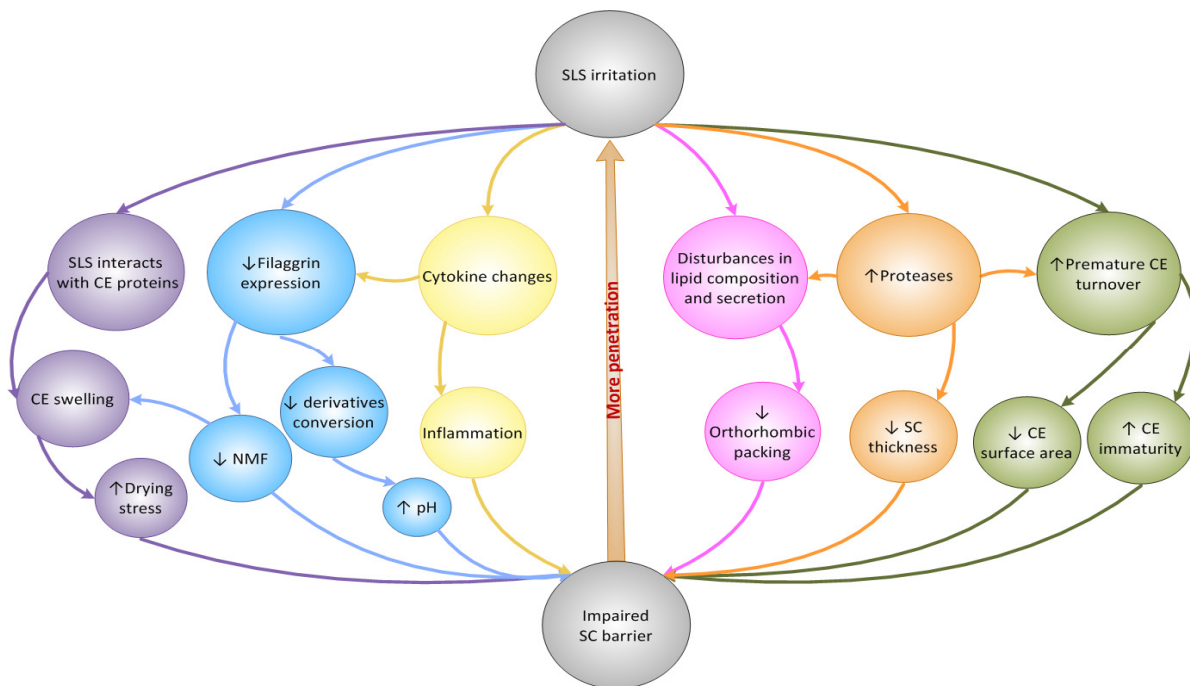
Figure 21: Proposed mechanisms of SLS damage to the SC barrier.

Several mechanisms may be associated with SLS damage to the skin barrier:

- SLS binds to SC proteins resulting in conformational changes in SC structure leading to transient swelling and hydration of corneocytes [59]. This in turn changes the water-holding capacity of the SC; in other words, the SC absorbs more water when hydrated but loses it more easily in dry condition [60]. One possible result of this effect is depletion of NMF. In any case, alterations in both conformational structure and water-holding capacity will introduce stress on drying and physical damage due to cracking of the skin [61].

- As shown in this study, SLS causes prolonged depletion of NMF possibly by reducing filaggrin expression. It also decreases the conversion of several amino acid derivatives, including PCA and t-UA, which are believed to be important in maintaining the pH of healthy skin. In addition, since SLS is slightly basic in nature and easily penetrated into the SC [62], it may function as a superbase to increase SC pH. This increase in pH could potentially enhance the SLS damage [63] to the SC.

- Immunological processes play an important role in irritant exposure. Several studies have demonstrated release of pro-inflammatory cytokines in vivo after SLS irritation, including IL-1α, IL-6, IL-8, etc. [45, 62, 64]. These cytokines activate the inflammatory cascade, which then initiates barrier repair. However, over-expression of the inflammatory response is associated with skin diseases, such as irritant contact and atopic dermatitis.

- SLS irritation introduces changes in lipid lamella composition and arrangement [30, 39, 65]. Microscopic images reveal changes in lamellar body secretion and the presence of lipid droplets in the matrix of corneocytes [38]. The change in lipid organisation is confirmed in this study, where predominately hexagonal lipid packing is observed at SLS-treated skin sites.

- Desquamation is controlled by the balance of proteases and protease inhibitors. After SLS irritation, proteases are up-regulated [66], which may be partially responsible for a reduced SC thickness and further modification of SC barrier function [67-70].

- Increase in cell turnover after SLS irritation leads to smaller corneocyte surface area and to less mature corneocytes. Both changes compromise the competency of SC barrier function.

In sum, SLS damages the SC barrier by manifold mechanisms which in turn allow more penetration of the irritant into the skin. The results from this work confirm that negative environmental factors compromise the health of the skin barrier, and may contribute to the development of skin disease, e.g., AD and ICD. The low concentration (0.1% w/v) of SLS used was chosen to mimic the typical everyday contact of surfactants. In fact, surfactants like SLS are found at much higher concentrations in many commercially available washing products and moisturizers (e.g., Aqueous Cream BP which contains 0.9% w/w). The daily use of Aqueous Cream BP has recently been shown to damage the SC barrier [19, 31]. Moreover, frequent washing has been identified as a risk factor for development of AD [71-72]. It is therefore important to minimize, whenever possible, exposure to soaps, detergents, etc., and to carefully choose emollients, for individuals who are at high risk of developing AD and ICD.

With respect to assessing skin barrier function, robust, minimally invasive and sensitive methods have been used to reveal the mechanisms of SLS induced SC damage. Among all the methods used, tape-stripping accompanied with NMF extraction and FTIR measurements appear to be the most promising techniques.

7. Conclusions

This result suggests that severe SC barrier damage occurs after prolonged exposure to a low concentration of SLS. Changes in SC morphology, depletion of NMF and lipid disordering are clear. Several minimally invasive methods have been developed and used to identify these changes and to successfully assess skin barrier function.

8. Reference

1. Chew A-L and Maibach HI, *Occupational issues of irritant contact dermatitis.* International Archives of Occupational and Environmental Health, 2003. **76**(5): p. 339-346.

2. Cork MJ, Robinson DA, Vasilopoulos Y, Ferguson A, Moustafa M, MacGowan A, Duff GW, Ward SJ, and Tazi-Ahnini R, *New perspectives on epidermal barrier dysfunction in atopic dermatitis: Gene-environment interactions.* Journal of Allergy and Clinical Immunology, 2006. **118**(1): p. 3-21.

3. McFadden JP, Wakelin SH, and Basketter DA, *Acute irritation thresholds in subjects with Type I-Type VI skin.* Contact Dermatitis, 1998. **38**(3): p. 147-149.

4. De Jongh C, John S, Bruynzeel D, Calkoen F, van Dijk F, Khrenova L, Rustemeyer T, Verberk M, and Kezic S, *Cytokine gene polymorphisms and susceptibility to chronic irritant contact dermatitis.* Contact Dermatitis, 2008. **58**(5): p. 269-277.

5. De Jongh C, Verberk M, Withagen C, Jacobs J, Rustemeyer T, and Kezic S, *Stratum corneum cytokines and skin irritation response to sodium lauryl sulfate.* Contact Dermatitis, 2006. **54**(6): p. 325-333.

6. Coenraads P-J and Diepgen TL, *Risk for hand eczema in employees with past or present atopic dermatitis.* International Archives of Occupational and Environmental Health, 1998. **71**(1): p. 7-13.

7. Terui T, Hirao T, Sato Y, Uesugi T, Honda M, Iguchi M, Matsumura N, Kudoh K, Aiba S, and Tagami H, *An increased ratio of interleukin-1 receptor antagonist to interleukin-1α in inflammatory skin diseases.* Experimental Dermatology, 1998. **7**(6): p. 327-334.

8. Muller S, Marenholz I, Lee Y, Sengler C, Zitnik S, Griffioen R, Meglio P, Wahn U, and Nickel R, *Association of filaggrin loss-of-function-mutations with atopic dermatitis and asthma in the Early Treatment of the Atopic Child (ETAC) population.* Pediatric Allergy and Immunology, 2009. **20**(4): p. 358-361.

9. Weidinger S, O'Sullivan M, Illig T, Baurecht H, Depner M, Rodriguez E, Ruether A, Klopp N, Vogelberg C, Weiland SK, McLean WHI, von Mutius E, Irvine AD, and Kabesch M, *Filaggrin mutations, atopic eczema, hay fever, and asthma in children.* Journal of Allergy and Clinical Immunology, 2008. **121**(5): p. 1203-1209.

10. S.J. Brown HJC, *Are filaggrin mutations associated with hand eczema or contact allergy? - we do not know.* British Journal of Dermatology, 2008. **158**(6): p. 1383-1384.

11. Nomura T, Akiyama M, Sandilands A, Nemoto-Hasebe I, Sakai K, Nagasaki A, Palmer CNA, Smith FJD, McLean WHI, and Shimizu H, *Prevalent and rare mutations in the gene encoding filaggrin in Japanese patients with ichthyosis vulgaris and atopic dermatitis.* J Invest Dermatol, 2008. **129**: p. 1302-1305.

12. Rawlings A and Harding C, *Moisturization and skin barrier function.* Dermatologic Therapy, 2004. **17**(s1): p. 43-48.

13. Levin J and Maibach H, *Human skin buffering capacity: an overview.* Skin Research and Technology, 2008. **14**(2): p. 121-126.

14. Kezic S, Kemperman PMJH, Koster ES, de Jongh CM, Thio HB, Campbell LE, Irvine AD, McLean IWH, Puppels GJ, and Caspers PJ, *Loss-of-Function mutations in the filaggrin gene lead to reduced level of natural moisturizing factor in the stratum corneum.* J Invest Dermatol, 2008. **128**(8): p. 2117-2119.

15. Takahashi M and Tezuka T, *The content of free amino acids in the stratum corneum is increased in senile xerosis.* Archives of Dermatological Research, 2004. **295**(10): p. 448-452.

16. Novak N, Baurecht H, Schafer T, Rodriguez E, Wagenpfeil S, Klopp N, Heinrich J, Behrendt H, Ring J, Wichmann E, Illig T, and Weidinger S, *Loss-of-function mutations in the filaggrin gene and allergic contact sensitization to nickel.* J Invest Dermatol, 2007. **128**(6): p. 1430-1435.

17. Howell MD, Kim BE, Gao P, Grant AV, Boguniewicz M, DeBenedetto A, Schneider L, Beck LA, Barnes KC, and Leung DYM, *Cytokine modulation of atopic dermatitis filaggrin skin expression.* Journal of Allergy and Clinical Immunology, 2009. **124**(3, Supplement 2): p. R7-R12.

18. Torma H, Lindberg M, and Berne B, *Skin barrier disruption by sodium lauryl sulfate-exposure alters the expressions of involucrin, transglutaminase 1, profilaggrin, and kallikreins during the repair phase in human skin in vivo.* J Invest Dermatol, 2007. **128**(5): p. 1212-1219.

19. Mohammed D, Matts PJ, Hadgraft J, and Lane ME, *Influence of Aqueous Cream on corneocyte size, maturity, skin protease activity, protein content and Trans-Epidermal Water Loss.* British Journal of Dermatology, 2011. **164**(6): p. 1304-1310.

20. Kalia YN, Alberti I, Sekkat N, Curdy C, Naik A, and Guy RH, *Normalization of Stratum Corneum Barrier Function and Transepidermal Water Loss In Vivo.* Pharmaceutical Research, 2000. **17**(9): p. 1148-1150.

21. Damien F and Boncheva M, *The Extent of Orthorhombic Lipid Phases in the Stratum Corneum Determines the Barrier Efficiency of Human Skin In Vivo.* J Invest Dermatol, 2009. **130**(2): p. 611-614.

22. Hirao T, Denda M, and Takahashi M, *Identification of immature cornified envelopes in the barrier-impaired epidermis by characterization of their hydrophobicity and antigenicities of the components.* Experimental Dermatology, 2001. **10**(1): p. 35-44.

23. Russell L, *Dermato-pharmacokinetics: an approach to evaluate topical drug bioavailabilty*, in *Department of Pharmacy and Pharmacology*. 2008, University of Bath: Bath.

24. Russell LM, Wiedersberg S, and Delgado-Charro MB, *The determination of stratum corneum thickness An alternative approach.* European Journal of Pharmaceutics and Biopharmaceutics, 2008. **69**(3): p. 861-870.

25. Judge MR, Griffiths HA, Basketter DA, Whitte IR, Rycroft RJG, and McFadden JP, *Variation in response of human skin to irritant challenge.* Contact Dermatitis, 1996. **34**(2): p. 115-117.

26. Lammintausta K, Maibach HI, and Wilson D, *Susceptibility to cumulative and acute irritant dermatitis An experimental approach in human volunteers.* Contact Dermatitis, 1988. **19**(2): p. 84-90.

27. Mohammed D, Matts PJ, Hadgraft J, and Lane ME, *Depth profiling of stratum corneum biophysical and molecular properties.* British Journal of Dermatology, 2011. **164**(5): p. 957-965.

28. Hadgraft J and Lane ME, *Transepidermal water loss and skin site: A hypothesis.* International Journal of Pharmaceutics, 2009. **373**(1-2): p. 1-3.

29. Fisher LB and Maibach HI, *Effect of some irritants on human epidermal mitosis.* Contact Dermatitis, 1975. **1**(5): p. 273-276.

30. Willis CM, Stephens CJM, and Wilkinson JD, *Epidermal Damage Induced by Irritants in Man: A Light and Electron Microscopic Study.* J Invest Dermatol, 1989. **93**(5): p. 695-699.

31. Tsang M and Guy RH, *Effect of Aqueous Cream BP on human stratum corneum in vivo.* British Journal of Dermatology, 2010. **163**(5): p. 954-958.

32. Ongpipattanakul B, Burnette R, Potts R, and Francoeur M, *Evidence that Oleic Acid Exists in a Separate Phase Within Stratum Corneum Lipids.* Pharmaceutical Research, 1991. **8**(3): p. 350-354.

33. Bouwstra J, Gooris G, and Ponec M, *The Lipid Organisation of the Skin Barrier: Liquid and Crystalline Domains Coexist in Lamellar Phases.* Journal of Biological Physics, 2002. **28**(2): p. 211-223.

34. Pilgram G, Vissers D, van der Meulen H, Pavel S, Lavrijsen S, Bouwstra J, and Koerten H, *Aberrant Lipid Organization in Stratum Corneum of Patients with Atopic Dermatitis and Lamellar Ichthyosis.* J Invest Dermatol, 2001. **117**(3): p. 710-717.

35. Bouwstra JA and Ponec M, *The skin barrier in healthy and diseased state.* Biochimica et Biophysica Acta (BBA) - Biomembranes, 2006. **1758**(12): p. 2080-2095.

36. Pilgram G, Pelt E, Bouwstra J, and Koerten H, *Electron Diffraction Provides New Information on Human Stratum Corneum Lipid Organization Studied in Relation to Depth and Temperature.* J Invest Dermatol, 1999. **113**(3): p. 403-409.

37. Froebe CL, Simion FA, Rhein LD, Cagan RH, and Kligman A, *Stratum corneum Lipid Removal by Surfactants: Relation to in vivo Irritation.* Dermatology, 1990. **181**(4): p. 277-283.

38. Fartasch M, *Ultrastructure of the epidermal barrier after irritation.* Microscopy Research and Technique, 1997. **37**(3): p. 193-199.

39. Fulmer AW and Kramer GJ, *Stratum Corneum Lipid Abnormalities in Surfactant-Induced Dry Scaly Skin.* J Invest Dermatol, 1986. **86**(5): p. 598-602.

40. Warner RR, Boissy YL, Lilly NA, Spears MJ, McKillop K, Marshall JL, and Stone KJ, *Water Disrupts Stratum Corneum Lipid Lamellae: Damage is Similar to Surfactants.* J Invest Dermatol, 1999. **113**(6): p. 960-966.

41. Bouwstra JA, de Graaff A, Gooris GS, Nijsse J, Wiechers JW, and van Aelst AC, *Water Distribution and Related Morphology in Human Stratum Corneum at Different Hydration Levels.* J Invest Dermatol, 2003. **120**(5): p. 750-758.

42.   Krafft C, Steiner G, Beleites C, and Salzer R, *Disease recognition by infrared and Raman spectroscopy.* Journal of Biophotonics, 2009. **2**(1-2): p. 13-28.

43.   Scott IR and Harding CR, *Filaggrin breakdown to water binding compounds during development of the rat stratum corneum is controlled by the water activity of the environment.* Developmental Biology, 1986. **115**(1): p. 84-92.

44.   Harding CR and Scott I, *Alterations in the processing of human filaggrin following skin occlusion in vivo and in vitro.* Journal of investigative dermatology, 1993. **100**(4): p. 579.

45.   Ulfgren A, Klareskog L, and Lindberg M, *An immunohistochemical analysis of cytokine expression in allergic and irritant contact dermatitis.* Acta Derm Venereol, 1000. **80**: p. 167-170.

46.   Steven AC and Steinert PM, *Protein composition of cornified cell envelopes of epidermal keratinocytes.* Journal of Cell Science, 1994. **107**(2): p. 693-700.

47.   Barrett JG and Scott IR, *Pyrrolidone Carboxylic Acid Synthesis in Guinea Pig Epidermis.* J Invest Dermatol, 1983. **81**(2): p. 122-124.

48.   Scott I, *Factors controlling the expressed activity of histidine ammonia-lyase in the epidermis and the resulting accumulation of urocanic acid.* Biochem J, 1981. **194**(3): p. 829-838.

49.   Abeyakirthi S, Mowbray M, Bredenkamp N, Overloop Lv, Declercq L, Davis PJ, Matsui MS, and Weller RB, *Arginase is overactive in psoriatic skin.* British Journal of Dermatology, 2010. **163**(1): p. 193-196.

50.   Chavanas S, Méchin M-C, Nachat R, Adoue V, Coudane F, Serre G, and Simon M, *Peptidylarginine deiminases and deimination in biology and pathology: Relevance to skin homeostasis.* Journal of Dermatological Science, 2006. **44**(2): p. 63-72.

51.   Horii I, Kawasaki K, Koyama J, Nakayama Y, Nakajima K, Okazaki K, and Seiji M, *Histidine-rich protein as a possible origin of free amino acids of stratum corneum.* Curr Probl Dermatol, 1983. **11**: p. 301-315.

52.   Schnorr O, Schuier M, Kagemann G, Wolf R, Walz M, Ruzicka T, Mayatepek E, Laryea M, Suschek CV, Kolb-Bachofen V, and Sies H, *Arginase-1 overexpression induces cationic amino acid transporter-1 in psoriasis.* Free Radical Biology and Medicine, 2005. **38**(8): p. 1073-1079.

53.   Bruch-Gerharz D, Schnorr O, Suschek C, Beck K-F, Pfeilschifter J, Ruzicka T, and Kolb-Bachofen V, *Arginase 1 overexpression in psoriasis: limitation of inducible nitric oxide synthase activity as a molecular mechanism for keratinocyte hyperproliferation.* Am J Pathol, 2003. **162**(1): p. 203-211.

54.   Kampfer H, Pfeilschifter J, and Frank S, *Expression and Activity of Arginase Isoenzymes During Normal and Diabetes-Impaired Skin Repair.* J Invest Dermatol, 2003. **121**(6): p. 1544-1551.

55.   Koyama J, Horii I, Kawasaki K, Nakayama Y, Morikawa Y, Mitsui T, and Kumagai H, *Free amino acids of stratum corneum as a biochemical marker to evaluate dry skin.* J Soc Cosmet Chem, 1984. **35**: p. 183-195.

56.   Wolfersberger MG and Tabachnik J, *Pyrrolidone carboxylic acid (pyroglutamic acid) in normal plasma.* Cellular and Molecular Life Sciences, 1973. **29**(3): p. 346-347.

57.   Kingsbury KJ, Kay L, and Hjelm M, *Contrasting plasma free amino acid patterns in elite athletes: association with fatigue and infection.* British Journal of Sports Medicine, 1998. **32**(1): p. 25-32.

58.   Wilhelm K-P, Freitag G, and Wolff HH, *Surfactant-induced skin irritation and skin repair: Evaluation of a cumulative human irritation model by noninvasive techniques.* Journal of the American Academy of Dermatology, 1994. **31**(6): p. 981-987.

59.   Ananthapadmanabhan KP, Moore DJ, Subramanyan K, Misra M, and Meyer F, *Cleansing without compromise: the impact of cleansers on the skin barrier and the technology of mild cleansing.* Dermatologic Therapy, 2004. **17**: p. 16-25.

60.   Mizushima J, Kawasaki K, ino Y, Sakamoto K, and Maibach HI, *Effect of surfactants on human stratum corneum utilizing electron paramagnetic resonance spectroscopy-from the point of view of water contents.* J Japanese Cosmetic Science Society, 2001. **25**: p. 130-135.

61.   Levi K, Weber RJ, Do JQ, and Dauskardt RH, *Drying stress and damage processes in human stratum corneum.* International Journal of Cosmetic Science, 2010. **32**(4): p. 276-293.

62.   De Jongh CM, Jakasa I, Verberk MM, and Kezic S, *Variation in barrier impairment and inflammation of human skin as determined by sodium lauryl sulphate penetration rate.* British Journal of Dermatology, 2006. **154**(4): p. 651-657.

63.   Ananthapadmanabhan KP, Lips A, Vincent C, Meyer F, Caso S, Johnson A, Subramanyan K, Vethamuthu M, Rattinger G, and Moore DJ, *pH-induced alterations in stratum corneum properties.* International Journal of Cosmetic Science, 2003. **25**(3): p. 103-112.

64.   De Jongh CM, Lutter R, Verberk MM, and Kezic S, *Differential cytokine expression in skin after single and repeated irritation by sodium lauryl sulphate.* Experimental Dermatology, 2007. **16**(12): p. 1032-1040.

65.   Friberg SE, Goldsmith L, Suhaimi H, and Rhein LD, *Surfactants and the stratum corneum lipids.* Colloids and Surfaces, 1987. **30**(1): p. 1-12.

66.   Suzuki Y, Nomura J, Hori J, Koyama J, Takahashi M, and Horii I, *Detection and characterization of endogenous protease associated with desquamation of stratum corneum.* Archives of Dermatological Research, 1993. **285**(6): p. 372-377.

67.   Nylander-lundgvist E and Egelrud T, *Formation of active IL-1 beta from pro-IL-1 beta catalyzed by stratum corneum chymotryptic enzyme in vitro.* Acta Derm Venereol. , 1997. **77**(3): p. 203-206.

68.   Yamasaki K, Schauber J, Coda A, Lin H, Dorschner RA, Schechter NM, Bonnart C, Descargues P, Hovnanian A, and Gallo RL, *Kallikrein-mediated proteolysis regulates the antimicrobial effects of cathelicidins in skin.* The FASEB Journal, 2006. **20**(12): p. 2068-2080.

69.   Hachem J-P, Man M-Q, Crumrine D, Uchida Y, Brown BE, Rogiers V, Roseeuw D, Feingold KR, and Elias PM, *Sustained Serine Proteases Activity by Prolonged Increase in pH Leads to Degradation of Lipid Processing Enzymes and Profound Alterations of Barrier Function and Stratum Corneum Integrity.* J Invest Dermatol, 2005. **125**(3): p. 510-520.

70.   Oikonomopoulou K, Hansen KK, Saifeddine M, Vergnolle N, Tea I, Blaber M, Blaber SI, Scarisbrick I, Diamandis EP, and Hollenberg MD, *Kallikrein-mediated cell signalling: targeting proteinase-activated receptors (PARs).* Biological Chemistry, 2006. **387**(6): p. 817-824.

71.   Hogewoning AA, Larbi IA, Addo HA, Amoah AS, Boakye D, Hartgers F, Yazdanbakhsh M, Van Ree R, Bouwes Bavinck JN, and Lavrijsen APM, *Allergic characteristics of urban schoolchildren with atopic eczema in Ghana.* Journal of the European Academy of Dermatology and Venereology, 2010. **24**(12): p. 1406-1412.

72.   Sherriff A and Golding J, *Hygiene levels in a contemporary population cohort are associated with wheezing and atopic eczema in preschool infants.* Archives of Disease in Childhood, 2002. **87**(1): p. 26-29.

Conclusions

In this thesis, the use of various minimally invasive bioengineering techniques to assess skin barrier function has been investigated. The specific objectives were: 1) to evaluate reverse iontophoresis and tape-stripping for the extraction of natural moisturizing factor (NMF) constituents from the stratum corneum (SC); 2) to analyse NMF composition at different body sites, and after skin irritation; and 3) to examine other bioengineering methods, including infrared spectrometry (IR) measurement and immunochemical staining, to evaluate skin barrier function. The ultimate objective is to underpin a non-invasive technology with which to diagnose and monitor individuals, especially infants pre-disposed to atopic dermatitis (AD).

As tape-stripping was a major technique employed in this thesis, Chapter 2 evaluated and compared a novel imaging method against the traditional gravimetric approach to quantify the SC removed on the tapes. This novel imaging method offers fast, simple, reproducible SC quantification on the tapes with a good signal-to-noise ratio. Correlation with infrared densitometry confirms that the imaging approach primarily evaluates the amount of SC via its protein content and it is thus not subject to interference when attempting to quantify SC thickness at skin sites where high levels of sebaceous lipids (e.g., forehead) are found. The imaging approach also correlates with the traditional gravimetric technique and, with further validation, may therefore offer a better standard method for SC quantification in the future.

Filaggrin expression is essential for SC hydration, as it is the precursor protein for the amino-acid-derived components of the natural moisturizing factor (NMF), a complex mixture of low molecular weight humectants. Due to low molecular weight, polarity and water solubility of NMF components, it was hypothesised that reverse iontophoresis could be used to monitor these molecules is a minimally invasive fashion. As expected, the extraction of NMF components was enhanced by reverse iontophoresis relative to passive extraction, and was influenced by molecular charge and the size of the so-called SC "reservoir". Chapter 3 demonstrated an abundant amino-acid-derived NMF reservoir in the SC and that a 4-hour iontophoretic extraction period is insufficient to deplete this material 'reservoir' in healthy human volunteers (with the exception of those components that are

charged or present only in minimal amounts in the SC, e.g., lysine). Therefore, reverse iontophoresis is a potentially useful tool with which to extract NMF from the SC.

In Chapter 4, attenuated total reflectance-fourier transform infrared spectroscopy (ATR-FTIR) in conjunction with *in vivo* NMF extraction was performed on the forearm and forehead of healthy volunteers. SC lipids on the forehead were more disordered, especially near the surface due to an extensive contribution from sebum. The concentrations of amino-acid derived NMF components at both sites were similar. However, forehead SC was thinner and generally contained a lower total amount of NMF. Reverse iontophoresis efficiently extracted charged NMF relative to passive extraction; however, only modest enhancement was achieved for zwitterionic amino acid constituents.

Repeated exposure to a low concentration of the irritant sodium lauryl sulphate (SLS) on healthy volunteers was used to model a damaged skin that is similar to AD and to chronic irritant contact dermatitis. The SC 'reservoir' of NMF was quantified with and without SLS-induced irritation and it was found that the components typically present at high and moderate levels were dramatically reduced; on the other hand, constituents present in low levels did not change. Zwitterions were best extracted by tape-stripping, as reverse iontophoresis cannot completely differentiate the origin from which the amino acids are extracted. In terms of a diagnostic matter, pyrrolidone carboxylic acid shows promise as it is reliably and completely extracted by reverse iontophoresis (confirmed by tape-stripping) and the amount obtained is not "contaminated" by material from a deeper compartment, such as the plasma, where it is present at very low concentration. Glutamine may also be a useful marker for impaired barrier function as it has been found at higher level in both SLS-treated skin sites and on the forehead.

All methods used were sensitive enough to differentiate the effect of SLS treatment. IR spectroscopy identified prolonged lipid disorder while fluorescent staining method demonstrated formation of smaller, immature corneocytes after surfactant exposure. However, changes in NMF composition inversely correlated with both basal TEWL and changes in TEWL after SLS-induced irritation, and may therefore prove to be useful as a potential marker for skin 'health'.

Although a relatively low concentration (0.1% w/v) SLS was used in the final component of this work, skin barrier damage was clearly evident. This highlights, therefore, the importance of minimising exposure to surfactant in the course of everyday life and to

choose carefully any moisturizer deemed necessary to maintain a well-hydrated skin. The techniques used and developed in this thesis may not only be used to identify people who have a compromised SC barrier, but also to assess changes in skin barrier function due to change in environmental conditions, work habits, dermatological therapy, etc. Multiple further studies exploring various exposure scenarios maybe envisaged, therefore, to confirm the finding of this work and to validate the approaches described for diagnostic and monitoring purposes.

Appendix 1. Analytical method for the detection of NMF components

1. Method

NMF components were analyzed using Shimadzu LCMS-2010EV with a single quadrupole and a dual ion source (containing both electrospray and atmospheric pressure chemical ionization). The MS was operated in positive ion mode with the ionspray voltage set at 1.5 kV. Nitrogen was used both as a nebulising and drying gas at a flow rate of 1.5 L/min with a heat block temperature of 480°C and curved desolvation line (CDL) temperature of 230°C. The quadrupole was operated in the selected ion monitoring (SIM) mode and protonated molecules $[M+H]^+$ (Table 1) were used for quantification

Table 1: Molecules for quantification

Molecules	Abbr.	$[M+H]^+$	Molecules	Abbr.	$[M+H]^+$
Alanine	Ala	90	Arginine	Arg	175
Asparagine	Asn	133	Aspartic acid	Asp	134
Citruline	Cit	176	Glutamic acid	Glu	148
Glutamine	Gln	147	glutamine-D5		152
Glycine	Gly	76	Glycine-D2		78
Histidine	His	156	Isoleucine	Ile	132
Leucine	Leu	132	Lysine	Lys	147
Methionine	Met	150	Ornithine	Orn	133
Phenylalanine	Phe	166	Proline	Pro	116
Pyrrolidone carboxylic acid	PCA	130	Taurine	Tau	126
Serine	Ser	106	Serine-D3		109
Theonine	Thr	120	Tryptophan	Try	205
Tyrosine	Tyr	182	Urea		61

Trans-urocanic acid	t-UA	139	Cis-urocanic acid	c-UA	139
Valine	Val	118			

Separation was carried out on a Gemini C18 column (50x4.6 mm, 3 μm, 110Å, Phenomenex, USA). All analyses were carried out at 40ºC with a flow-rate of 0.3 ml/min. A gradient was used with eluent A being a 20 mM nonafluoropentanoic acid (NFPA) solution in water and eluent B acetonitrile. The gradient elution started with 99:1(v/v) A:B for 5 minutes, followed by a linear change to 86:14(v/v) A:B over 9 minutes, then 86:14(v/v) for 5 minutes, and subsequently altered linearly to 64:36(v/v) over 14 minutes. The MS was then switched to negative ion mode with 20/80 (v/v) A:B for 3 minutes to wash the column and finally equilibrated for 20 minutes under the initial conditions.

2. Results

Because of their volatility, perfluorinated carboxylic acids are suitable for use with MS. The method has been shown to give adequate resolution in both LCMS and LCMS/MS [1-3]. In MS, the positive ionisation mode generally shows higher sensitivity than the negative mode [4] for amino acid analysis. Perfluorinated carboxylic acids are strong acids, and therefore amino acids are protonated by these compounds. The separation profile is shown in Figure 1.
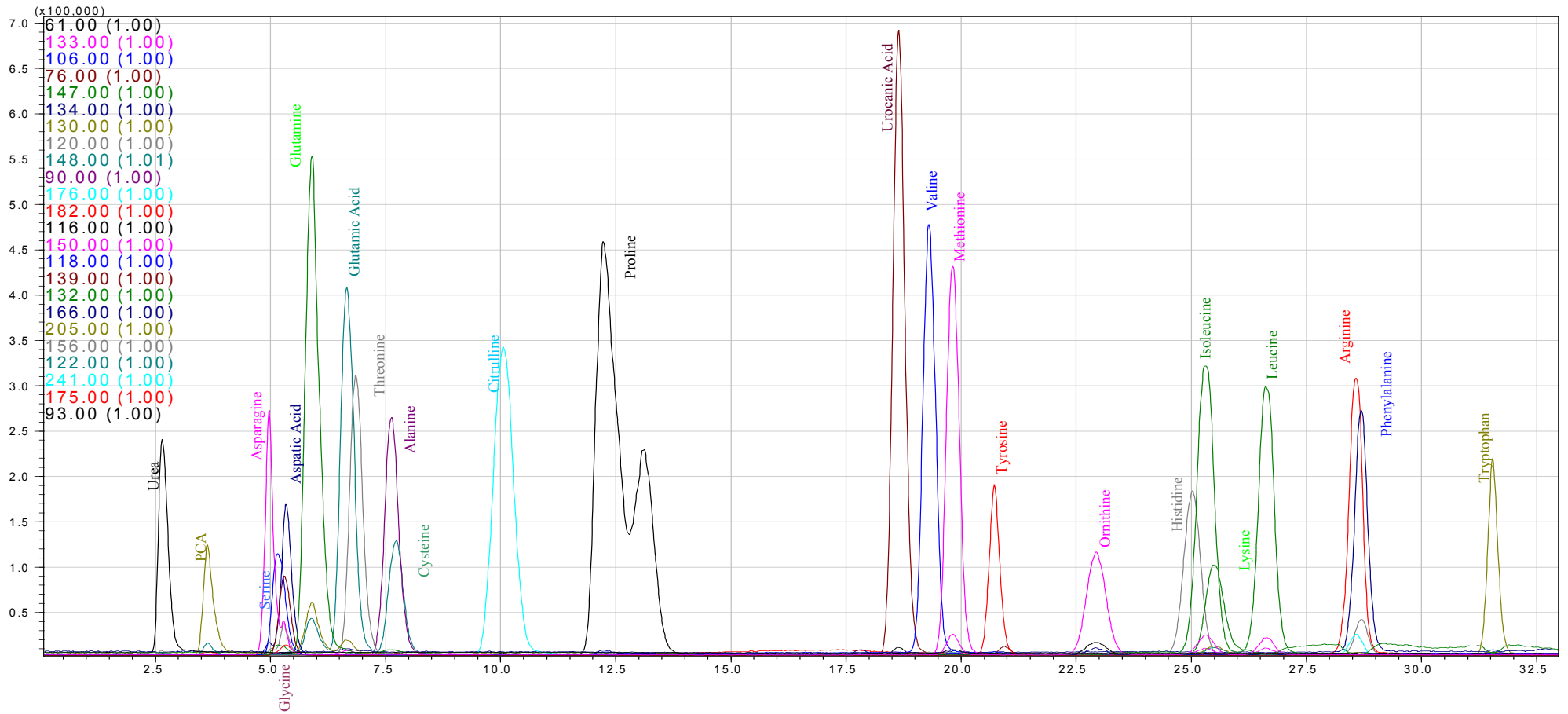
Figure1: Sample separation and detection of NMF standards (5µg/ml) by LCMS

3. Method Validation

3.1 Reasons for exclusion of quantification

Twenty-one NMF components were successfully quantified; others were detected in the samples but could not be quantified for the reasons listed below:

Table2: Reasons for exclusion of quantification in skin samples.

Analytes	Reasons for exclusion of quantification
Asparagine	Severe ion suppression at cathode
Aspartic Acid	Co-elution with other unidentified molecules and present with severe ion suppression
Methionine	Signals were between limit of detection (LOD) and limit of quantification (LOQ).
Taurine	Signals were between LOD and LOQ
Cis-Urocanic Acid	Signals were between LOD and LOQ.

3.2 LOQ and repeatability

The repeatability and LOQ for each analyte are summarized in Table 3. Intra-day RSD was obtained from 5 injections of an NMF mixture at 3µg/ml on the same day, while inter-day RSD was obtained from repeated injections (3µg/ml) on 5 consecutive days. Serine and glycine had very high inter-day RSD levels (>15%) due to ion suppression, and were therefore normalised by introducing the corresponding deuterated amino acids, this resulted in the RSDs being significantly reduced.

Table 3: LQL and repeatability of the LCMS method with NFPA as the ion pairing agent

Analytes	Intra-day RSD (%)	Inter-day RSD (%)	LOQ (µM)
	(n=5)	(n=5)	
Alanine	2.6	4	0.3
Arginine	4.4	3.7	0.8
Asparagine	5.9	8.4	1.5
Aspartic Acid	5.7	10.4	1.5
Citrulline	3.1	4.3	0.1
cis-Urocanic Acid	2.8	7.7	0.1
Glutamic acid	6	7	0.2
Glutamine	4.7	9	0.1
Glycine	0.8	1.3	1.3
Histidine	7	4.2	0.9
Isoleucine	2.4	4.4	0.2
Leucine	3.7	3.6	0.2
Lysine	5.8	5.1	2.1
Methionine	4.9	4.5	0.1
Ornithine	5.9	3.8	0.8
PCA	3	5	0.8
Phenylalanine	3.3	3.6	0.2
Proline	1.9	9.2	0.2
Serine	0.6	1.2	3.8
Taurine	5.6	20.9	0.3
Threonine	1.6	7.9	0.3
Tryptophan	4.6	4.3	0.2
t-UA	2.9	3.2	0.1
Tyrosine	3.8	4.9	0.2
Urea	3	7.8	1
Valine	2.2	3.7	0.3

3.3 Analysis of matrix effects

Matrix effects in an analytical method are caused by the co-elution of other components of the sample with the specific compound to be quantified. It has a high incidence in MS, and is believed to result from the competition of analyte ions and matrix components to access the electrosprayed droplet surface for gas-phase emission in MS. Although it can lead to either ion enhancement or ion suppression with a consequent error in the quantification of the analyte of interest, in most cases ion suppression is the main problem.

3.3.1 Matrix effects caused by salts

Matrix effects were detected in the MS analysis of the initial reverse iontophoresis samples, in which sodium chloride was used as background electrolyte. Significant ion suppression for most of the amino acid analytes was observed in the presence of 20mM sodium chloride. Consequently, ammonium chloride, a volatile salt, was chosen instead, resulting in much less suppression.

3.3.1 Matrix effects caused by *in vivo* samples

The *in vivo* samples for reverse iontophoresis, passive diffusion and tape stripping comprised a volume of only 1-1.6ml of aqueous solution. As these samples were collected at different times and by different methods, they were expected to result in different matrix effects making their resolution difficult. To deal with this problem, it was therefore decided to employ a technique called post-column infusion[5] (PCI).

3.3.1 PCI Method

The PCI setup is shown in Figure 2.
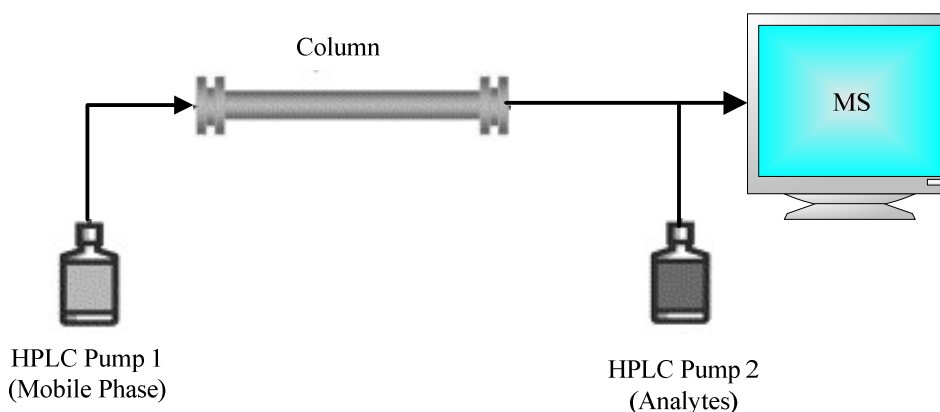
Figure 2: Schematic diagram of post-column infusion set up (Redrawn from Souverain et.al [5]).

All experiments were performed on Shimadzu LCMS-2010EV with a single quadrupole and a dual ion source; a Jasco LC pump (PU-980) was used as an additional pump after the column. The LC/MS parameters were exactly the same as the in vivo sample analysis mentioned previously. MS detection was conducted in the selected ion monitoring (SIM) mode, and protonated molecules were detected. The analyte solution was a standard NMF mixture with a concentration of 20µg/ml at a flow rate of 0.15ml/min.

Results

As a large amount of NMF standards was infused constantly, the baseline increased for all the compounds of interest. If ion suppression occurs, injection of the sample causes a dip in the chromatogram, the size of which indicates the magnitude of the suppression.

As expected, different matrices provoked different effects. Water was injected first, as a control, and it showed no suppression on any signals nor on the total ion count (Figure 3a). As seen in Figures 3(b-e), when other matrices were injected, two main ion suppressions were observed at 2 and 5 minutes. Figures 4 (a-c) show an example: arginine, is affected by ion suppression but not at the time it elutes. Similar to arginine, most analytes are protonated easily and elute at different times from those of which ion suppression occurs, therefore they are not affected by the matrix effects. The compounds, which are affected, are asparagine, aspartic acid, serine, glycine, and glutamine. To correctly interpret the subsequently obtained data, deuterated amino acids were employed.

The magnitude of the ion suppression differs between matrices. Cathode samples as expected had the most ion suppression, while anode, passive diffusion and tape stripping samples showed similar levels of suppression.   Samples from different time points had only small differences between them.
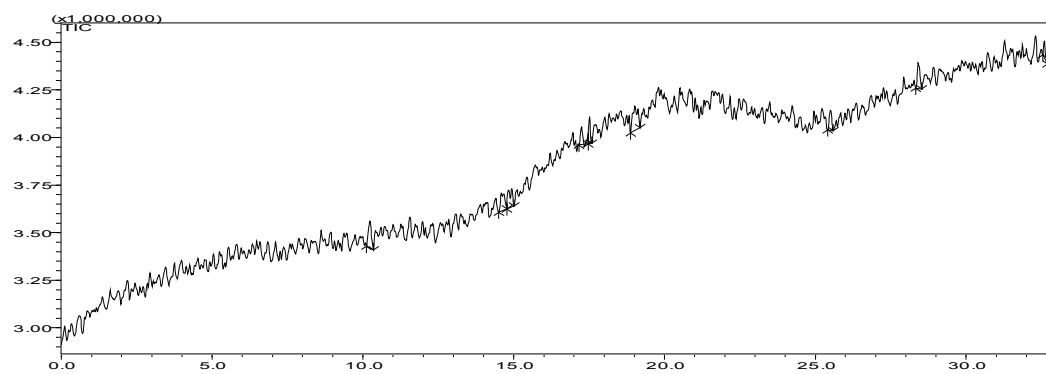
Figure 3a: Total ion count in MS after water injection.
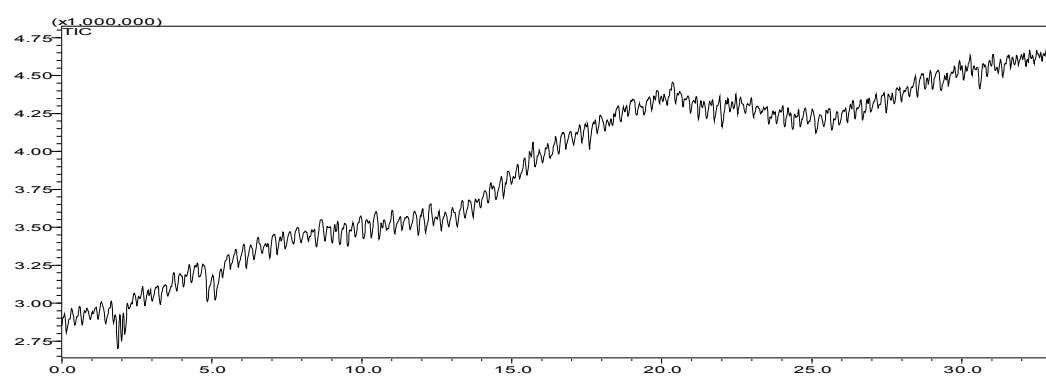
Figure 3b: Total ion count in MS after injection of buffer solution.
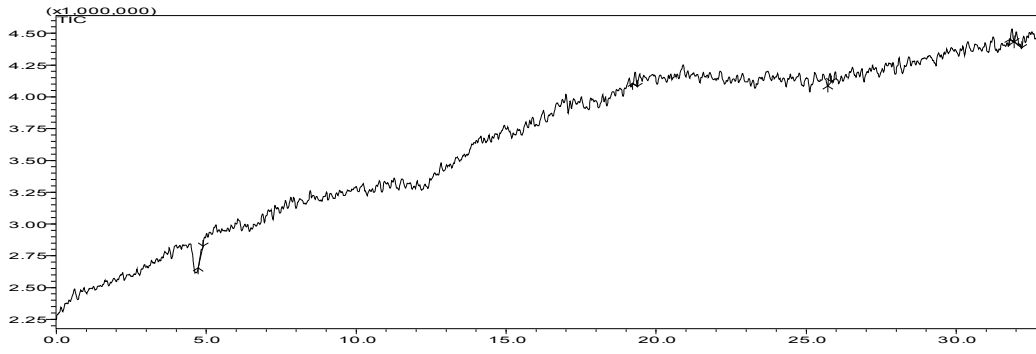
Figure 3c: Total ion count in MS after injection of samples from extracted tapes.
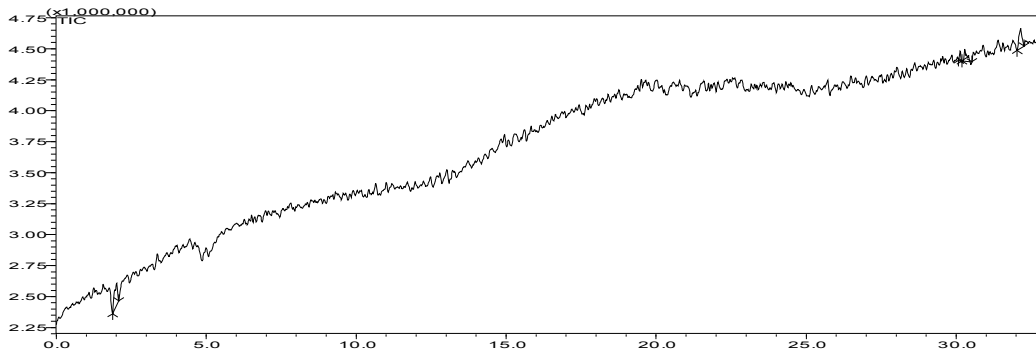
Figure 3d: Total ion count in MS after injection of samples extracted from anode.
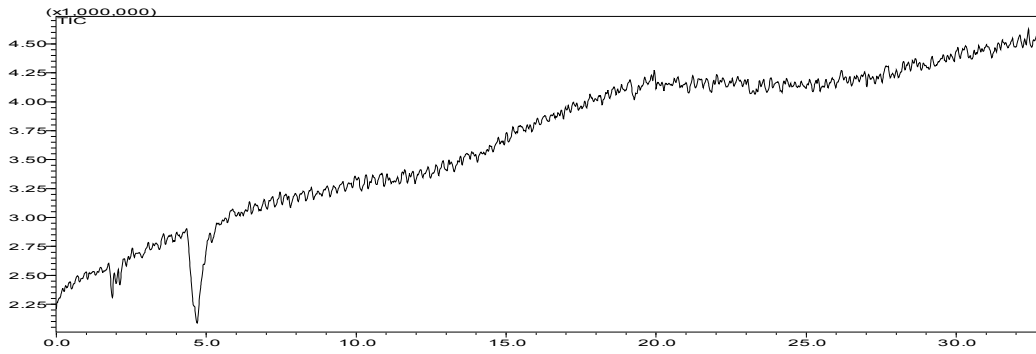
Figure 3e: Total ion count in MS after injection of samples extracted from cathode.

Example that is affected by matrix, but not at the time of separation. ---Arginine
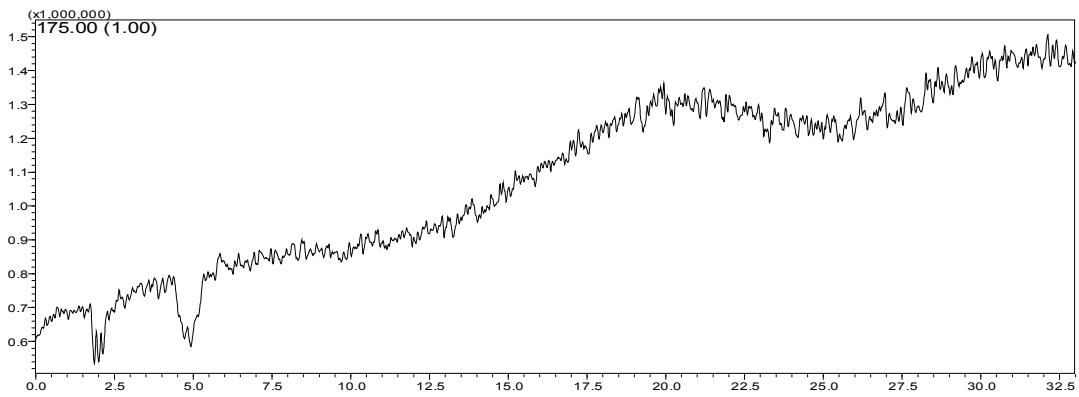
Figure 4a: Ion suppression at 2 and 5 minutes, but the analyte elutes at 27 minutes, which is not affected by injection sample from cathode at 1hour collection point.
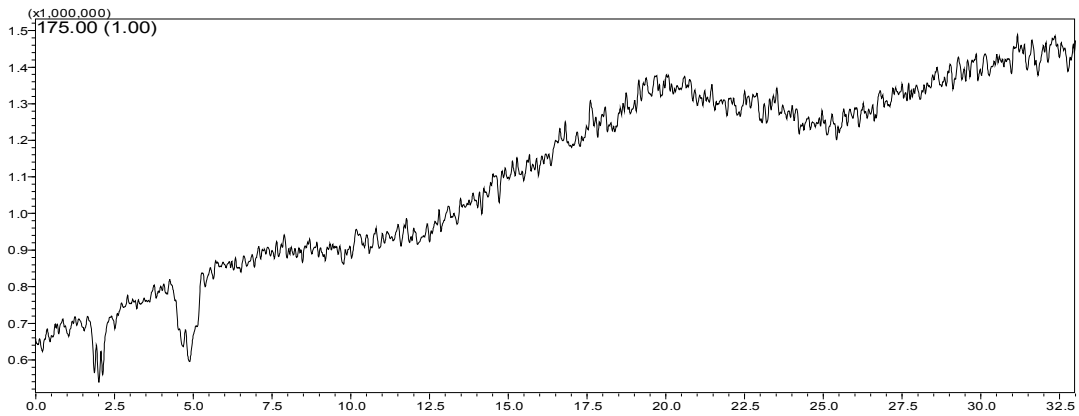
Figure 4b: Ion suppression at 2 and 5 minutes, but the analyte elutes at 27 minutes, which is not affected by injection sample from cathode at 3.5hour collection point
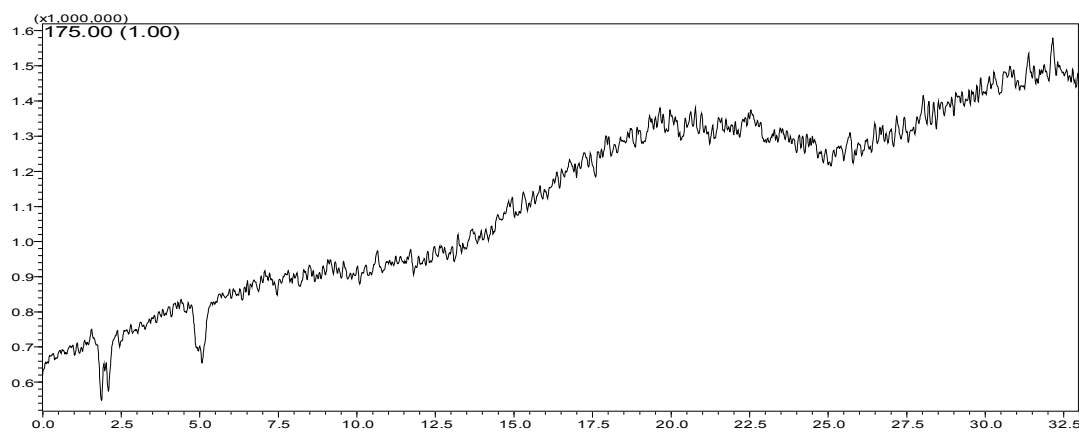
Figure 4c: Ion suppression at 2 and 5 minutes, but the analyte elutes at 27 minutes, which is not affected by injection samples from anode at 3hr collection point.

4. Reference:

1.   Piraud, M., et al., *Ion-pairing reversed-phase liquid chromatography / electrospray ionization mass spectrometric analysis of 76 underivatized amino acids of biological interest: a new tool for the diagnosis of inherited disorders of amino acid metabolism.* Rapid Communications in Mass Spectrometry, 2005. **19**(12): p. 1587-1602.

2.   Petritis, K.N., et al., *Ion-pair reversed-phase liquid chromatography for determination of polar underivatized amino acids using perfluorinated carboxylic acids as ion pairing agent.* Journal of Chromatography A, 1999. **833**(2): p. 147-155.

3.   Henriksen, T., et al., *The relative influences of acidity and polarity on responsiveness of small organic molecules to analysis with negative ion electrospray ionization mass spectrometry (ESI-MS).* Journal of the American Society for Mass Spectrometry, 2005. **16**(4): p. 446-455.

4.   Chaimbault, P., et al., *Determination of 20 underivatized proteinic amino acids by ion-pairing chromatography and pneumatically assisted electrospray mass spectrometry.* Journal of Chromatography A, 1999. **855**(1): p. 191-202.

5.   Souverain, S., S. Rudaz, and J.-L. Veuthey, *Matrix effect in LC-ESI-MS and LC-APCI-MS with off-line and on-line extraction procedures.* Journal of Chromatography A, 2004. **1058**(1-2): p. 61-66.

Appendix 2. Calibration Curve for NMF components
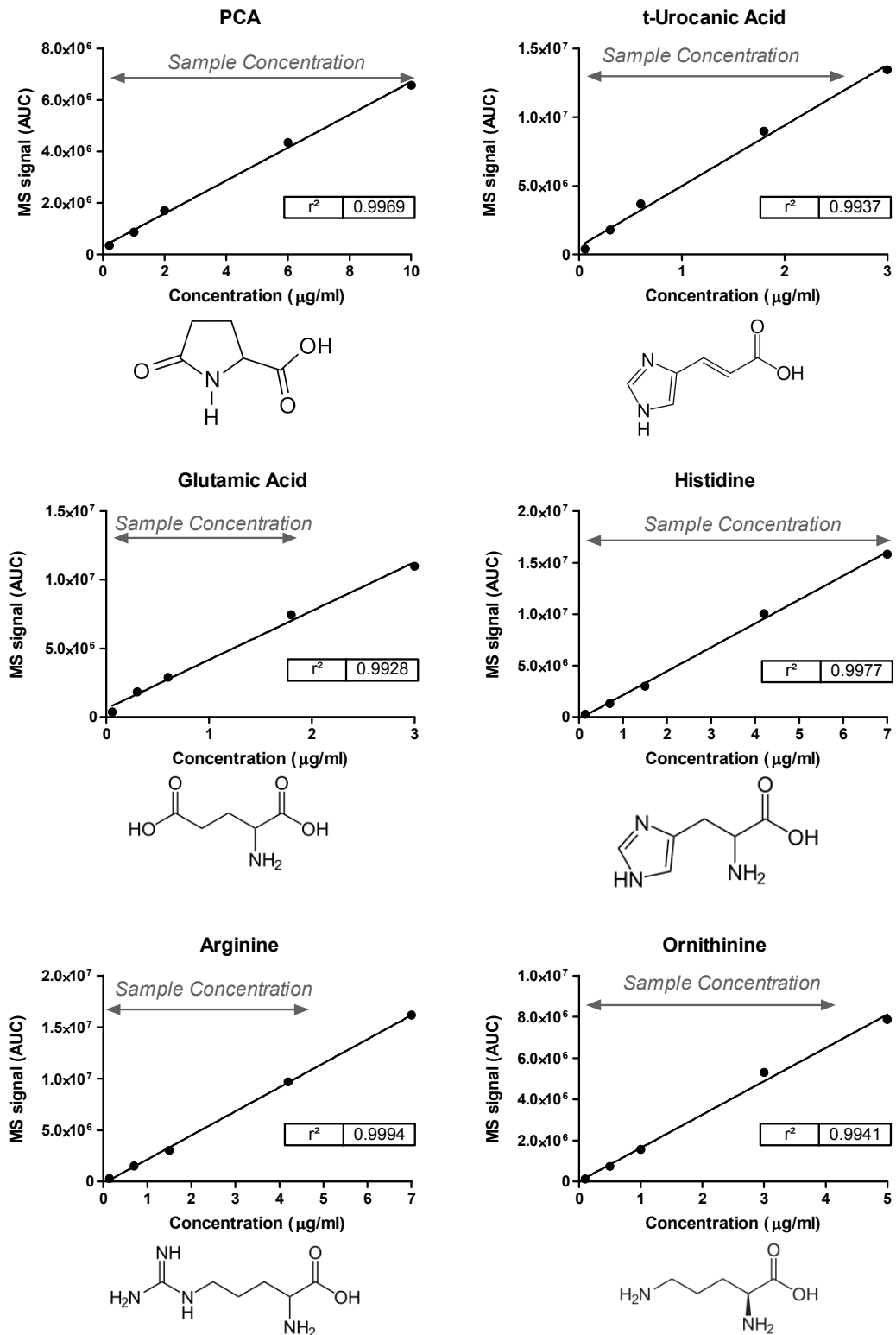
Figure 1: Analytes calibration curves. (Normal sample concentrations range are illustrated by the solid grey line with arrows)
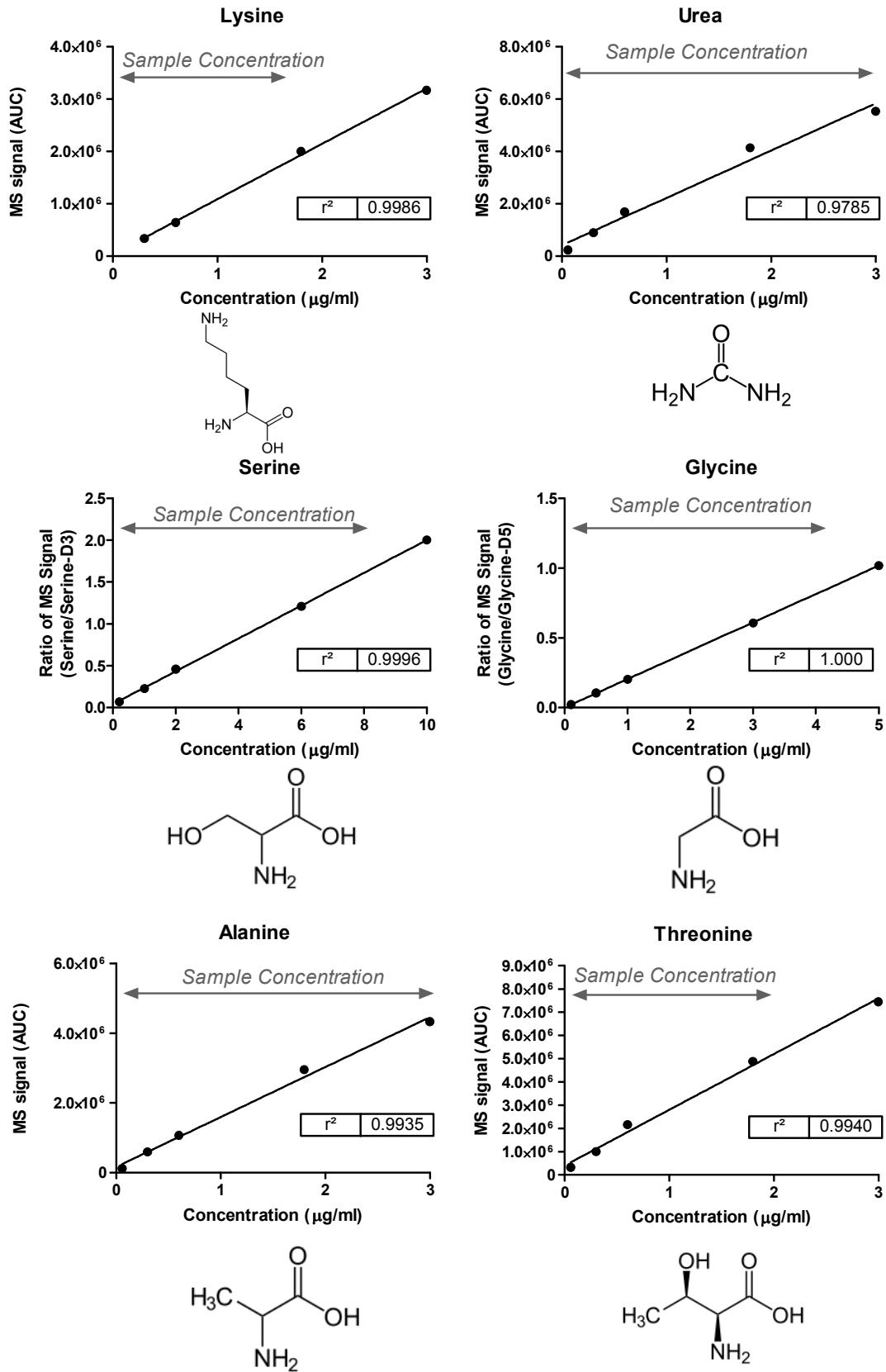
Figure 2: Analytes calibration curves. (Normal sample concentrations range are illustrated by the solid grey line with arrows)
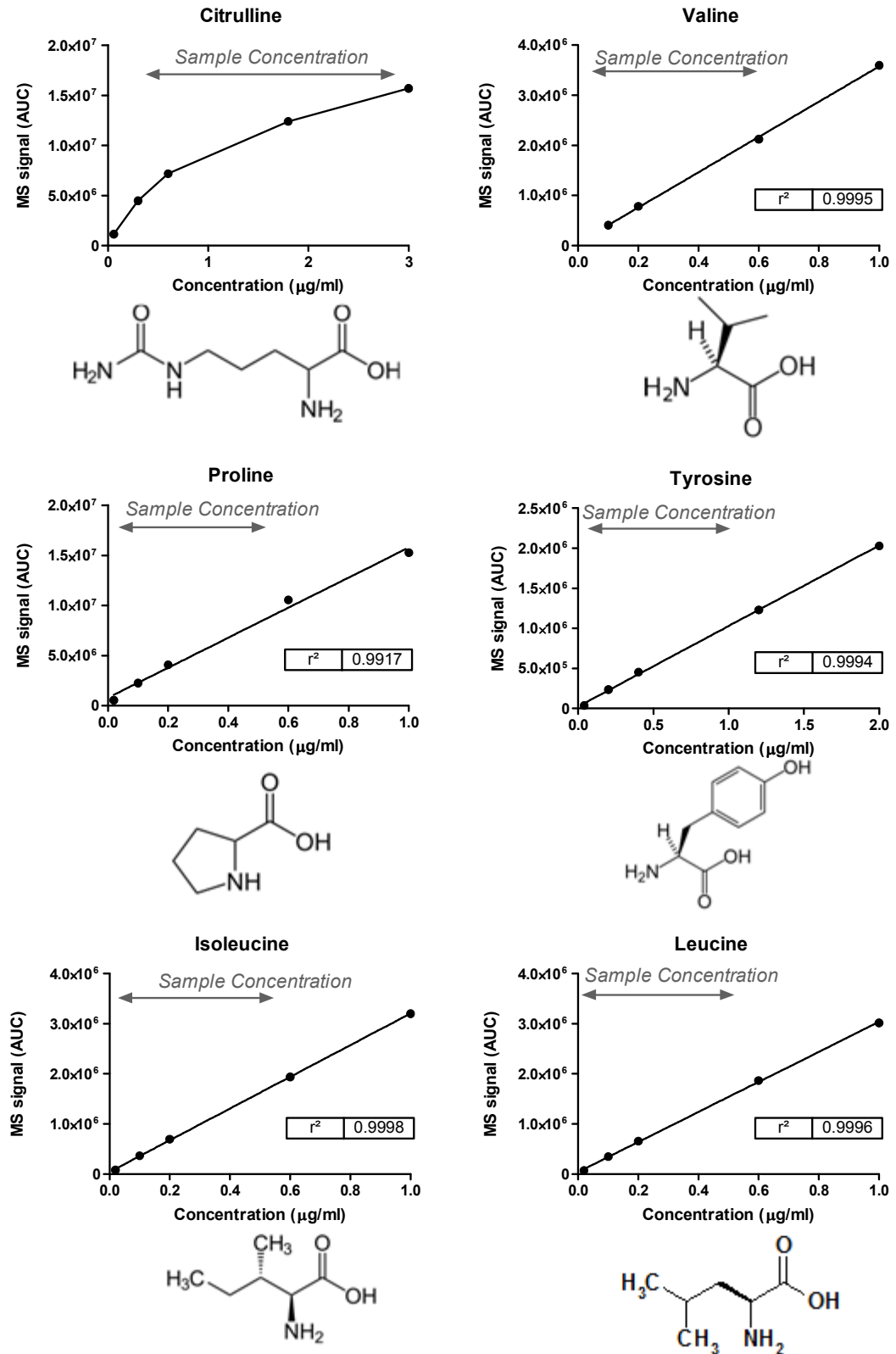
Figure 3: Analytes calibration curves. (Normal sample concentrations range are illustrated by the solid grey line with arrows)
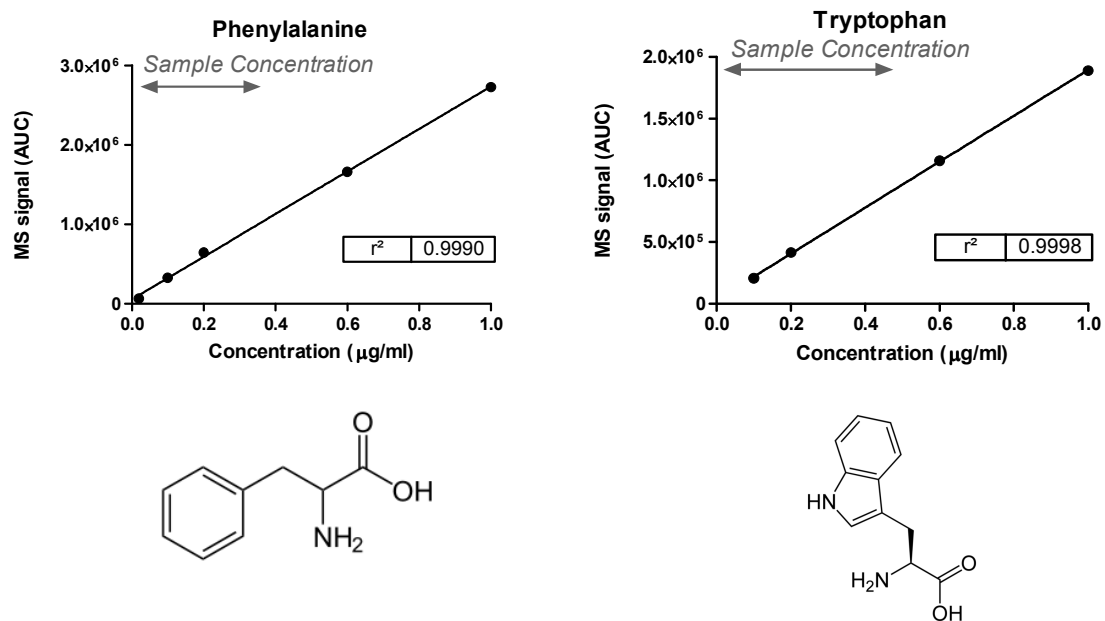
Figure 4: Analytes calibration curves. (Normal sample concentrations range are illustrated by the solid grey line with arrows)

Appendix 3. Complements to Chapter 3

1. SC content determined by tape-stripping
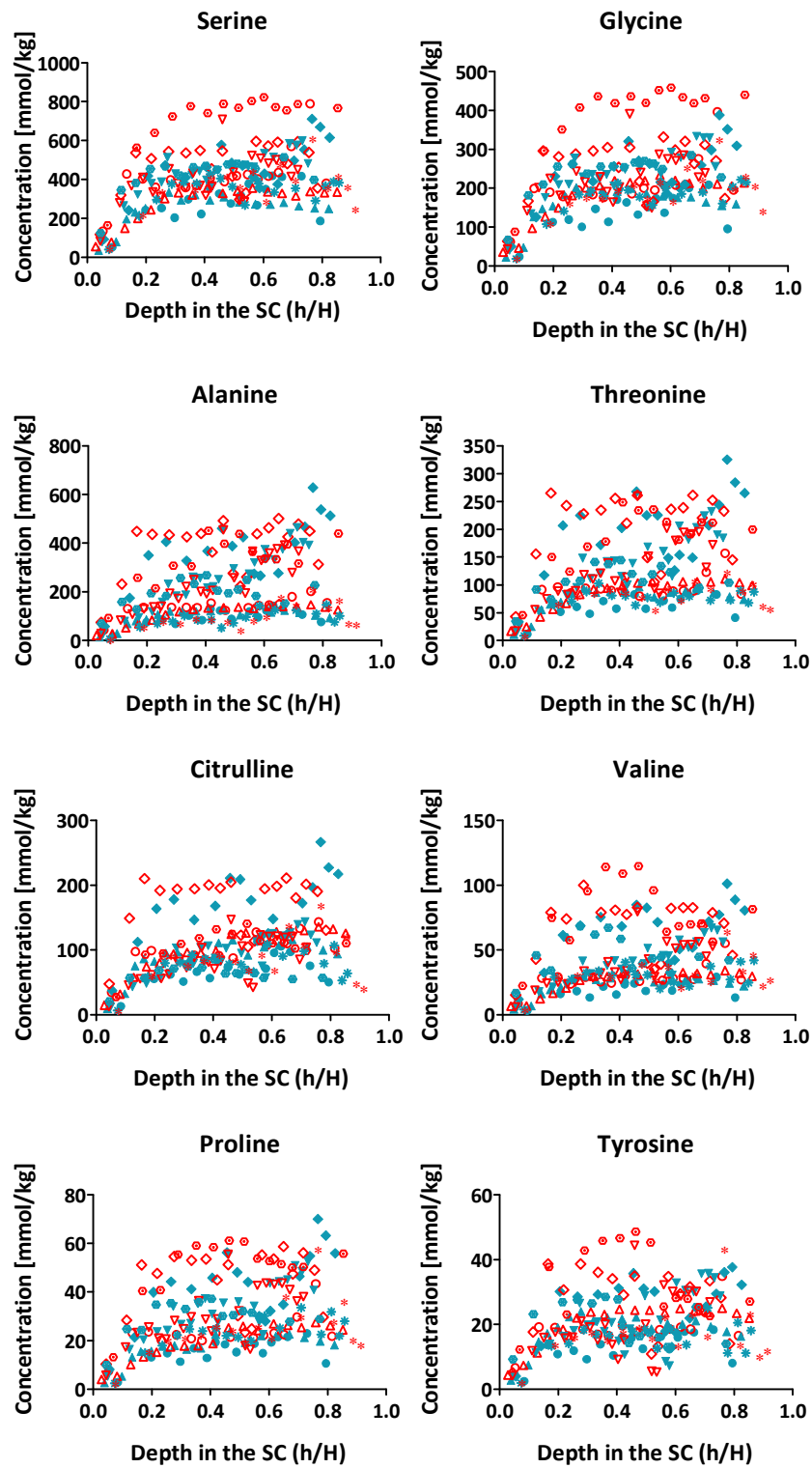
Figure 1a: Concentration profiles of NMF components as a function of position in the SC in 6 human volunteers determined using the gravimetric (cyan) and imaging (red) methods.
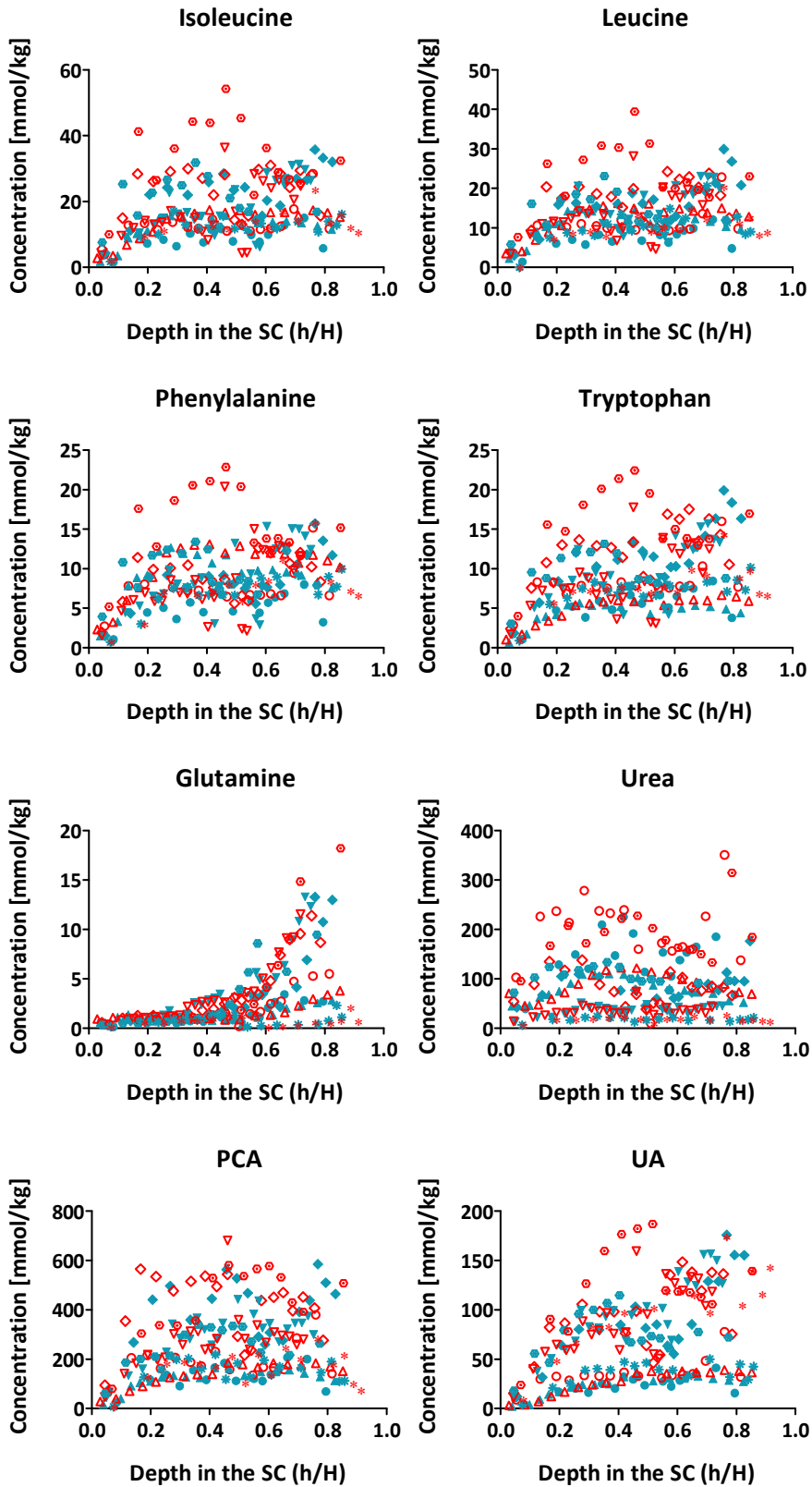
Figure 1b: Concentration profiles of NMF components as a function of position in the SC in 6 human volunteers determined using the gravimetric (cyan) and imaging (red) methods.
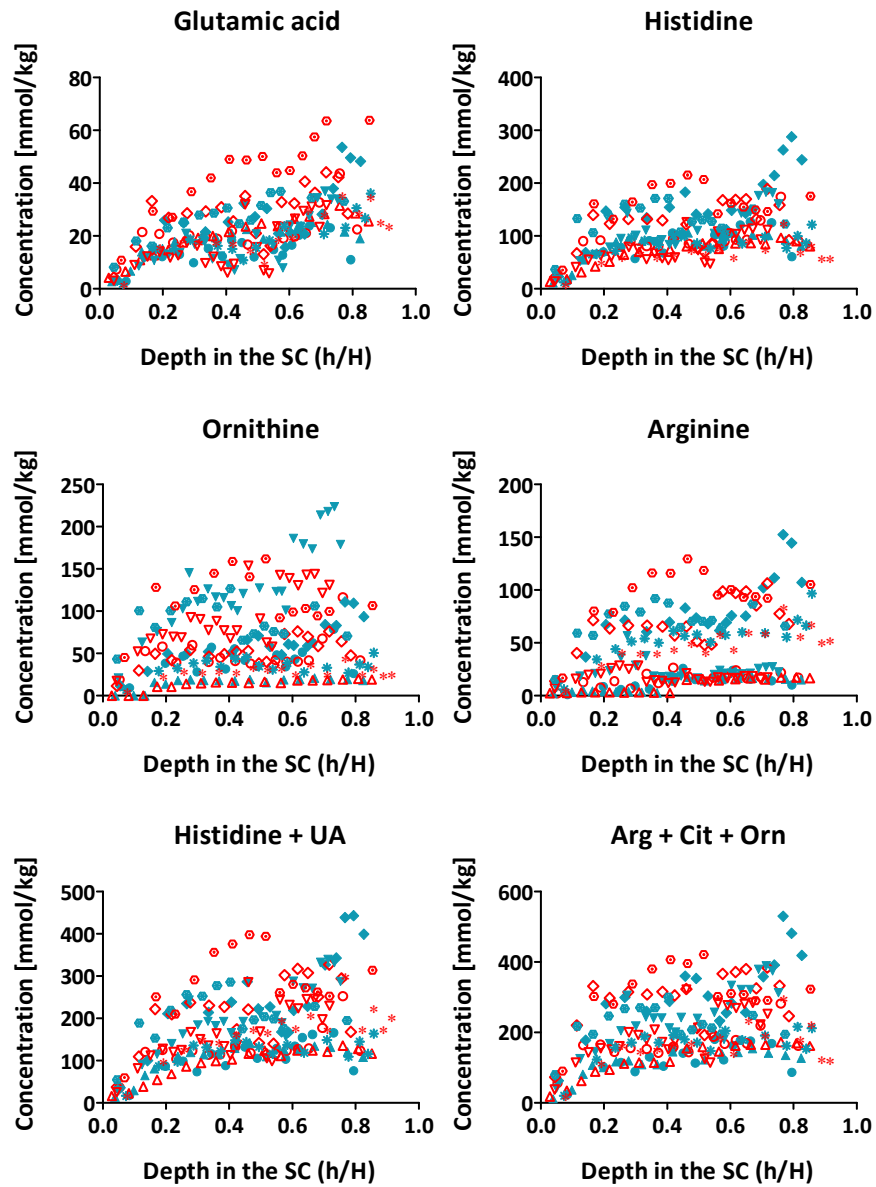
Figure 1c: Concentration profiles of NMF components as a function of position in the SC in 6 human volunteers determined using the gravimetric (cyan) and imaging (red) methods.
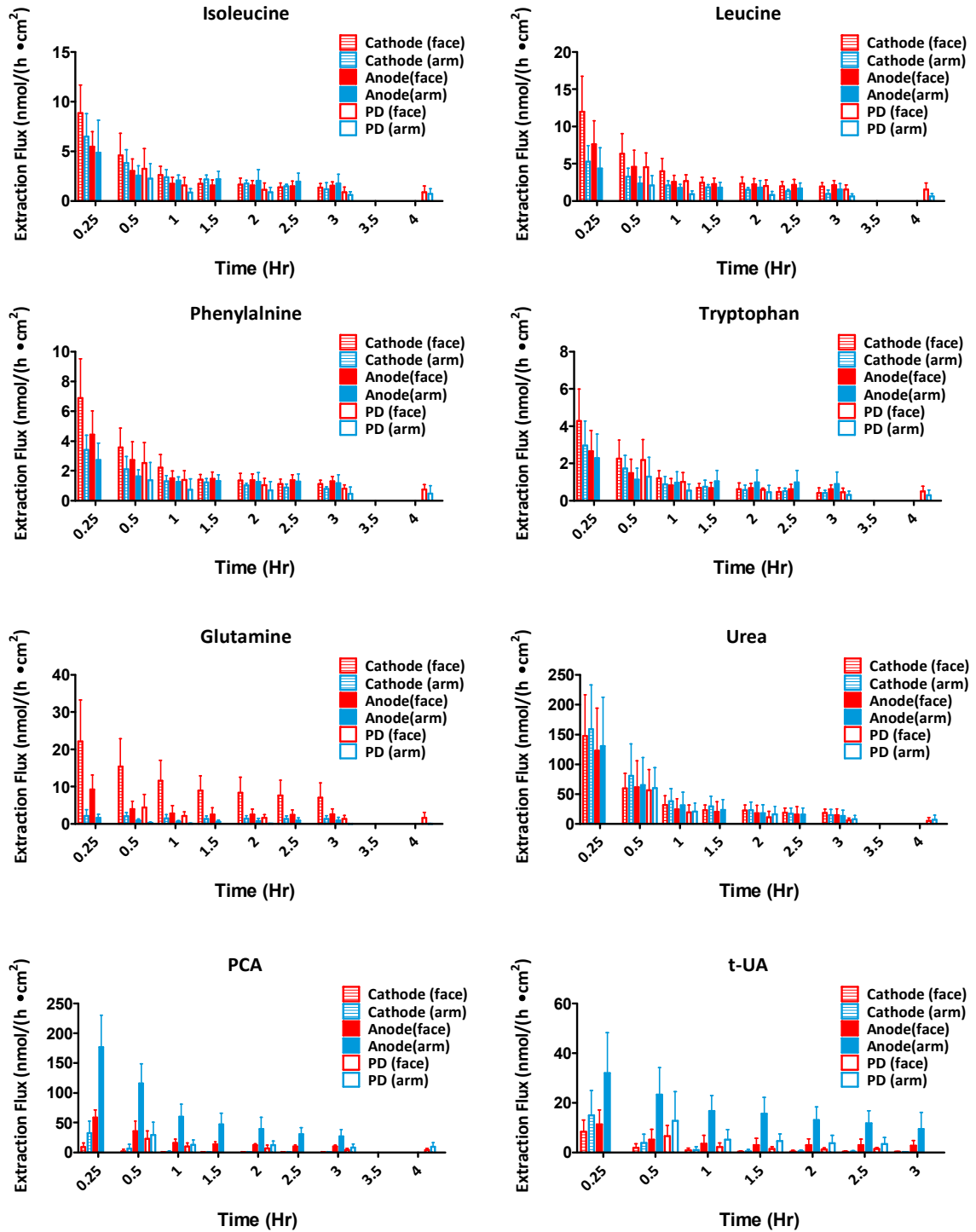
2. Extraction by reverse iontophoresis and passive diffusion

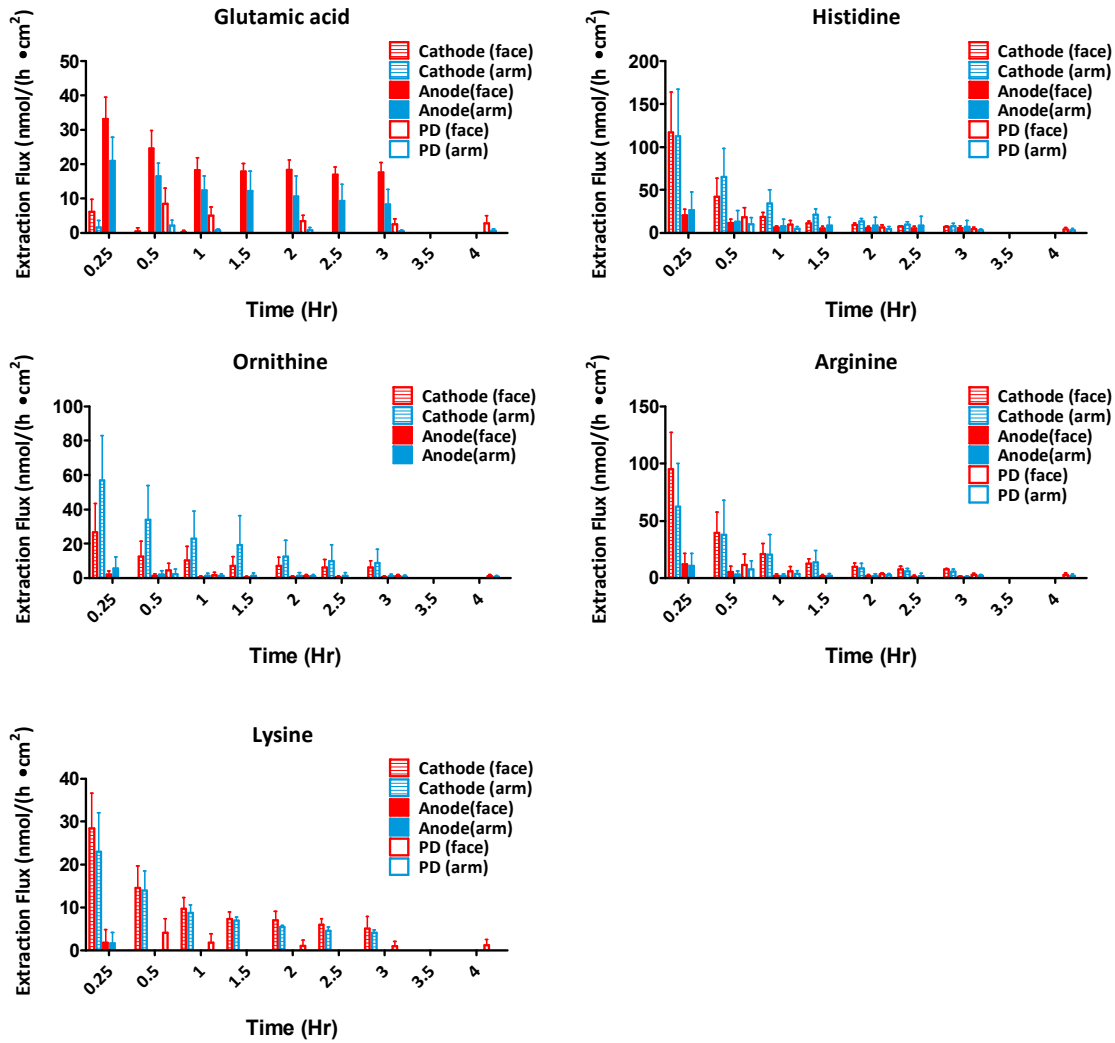Figure 2a: Reverse iontophoretic and passive extraction fluxes (mean ± SD) of NMF components *in vivo* in human volunteers (n=6) as a function of time.

Figure 2b: Reverse iontophoretic and passive extraction fluxes (mean ± SD) of NMF components *in vivo* in human volunteers (n=6) as a function of time.

Figure 2c: Reverse iontophoretic and passive extraction fluxes (mean ± SD) of NMF components *in vivo* in human volunteers (n=6) as a function of time.

3. Origins of NMF extracted

Figure 3a: Cumulative amounts of NMF components extracted (mean ± SD) by reverse iontophoresis and by passive diffusion as a function of time (n=6). The average quantities in the SC determined by tape-stripping are shown for comparison by the solid horizontal lines, with the ±SD indicated by the dashed lines.

Figure 3b: Cumulative amounts of NMF components extracted (mean ± SD) by reverse iontophoresis and by passive diffusion as a function of time (n=6). The average quantities in the SC determined by tape-stripping are shown for comparison by the solid horizontal lines, with the ±SD indicated by the dashed lines.
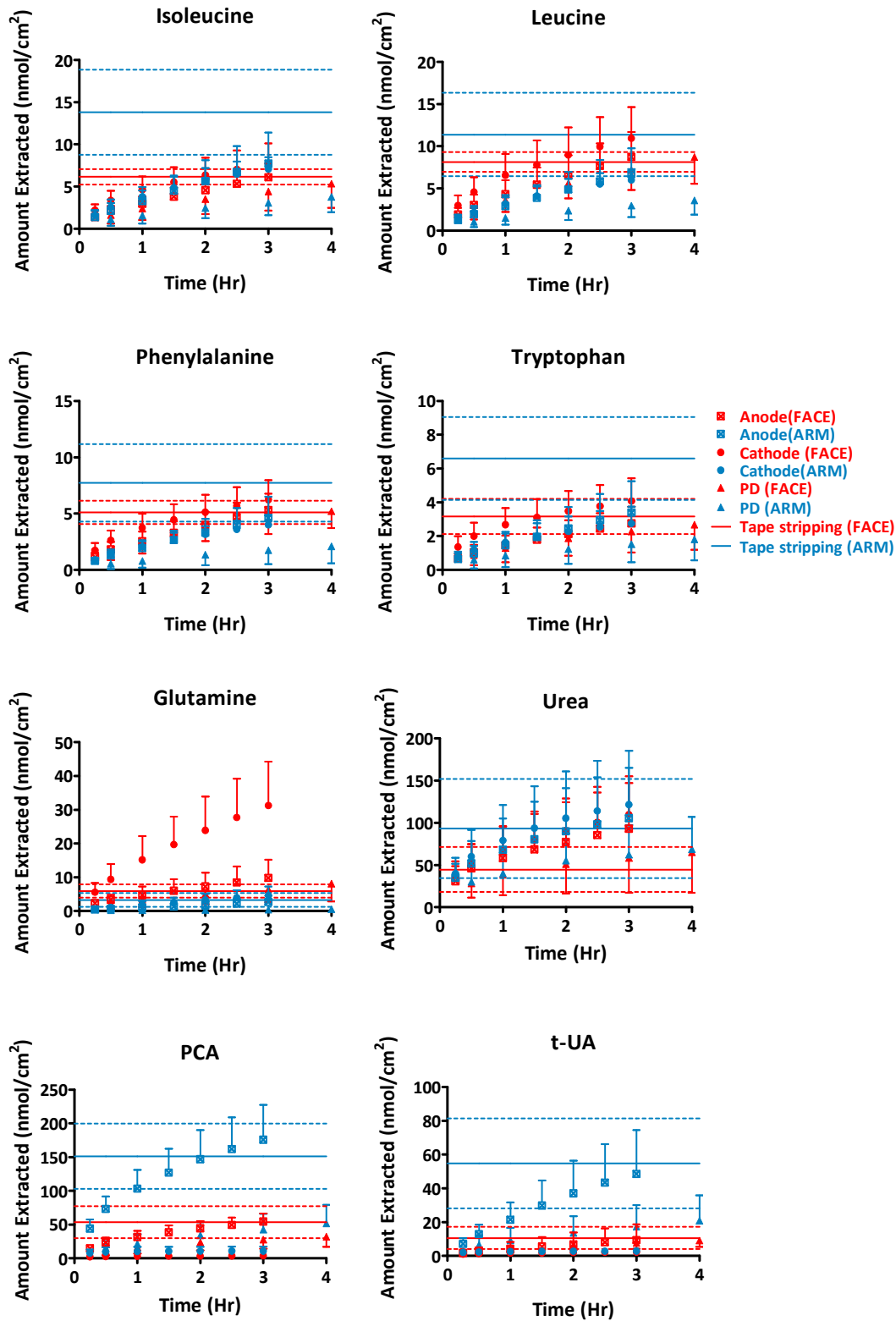
Figure 3c: Cumulative amounts of NMF components extracted (mean ± SD) by reverse iontophoresis and by passive diffusion as a function of time (n=6). The average quantities in the SC determined by tape-stripping are shown for comparison by the solid horizontal lines, with the ±SD indicated by the dashed lines.
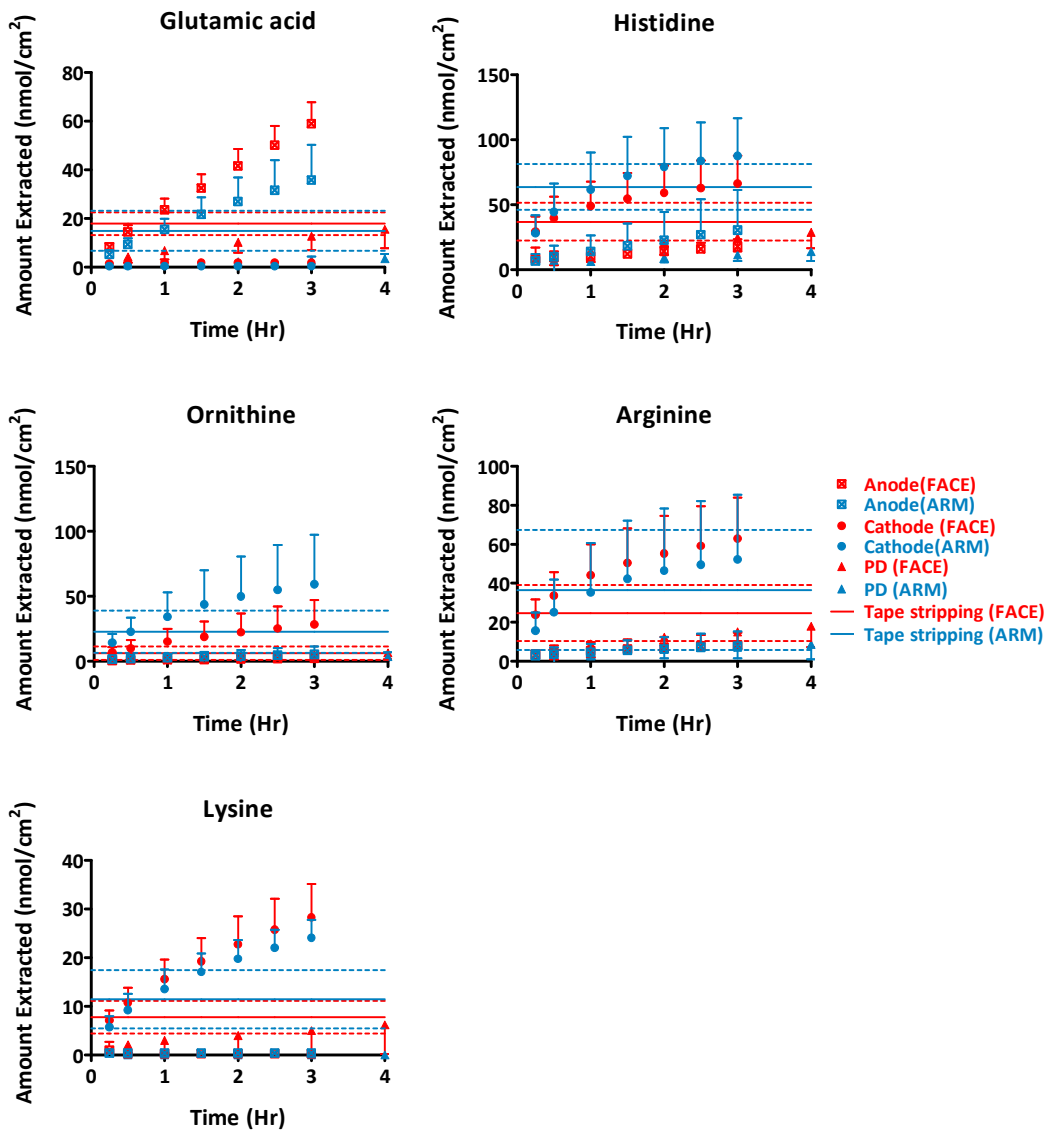
Appendix 4. Complements to Chapter 4

1. SC content determined by tape-stripping
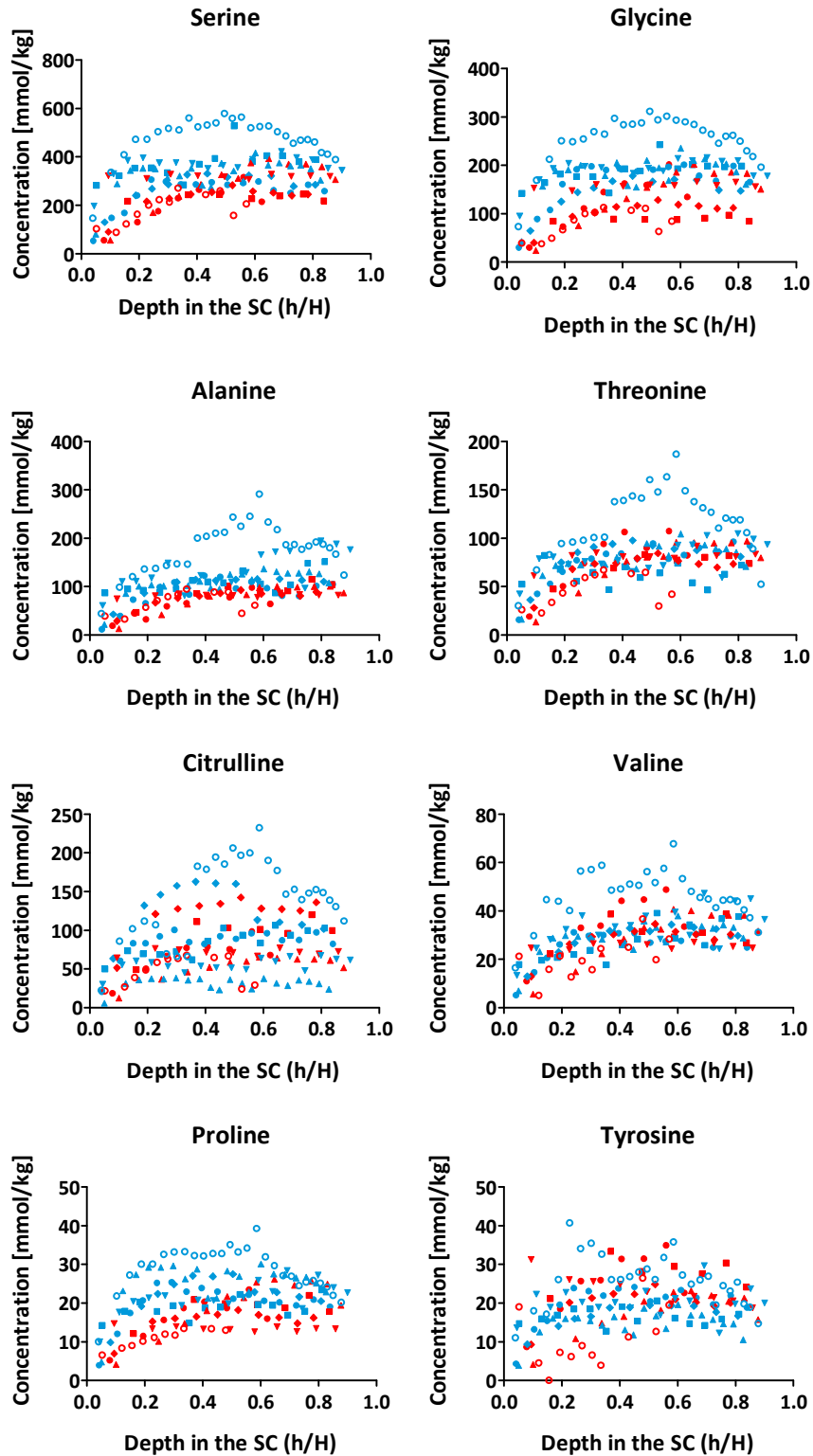
Figure 1a: Concentration profiles of NMF components as a function of position in the SC on forehead (red) and forearm (blue) in 6 human volunteers.
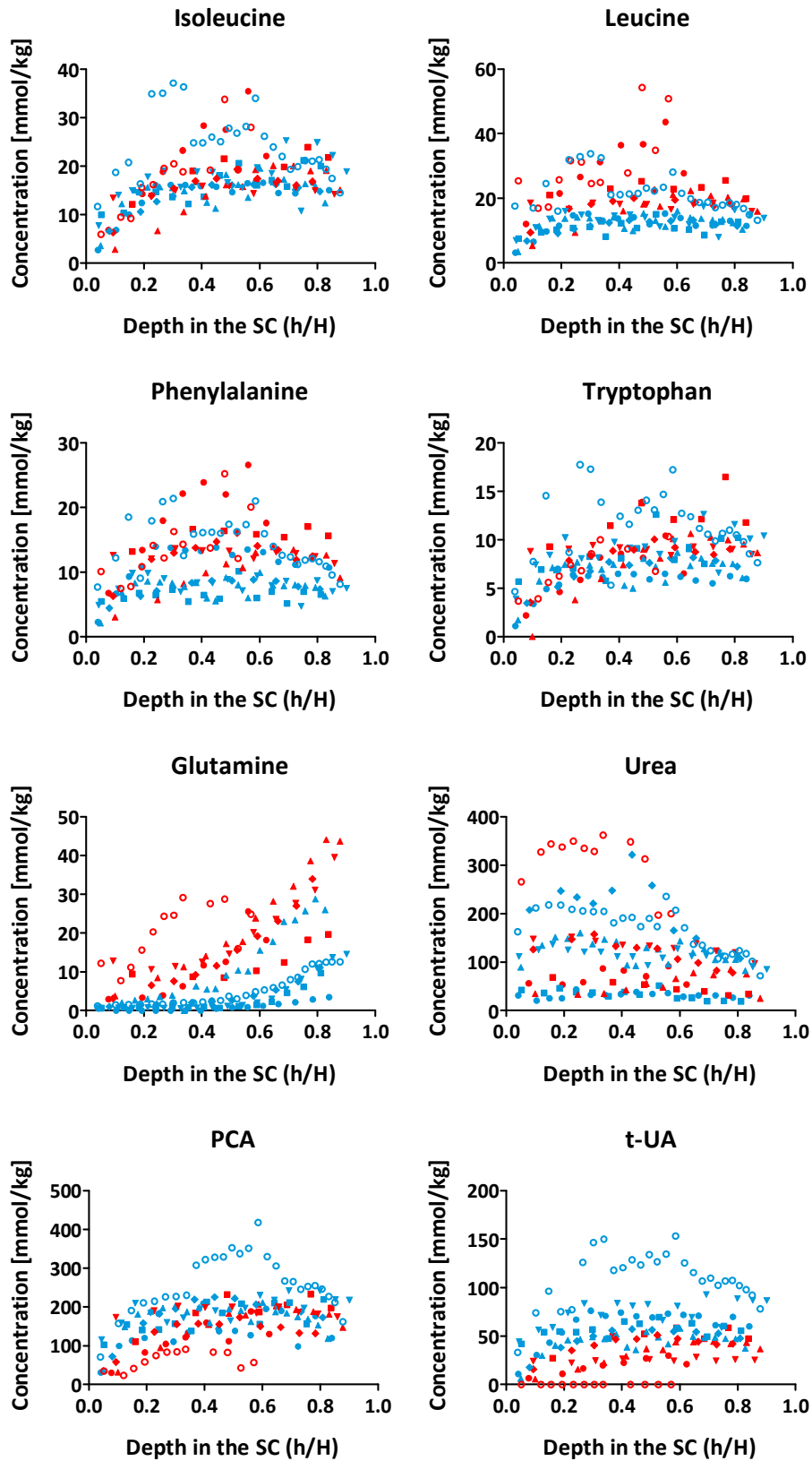
Figure 1b: Concentration profiles of NMF components as a function of position in the SC on forehead (red) and forearm (blue) in 6 human volunteers.
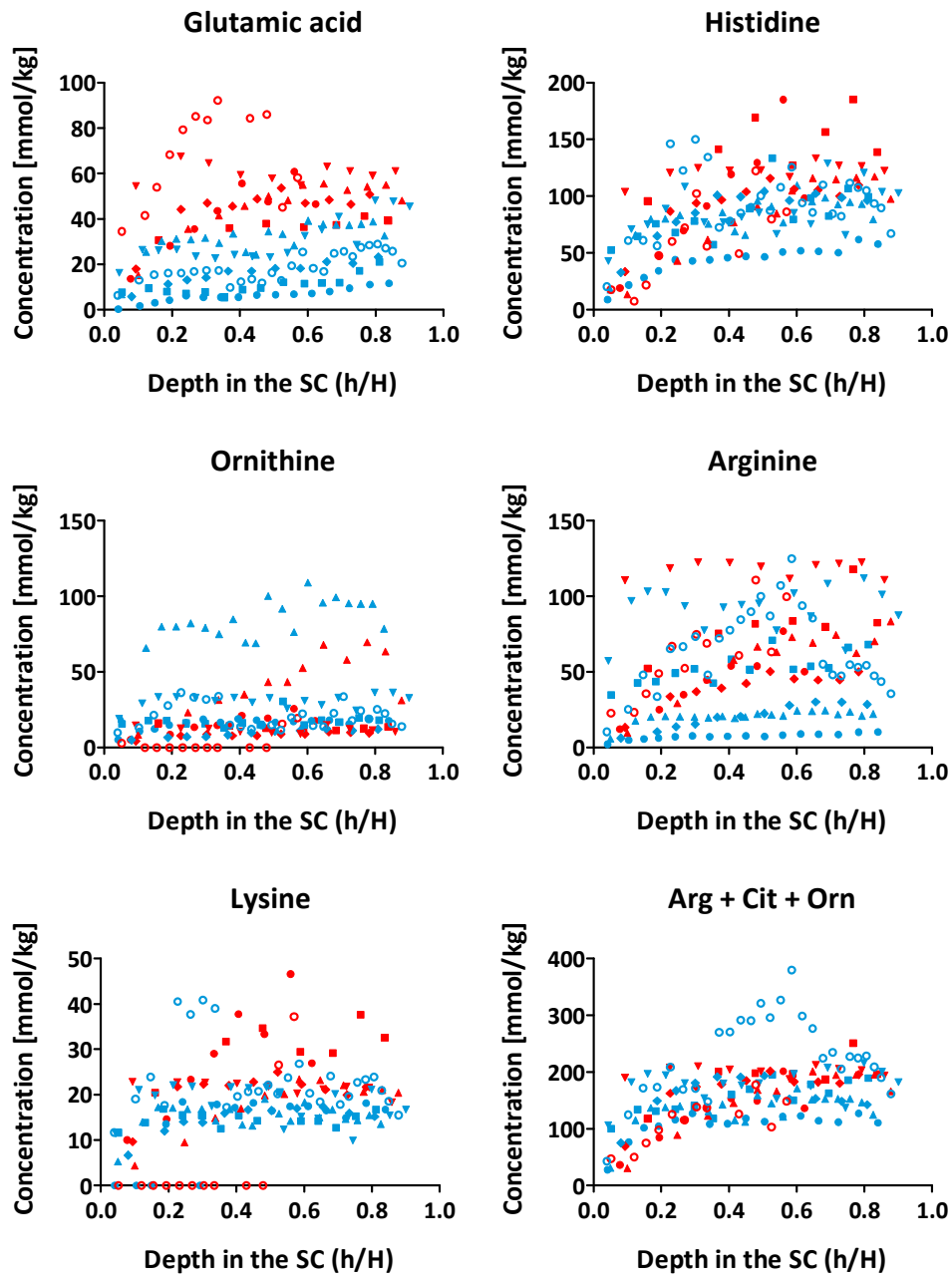
Figure 1c: Concentration profiles of NMF components as a function of position in the SC on forehead (red) and forearm (blue) in 6 human volunteers.

2. Extraction by reverse iontophoresis and passive diffusion

Figure 2a: Reverse iontophoretic and passive extraction flux (mean ± SD) of NMF components *in vivo* in human volunteers (n=6) from forehead (red) and forearm (blue) skin as a function of time.

Figure 2b: Reverse iontophoretic and passive extraction flux (mean ± SD) of NMF components *in vivo* in human volunteers (n=6) from forehead (red) and forearm (blue) skin as a function of time.

Figure 2c: Reverse iontophoretic and passive extraction flux (mean ± SD) of NMF components *in vivo* in human volunteers (n=6) from forehead (red) and forearm (blue) skin as a function of time.

3. Origins of NMF extracted

Figure 3a: Cumulative amounts of NMF components extracted (n=6; mean ± SD) by iontophoresis at both electrodes and by passive diffusion as a function of time from the forehead (red) and forearm (blue). The average quantities in the SC determined by tape-stripping are shown for comparison by the solid horizontal lines, with the ±SD indicated by dashed lines.

Figure 3b: Cumulative amounts of NMF components extracted (n=6; mean ± SD) by iontophoresis at both electrodes and by passive diffusion as a function of time from the forehead (red) and forearm (blue). The average quantities in the SC determined by tape-stripping are shown for comparison by the solid horizontal lines, with the ±SD indicated by dashed lines.

Figure 3c: Cumulative amounts of NMF components extracted (n=6; mean ± SD) by iontophoresis at both electrodes and by passive diffusion as a function of time from the forehead (red) and forearm (blue). The average quantities in the SC determined by tape-stripping are shown for comparison by the solid horizontal lines, with the ±SD indicated by dashed lines.

Appendix 5. Complements to Chapter 5

1. SC content determined by tape-stripping
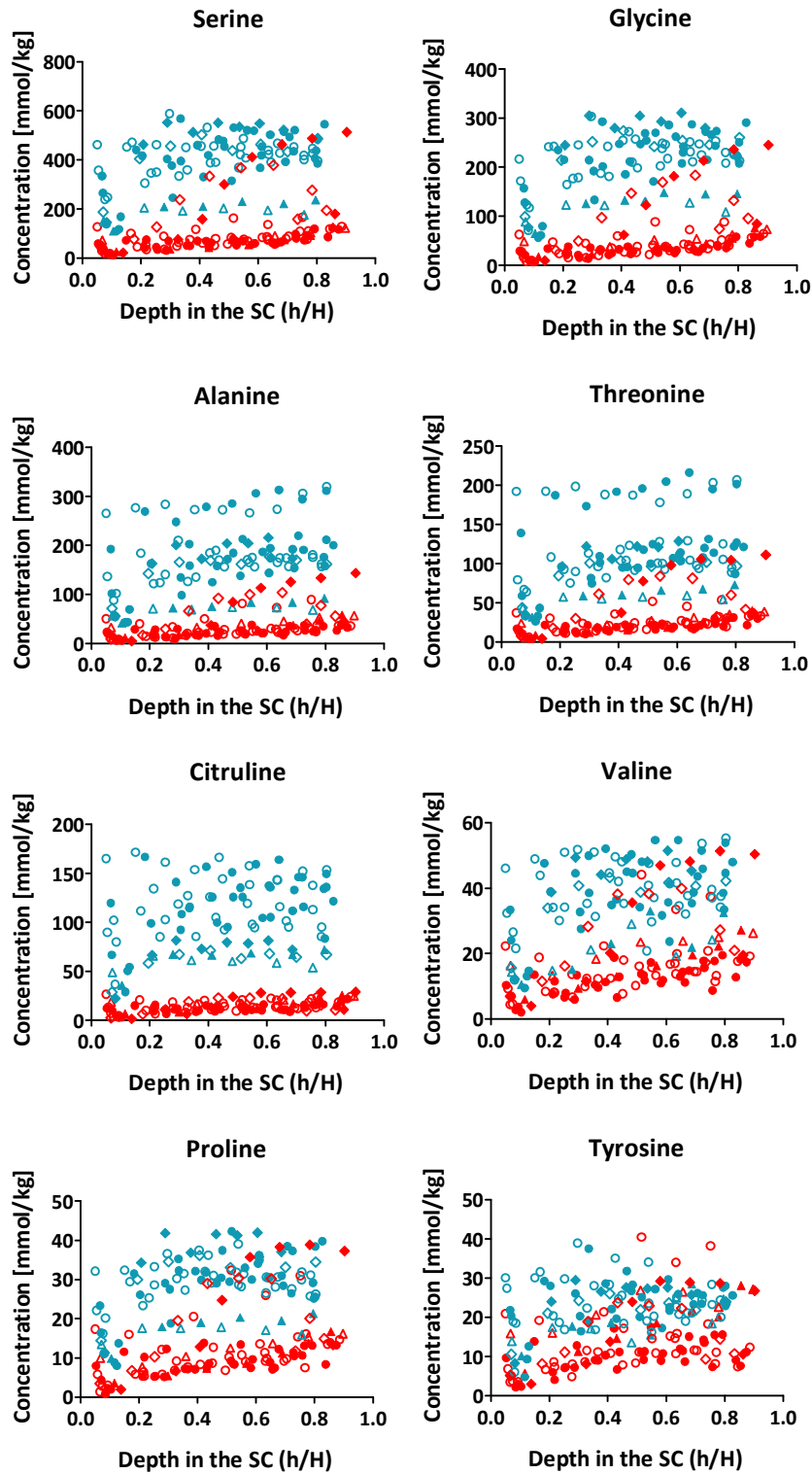
Figure 1a: Concentration profiles of NMF components as a function of SC depth on SLS-treated (red) and untreated, control (blue) forearms (n=7, Volunteer 7: diamond; Volunteer 4: triangle; other volunteers: circles; gravimetric method: solid symbols; imaging method: open symbols).
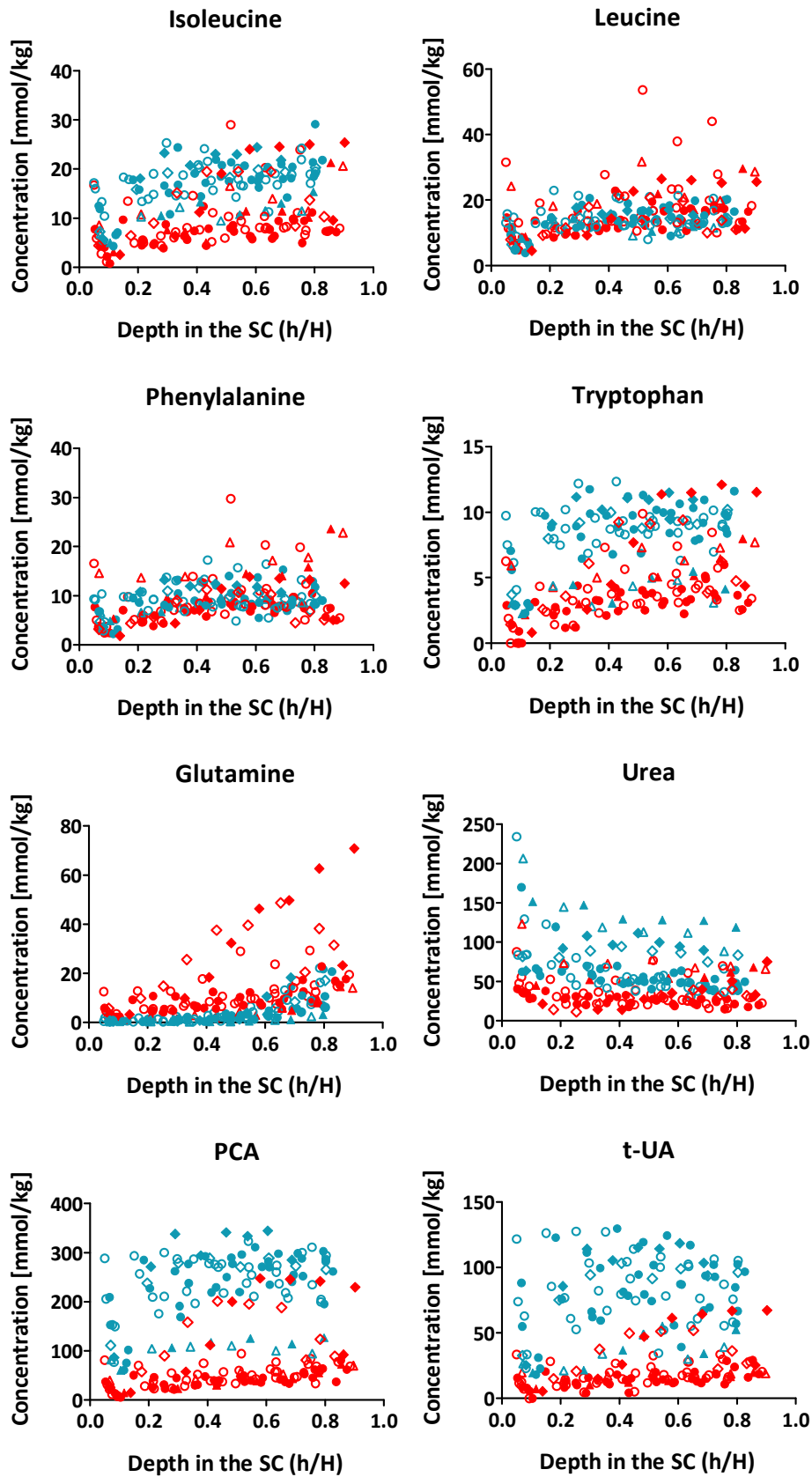
Figure 1b: Concentration profiles of NMF components as a function of SC depth on SLS-treated (red) and untreated, control (blue) forearms (n=7, Volunteer 7: diamond; Volunteer 4: triangle; other volunteers: circles; gravimetric method: solid symbols; imaging method: open symbols).
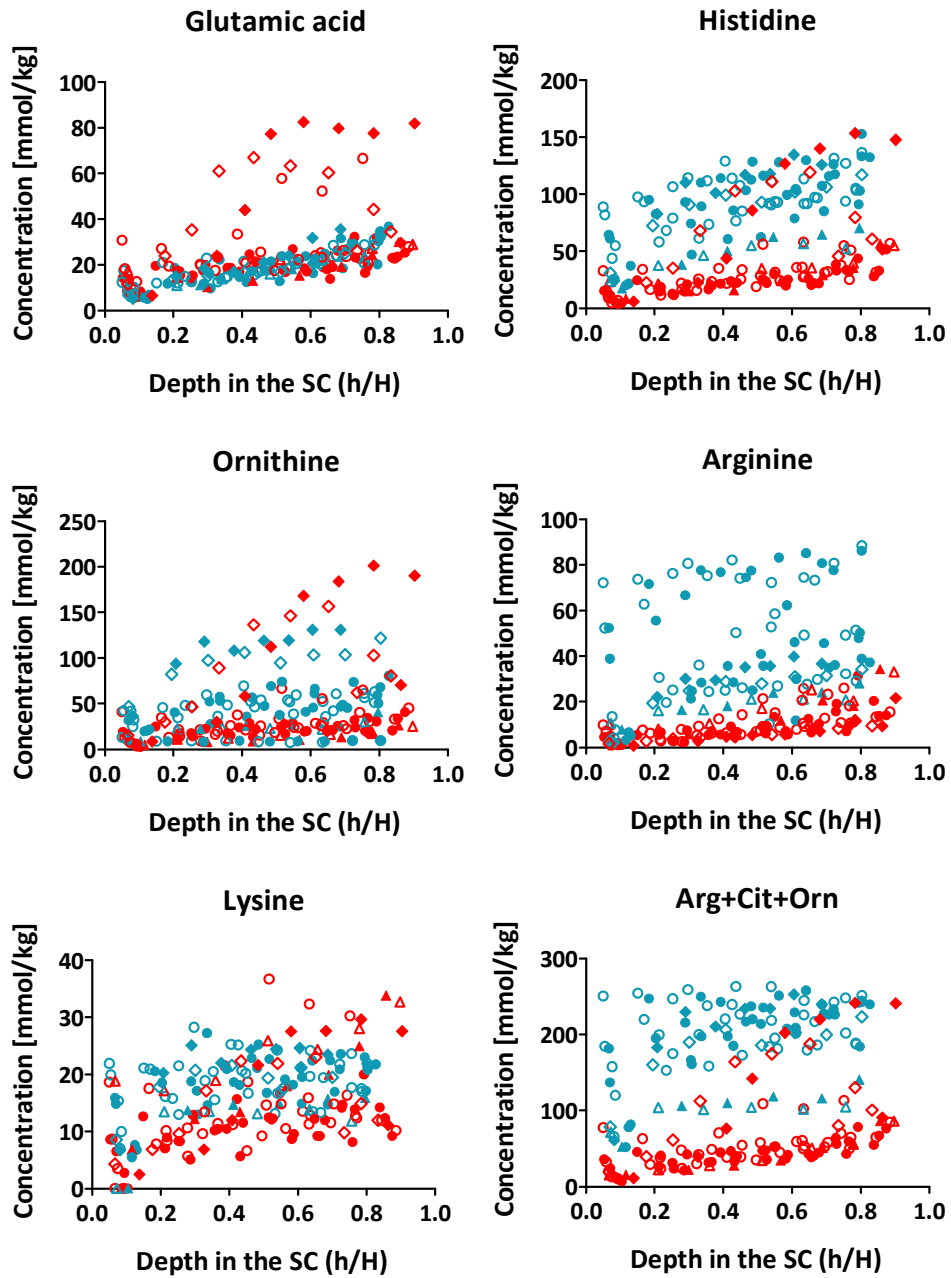
Figure 1c: Concentration profiles of NMF components as a function of SC depth on SLS-treated (red) and untreated, control (blue) forearms (n=7, Volunteer 7: diamond; Volunteer 4: triangle; other volunteers: circles; gravimetric method: solid symbols; imaging method: open symbols).

2. Extraction by reverse iontophoresis and passive diffusion

Figure 2a: Reverse iontophoretic and passive extraction flux (mean ± SD) of NMF components *in vivo* in human volunteers (n=6) from the SLS treated (red) and control (blue) forearms as a function of time.
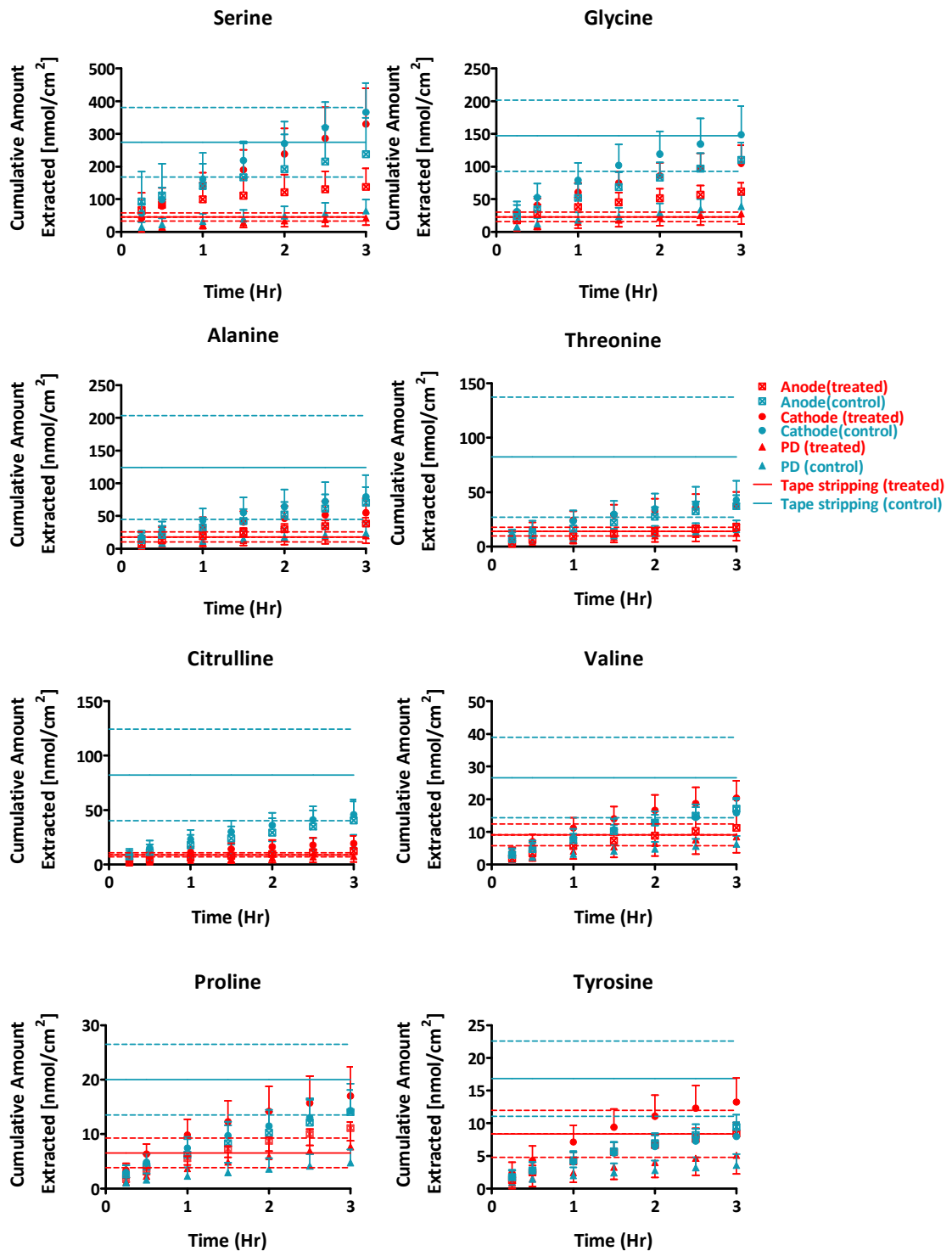
Figure 2b: Reverse iontophoretic and passive extraction flux (mean ± SD) of NMF components *in vivo* in human volunteers (n=6) from the SLS treated (red) and control (blue) forearms as a function of time.

Figure 2c: Reverse iontophoretic and passive extraction flux (mean ± SD) of NMF components *in vivo* in human volunteers (n=6) from the SLS treated (red) and control (blue) forearms as a function of time.
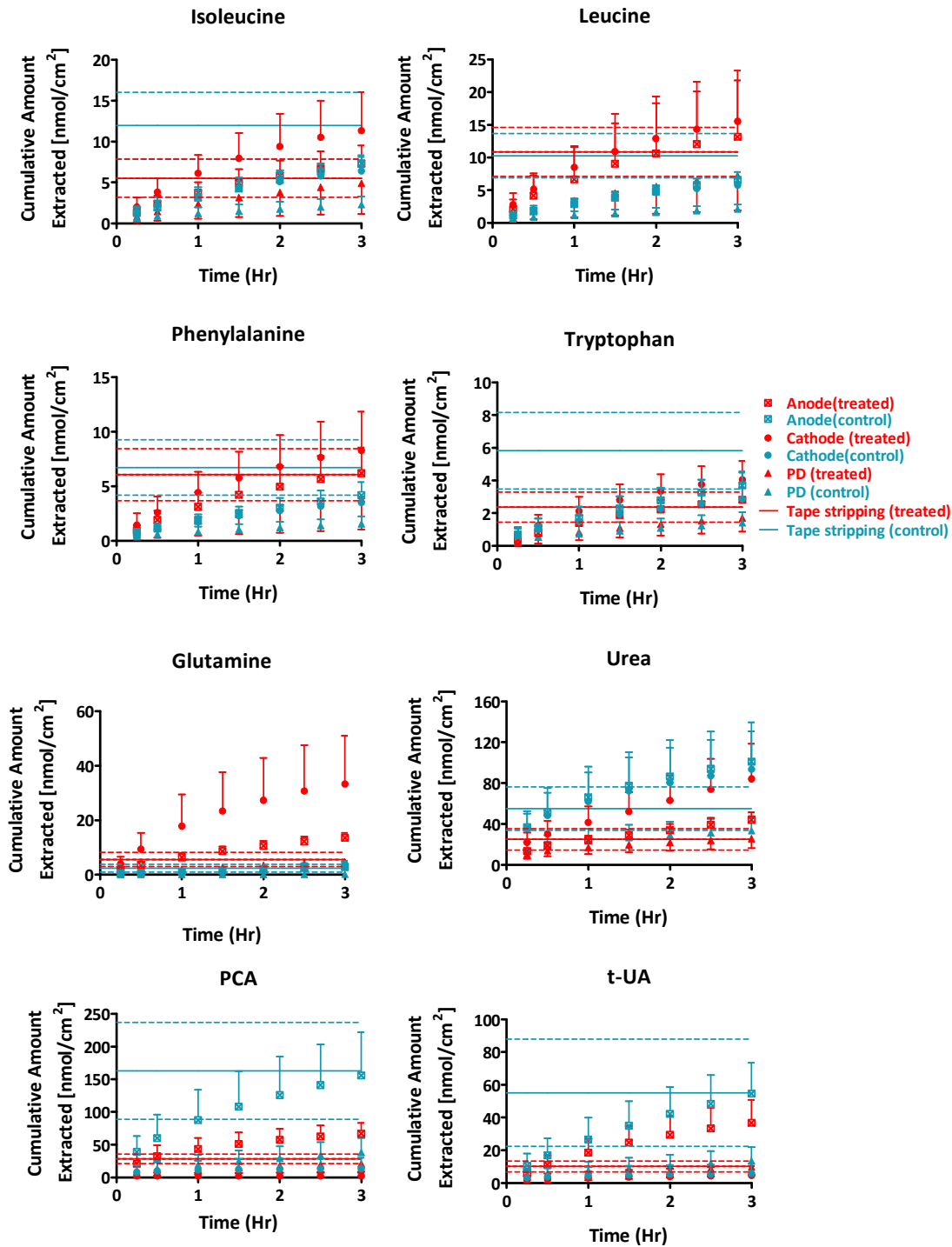
3. Origins of NMF extracted

Figure 3a: Cumulative amounts of NMF components extracted (mean ± SD; n=6) by iontophoresis at both electrodes and by passive diffusion as a function of time from the SLS-treated (red) and untreated, control (blue) forearms. The average quantities in the SC determined by tape-stripping are shown for comparison by the solid horizontal lines, with the ±SD indicated by dashed lines.
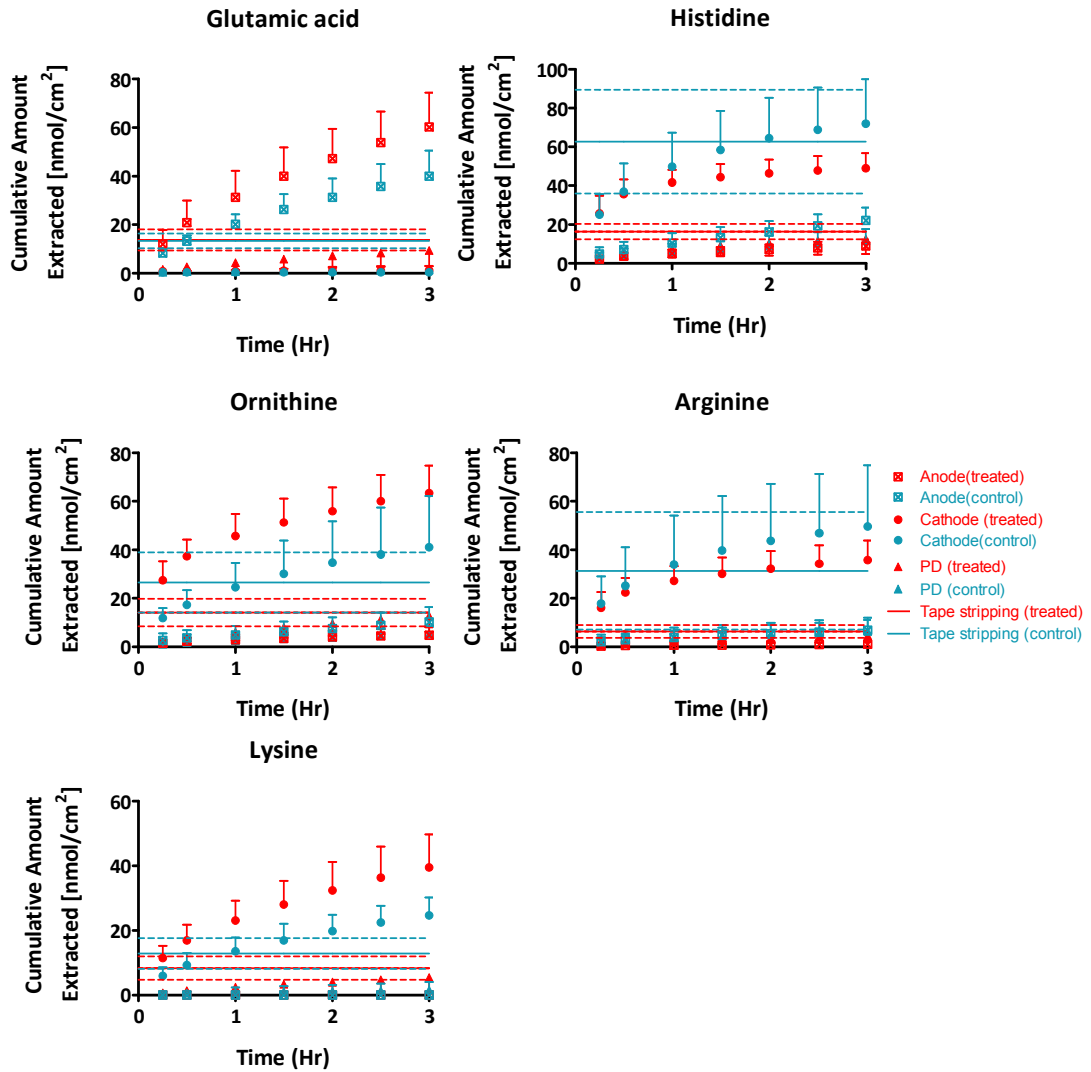
Figure 3b: Cumulative amounts of NMF components extracted (mean ± SD; n=6) by iontophoresis at both electrodes and by passive diffusion as a function of time from the SLS-treated (red) and untreated, control (blue) forearms. The average quantities in the SC determined by tape-stripping are shown for comparison by the solid horizontal lines, with the ±SD indicated by dashed lines.

Figure 3c: Cumulative amounts of NMF components extracted (mean ± SD; n=6) by iontophoresis at both electrodes and by passive diffusion as a function of time from SLS-treated (red) and untreated, control (blue) forearms. The average quantities in the SC determined by tape-stripping are shown for comparison by the solid horizontal lines, with the ±SD indicated by dashed lines.
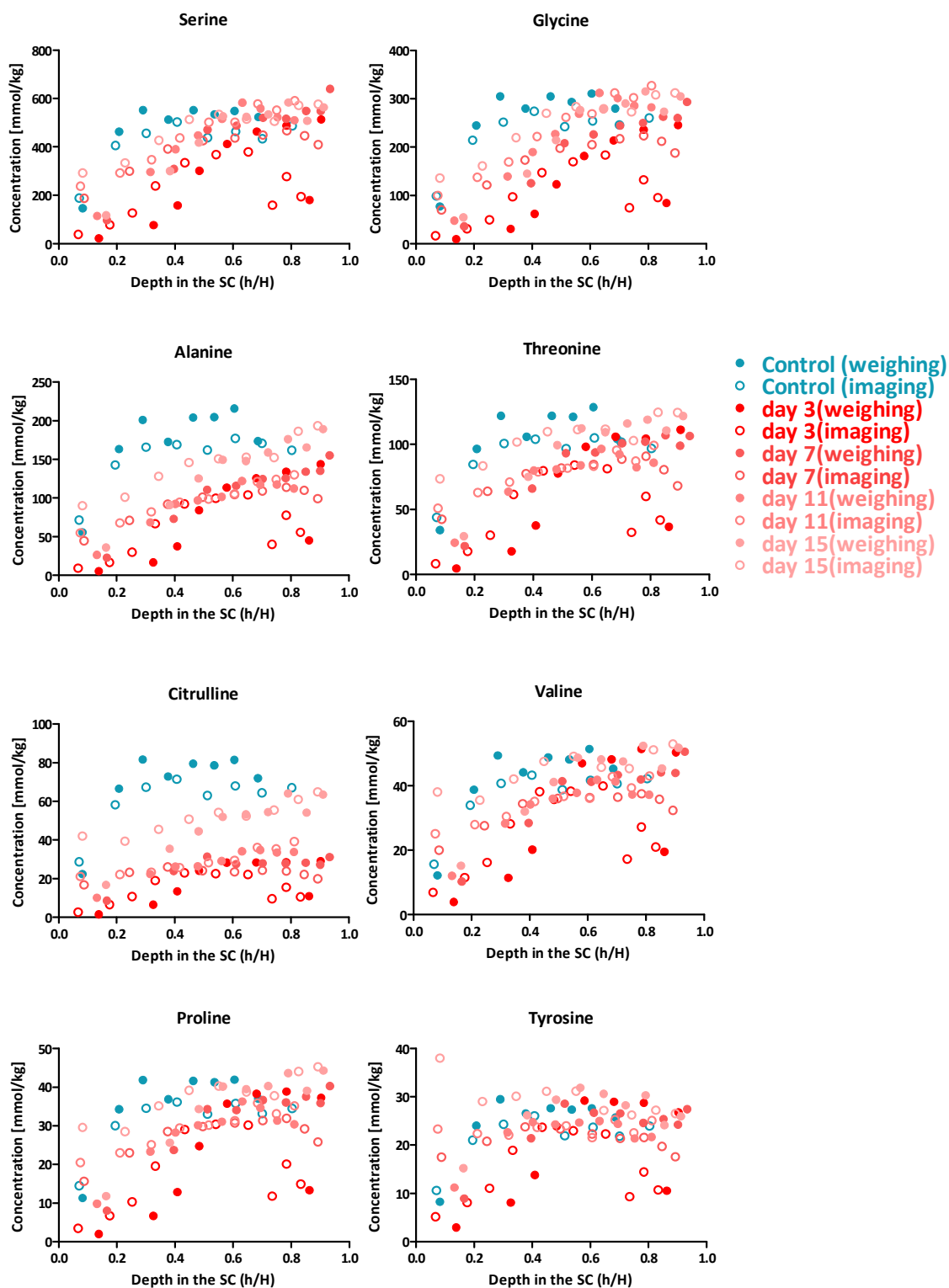
Figure 4a: Concentration profiles of NMF components as a function of SC depth on SLS treated (red) and untreated, control (blue) forearms from volunteer 7 on day 3, 7, 11, 15 after the final SLS application (gravimetric method : solid circles, imaging method: open circles).
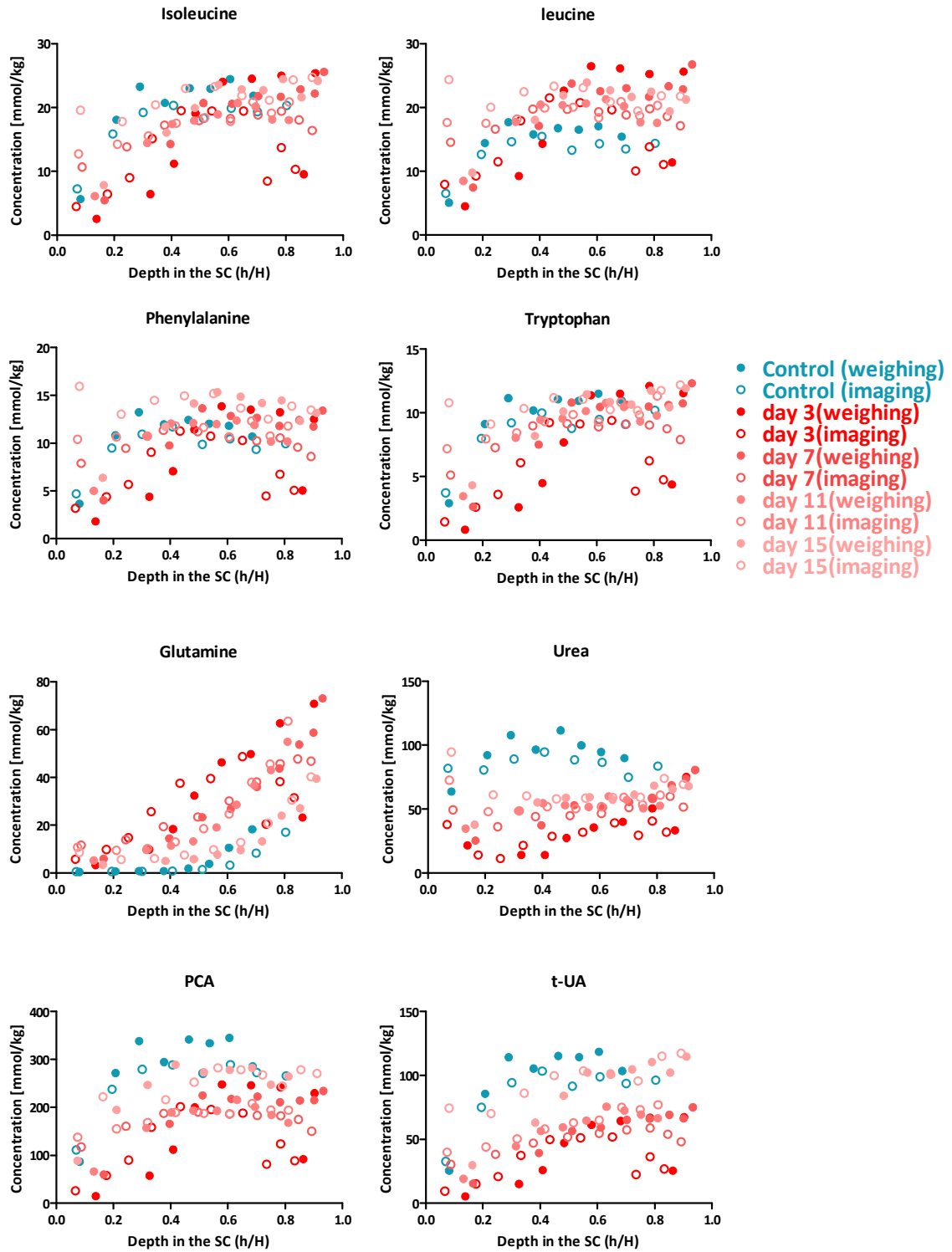
Figure 4b: Concentration profiles of NMF components as a function of SC depth on SLS treated (red) and untreated, control (blue) forearms from volunteer 7 on day 3, 7, 11, 15 after the final SLS application (gravimetric method : solid circles, imaging method: open circles).
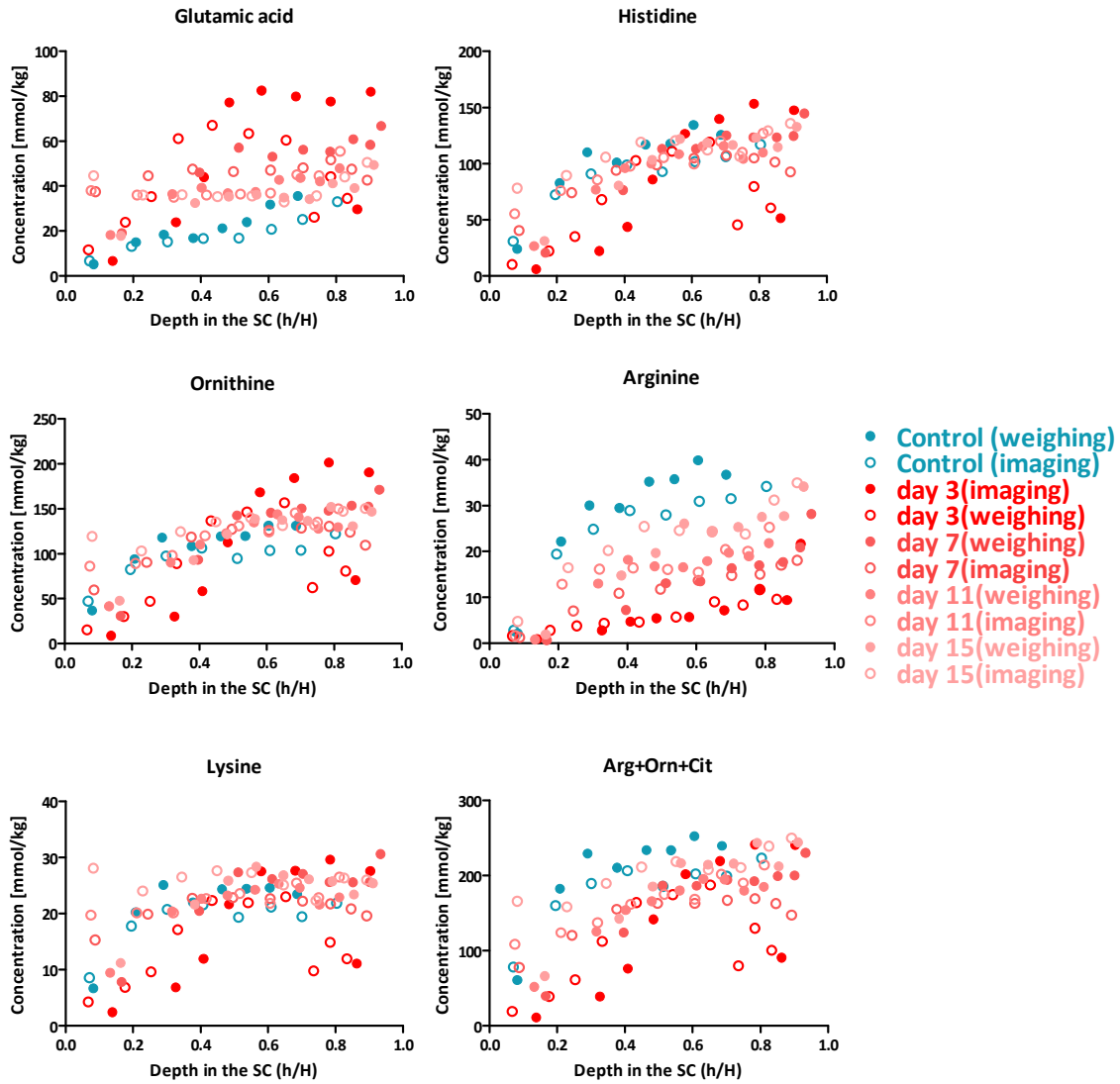
Figure 4c: Concentration profiles of NMF components as a function of SC depth on SLS treated (red) and untreated, control (blue) forearms from volunteer 7 on day 3, 7, 11, 15 after the final SLS application (gravimetric method : solid circles, imaging method: open circles).